ANL-ART-155

Sodium Freezing and Remelting Tests in FY 2018

Nuclear Science and Engineering Division

About Argonne National Laboratory
Argonne is a U.S. Department of Energy laboratory managed by UChicago Argonne, LLC under contract DE-AC02-06CH11357. The Laboratory's main facility is outside Chicago, at 9700 South Cass Avenue, Argonne, Illinois 60439. For information about Argonne and its pioneering science and technology programs, see www.anl.gov.

DOCUMENT AVAILABILITY

Online Access: U.S. Department of Energy (DOE) reports produced after 1991 and a growing number of pre-1991 documents are available free via DOE's SciTech Connect (http://www.osti.gov/scitech/)

Reports not in digital format may be purchased by the public from the National Technical Information Service (NTIS):

U.S. Department of Commerce
National Technical Information Service
5301 Shawnee Rd
Alexandra, VA 22312
www.ntis.gov
Phone: (800) 553-NTIS (6847) or (703) 605-6000
Fax: (703) 605-6900
Email: **orders@ntis.gov**

Reports not in digital format are available to DOE and DOE contractors from the Office of Scientific and Technical Information (OSTI):

U.S. Department of Energy
Office of Scientific and Technical Information
P.O. Box 62
Oak Ridge, TN 37831-0062
www.osti.gov
Phone: (865) 576-8401
Fax: (865) 576-5728

Disclaimer
This report was prepared as an account of work sponsored by an agency of the United States Government. Neither the United States Government nor any agency thereof, nor UChicago Argonne, LLC, nor any of their employees or officers, makes any warranty, express or implied, or assumes any legal liability or responsibility for the accuracy, completeness, or usefulness of any information, apparatus, product, or process disclosed, or represents that its use would not infringe privately owned rights. Reference herein to any specific commercial product, process, or service by trade name, trademark, manufacturer, or otherwise, does not necessarily constitute or imply its endorsement, recommendation, or favoring by the United States Government or any agency thereof. The views and opinions of document authors expressed herein do not necessarily state or reflect those of the United States Government or any agency thereof, Argonne National Laboratory, or UChicago Argonne, LLC

ANL-ART-155

Sodium Freezing and Remelting Tests in FY 2018

---

prepared by
Q. Lv, Y. Momozaki, E. Boron, D. B. Chojnowski, J. J. Sienicki, and C. B. Reed
Nuclear Science and Engineering Division, Argonne National Laboratory

September 27, 2018

ABSTRACT

In FY 2017 and FY 2018, a total of thirteen tests were successfully performed in the Sodium Freezing and Remelting test facility. Each new test was carefully designed based upon the results and findings of the previous test to investigate the effects of different factors on the sodium freezing phenomena, including dissolved Ar cover gas versus vacuum, test section cooling rate during freezing, different freezing patterns (e.g., from the free surfaces inward toward the center versus from the center toward the free surfaces), and Ar cover gas pressure. The freezing results were found to depend upon a combination of phenomena. As more tests were conducted and lessons learned, the conduct of the tests improved. In particular, the last three experiments, Tests 11 through 13, may be singled out as providing representative data under well controlled conditions.

The maximum stresses arising from sodium freezing are measured to be quite mild. In the tests, a maximum strain change of 60 radial micro strains was measured, equivalent to a stress/negative pressure of 77 psi. This mild maximum stress is thought to reflect the low yield stress of solid sodium near the freezing temperature. Evidence for yielding of solid sodium is provided by the visual observation of a depression in the frozen sodium free surface inside of the sodium reservoir in one test. It is thought that contraction of sodium in the test section during freezing pulled downward on the frozen sodium at the free surface creating the depression. The authors are not aware of any data for the yield stress of solid sodium or the stress versus strain behavior of solid sodium (sodium is not a structural material). It is thus not possible to directly compare with the solid sodium yield strength. However, stress versus strain data at different temperatures up to the freezing temperature are available for solid lithium which is also a alkali metal and has a low yield strength similar to the maximum stresses determined from the Sodium Freezing and Remelting tests providing support for the interpretation of the results in terms of yielding of solid sodium. This is a good result for Sodium-Cooled Fast Reactors and sodium facilities. The maximum stress due to frozen sodium pulling inward upon a structural wall wetted by sodium and to which the sodium adheres will be limited by the low sodium yield stress.

Argon has a significant solubility in sodium. Cavitation due to nucleation of dissolved argon can offset the effects of sodium thermal contraction and alleviate the formation of stress/negative pressure. This is also a good result for Sodium-Cooled Fast Reactors and sodium facilities that operate with an argon cover gas. In the tests, it was found that due to the cavitation, the maximum measured strain change during sodium freezing was limited to 10 axial micro strains, or equivalently 55 psi of negative pressure.

Table of Contents

LIST OF FIGURES

LIST OF TABLES

1 Introduction

Research and development on advanced energy conversion systems for Sodium-Cooled Fast Reactors (SFRs) is being carried out to identify energy conversion approaches that offer capital cost, safety, and efficiency benefits beyond the current Rankine superheated steam cycle. The current focus in the U.S. is on the supercritical carbon dioxide (sCO_2) Brayton cycle. The sCO_2 Brayton cycle is well suited for application to SFRs. The cycle is highly recuperated and will operate with a CO_2 temperature rise through the sodium-to-CO_2 heat exchanger of about 150°C. This is approximately equal to the temperature rise through the SFR core, providing an excellent match.

The sCO_2 Brayton cycle offers a number of benefits over the traditional Rankine superheated steam cycle. Foremost is eliminating sodium-water reactions. Sodium reacts energetically with water releasing heat and generating combustible hydrogen gas. With the Rankine water/steam cycle, the designer must incorporate design features for sodium-heated steam generators to detect small leakages of water/steam into sodium before the leaks grow in size and to accommodate sodium-water reactions following the postulated double-ended guillotine rupture of a steam generator tube failure. Those design features add to the capital cost of the SFR. While the sCO_2 Brayton cycle eliminates sodium-water reactions, there is a need to understand and accommodate the effects of sodium-CO_2 interactions.

The sCO_2 Brayton cycle offers the potential for lower capital cost than the Rankine steam cycle. The sCO_2 cycle provides higher cycle efficiency than the steam cycle for higher SFR core outlet temperatures further reducing the plant cost per unit electrical power and increasing the plant net present value. The sCO_2 cycle turbomachinery is remarkably small giving rise to the expectation of significant cost savings provided that reliable and cost effective compact heat exchangers can be utilized for the sodium-to-CO_2 heat exchangers, high temperature recuperator, low temperature recuperator, and CO_2-to-water cooler.

Utilization of the sCO_2 Brayton cycle requires that suitably reliable and economical sodium-to-CO_2 heat exchangers are designed. Development of the sCO_2 cycle at Argonne National Laboratory (Argonne) envisions use of compact diffusion-bonded heat exchangers such as those manufactured by Heatric Division of Meggitt (UK) Ltd [1, 2]. Heat transfer from sodium to sCO_2 does not involve boiling as with the steam cycle such that heat transfer can take place inside of compact diffusion-bonded heat exchangers. Compact diffusion-bonded heat exchangers potentially offer high reliability in terms of the expectation of a low failure rate. Compact diffusion-bonded heat exchangers also offer long life and significantly smaller volume relative to other heat exchanger types.

In the Argonne AFR-100 SFR design developed under the Advanced Reactor Technologies Program, sodium enters the sodium-to-CO_2 heat exchangers at 528°C and exits at 373°C. At these temperatures, the heat exchanger stainless steel is expected to be wetted by the sodium within days. In reality, the heat exchanger would likely already have been wetted from exposure to sodium at lower temperatures of about 200°C during the lengthy startup of the reactor.

The utilization of compact diffusion-bonded sodium-to-CO_2 heat exchangers requires that fundamental phenomena for such heat exchangers be understood. This will enable heat exchangers to be reliably designed for the complete spectrum of normal and off-normal transient operating conditions. Three particular phenomena that have been identified for which knowledge and understanding are crucial are:

- Thermal shock-induced failure of the heat exchanger;
- Failure to efficiently drain sodium from heat exchanger sodium channels; and
- Heat exchanger failure due to freezing or melting of inadvertently trapped sodium remaining inside of heat exchanger sodium channels following draining.

To investigate and gain knowledge and understanding of the third phenomenon listed above, a Sodium Freezing and Remelting test facility has been designed and built at Argonne. The sodium freezing and remelting campaign dates back to FY 2010 [3] when the concept for an experiment facility was developed. In FY 2011 [4], it was decided to design and assemble a small-scale facility for fundamental sodium freezing and remelting testing. In parallel, the formulation and design of fundamental sodium freezing experiments to conduct in the sodium freezing and remelting facility was undertaken. To this end, an investigation into the fundamental freezing and remelting behavior of sodium inside of stainless steel channels was undertaken using analytical models. In FY 2012 [5], the Sodium Freezing and Remelting test facility was designed, fabricated, and assembled; and shakedown tests were initiated. From FY 2013 to FY 2016 [6, 7], the shakedown tests were continued and a series of freezing and remelting tests were performed. Due to the temperature limits of the strain gages implemented on the test sections, those experiments were limited to 300ºC and did not reach wetting of the test section inner surface, a critical phenomenon that needs to be achieved in order to observe excess stress/strain when sodium freezing/melting occurs. This limitation was due to specification of the wrong bonding material to attach the strain gages to the stainless steel test sections. The bonding material was limited to 350ºC.

It was therefore decided to replace the old test sections with a new design with high-temperature strain gages (temperature limit of 980ºC) implemented. The design of the new single test section incorporates a thin wall to enhance the strains achieved. In FY 2017 [8], the Sodium Freezing and Remelting test facility was upgraded with the work mainly focusing on replacing the old test sections with the new test section. With the upgraded test facility, two tests were performed in FY 2017, including a shakedown test at ~ 200ºC mainly to confirm the availability of sodium flow and a formal test at ~ 400ºC in the test section. Strain drop (negative pressure) during sodium freezing was clearly observed in the 400ºC test, although it was only in the order of ~ 10 microstrains. Continuing in FY 2018, a total of 8 freezing tests were performed, with the first test trying to wet the test section at ~ 500ºC for 24 hours. After the first test, each new test was designed based on the results from the previous test to investigate the effects of different factors on the freezing phenomenon, including dissolved Ar, test section cooling rate, different freezing patterns, and cover gas pressure. In this report, details of the work performed in FY 2018 are discussed.

2 Sodium Freezing and Remelting Test Facility Description

The upgraded Freezing and Remelting test facility, as shown in Figure 1 to Figure 3, is a simple closed loop system only partially filled with sodium. This test facility consists of four main components: the test section in the bottom, the DC EM pump located in the small vertical leg, the sodium reservoir located in the opposite leg, and the cold finger submerged into the sodium reservoir. The small tubing, including the pump duct, is ½ inch outer diameter (OD) tubing; the fill reservoir is made from a 4-inch Schedule 80 pipe. Swagelok VCR fittings are used on all non-welded connections, except the top flange for the sodium reservoir. The system must be vacuum tight for bake-out prior to the initial sodium loading, so the top flange is sealed with a Conflat knife-edge seal design. The sodium freezing and remelting test section is connected using quick change VCR fittings to elbows below the sodium fill reservoir and the electromagnetic sodium pump. The cold finger is submerged in the sodium reservoir, and sealed to the reservoir cap with a conflat flange. Details regarding the design and upgrades of the test facility can be found in the previous report [8].

Figure 1. Upgraded Sodium Freezing and Remelting test facility.

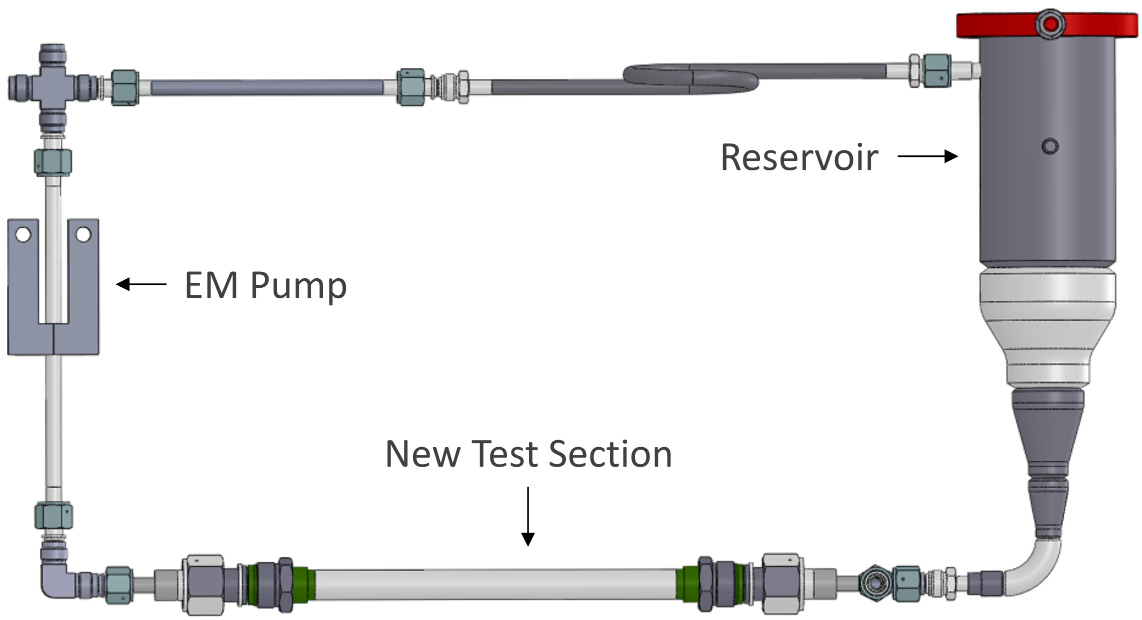

Figure 2. CAD drawing of the upgraded Sodium Freezing and Remelting test facility, not including the cold finger.

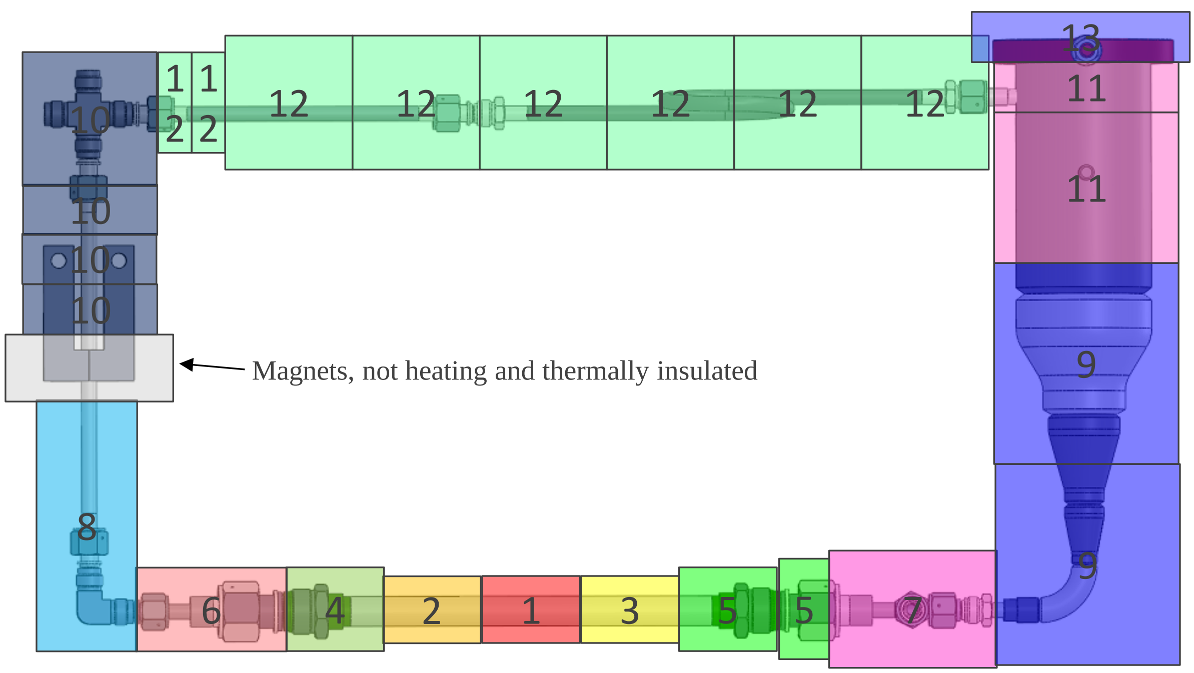

Figure 3. Updated heating zones for the Freezing and Remelting test facility.

3 Sodium Freezing and Remelting Tests

In FY 2017 [8], two tests were performed, including a shakedown test with sodium at a maximum temperature of ~ 200ºC mainly to confirm the availability of sodium flow and a formal test with sodium at a maximum temperature of ~ 400ºC in the test section. These two tests will also be included in this report, so that a more complete list of tests that have been performed on the Sodium Freezing and Remelting test facility so far can be presented. In FY 2018, after fixing the heating control issue encountered in the 400ºC formal test in FY 2017, a total of 8 freezing tests were performed, with the first test trying to wet the test section at ~ 500ºC for 24 hours. After the first test, each new test was designed based on the results from the previous test to investigate the effects of different factors on the freezing phenomenon, including dissolved Ar, test section cooling rate, different freezing patterns, and cover gas pressure. In what follows, the details of these tests will be discussed in the same order as how the tests were designed, to better show the learning and thinking process through the tests.

3.1 Test 1: Shakedown Test in FY 2017

In FY 2017 [8], a few upgrades including replacement of the new test section were made to the Sodium Freezing and Remelting test facility. During the disassembly of the old test facility, glove bags were used when breaking a VCR connection to avoid causing significant contamination (oxidation) of the sodium inside the loop. Even though all the disassembly and reassembly work has been performed quickly and carefully, contamination is inevitable. The contamination can potentially cause plugging of the loop. Therefore, upon completion of the reassembly of the new test facility, it was decided to first perform a shakedown test, mainly to confirm and establish the sodium flow. In the present Sodium Freezing and Remelting test facility, there is no flow meter implemented. The only indirect way that has been employed to confirm sodium flow is intentionally heating the different zones (see Figure 3) to different temperatures. By turning on the EM pump, if a sodium flow exists, the different zone temperatures should converge to approximately the same temperature. In this shakedown test, Zone 10 was heated to ~ 250°C considering the heat sink of the EM pump magnets; Zone 12 was heated to ~ 125°C; and the rest of the loop was heated to ~ 200°C. Once the system temperatures stabilized (there were still some oscillations in the Zone 10 temperatures mainly due to the heat loss to the EM pump magnets and on-off controlling of the heaters), the EM pump was turned on. The system temperatures before and after turning on the EM pump are shown in Figure 4. As can be clearly seen, before turning on the EM pump, a temperature gradient exists along the loop. However, once turning on the EM pump, the system temperatures converge to approximately the same temperature of ~ 200°C. This clearly demonstrates that a sodium flow has been established and the loop is operational.

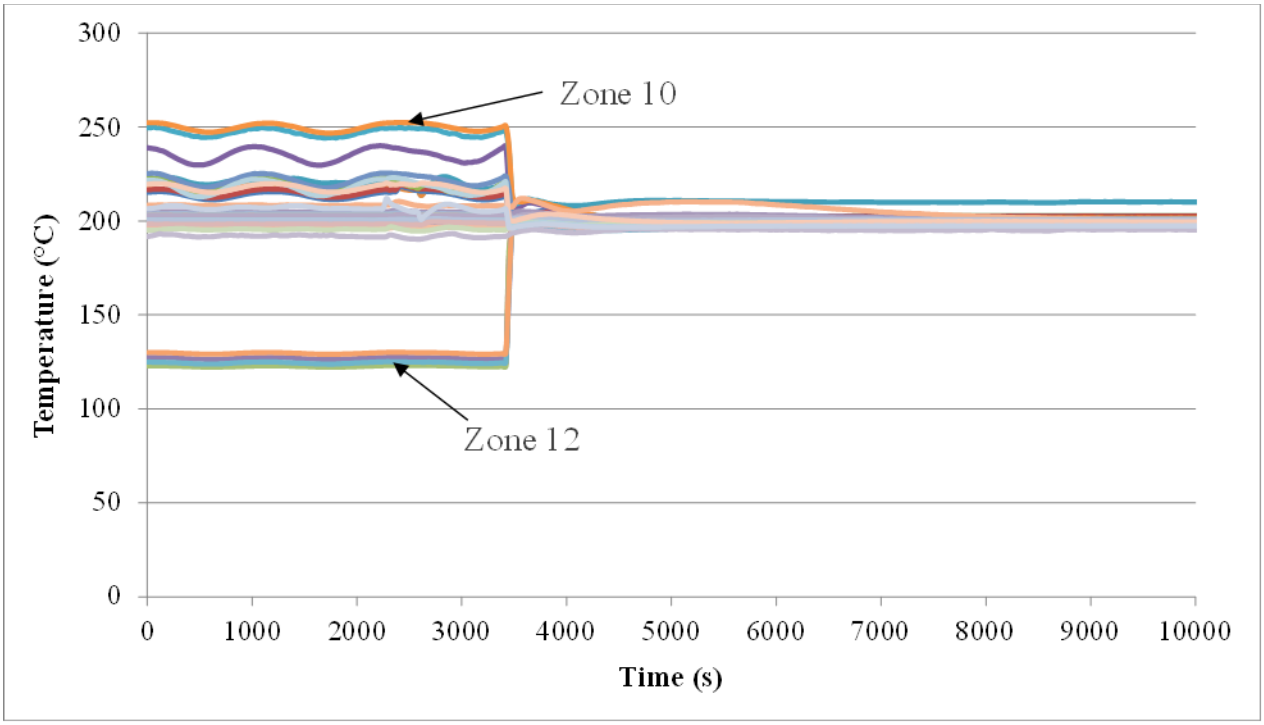

Figure 4. System temperatures before and after turning on the EM pump in Test 1.

3.2 Test 2: 400°C Test in FY 2017

After confirming the sodium flow in the shakedown test, it was decided to proceed with the formal tests. The Sodium Freezing and Remelting test facility had never been operated at temperatures higher than 300°C before, and, therefore, there was no well-established test procedure for tests at temperatures above 300°C. So the first test, although called a 'formal' test, was still a trial test, in which the test section temperatures were raised up slowly in multiple steps.

For this test, the loop was first evacuated to remove the cover gas at room temperature. This evacuation helped eliminate potential gas pocket formation in the test section as well as to reduce any dissolved gas in the sodium. It is known that the dissolved gas may become a seed of cavitation during the freezing. If such cavitation occurs, the expected inward pressure may be significantly reduced. The loop was then heated to melt the sodium from the free surfaces toward the center of the test section. Once the sodium was melted, the Zone 12 temperatures were raised to 125°C, Zone 10 temperatures to 225°C and the rest of the loop to 200°C. The EM pump was subsequently turned on, and the sodium flow was confirmed by observing the convergence of the loop temperatures. These steps were deemed as necessary to confirm sodium flow, and thus would be repeated for every future test. Once the sodium flow started, the cold finger was turned on by introducing cold air into it. The Zone 11 controller was then set to and fixed at a 150°C set temperature to keep it as the coldest region in the loop. This would ensure that the impurities deposit onto the cold finger in Zone 11, not any other region in the loop. The loop temperatures were then increased slowly in steps. With the cold finger on, there was competition between cooling and heating. Every time when the loop set temperatures (except for Zone 11) were increased, it took time for the system to stabilize and develop some temperature gradient. As the test continued and when the test section temperatures were raised to ~ 400°C, difficulties were encountered in controlling the loop temperatures. Large discrepancies in PID controller and limit controller readings were observed in Zones 3, 5, and 7. After a group discussion, it was concluded that the controlling thermocouples and heaters for those zones were not thermally coupled well, and improvement work would be needed to reposition those controlling thermocouples and heaters. It was then decided to stop increasing the system temperatures. The system was maintained at that state (~ 400°C in the test section) for approximately 2 hours (see Figure 5), before the sodium leak early warning system was triggered by an abnormal high temperature. When the warning system was triggered, immediate actions were taken to trace and identify the location of the VCR fitting with the high temperature. The information from the warning system led to the VCR fitting in Zone 12. However, no smoke was observed at that location. Also, the heater controller set temperature was lowered for that specific zone, the temperatures there (read from both the warning system and data acquisition system) started to decrease. This did not appear to be a real sodium leak. To be cautious, it was decided to lower the system temperatures and perform a freezing test.

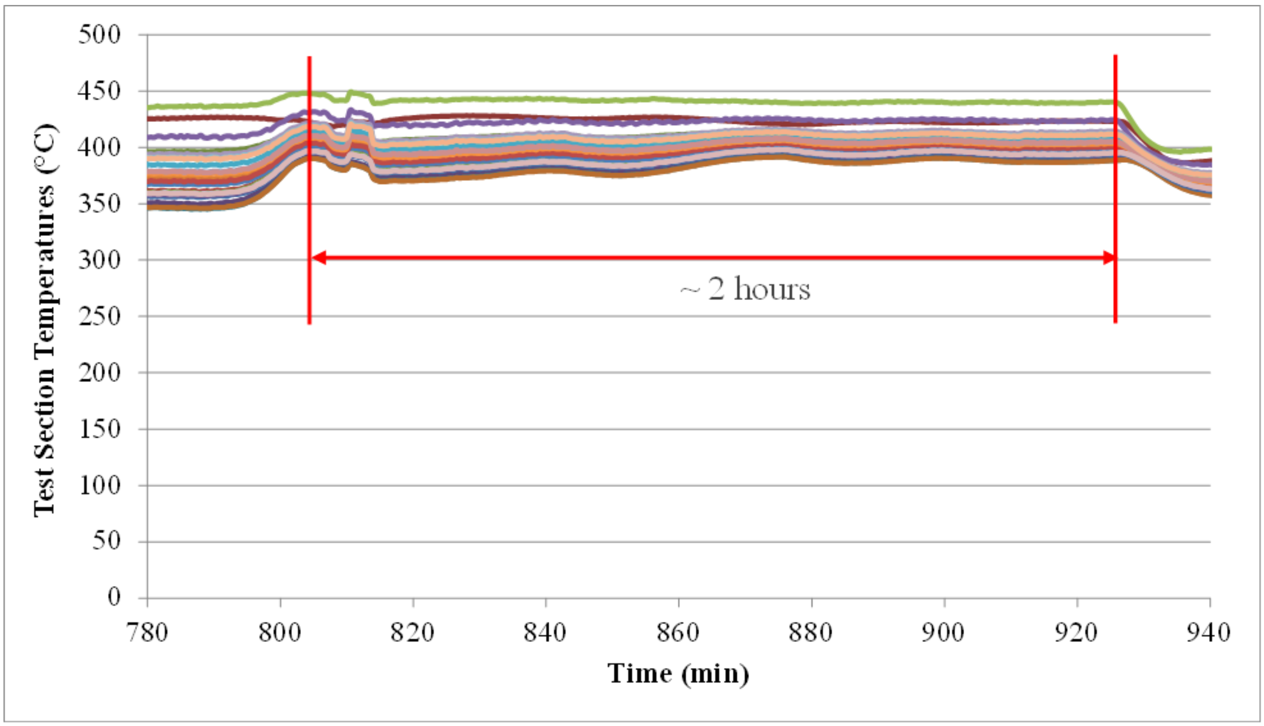

Figure 5. Test section maintained at ~ 400°C for ~ 2 hours in Test 2.

For the freezing test, the system temperatures were first lowered to ~ 110°C. The freezing was then started from the free surfaces by turning off the heaters in the corresponding zones (Zones 10 and 11). The free surfaces were first frozen so that the test section could detect the maximum strain change when sodium freezing occurred. When freezing started to occur in the test section, the freezing front was controlled to propagate from the ends of the test section toward its center, as shown in Figure 6.

The measured test section strains at three different axial locations during sodium freezing are plotted against the corresponding average temperature at each location, as shown in Figure 7 -

Figure 14. Among the 8 strain gages, the hoop strain gage at +4.8" location (Figure 10), two axial strain gages (Figure 11 and Figure 12) at the center, and one hoop strain gage at the center (Figure 13) clearly captured a drop and subsequent increase in the strain. The measured strain drop is clearly due to the thermal contraction during sodium freezing. For the subsequent strain increase, it was initially assumed to be due to the breakaway of solid sodium from the tube wall, which turned out to be incorrect. As it will be explained later, this was probably due to the Poisson effect. The maximum strain change measured in the present test is ~ 10 axial micro strains, corresponding to a negative pressure of only ~ 24 psi, if an ideal thin-walled tube is assumed.

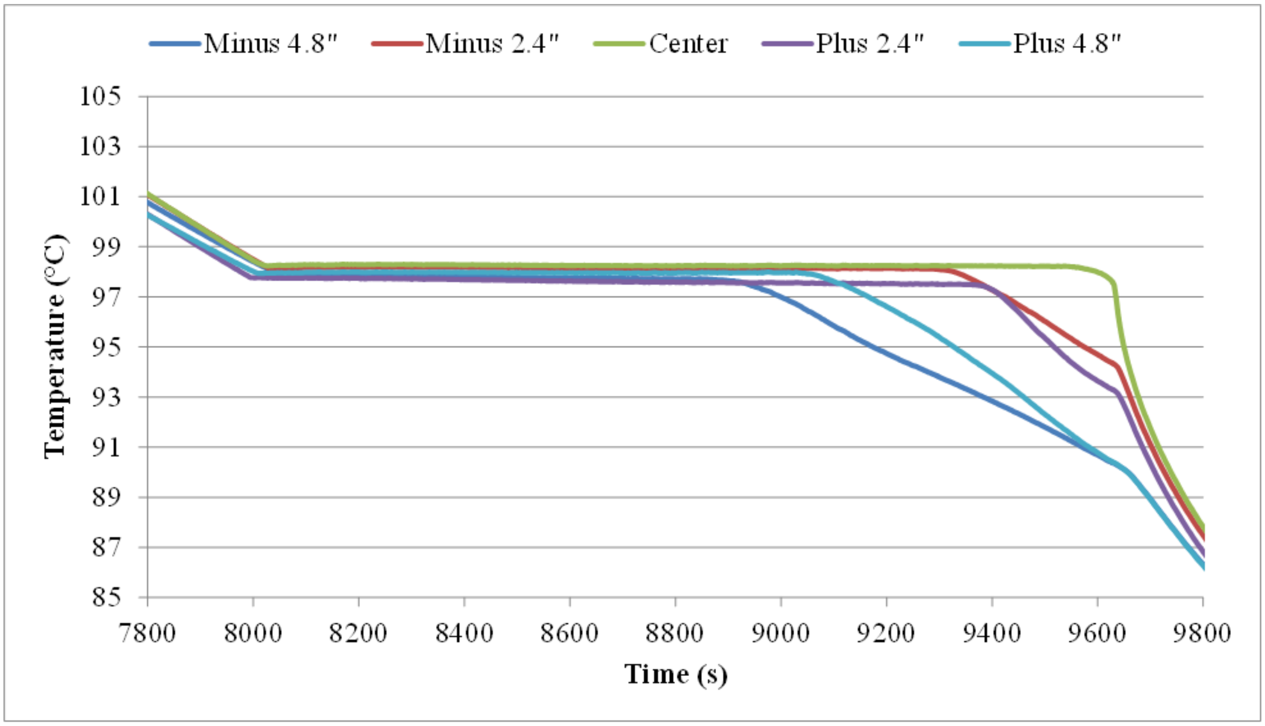

Figure 6. Propagation of freezing front from the ends toward the center of the test section in Test 2.

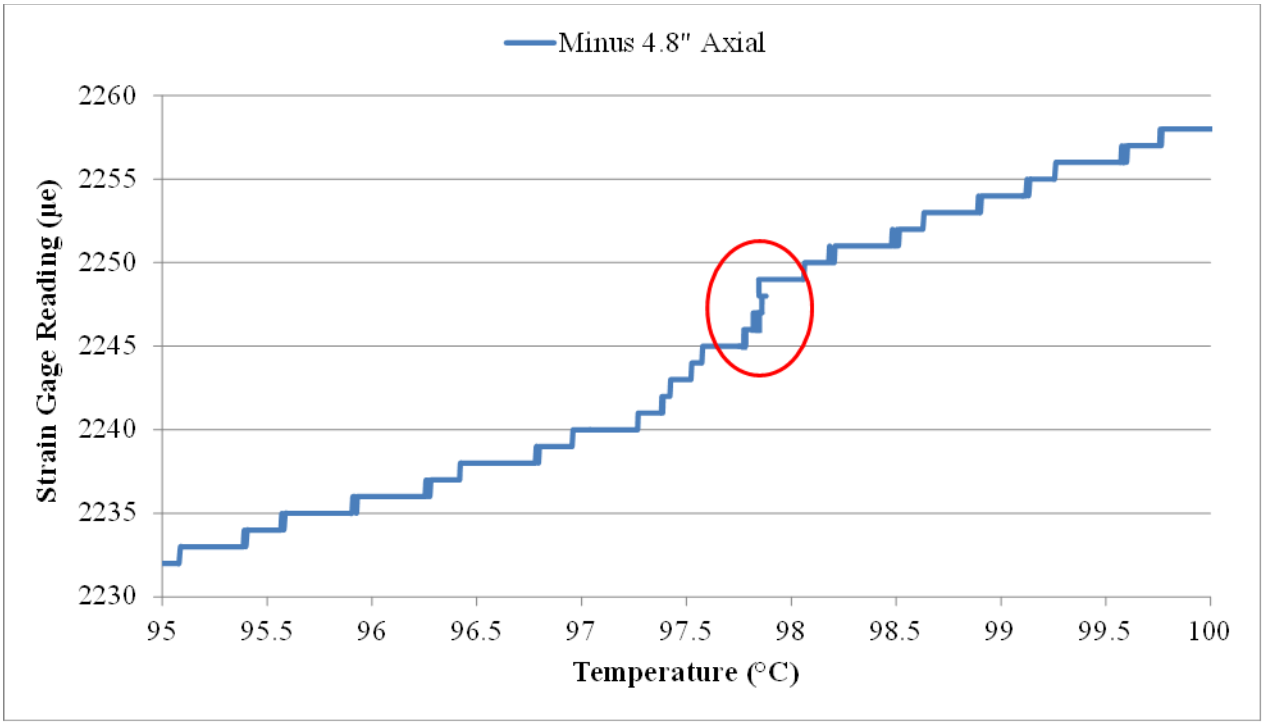

Figure 7. Axial strain vs temperature at –4.8" from the test section center in Test 2.

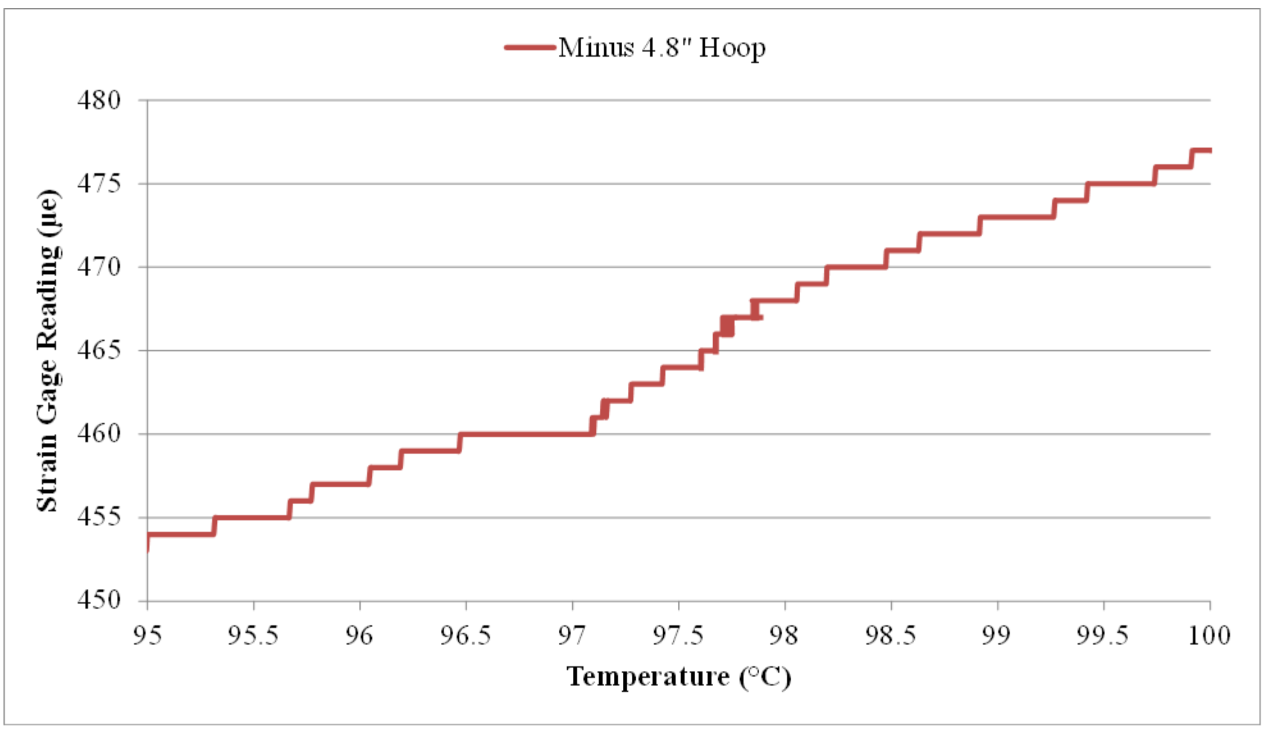

Figure 8. Hoop strain vs temperature at -4.8" from the test section center in Test 2.

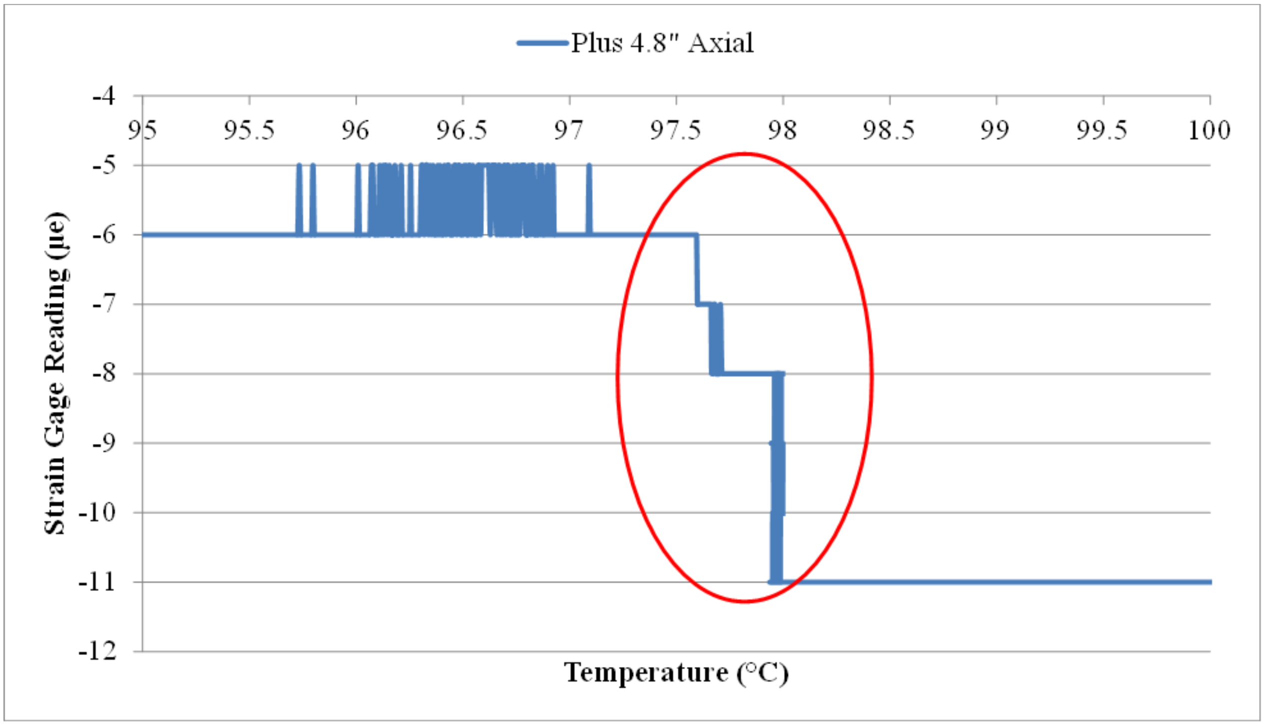

Figure 9. Axial strain vs temperature at +4.8" from the test section center in Test 2.

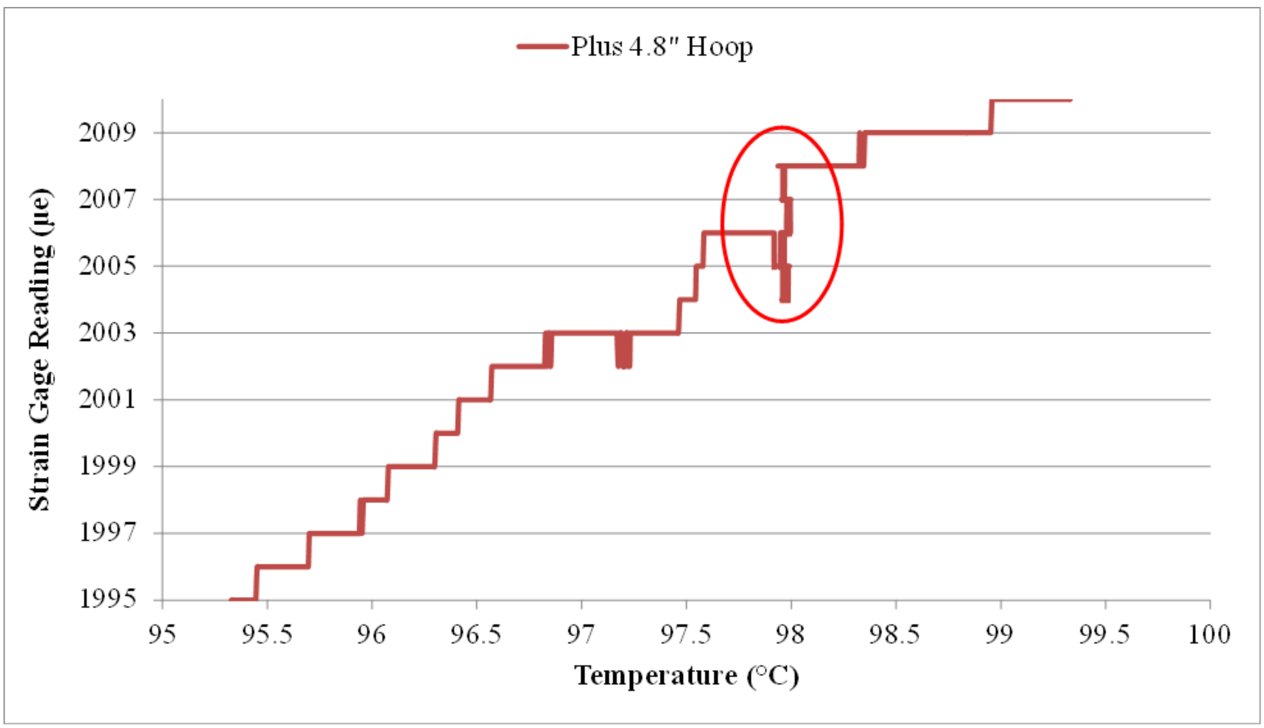

Figure 10. Hoop strain vs temperature at +4.8" from the test section center in Test 2.

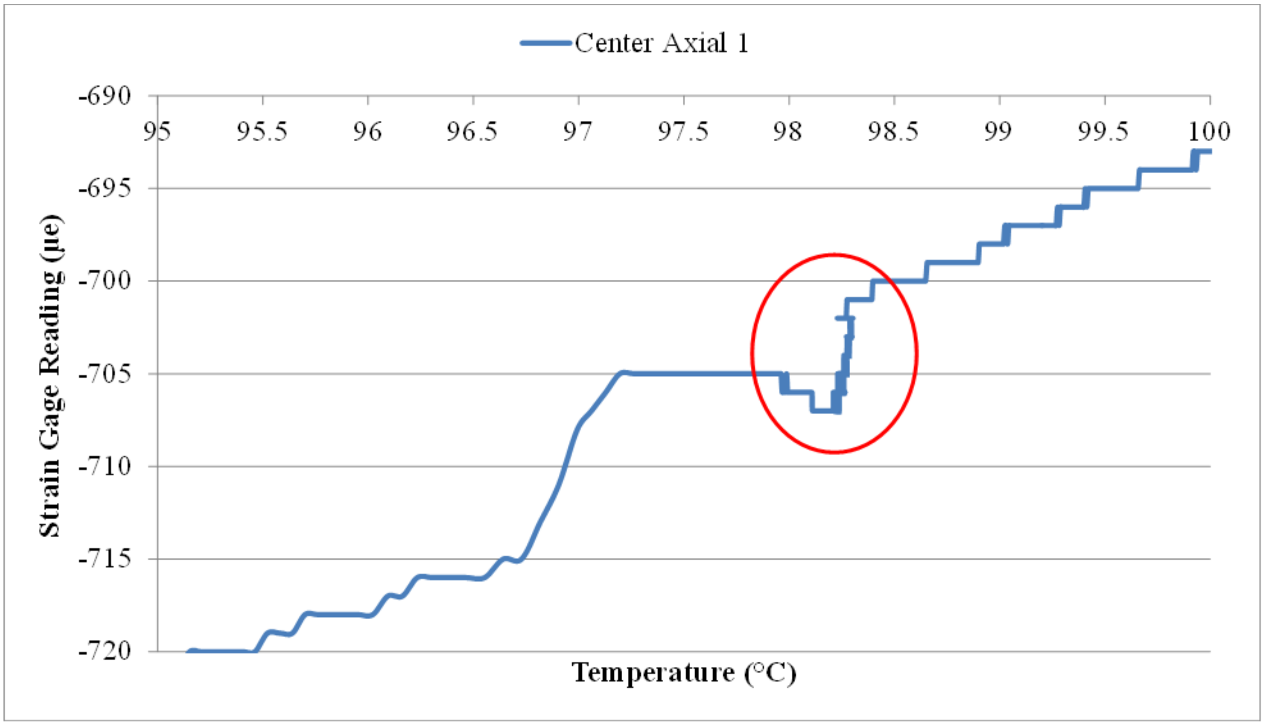

Figure 11. Axial Strain 1 vs temperature at the test section center in Test 2.

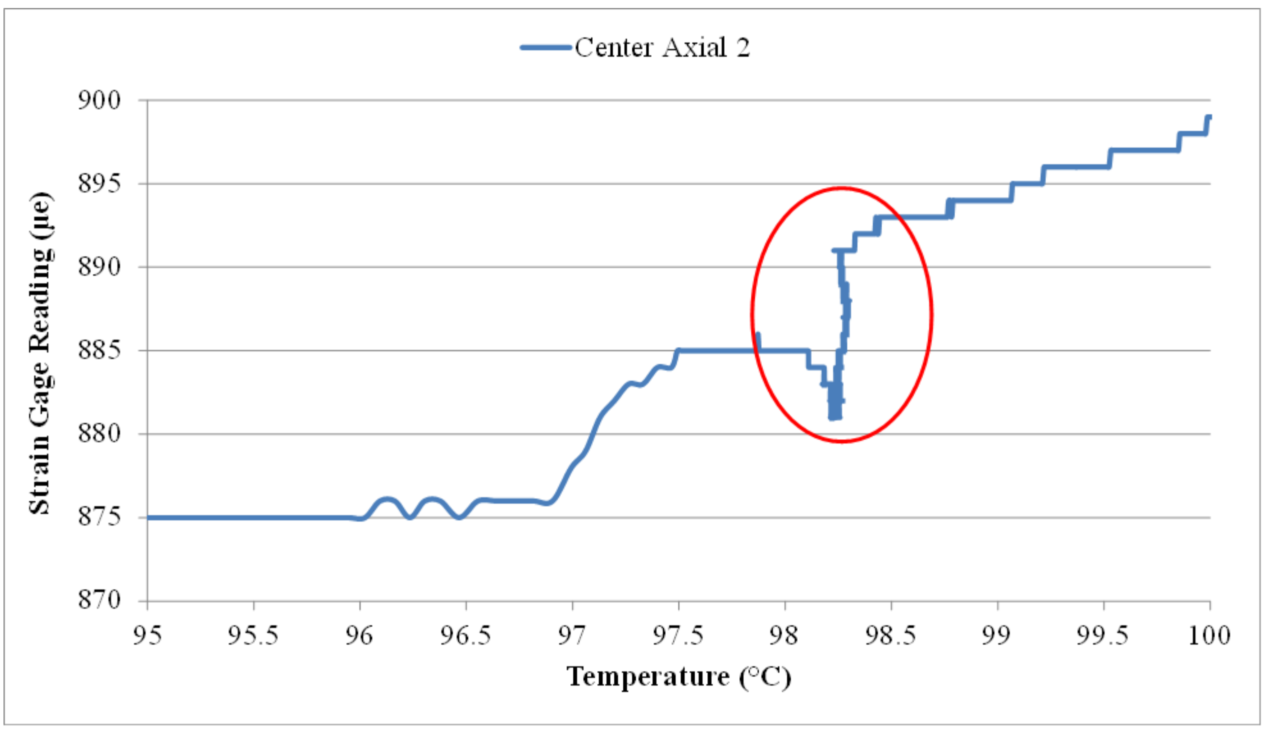

Figure 12. Axial Strain 2 vs temperature at the test section center in Test 2.

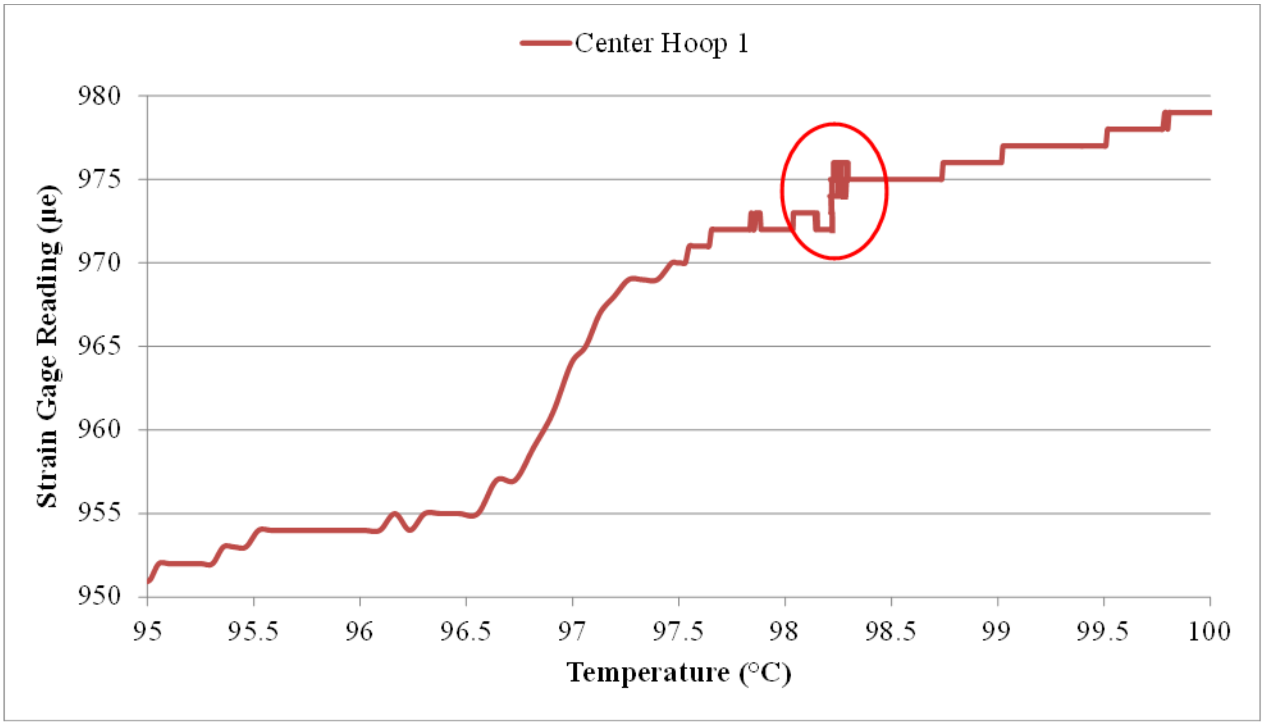

Figure 13. Hoop Strain 1 vs temperature at the test section center in Test 2.

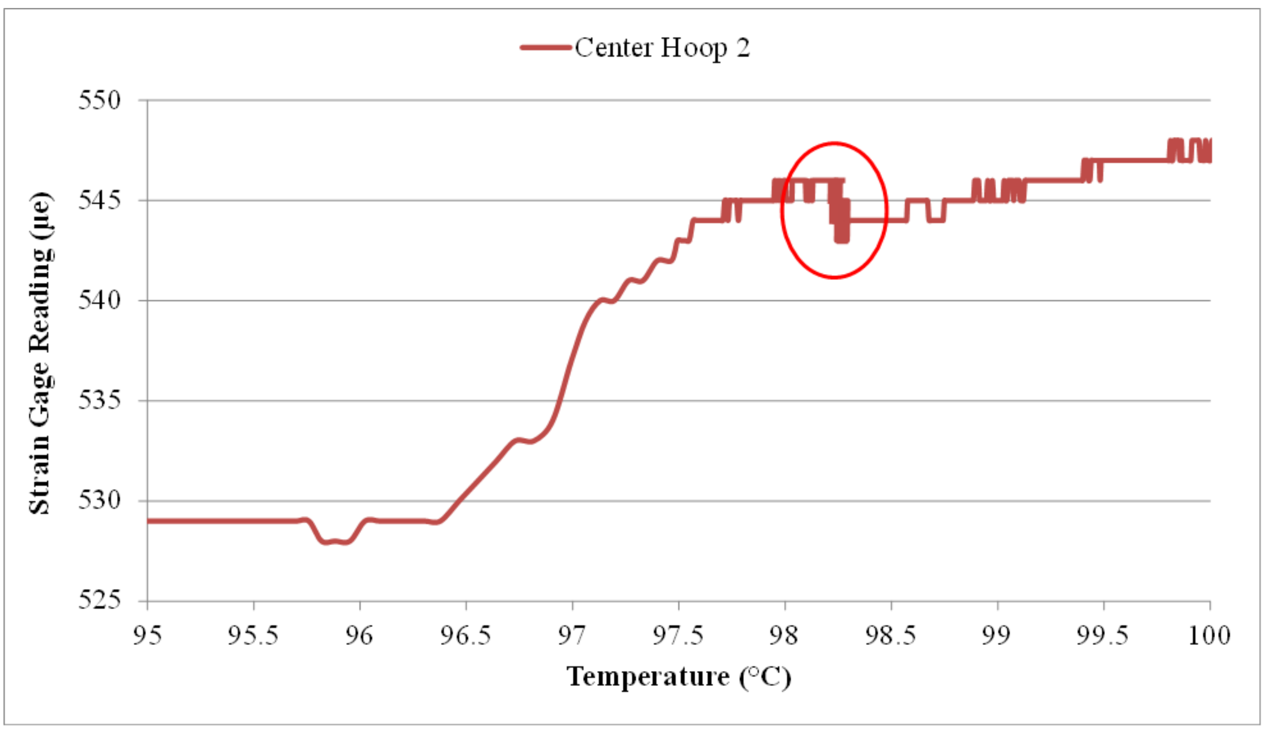

Figure 14. Hoop Strain 2 vs temperature at the test section center in Test 2.

3.3 Test 3: 500°C Wetting Test in FY 2018

As mentioned earlier, the sodium leak early warning system was triggered and issues with heater control were encountered in the 400°C test in FY 2017. Continuing in FY 2018, efforts were first made to fix these problems. Heaters in Zone 12 that triggered the sodium leak early warning system were removed and a visual inspection was performed on the VCR fittings in Zone 12. No sodium leak was visually observed in those VCR fittings. To further confirm the integrity of the system, a helium leak check was subsequently performed with no leak identified. To resolve the heater control issues, all the band heaters were first removed and the controlling thermocouples were traced to make sure they were in the right locations to control the individual heating zones. In addition, high temperature and high thermally conductive paste was applied to all the thermocouples to enhance their thermal coupling with the loop structure.

One thing that has been noticed in the previous modification work on the loop is a design defect of the cold finger. In the original design of the cold finger, a bellows that allows the cold finger probe to be lowered or elevated is employed. To support and guide the cold finger probe when it is moved, two of the six bolting holes in each piece of the conflat flanges in the cold finger are used to house the support/guide rods. This design feature will compromise the sealing capability of the conflat flanges when the cold finger probe is lowered or elevated. It was therefore decided to take out the cold finger and improve its design by employing additional support/guide pieces instead of using the conflat flange bolting holes. After taking out the cold finger, another issue was however identified. It was found that the cold finger probe was submerged in sodium by only ~ 1” in the previous tests while the probe was already lowered near its lowest possible position. Considering the OD of the cold finger probe being only 0.5”, the cold finger had definitely not been efficient in removing the impurities. Based on this finding, further improvement to the cold finger design to increase its impurity removal efficiency was deemed necessary before it could be installed back to the loop. For the first 500°C wetting test, it was decided to not use the cold finger (which ended up not being used for the rest of the tests performed in FY 2018 due to cost and time).

Before assembling back the heaters for the test section and starting the 500°C wetting test, it was also decided to measure the electrical resistances across the test section diameter at different axial locations as shown in Figure 15. The measurement was made by applying a DC current of 15 amps across the test section diameter and measuring the corresponding voltage with a handheld multimeter. It should be noted that these results are not meant to be accurate measurements but rather providing an order of magnitude feeling for the wetting extent. The measured results are summarized in Columns 2 and 3 in Table 1, as well as shown in Figure 16. As can be seen from the results, the electrical resistance generally decreases along the flow direction, indicating better wetting in the downstream. This is understandable since the temperature is always higher in the downstream than in the upstream. The same measurement was be made after the 500°C wetting test to see if there is any improvement in wetting with the high temperature heating.

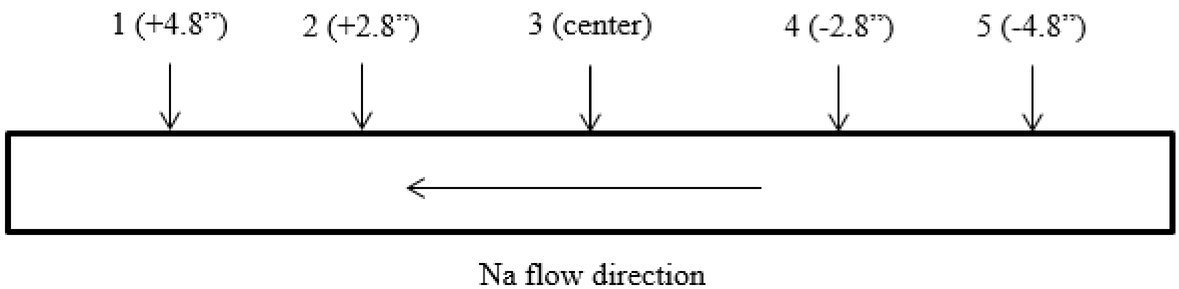

Figure 15. Electrical resistance measurement locations.

Table 1. Electrical resistance measurement results

Location	Post Test 2		Post Test 3		Post Test 5	
	Voltage, mV	Resistance, μΩ	Voltage, mV	Resistance, μΩ	Voltage, mV	Resistance, μΩ
1	0.080	5.33	0.066	4.40	0.098	6.53
2	0.160	10.67	0.096	6.40	0.073	4.87
3	0.134	8.93	0.080	5.33	0.058	3.87
4	0.190	12.67	0.117	7.80	0.054	3.60
5	1.360	90.67	0.183	12.20	0.140	9.33

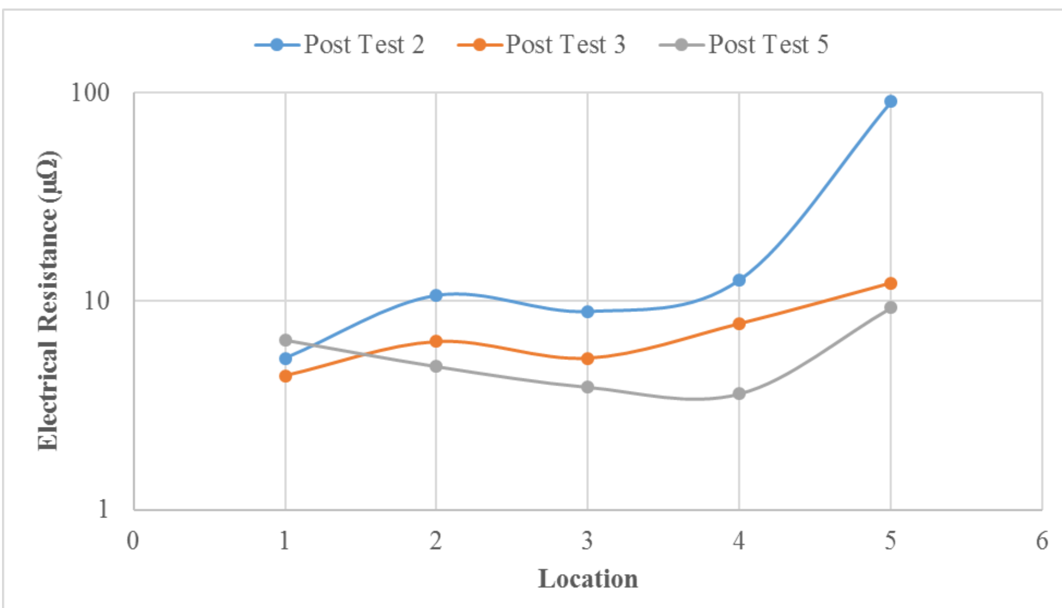

Figure 16. Electrical resistance measurement results.

The same steps up to the point of initiating sodium flow as performed in Test 2 were first carried out in Test 3. After confirming the sodium flow, the system temperatures were raised slowly until the test section set temperatures reached 500°C, as shown in Figure 17. Since the cold finger was not used for the wetting test, the temperatures in the rest of the loop were deliberately set at lower values, as shown in Figure 18, so that impurities would not deposit in the test section.

One question that once arose during the wetting test was how long the test section should be maintained at 500°C in order to reach wetting. Although the test section is rated at 530°C, it has a very thin wall of only 0.02”. It is important to determine the proper heating time that is long enough to wet the test section while not unnecessarily long to stress the system and reduce the system reliability. Based on the information on wetting rate vs temperature by [9], as shown in Figure 19, the time needed to reach wetting at 450°C, was estimated to be 18 hours. With the test section being heated at a higher temperature of ~ 500°C, 24 hours were deemed a good heating time. The actual wetting temperatures and time of the test section for this test are shown in Figure 20. During this 24-hour wetting period, the operators took shifts to monitor the loop operation to ensure safety.

In the current design of the test facility, wetting is monitored through monitoring the electrical resistance (i.e., voltage with a constant current applied) over the test section. With a constant current of 4 amps applied across the two ends of the test section, its measured electrical resistance/voltage during the heating period is shown in Figure 21. As can be seen, from 10 to 50 hours, the test section temperatures were first stable at ~ 400°C, then raised slowly to and eventually maintained at 500°C. Instead of increasing monotonically, at times over the same period, the measured test section electrical resistance/voltage decreased, a probable indication of wetting progression.

Figure 17. Heater set temperatures in the test section in Test 3.

Figure 18. Heater set temperatures in the rest of the loop in Test 3.

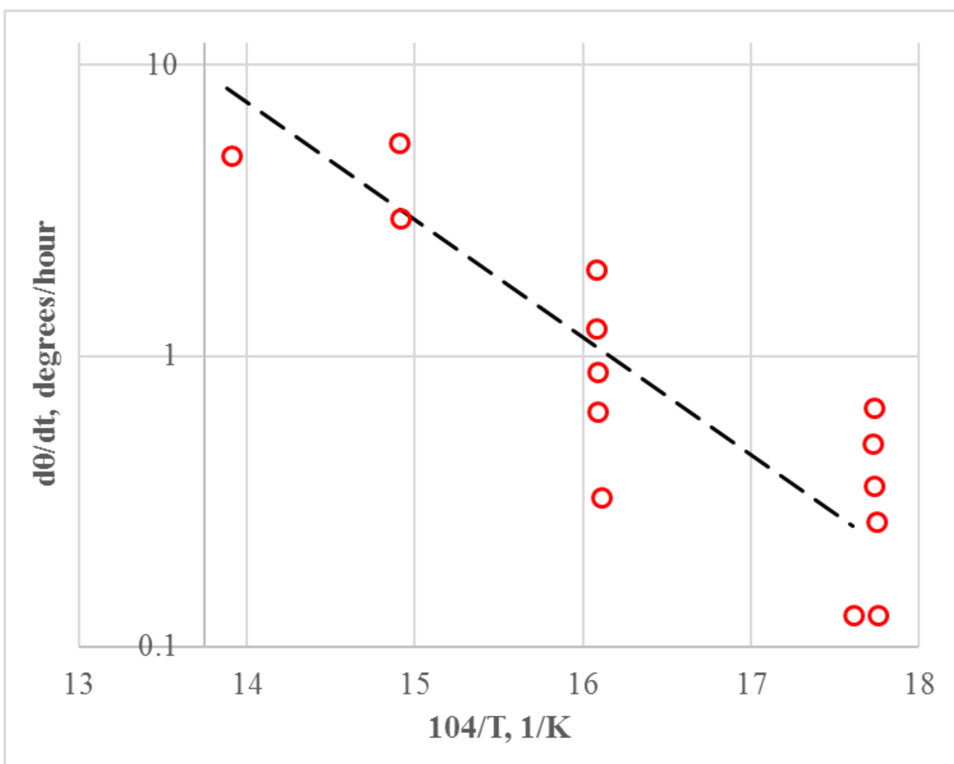

Figure 19. Contact angle decrease rate vs temperature by [9].

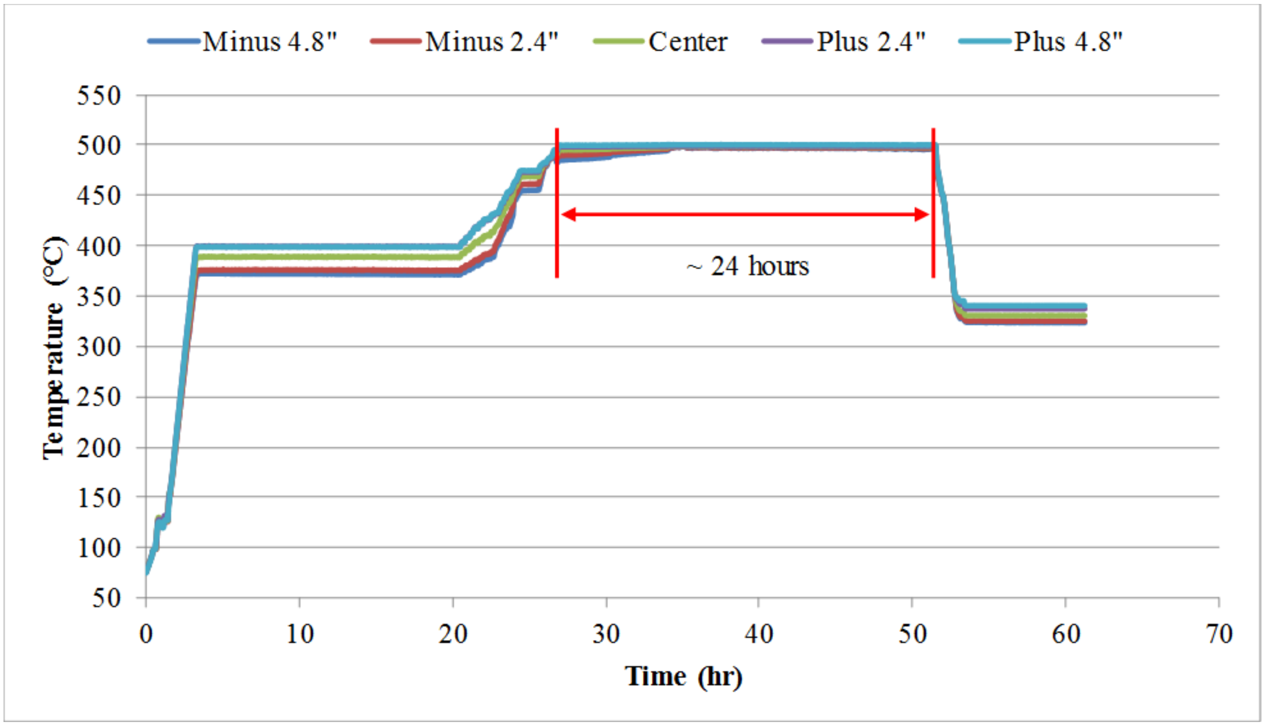

Figure 20. Heating history of the test section in in Test 3.

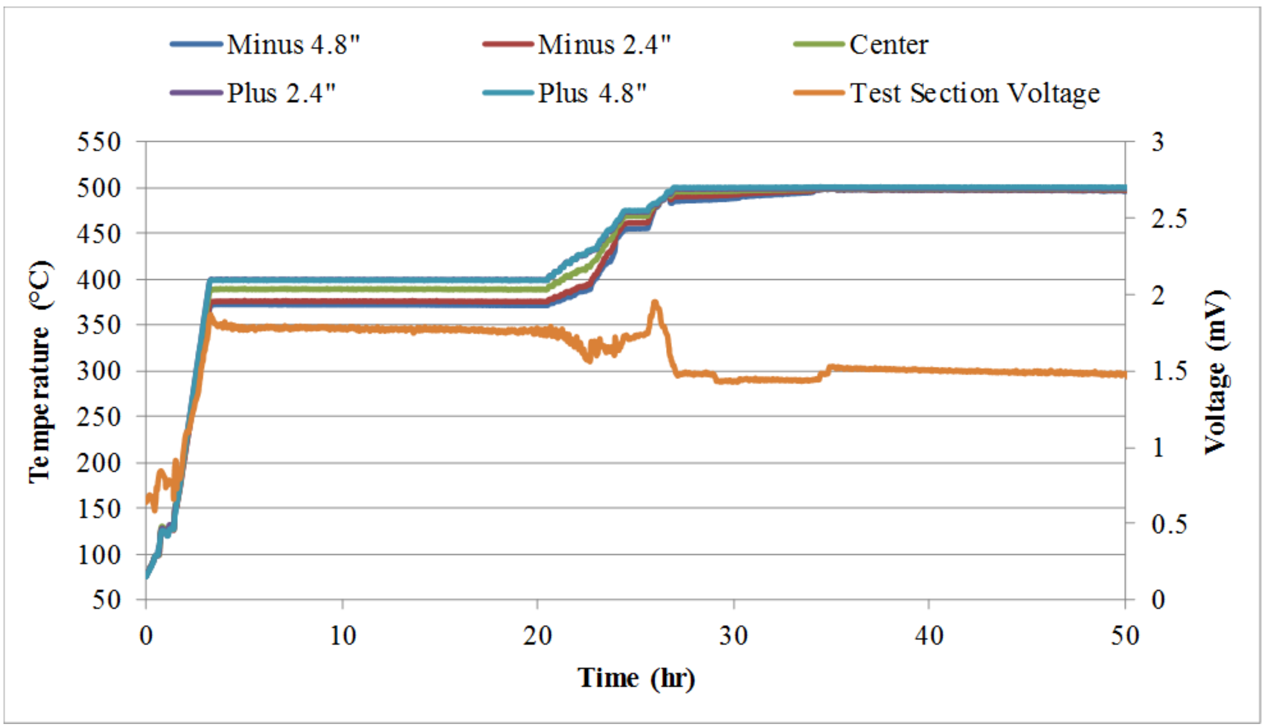

Figure 21. Test section electrical voltage/resistance monitoring in Test 3.

After heating the test section at 500°C for 24 hours, the system temperatures were lowered gradually. During the cooling down process, sodium was still circulated and a temperature difference between the test section and the rest of the loop was maintained to avoid impurity deposition in the test section. As the test section temperatures were lowered to and stable at ~

130°C, the sodium reservoir temperatures were near ~ 100°C. The EM pump was then turned off and Ar gas at approximately 10 psig was introduced to compress any voids that might exist inside sodium. The same as in Test 2, freezing in Test 3 was started from the free surfaces and controlled to propagate toward the center of the test section. Freezing front propagation in the test section is shown in Figure 22.

The measured test section strains during sodium freezing are shown in Figure 23 to Figure 30. Compared to the measured results in Test 2, overall the new results are similar. The maximum measured strain change during sodium freezing occurs at center axial Strain Gage 2, with a value of ~ 10 micro strains. Previously in Test 2, lack of wetting was deemed as the reason why only small strain changes were measured during sodium freezing. Because of this, efforts were made in the new Test 3, trying to reach wetting by heating the test section at 500°C. As mentioned earlier, the real time electrical resistance/voltage monitoring of the test section indicated wetting progression in Test 3. In addition, electrical resistance across the test section diameter at different axial locations was also checked post Test 3, as summarized in Table 1. As can be seen, compared with the post Test 2 results, there is a significant drop in the electrical resistance along the test section. This also confirms improvement in wetting in Test 3. However, no improvement was observed in the measured strain changes during sodium freezing in Test 3. This indicates that there are probably other factors than wetting dominant in the process of sodium freezing. The Sodium Freezing and Remelting experiment originated back to the finding in the previous liquid lithium experiment [4], in which significant stress to cause deformation of EM pump duct was observed. The same phenomenon has not been observed in the sodium freezing experiment, which leads to the question of what difference between lithium and sodium has caused the different freezing phenomenon. After some literature review, it was suspected that the cause might be due to the difference in Ar solubility in the two liquid metals. According to [10], at 0.1 MPa and below 800 K, the solubility of Ar in liquid sodium is at least 1.33E8 times that in liquid lithium. The much larger solubility of Ar in liquid sodium could have caused cavitation during sodium freezing, which compromised the measured strain drop (negative pressure). To investigate into this possibility, it was decided to perform a new freezing test under high vacuum.

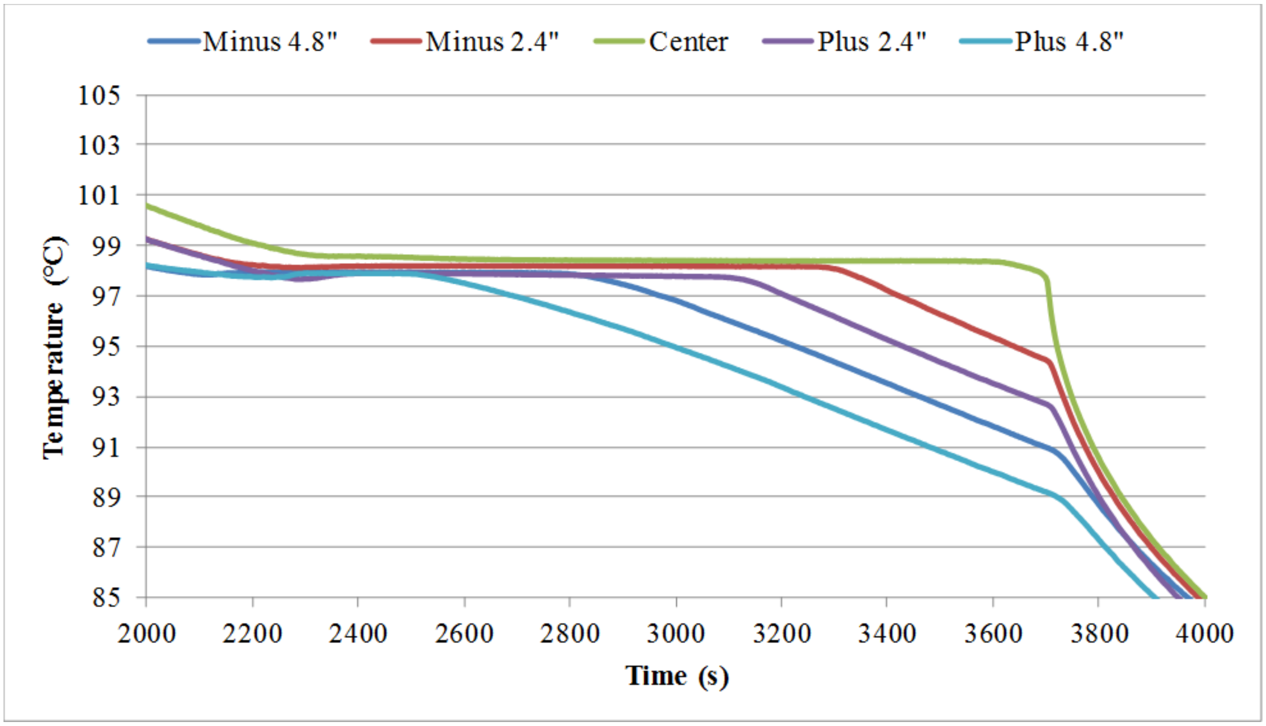

Figure 22. Freezing front propagation inside the test section in Test 3.

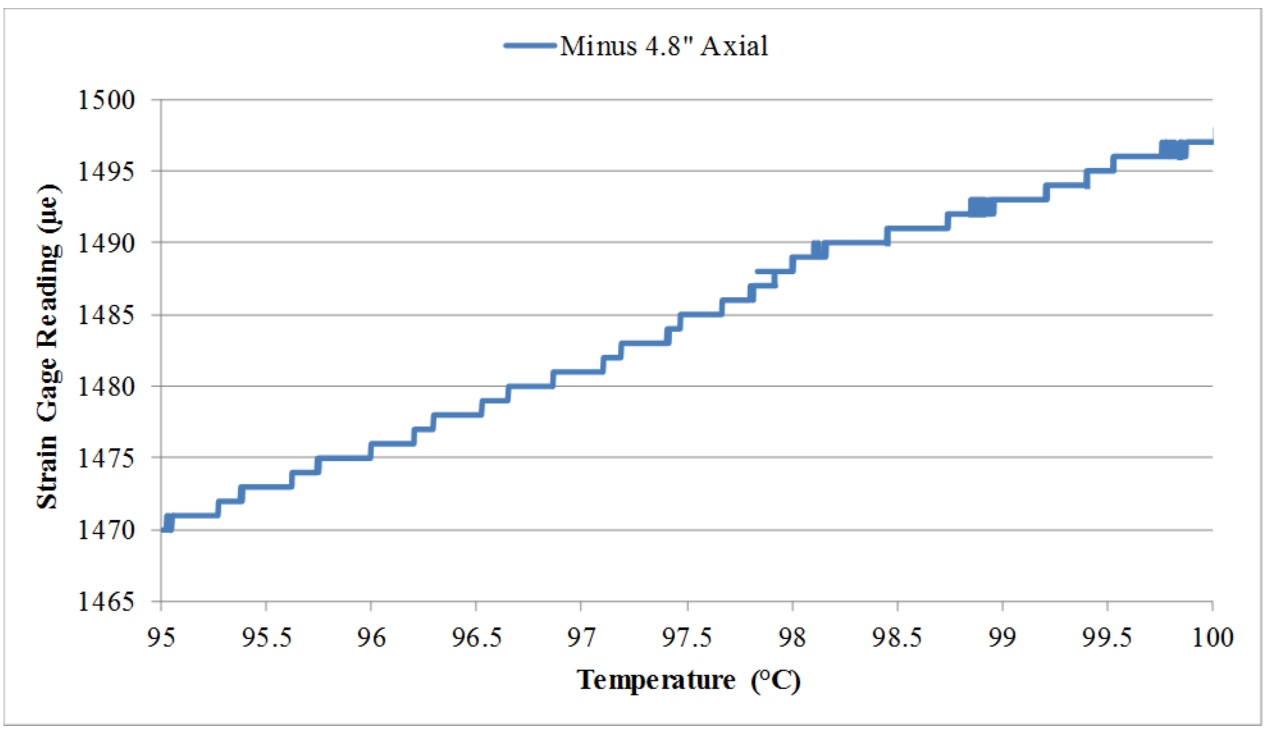

Figure 23. Axial strain vs temperature at –4.8" from the test section center in Test 3.

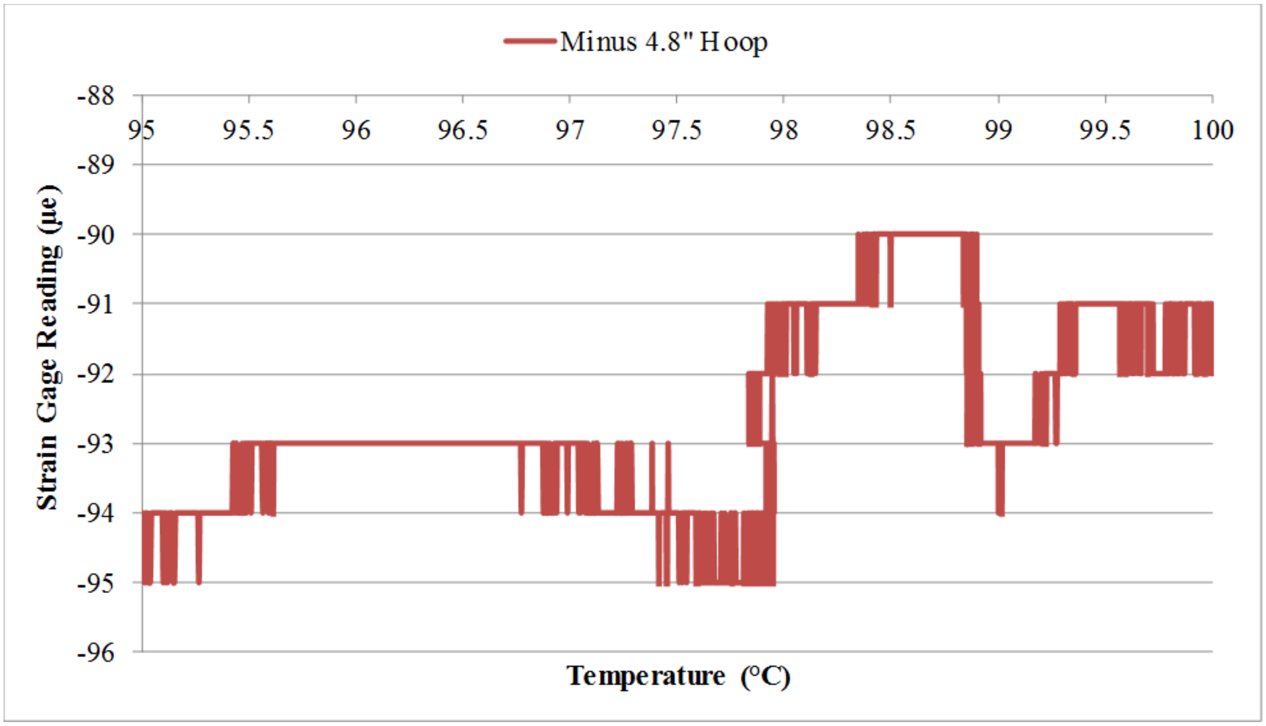

Figure 24. Hoop strain vs temperature at -4.8” from the test section center in Test 3.

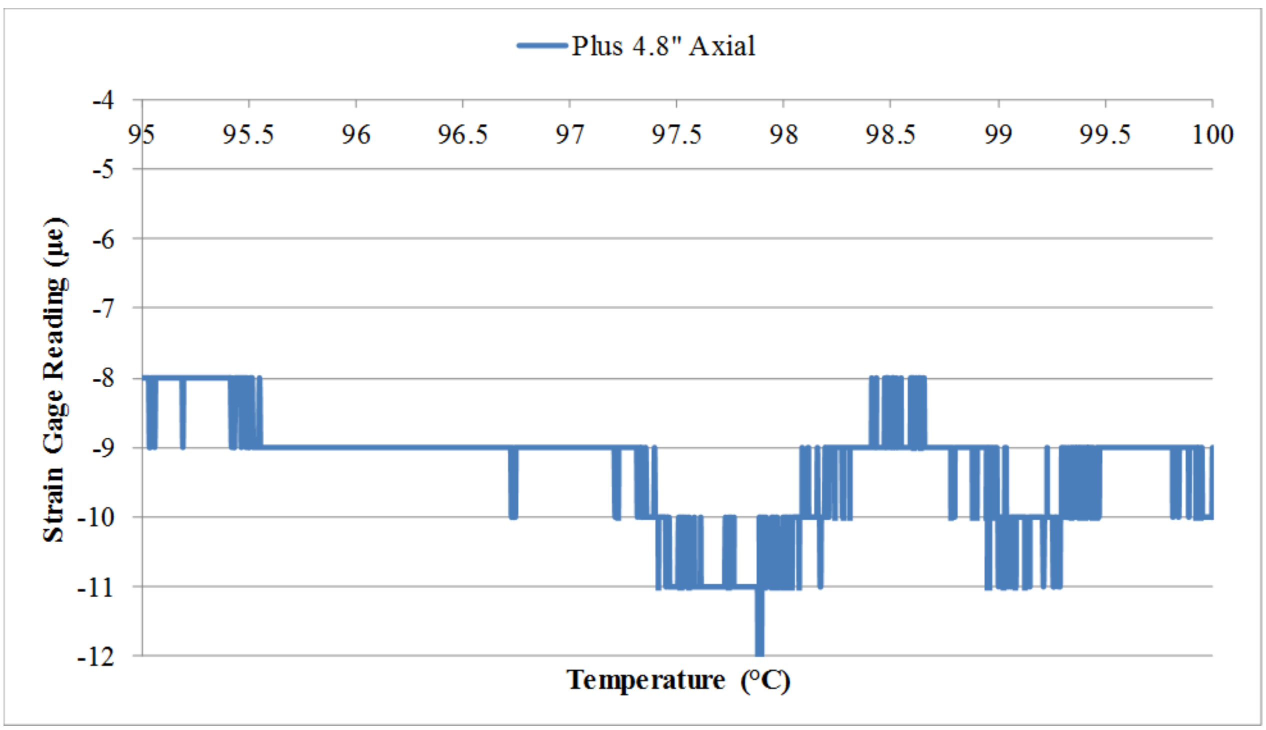

Figure 25. Axial strain vs temperature at +4.8” from the test section center in Test 3.

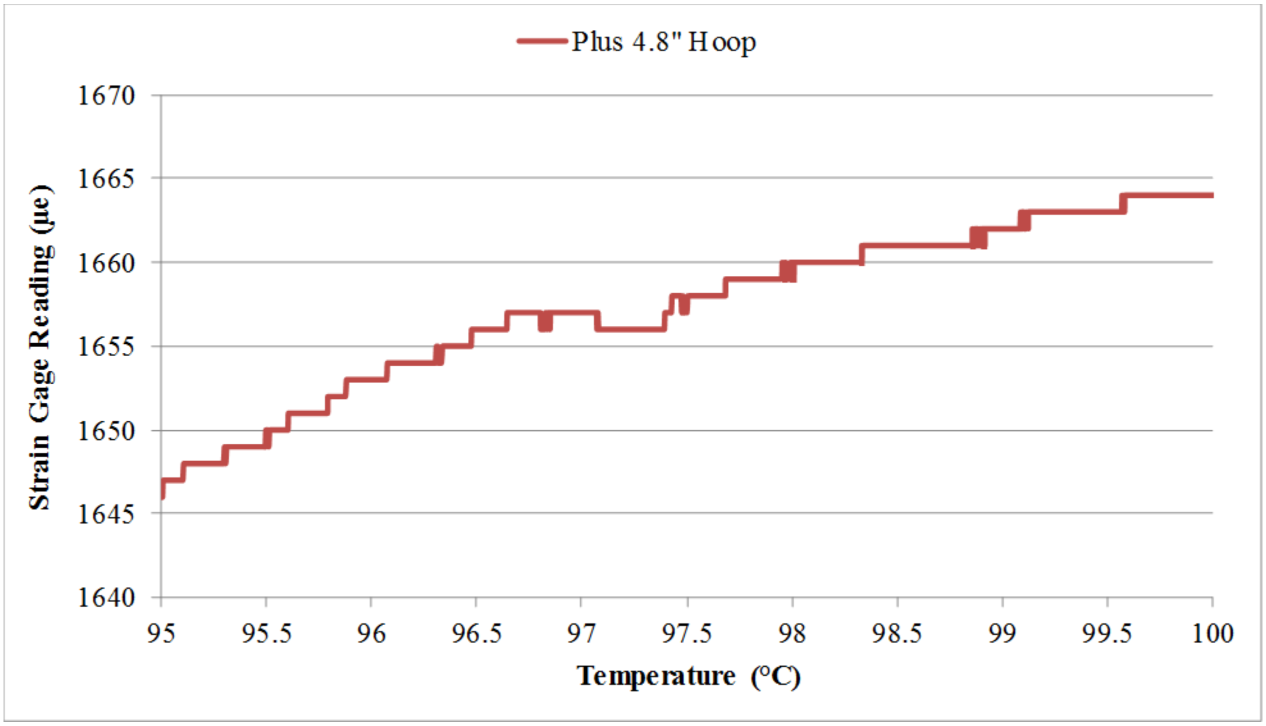

Figure 26. Hoop strain vs temperature at +4.8" from the test section center in Test 3.

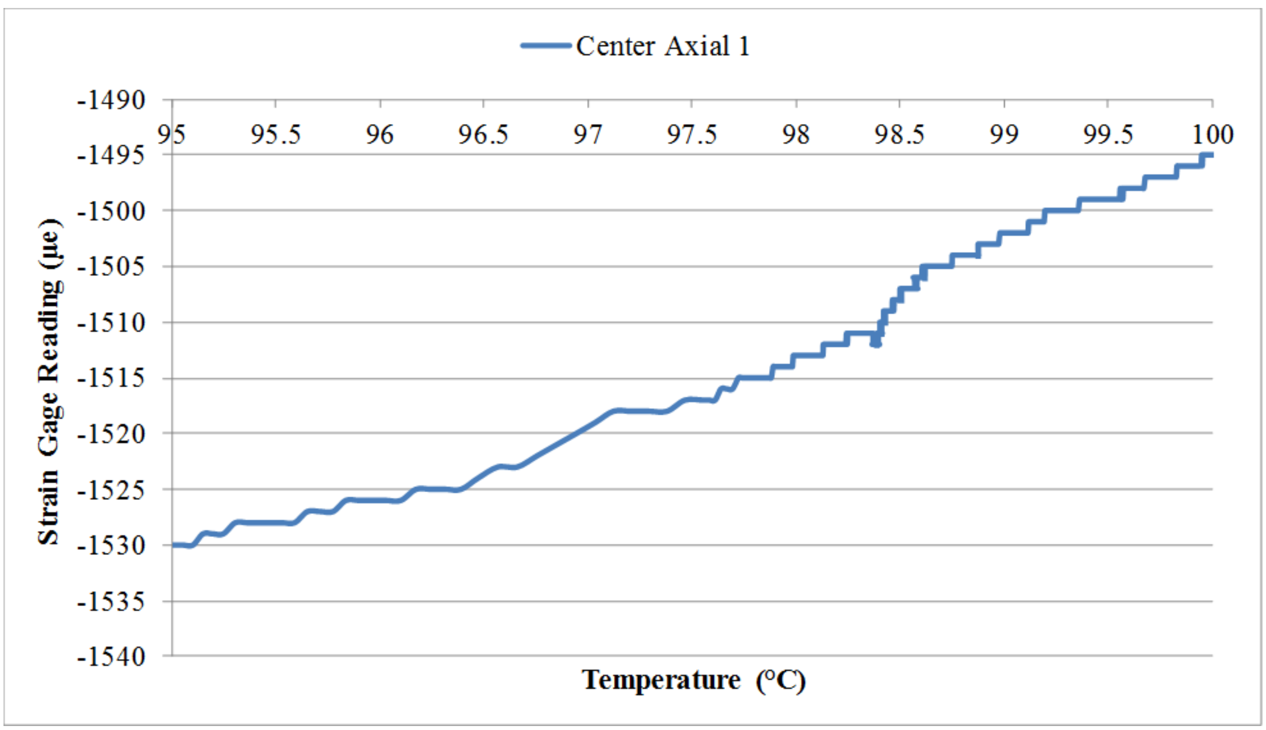

Figure 27. Axial Strain 1 vs temperature at the test section center in Test 3.

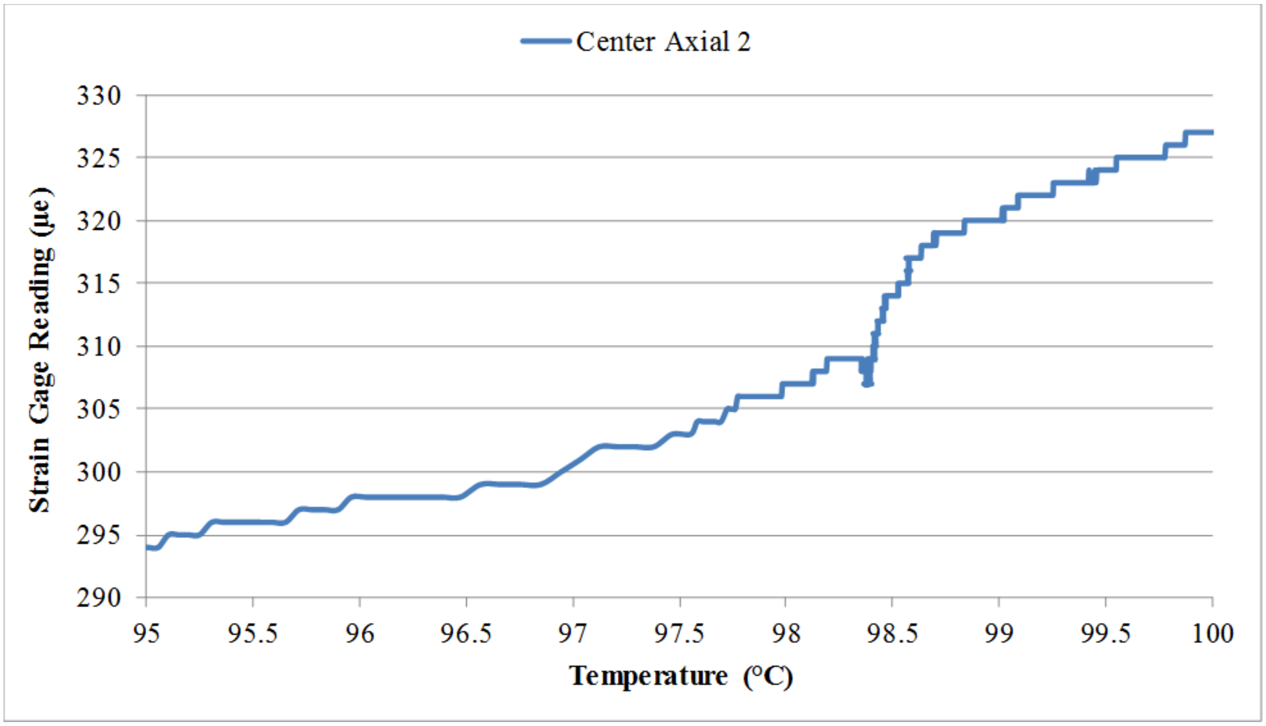

Figure 28. Axial Strain 2 vs temperature at the test section center in Test 3.

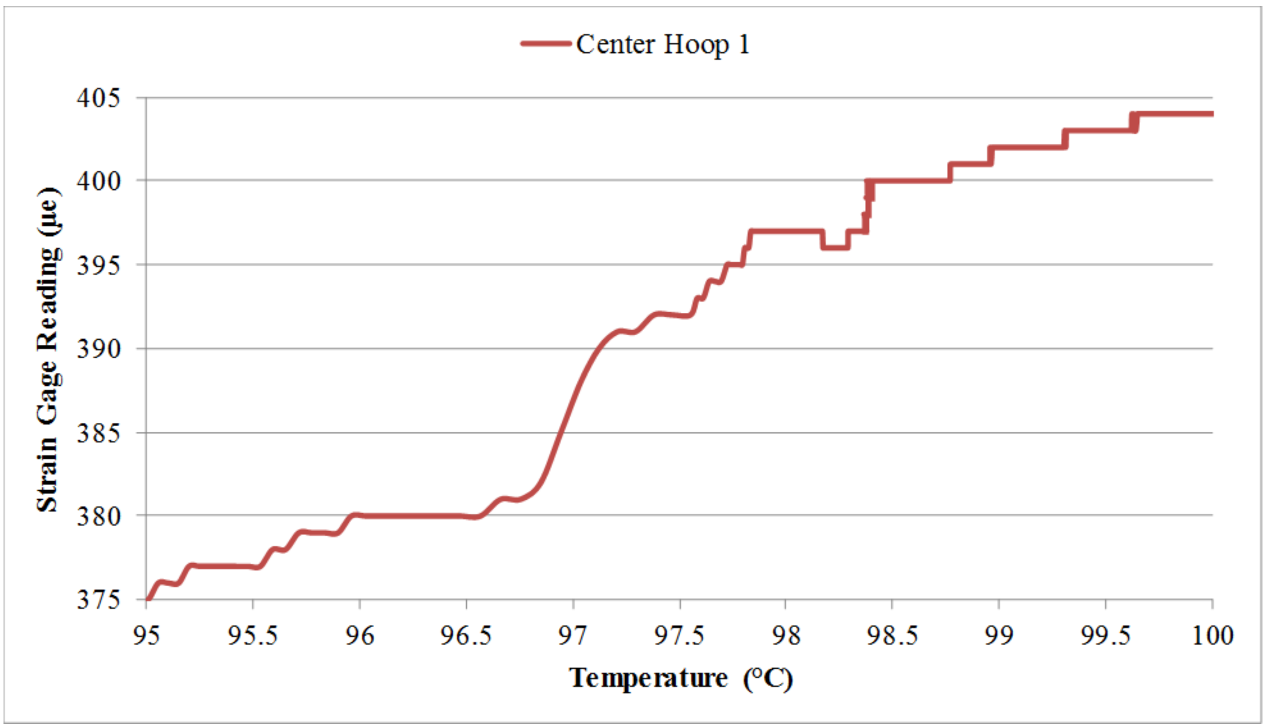

Figure 29. Hoop Strain 1 vs temperature at the test section center in Test 3.

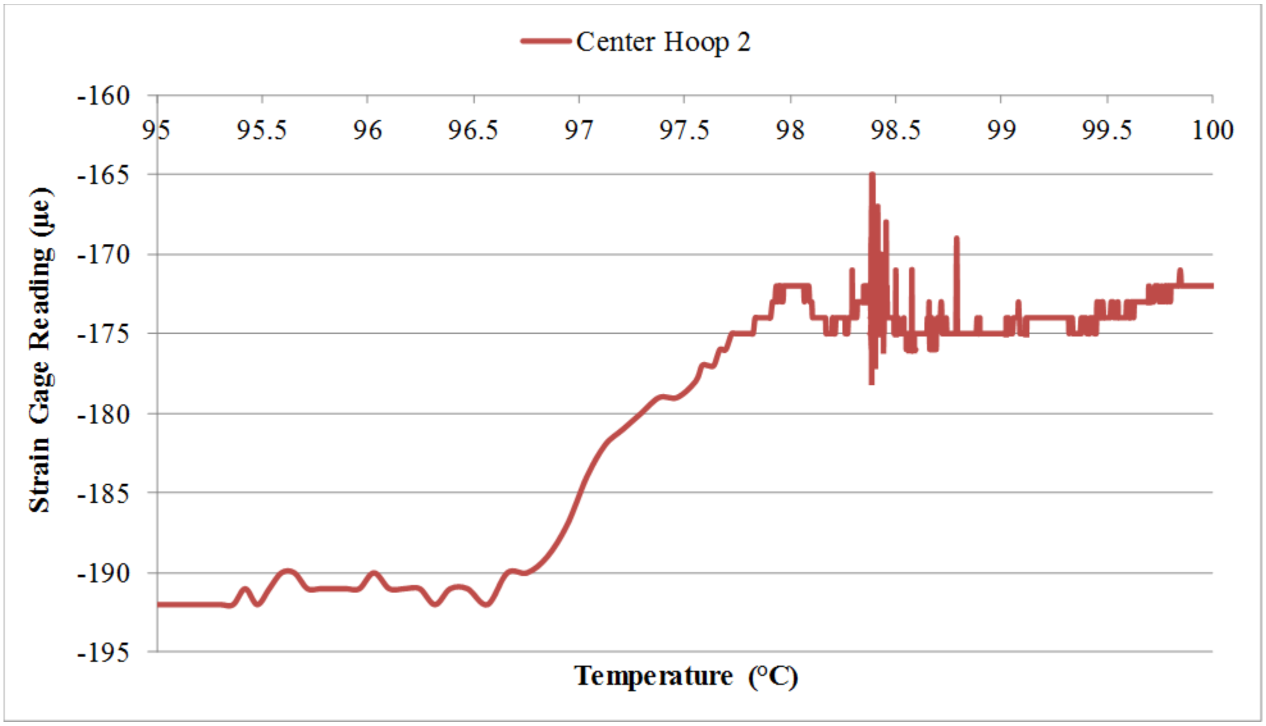

Figure 30. Hoop Strain 2 vs temperature at the test section center in Test 3.

3.4 Test 4: High Vacuum Test

This test was intended to examine the effect of dissolved Ar in the liquid sodium on the freezing phenomena. Before starting the test, modification to the loop was necessary. In place of the cold finger a cross connection was set up, with the bottom port connected to the reservoir, the side ports connected to a vacuum ion gage and a Convectron vacuum gage, and the top port connected to the leak detector through a big port valve. The setup is shown in Figure 31. A quick vacuum was first pulled when the loop was still at room temperature. The loop was then heated up while evacuating the system. During the heatup, slow outgassing was observed through the pressure monitoring system. As heating continued, sodium was melted from the free surfaces. When the sodium in the reservoir started to melt, drastic changes in the pressure reading was observed, which was a clear indication of trapped Ar gas inside of the sodium. Once all the sodium was melted, the EM pump was turned on to circulate the sodium, at which point no drastic change in the pressure reading was observed. The loop was then left to stabilize, with all the temperature controllers set at 105°C, sodium being circulated, and the loop being evacuated.

Figure 31. Setup for the vacuum test.

The degassing process was maintained until the vacuum ion gage reading was stable at ~ 1E-5 torr. The freezing test was then performed with freezing started from the free surfaces. The freezing front propagation inside the test section is similar to the results before, as shown in Figure 32. The measured strain changes during sodium freezing are shown in Figure 33 to Figure 40. Compared to Test 3, again, the new test results are similar and no improvement is observed. The measured maximum strain change is still ~ 10 micro strains at the axial Strain Gage 2. The absence of improvement in the measured strain changes does not necessarily mean that the previous hypothesis of cavitation during sodium freezing is not correct. As mentioned earlier, the solubility of Ar in liquid sodium is about 1.33E8 times that in liquid lithium. As an approximation, the vacuum has to be as deep as 5.64E-6 torr in order for the amount of dissolved Ar in liquid sodium to be comparable to that in liquid lithium at atmospheric pressure. Considering that the lithium experiment was performed under vacuum, the vacuum in the sodium experiment should be even deeper, if the same freezing phenomenon is ever expected to occur. However, limited by the available equipment, a vacuum only down to ~ 1E-5 torr was achieved in this experiment. This means the previous hypothesis of Ar cavitation during sodium freezing cannot be directly proved with the current equipment.

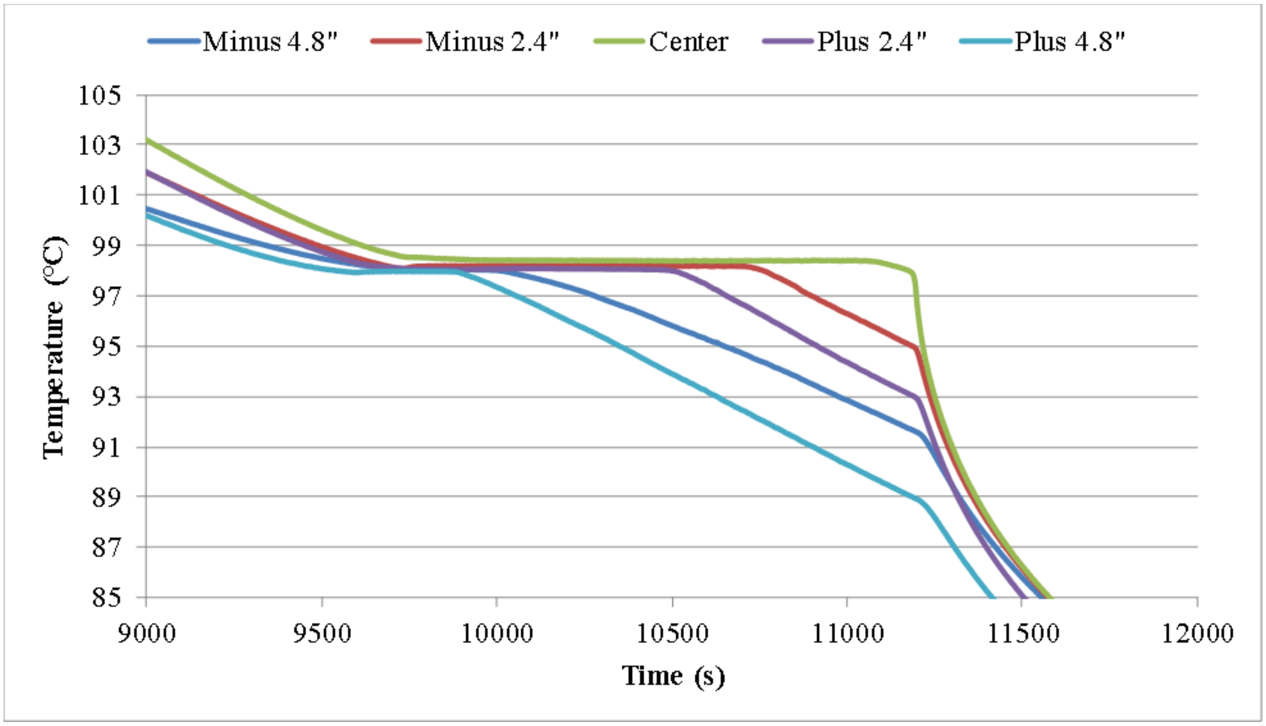

Figure 32. Freezing front propagation in the test section in Test 4.

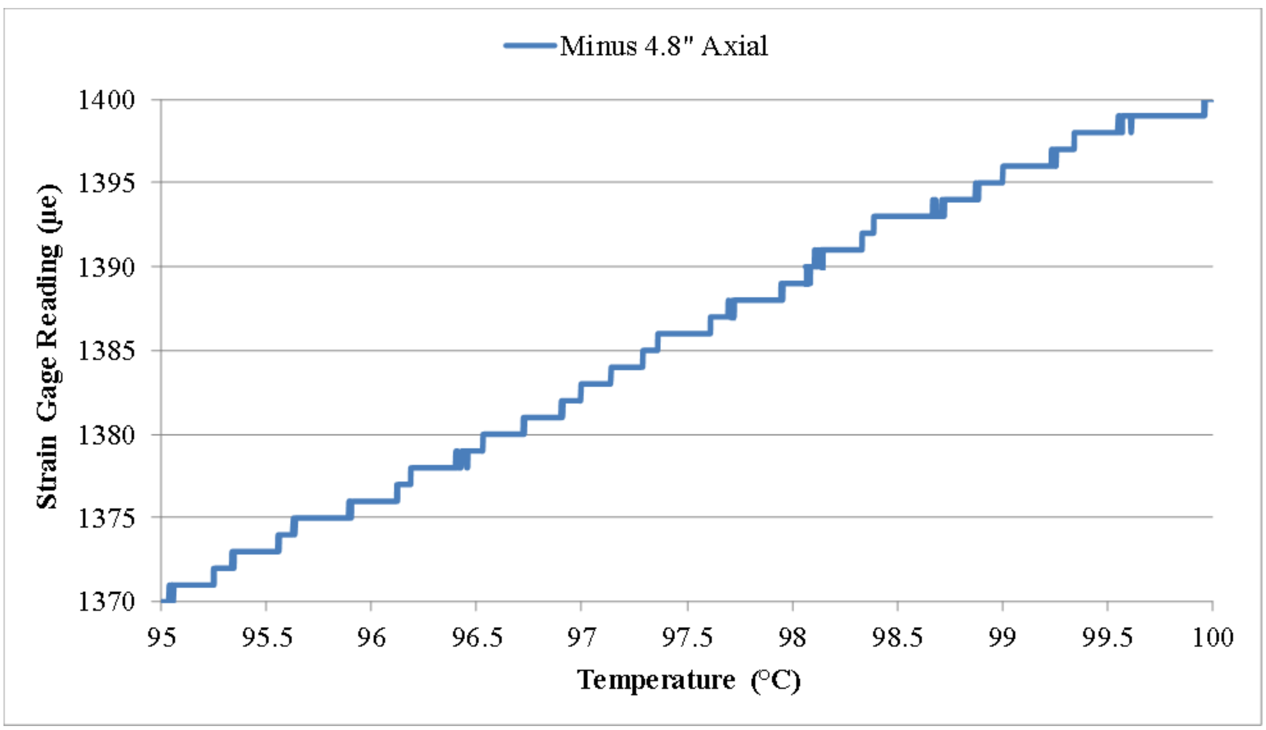

Figure 33. Axial strain vs temperature at –4.8" from the test section center in Test 4.

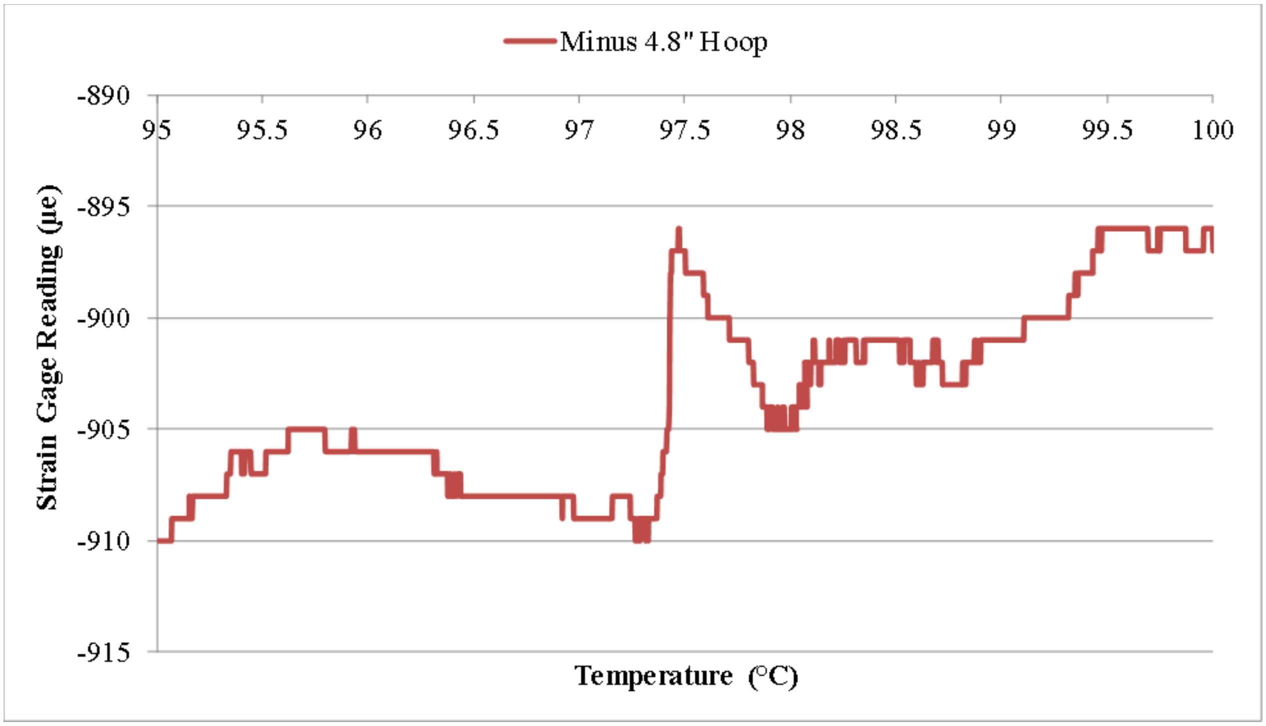

Figure 34. Hoop strain vs temperature at -4.8" from the test section center in Test 4.

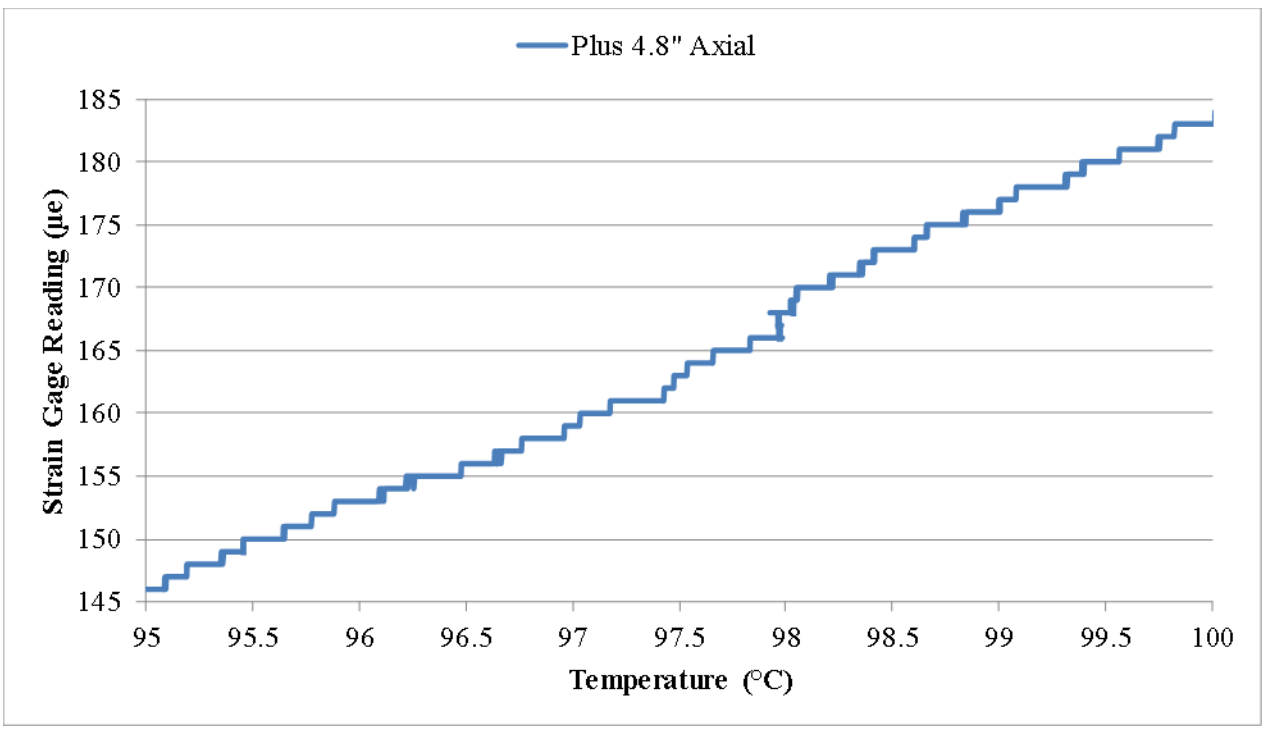

Figure 35. Axial strain vs temperature at +4.8" from the test section center in Test 4.

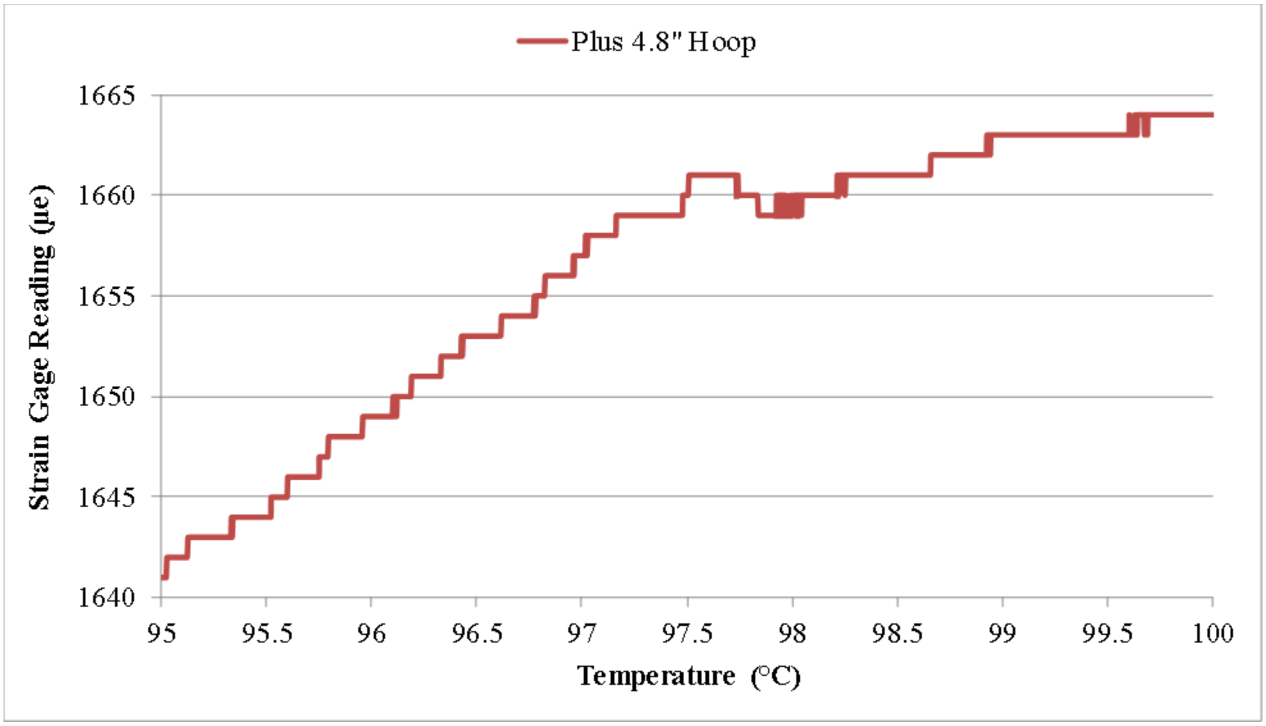

Figure 36. Hoop strain vs temperature at +4.8" from the test section center in Test 4.

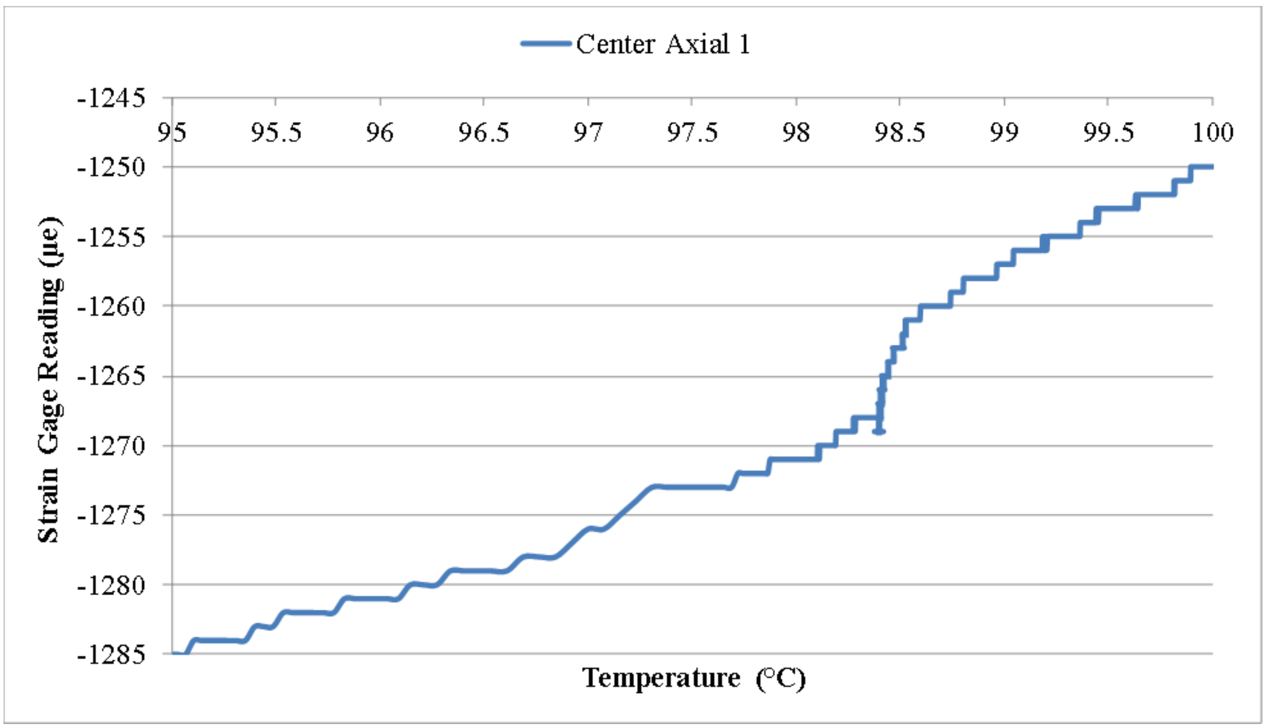

Figure 37. Axial Strain 1 vs temperature at the test section center in Test 4.

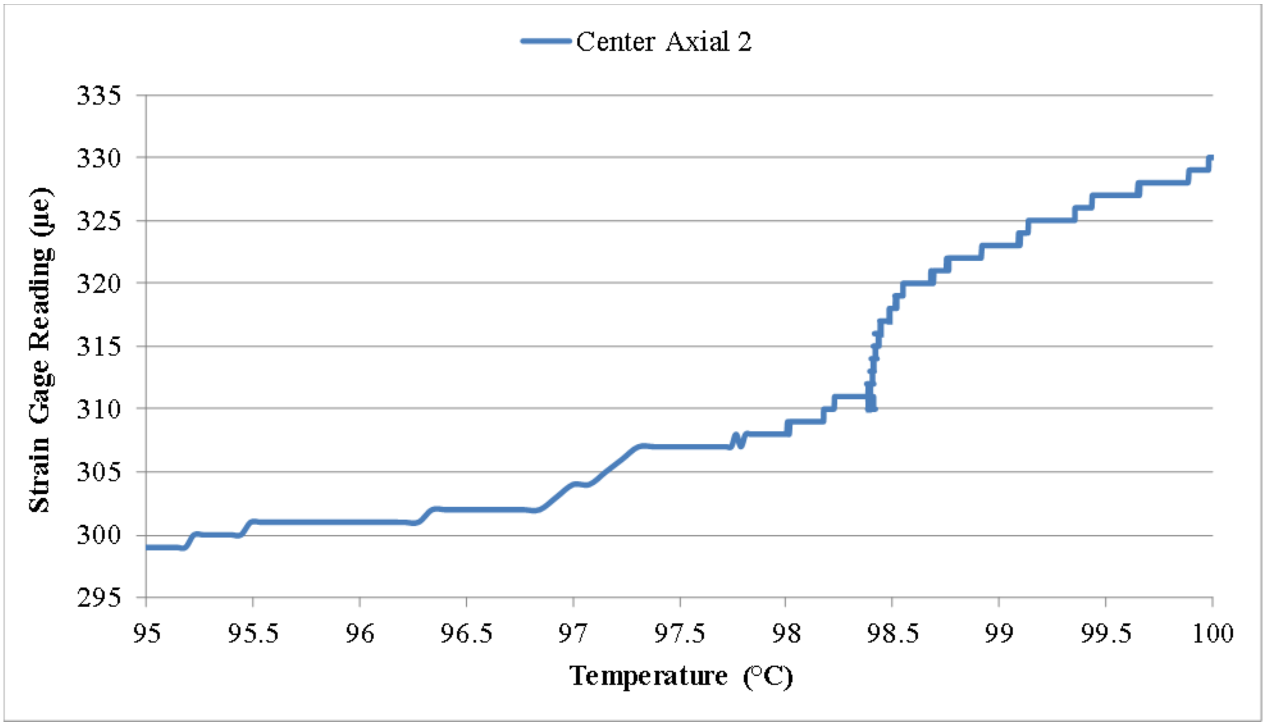

Figure 38. Axial Strain 2 vs temperature at the test section center in Test 4.

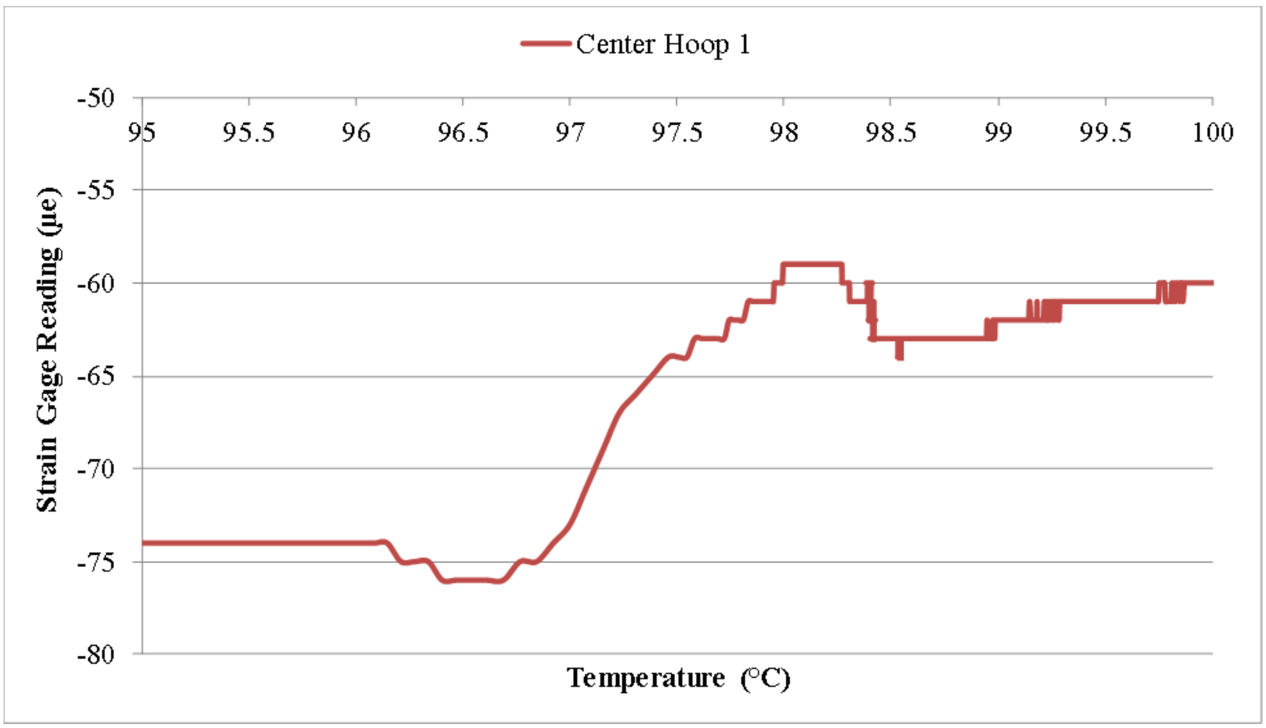

Figure 39. Hoop Strain 1 vs temperature at the test section center in Test 4.

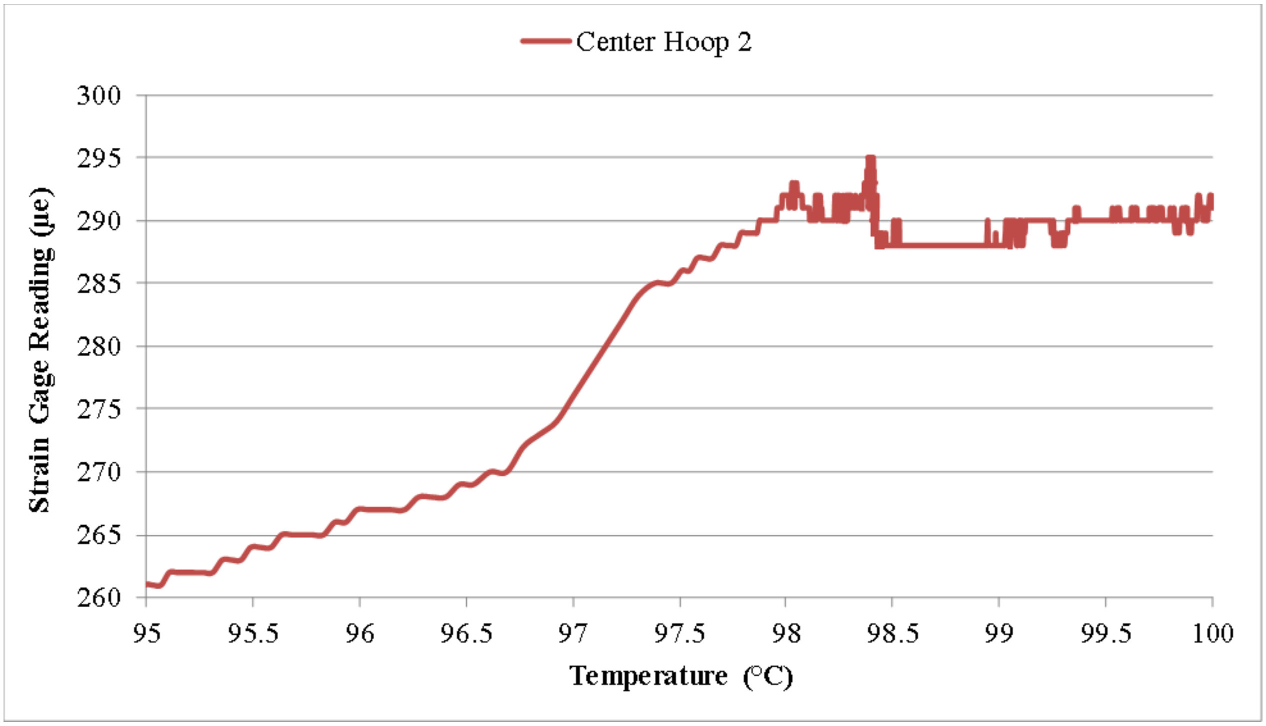

Figure 40. Hoop Strain 2 vs temperature at the test section center in Test 4.

3.5 Test 5: Fast Cooling Test

Due to the limits by the available vacuum equipment, the previous hypothesis of Ar cavitation dominating the sodium freezing process could not be proved. Other indirect ways were sought to prove (or disprove) this hypothesis. If cavitation does occur during sodium freezing, the measured strain drops (or negative pressure) will always be limited by the low yield strength of the solid sodium at its melting temperature. If the frozen sodium could be hardened somehow, there might be an increase in the measured strain drops during sodium freezing. Therefore, it was decided to use a fan to actively cool the test section and increase the strength of the frozen sodium. The same test procedure as in Test 4 was followed in Test 5 with the only difference that active cooling by a fan was applied to the test section when freezing started in it. The freezing front propagation in the test section with active cooling is shown in Figure 41. As can be seen, over the same time scale as in the previous test (Figure 32), the freezing time is shorter and the temperature drop rate is faster in the new test, a clear indication of active cooling. The measured strain changes during sodium freezing are shown in Figure 42 to Figure 49. Again, the new results are similar to those in Test 4, and there seems to be no effect of faster cooling rate on the freeing phenomena. After more thinking, it was realized that even with active cooling the frozen sodium near the freezing front would always be close to the melting temperature, imposing a limit on the strength of the frozen sodium. This may explain why the results are not changed in Test 5.

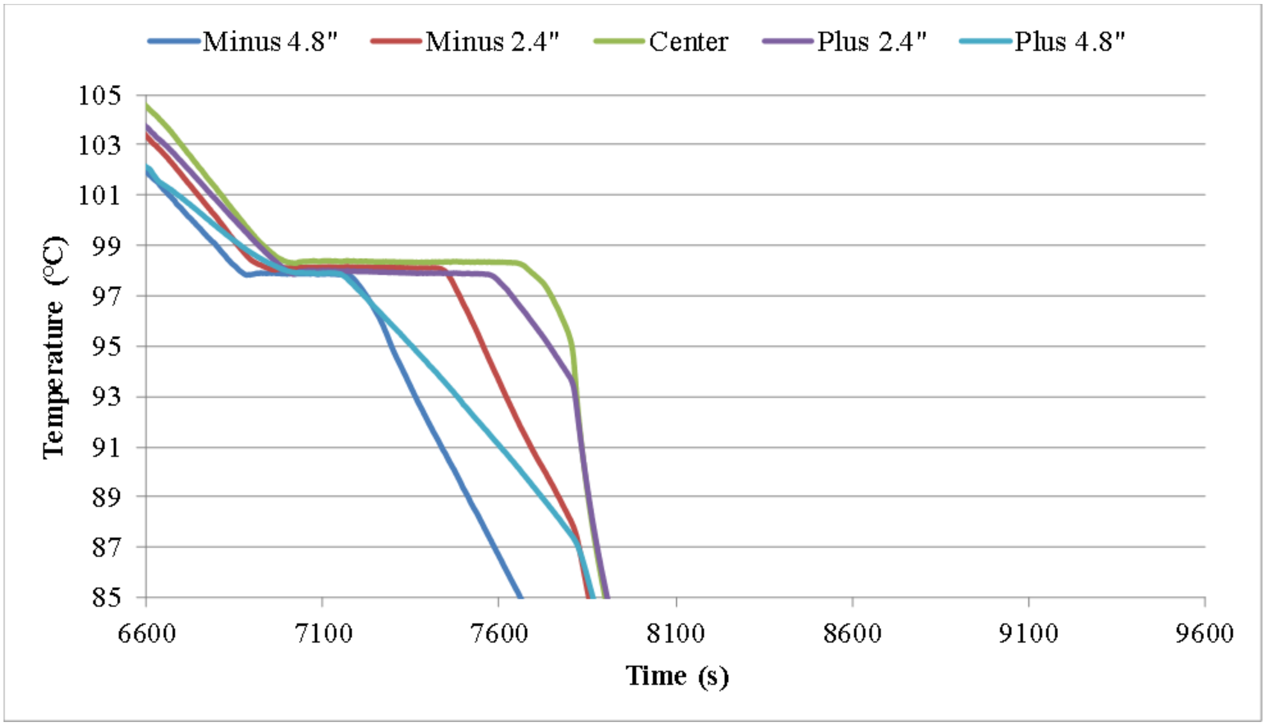

Figure 41. Freezing front propagation in the test section with active cooling in Test 5.

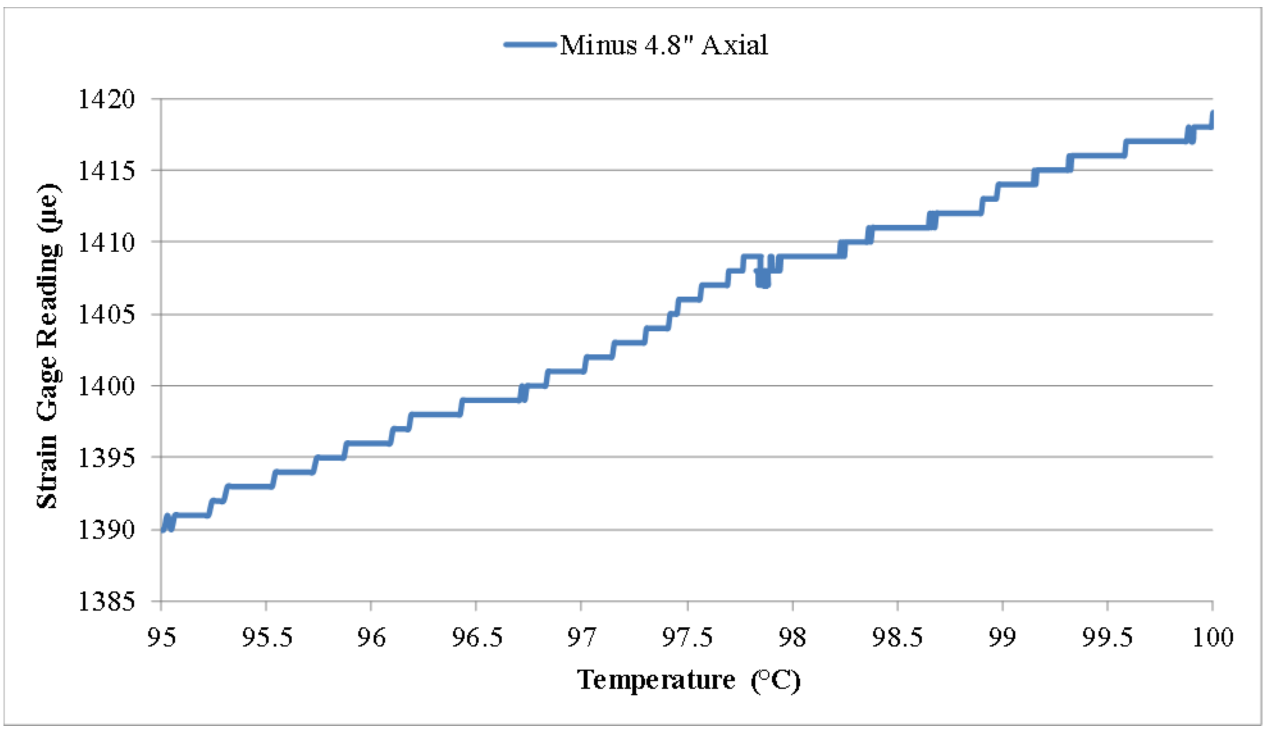

Figure 42. Axial strain vs temperature at –4.8" from the test section center in Test 5.

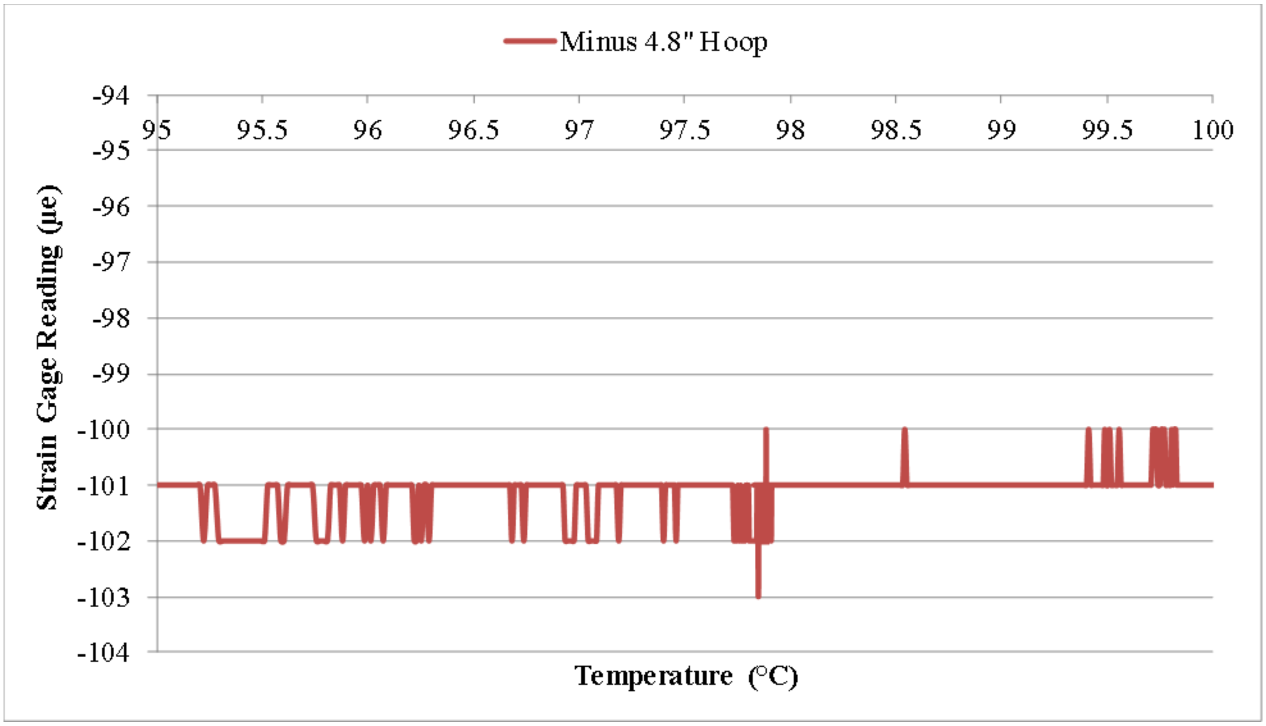

Figure 43. Hoop strain vs temperature at -4.8" from the test section center in Test 5.

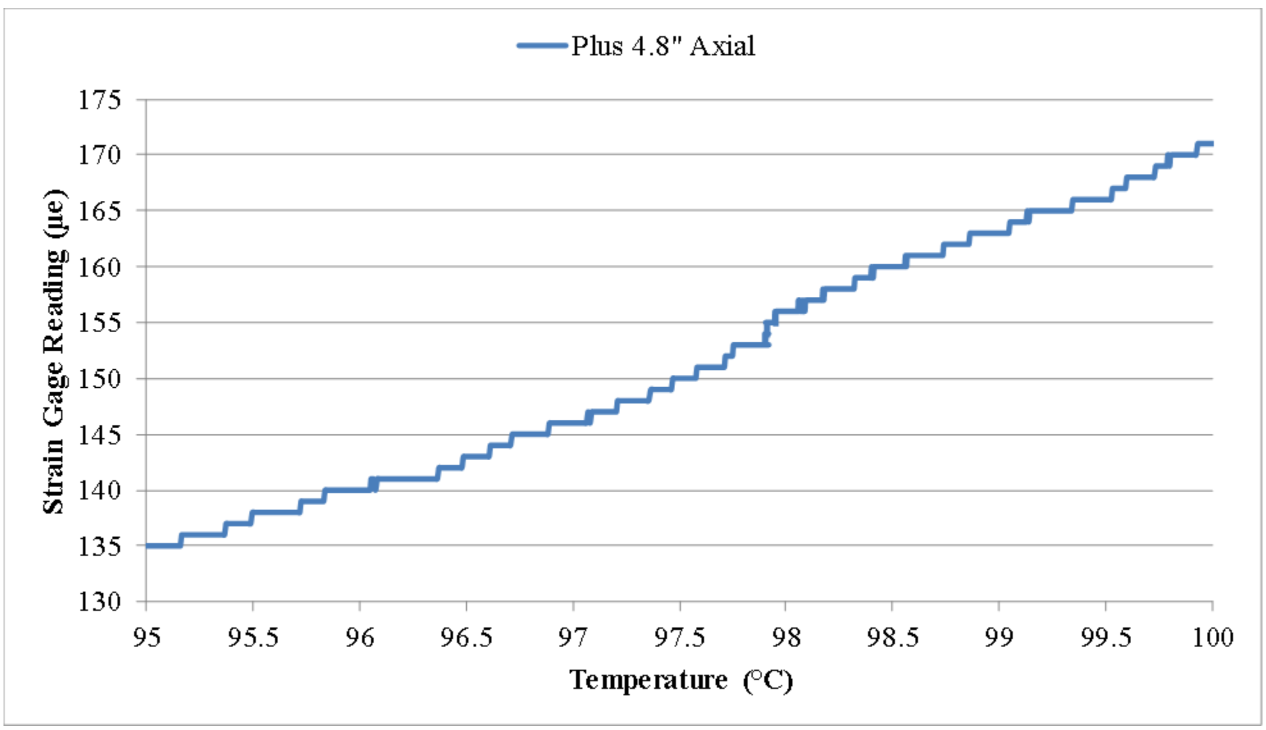

Figure 44. Axial strain vs temperature at +4.8" from the test section center in Test 5.

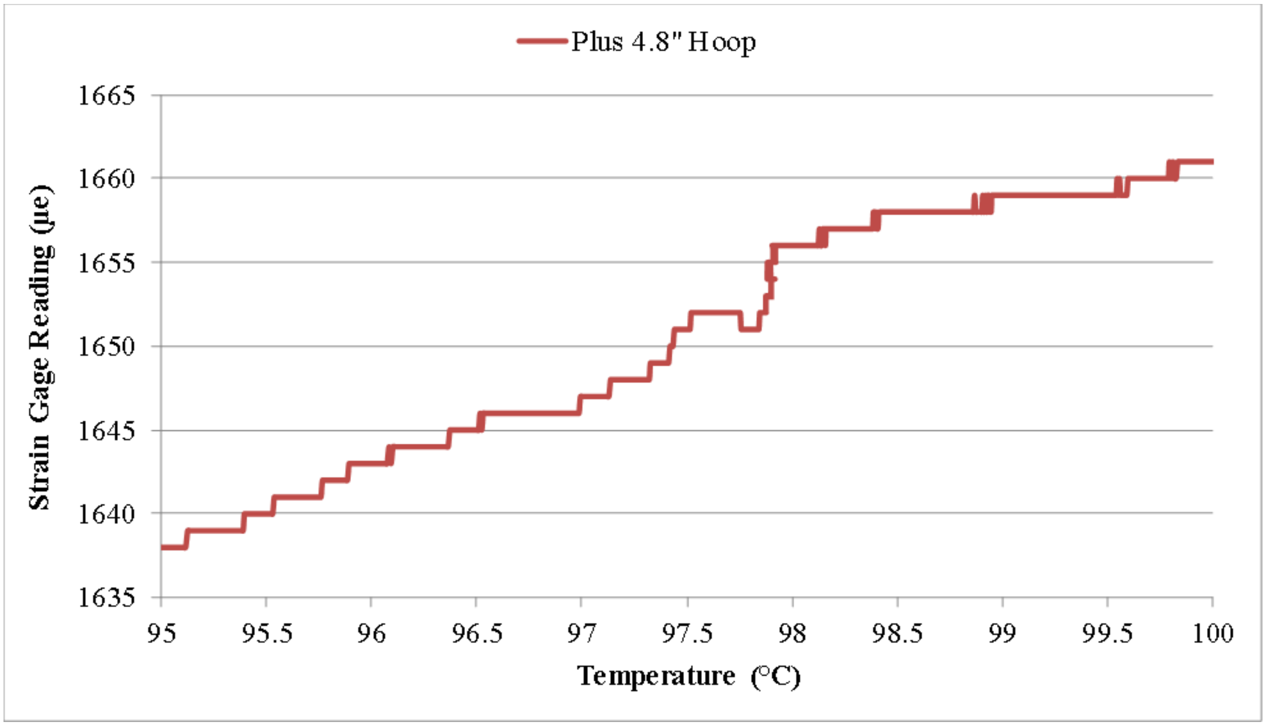

Figure 45. Hoop strain vs temperature at +4.8" from the test section center in Test 5.

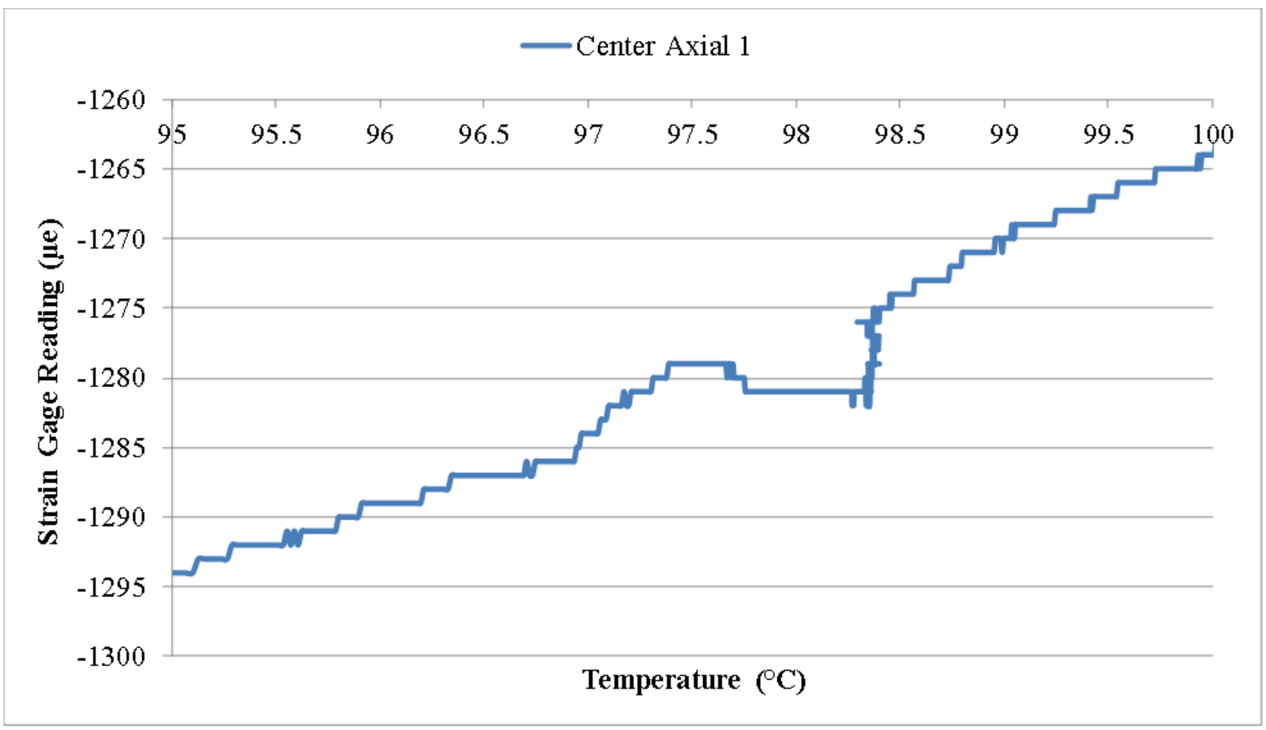

Figure 46. Axial Strain 1 vs temperature at the test section center in Test 5.

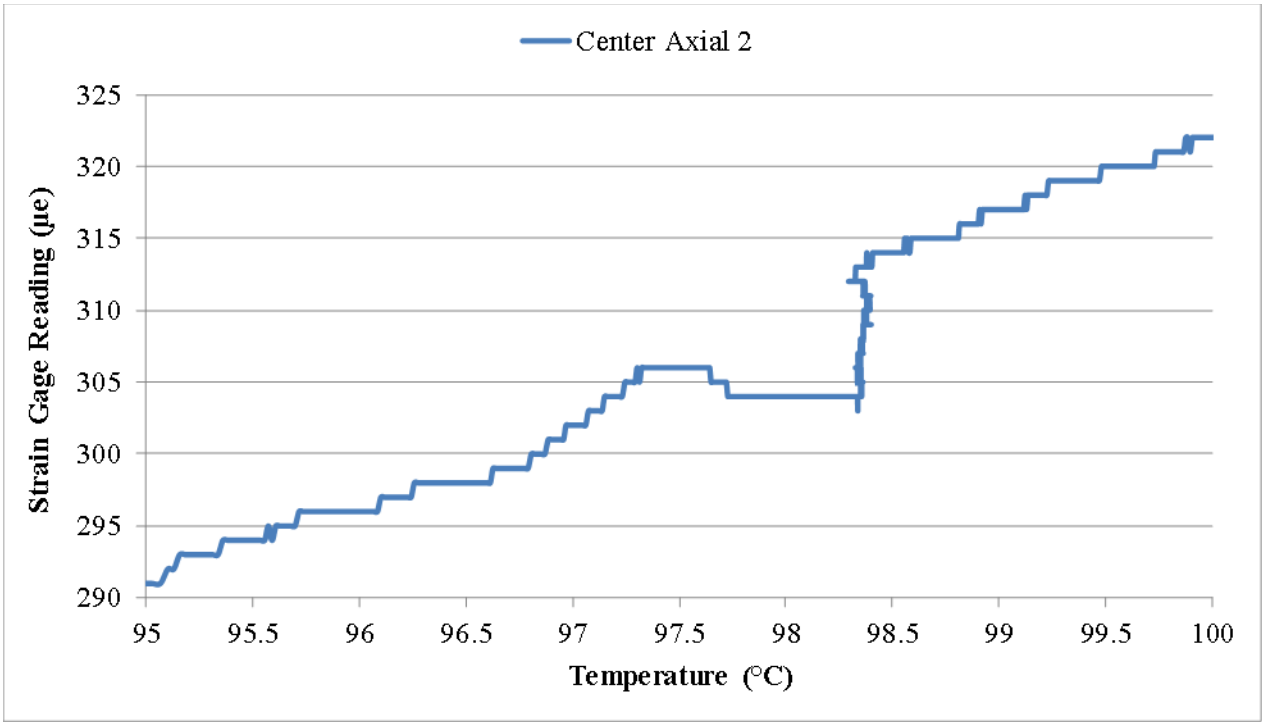

Figure 47. Axial Strain 2 vs temperature at the test section center in Test 5.

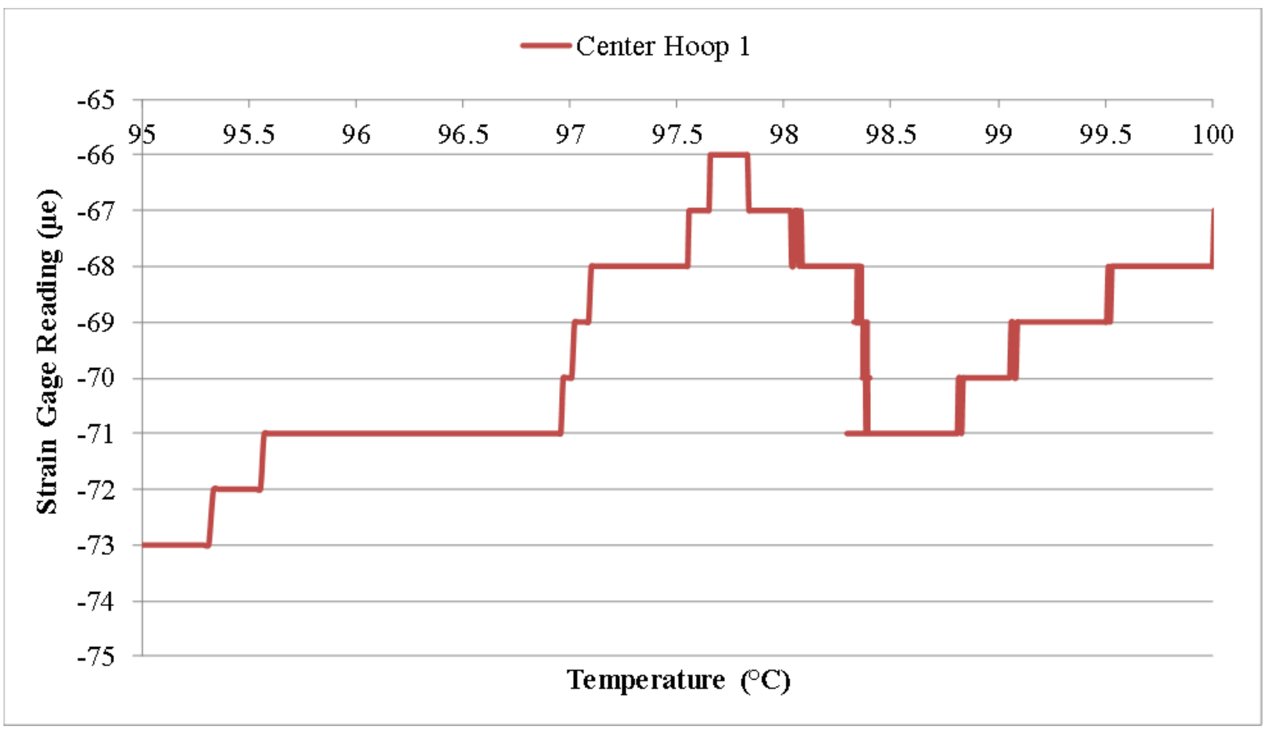

Figure 48. Hoop Strain 1 vs temperature at the test section center in Test 5.

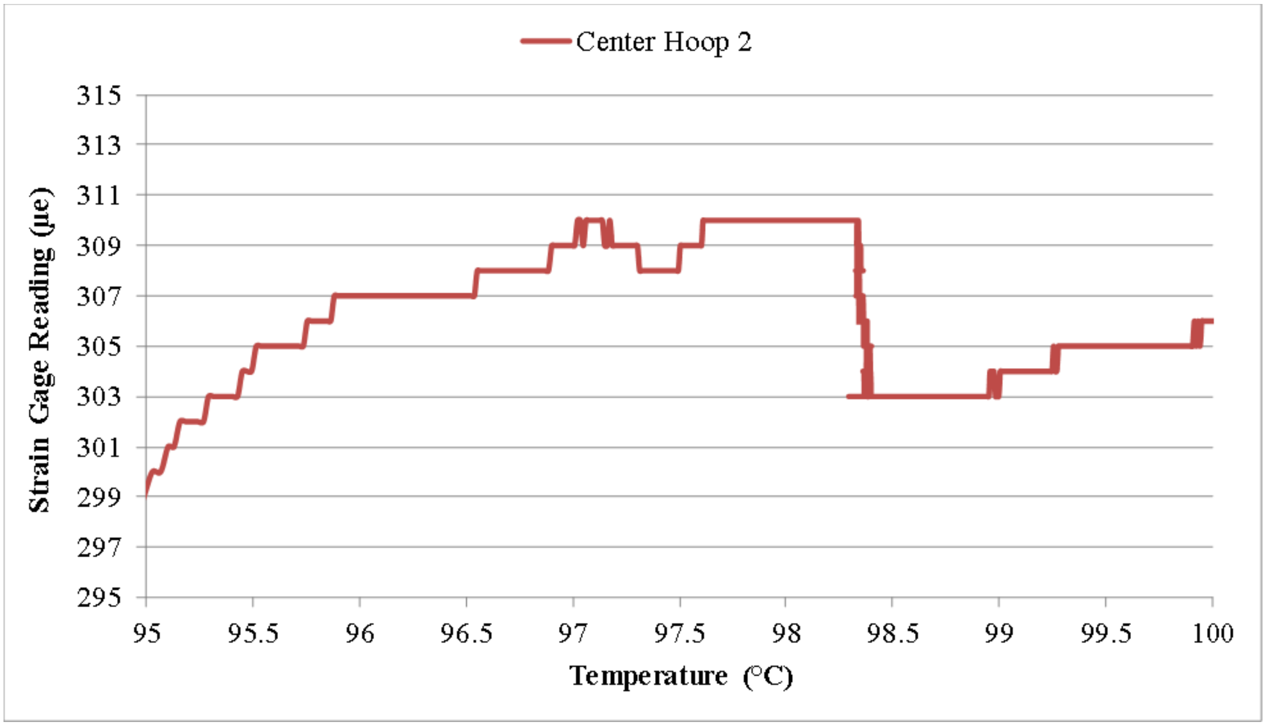

Figure 49. Hoop Strain 2 vs temperature at the test section center in Test 5.

Since it failed to prove the hypothesis of Ar cavitation through Test 5, it was decided to try another indirect method. Assuming that Ar cavitation always occurs at ~ 0 psia, if there is some initial cover gas pressure, the strain gages should first capture this pressure as strain drops, followed by the drops due to sodium contraction upon freezing. Therefore, the measured strain drops during sodium freezing should be higher if there is cover gas pressure applied. It was decided to perform a new freezing test, in which the maximum allowable cover gas pressure of 30 psig would be applied to potentially maximize the measured strain drops during sodium freezing. Since the test section would be pressurized at its rating pressure, it was decided to remove the test section heaters and perform a visual inspection of the test section to ensure safety. There was no deformation observed in the test section. Before assembling back the test section heaters, it was also decided to recheck the electrical resistance along the test section, as summarized in Table 1. Compared to post Test 3 results, there is no significant change in the electrical resistance after Test 5, further confirming the achievement of good wetting after the 500°C wetting test.

To perform the 30 psig test, the cross setup previously used in the vacuum test needed to be removed as the two vacuum gages could not withstand the 30 psig pressure. In the process of removing the cross setup, however, a deep depression was visually observed at the center of the solid sodium inside the reservoir, as shown in Figure 50. After a discussion within the group, it was suspected that the deep depression was caused by starting freezing from the free surfaces in the previous test. Once the free surfaces freeze, the sodium underneath will pull the frozen layer downward when it cools and freezes, causing a depression. If the depression propagated all the way to the test section in all previous tests, that could also explain the small strain changes measured during sodium freezing. It was therefore decided to postpone the 30 psig test and perform a new test with a different freezing pattern from the previous tests, when the sodium was still clean in terms of dissolved Ar gas. The cross setup for the vacuum test was installed back and the same test procedure as Test 4 except for the freezing pattern would be followed to eliminate any effect from the factor of dissolved Ar gas.

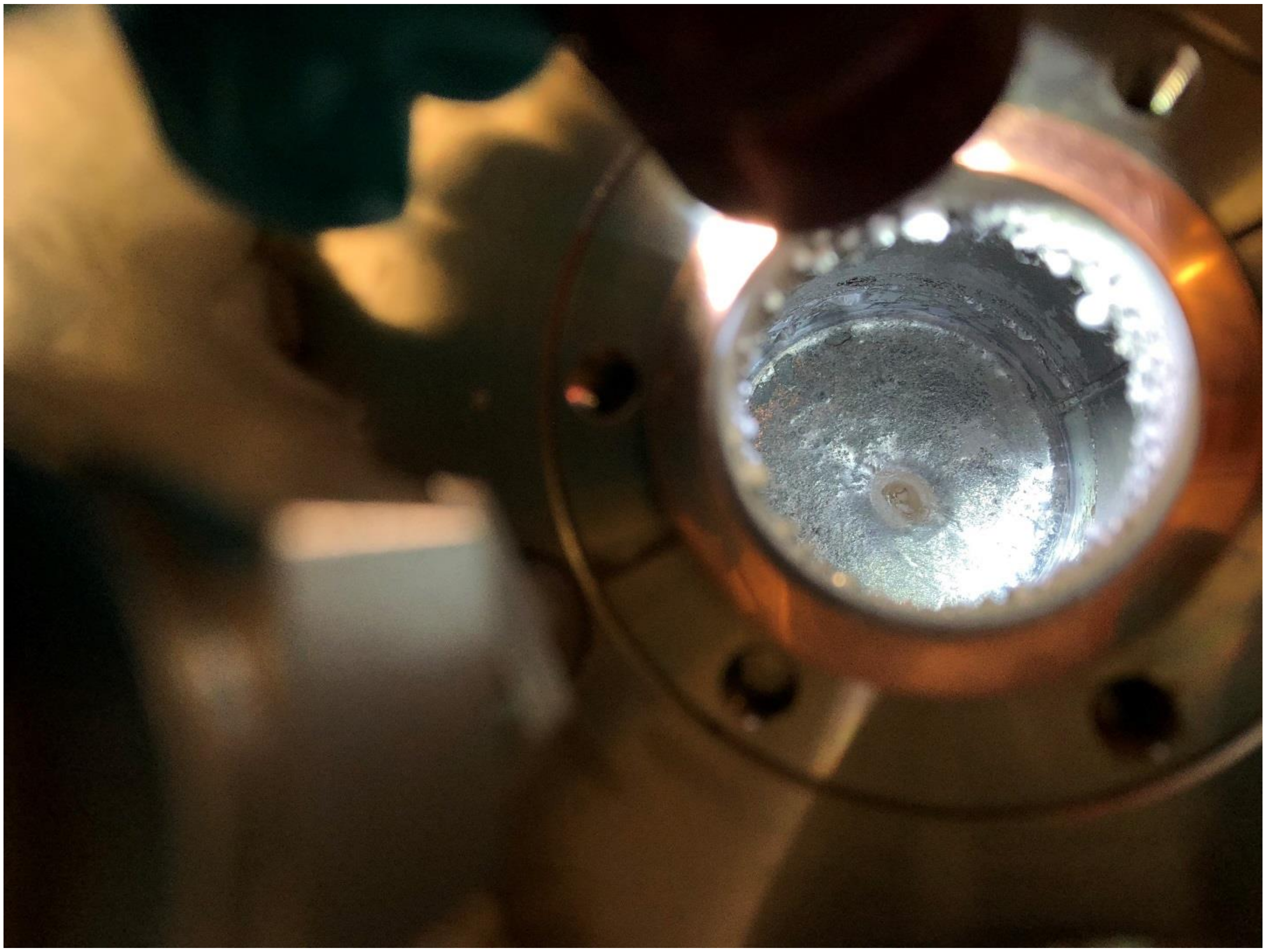

Figure 50. Deep depression observed in the sodium inside the reservoir.

3.6 Test 6: Test with Freezing Pattern 2

In this test, before starting the freezing, the same procedure as in Test 4 was followed. Freezing was started in the two zones upstream and downstream of the test section (Zones 7 and 6), and then continued toward the free surfaces. After freezing was complete at the free surfaces, the frozen plugs were left to further cool down. With the frozen plugs reaching their lowest temperatures, freezing was initiated in the test section, from the ends toward the center. With this new freezing pattern, the previously observed depression in the sodium inside the reservoir disappeared, as shown in Figure 51. The measured strain changes during sodium freezing are shown in Figure 52 to Figure 59. No improvement was observed in the measured strain changes during sodium freezing in the new test, which was actually not too surprising to the authors. Although a depression was not formed in the new test, eliminating the possibility of communicating with the free surfaces during sodium freezing in the test section, the measured strain changes would always be limited by the yield strength of the frozen sodium as long as cavitation occurred, according to the previous hypothesis.

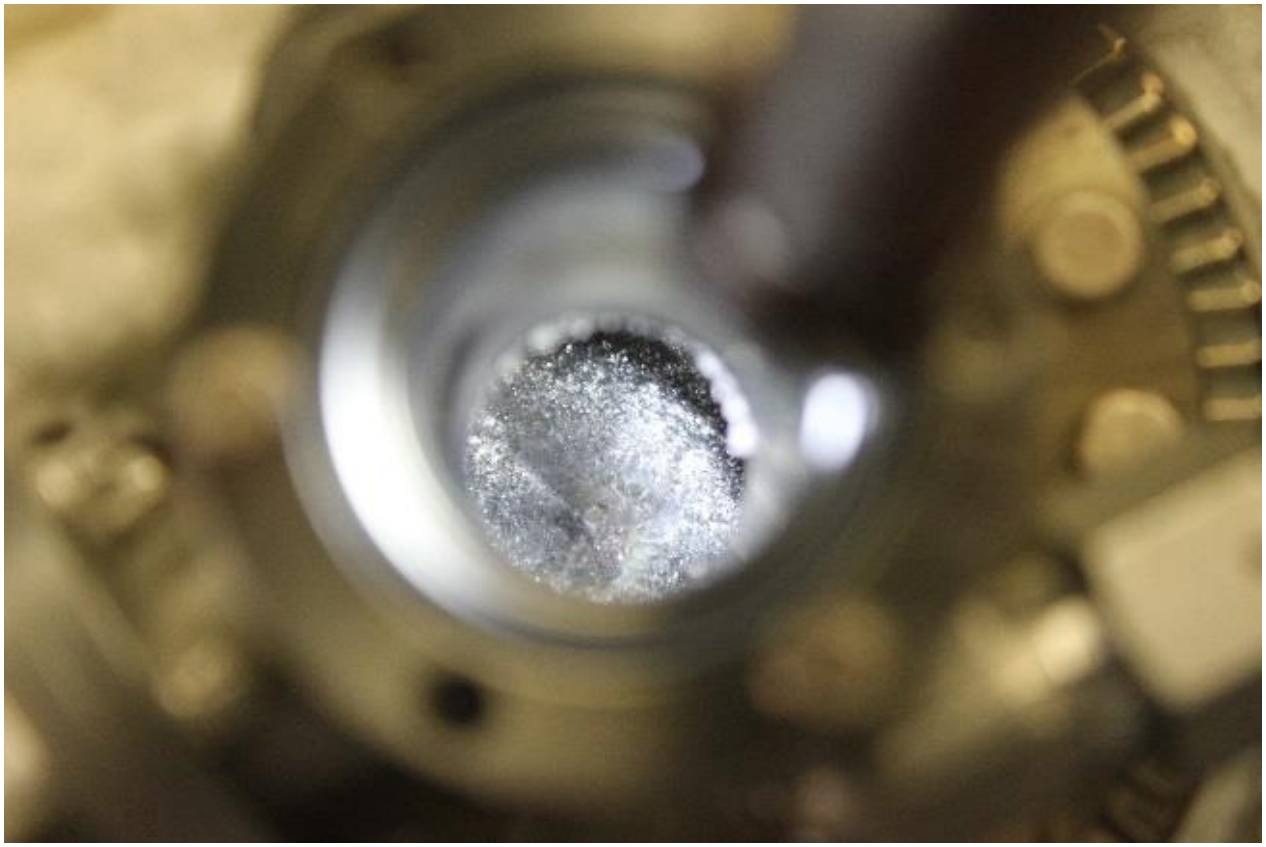

Figure 51. No deep depression observed with the new freezing pattern.

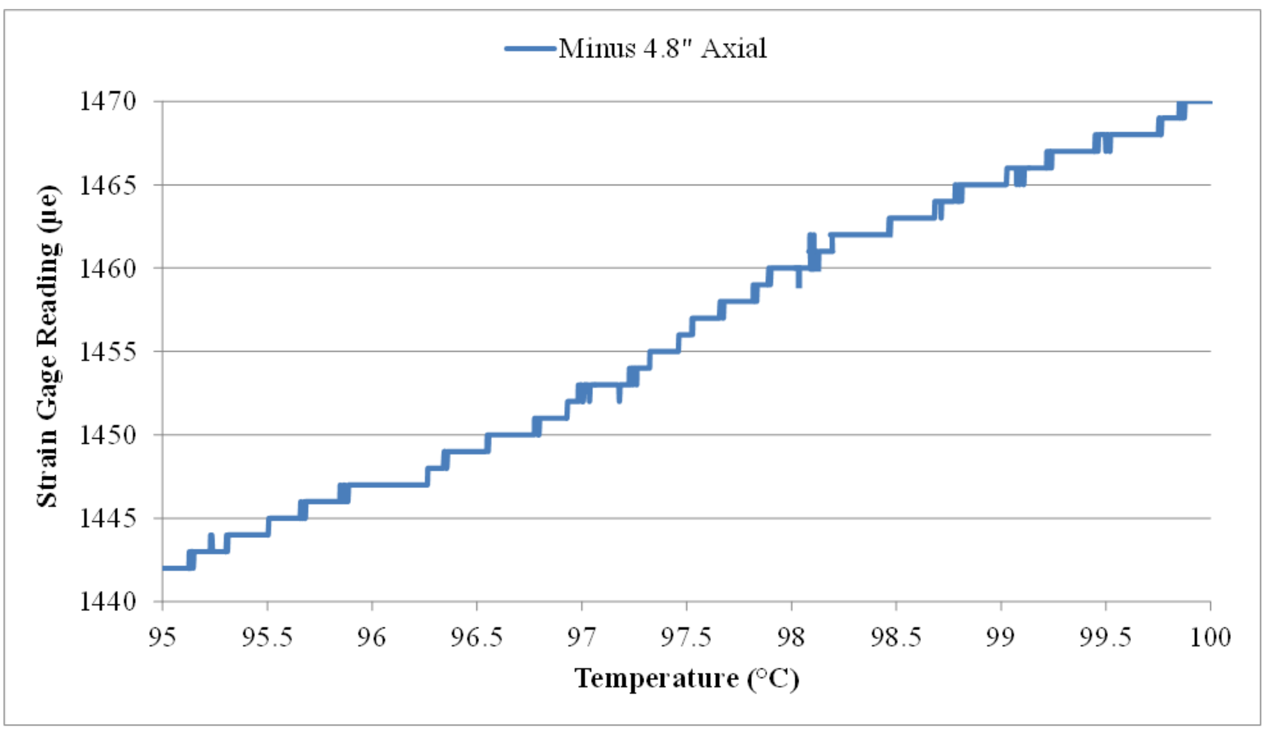

Figure 52. Axial strain vs temperature at –4.8" from the test section center in Test 6.

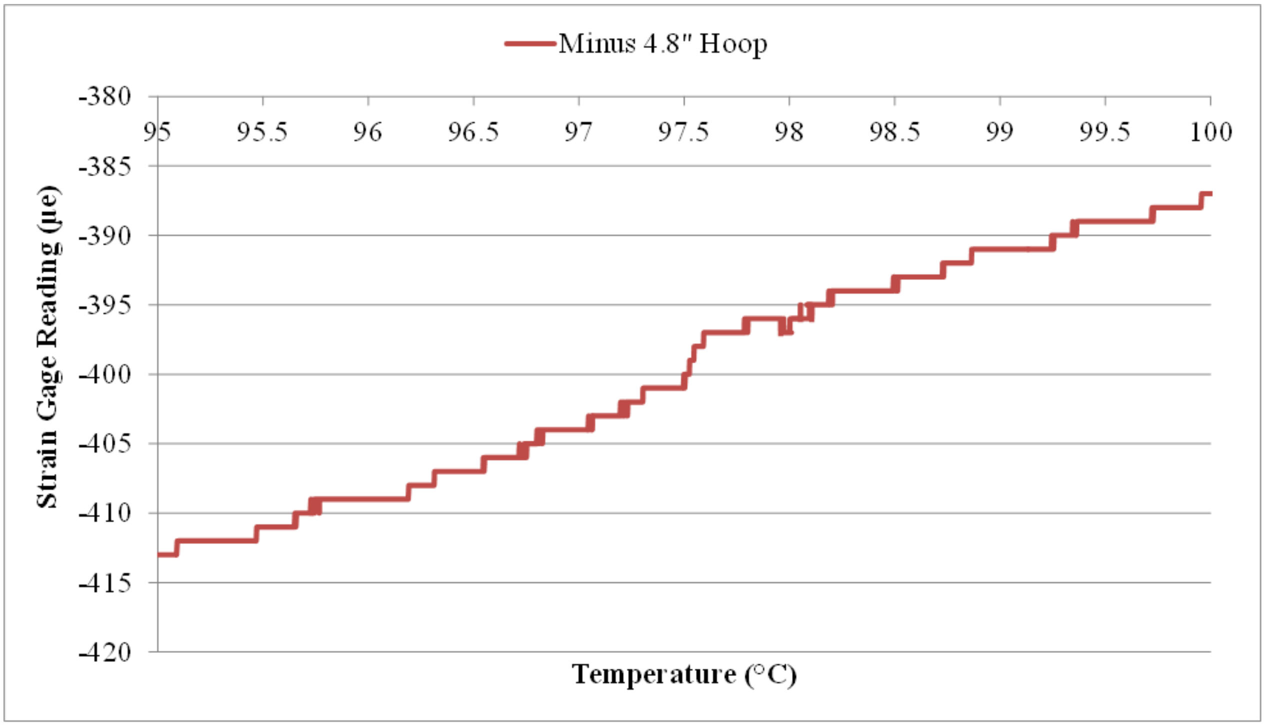

Figure 53. Hoop strain vs temperature at -4.8" from the test section center in Test 6.

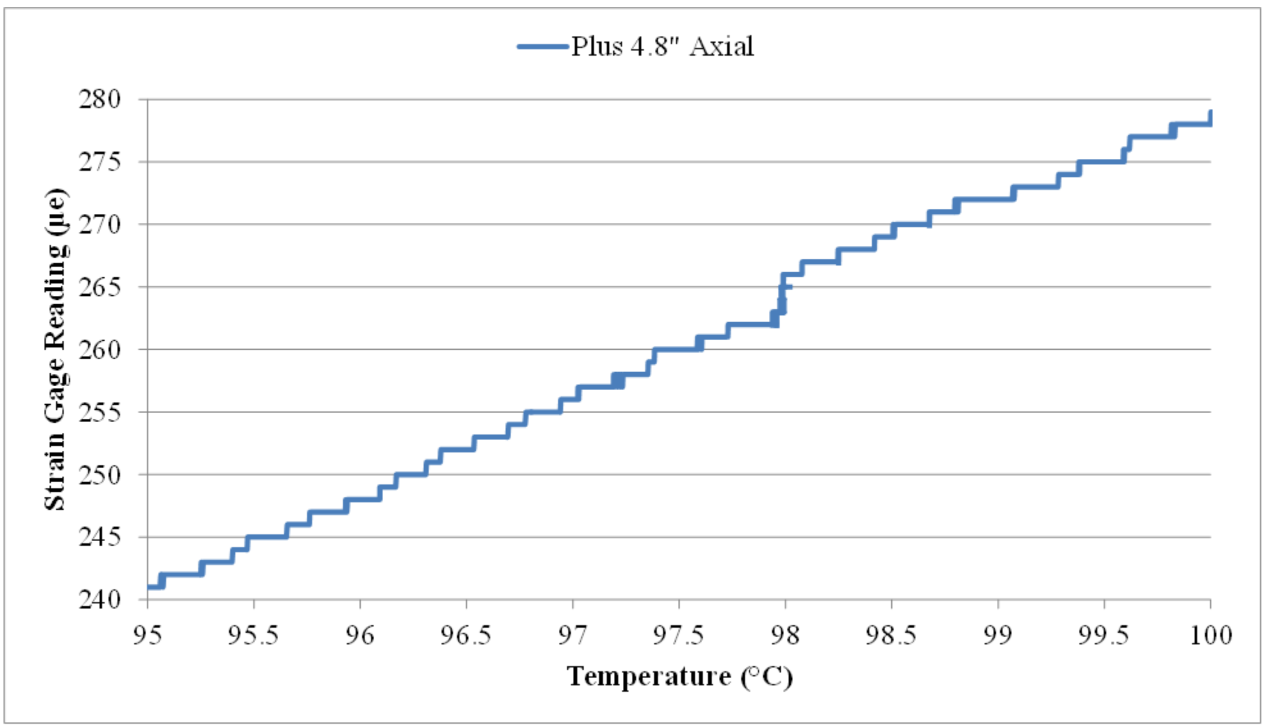

Figure 54. Axial strain vs temperature at +4.8" from the test section center in Test 6.

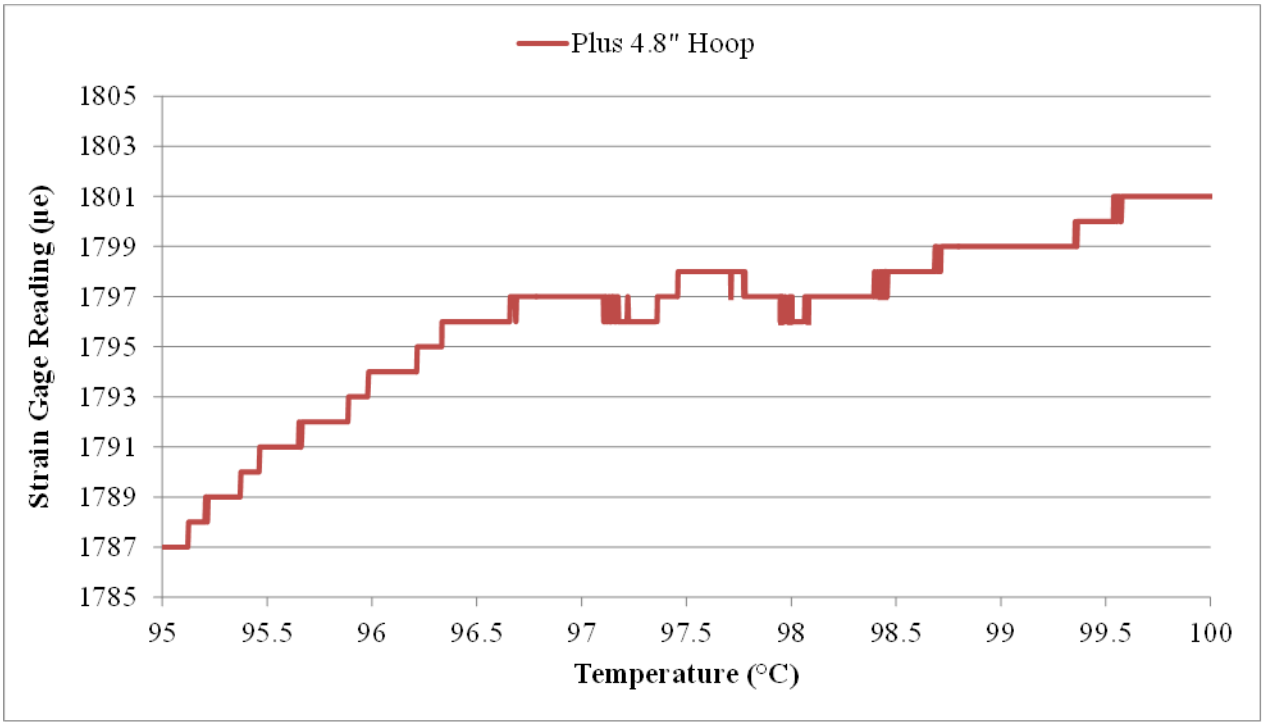

Figure 55. Hoop strain vs temperature at +4.8" from the test section center in Test 6.

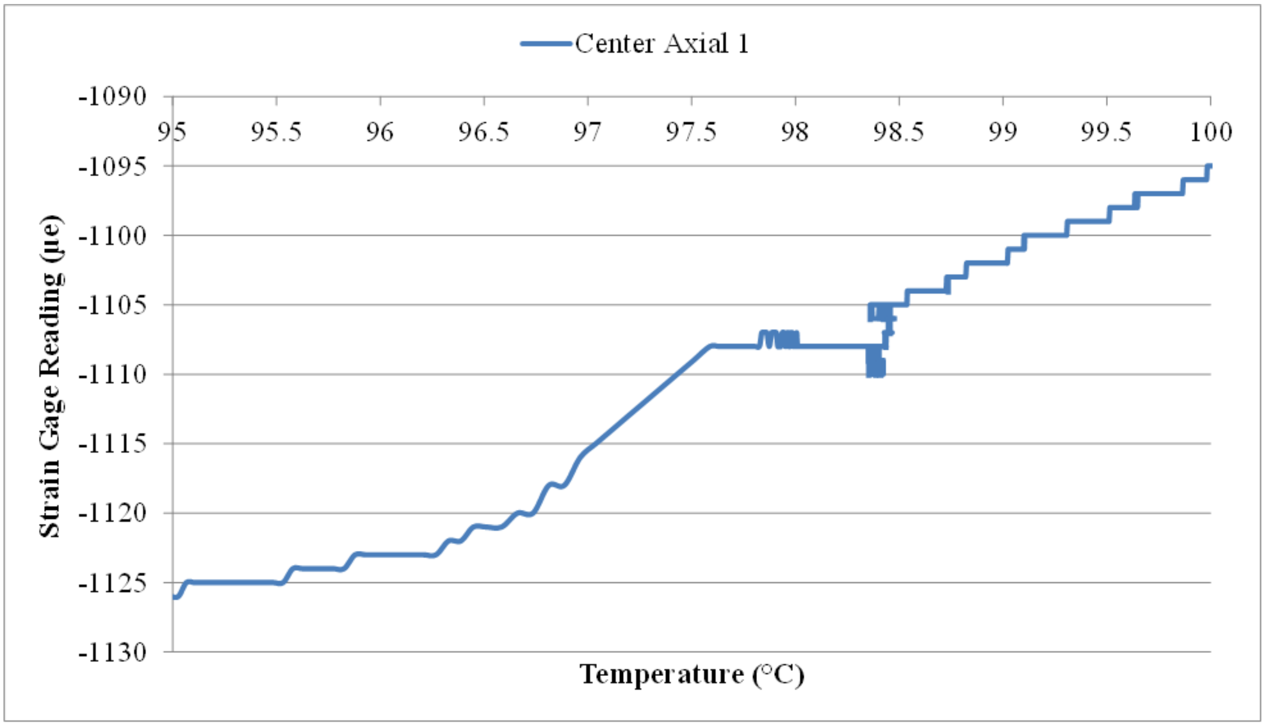

Figure 56. Axial Strain 1 vs temperature at the test section center in Test 6.

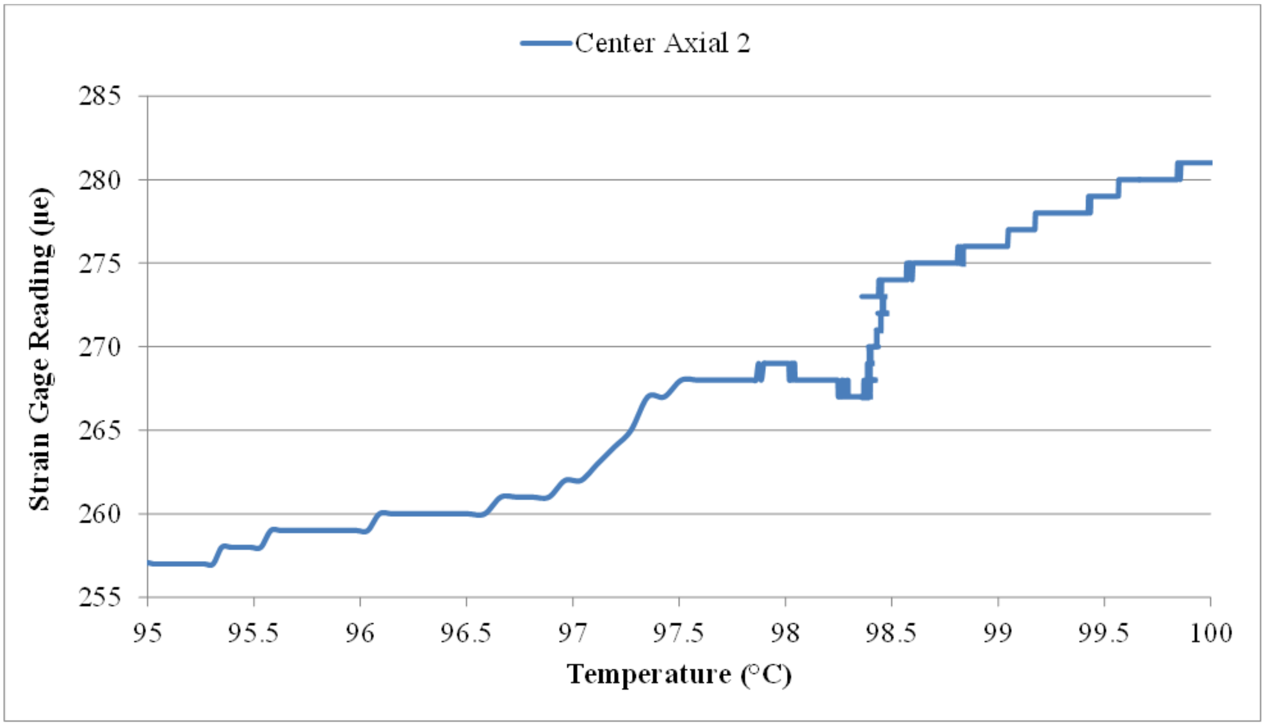

Figure 57. Axial Strain 2 vs temperature at the test section center in Test 6.

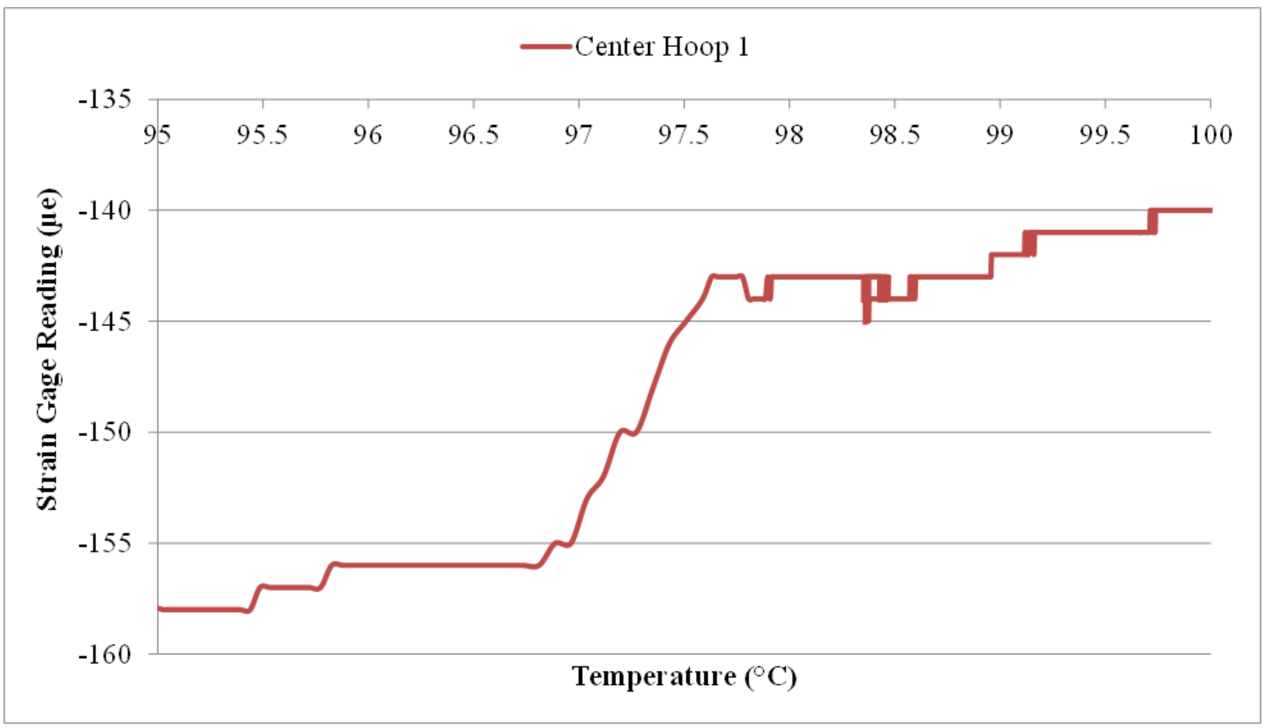

Figure 58. Hoop Strain 1 vs temperature at the test section center in Test 6.

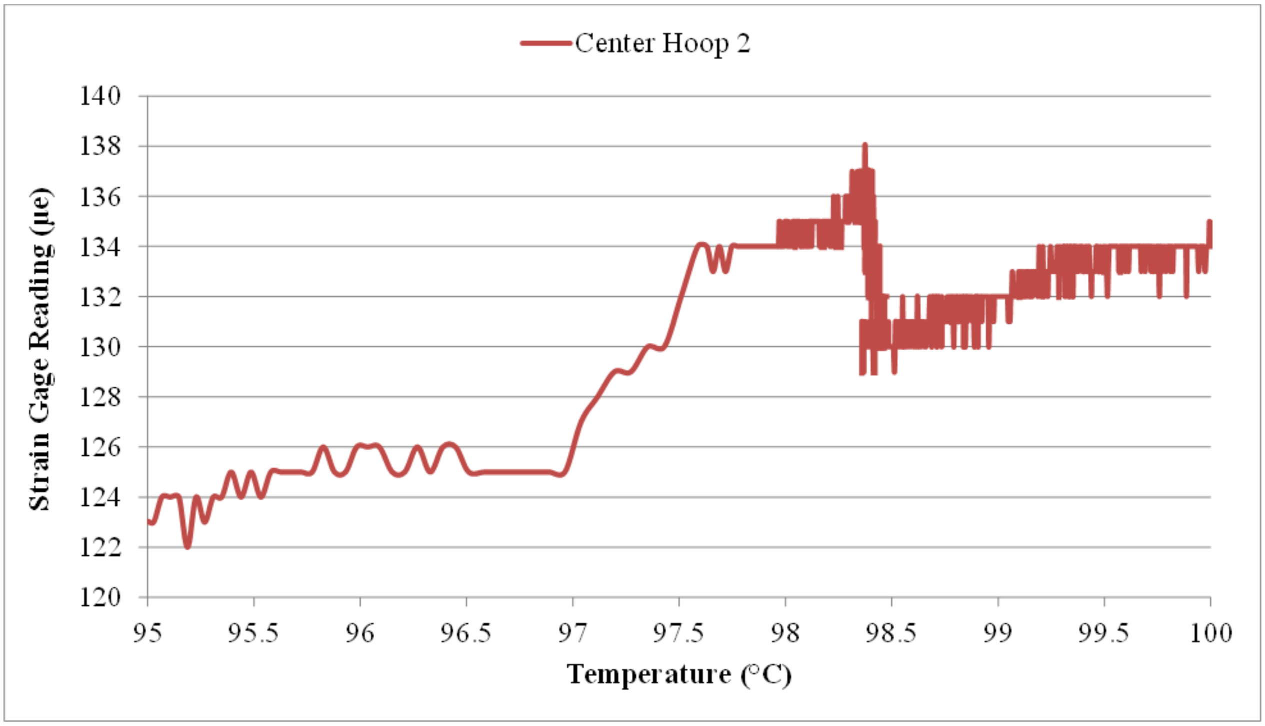

Figure 59. Hoop Strain 2 vs temperature at the test section center in Test 6.

From Test 1 to Test 6, the analysis has been focused on the sodium freezing region due to the initial impression of large thermal contraction upon sodium freezing. However, the expected large thermal contraction during sodium freezing was never detected in the previous 6 tests. It was decided to also look at the big picture and examine the entire strain history during each test. The measured strain histories by each strain gage in Test 6 are shown in Figure 60 to Figure 67. Each strain history consists of three parts, corresponding to the heating/melting phase, soaking phase, and freezing/cooling phase, respectively. During the heating/melting phase, there are pressure buildups due to trapped sodium melting and subsequent relaxations due to the melting front propagation. In Test 6, frozen plugs outside of the test section were formed before the soaking phase (at ~ 105°C), and were left to further cool down during the soaking phase. One interesting finding from these plots lies in the hoop strain at the +4.8" location. Passing the melting point, there is a slope change in the strain vs temperature plot, which indicates a change of thermal expansion coefficient. Curve fittings were applied to the plot right before and after the melting point, and slopes of ~ 2 με/°C and ~ 8 με/°C were obtained, respectively, as shown in Figure 68. According to [11], the linear thermal expansion coefficient of SS316 is approximately 18.2E-6 m/m-°C, while according to [12], the linear thermal expansion coefficient of solid sodium is approximately 75.3E-6 m/m-°C. The ratio of the SS316 and sodium thermal expansion coefficients coincide with the ratio of the strain vs temperature slopes before and after the melting point. Therefore, the measured hoop strain vs temperature slope change across melting point at the +4.8" location probably represents the physical phenomenon of frozen sodium pulling inward on the test section wall. As stress builds up during the pulling process, the frozen sodium eventually breaks away from the wall and the strain vs temperature slope recovers to that of the stainless steel tube, as shown in Figure 68. Before the frozen sodium breaks away from the wall, a strain drop of ~ 75 micro strains is attained, and ~ 60 micro strains of that are due to the thermal contraction of solid sodium. Lastly, in Figure 63, the slope of the cooling down part of the

Heating/Melting phase (in red) represents the thermal contraction of the SS316 tube, since sodium is still in liquid state during that phase. After formation of the frozen plugs and the soaking phase (at ~ 105°C), the first part of the Freezing/Cooling phase (in blue) should represent the thermal contraction of confined liquid sodium. Due to the higher thermal contraction coefficient of liquid sodium, a steeper slope is expected. However, as can be seen from Figure 63, there is no slope change before and after formation of frozen plugs. This indicates that during the thermal contraction of the confined liquid sodium, cavitation probably occurs. However, it is uncertain if the cavitation occurs inside the liquid sodium or at the liquid-solid sodium interface as the freezing front propagates.

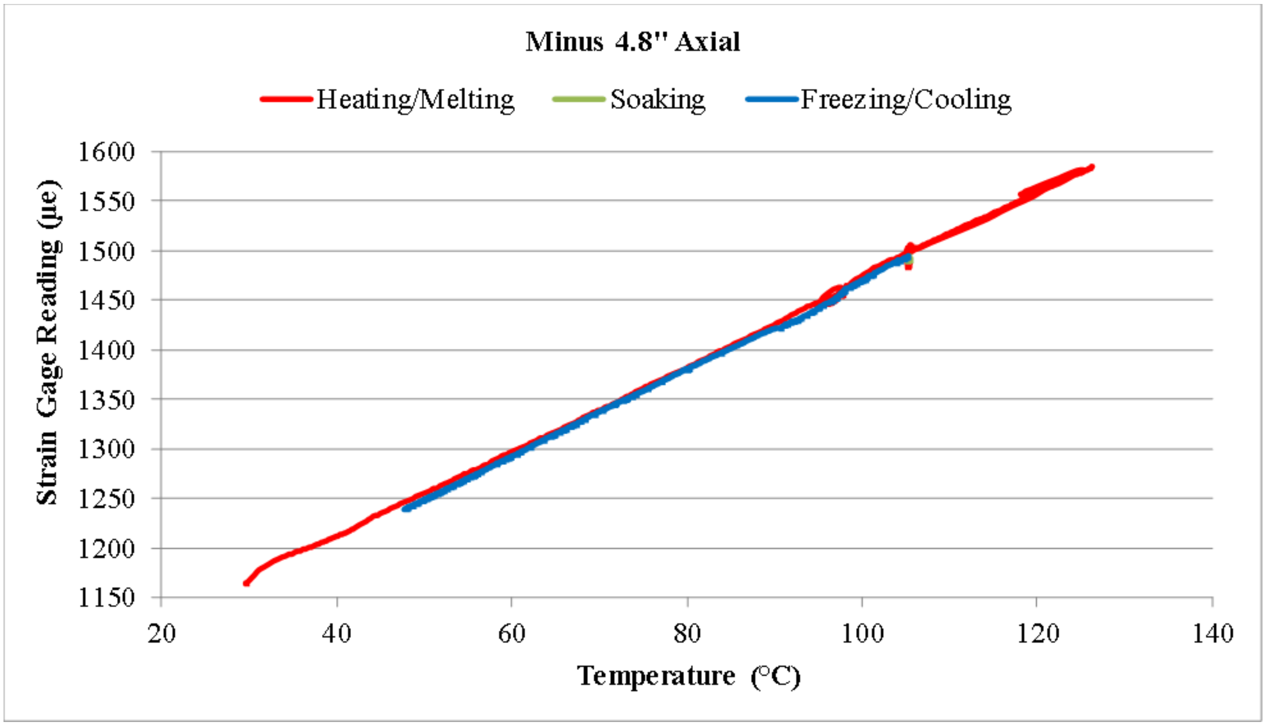

Figure 60. Entire axial strain history at –4.8" from the test section center in Test 6.

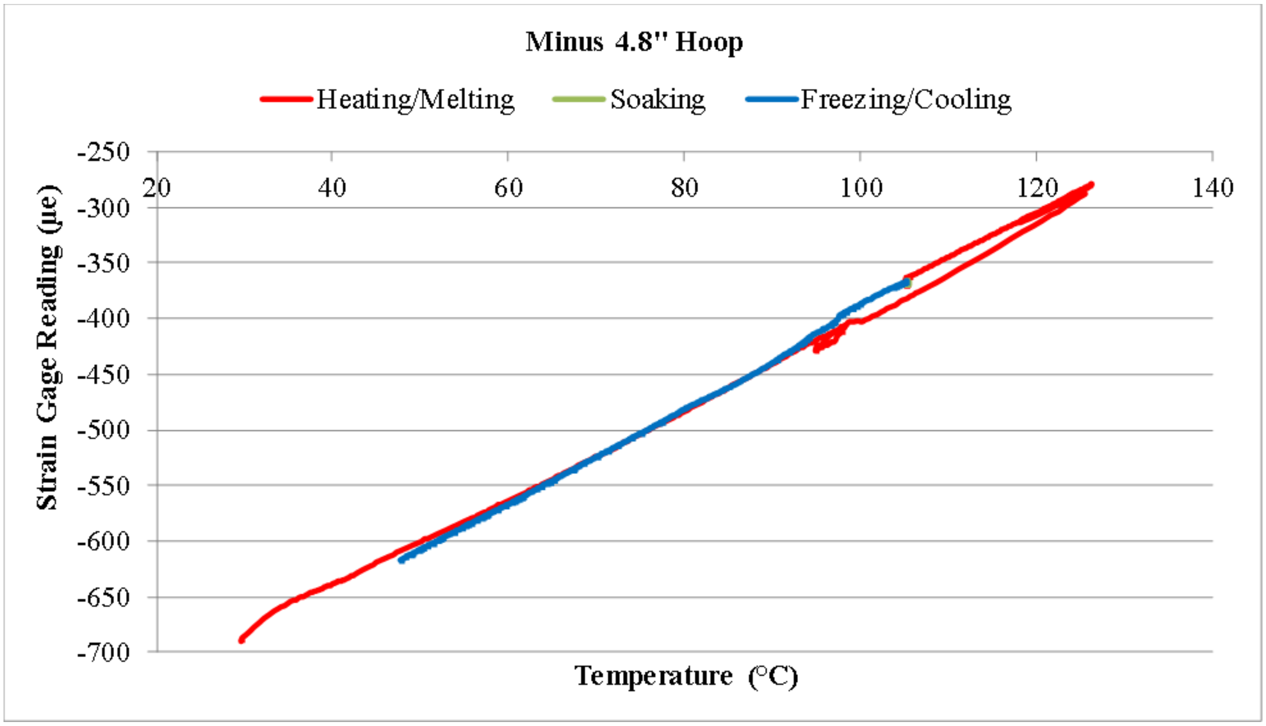

Figure 61. Entire hoop strain history at -4.8" from the test section center in Test 6.

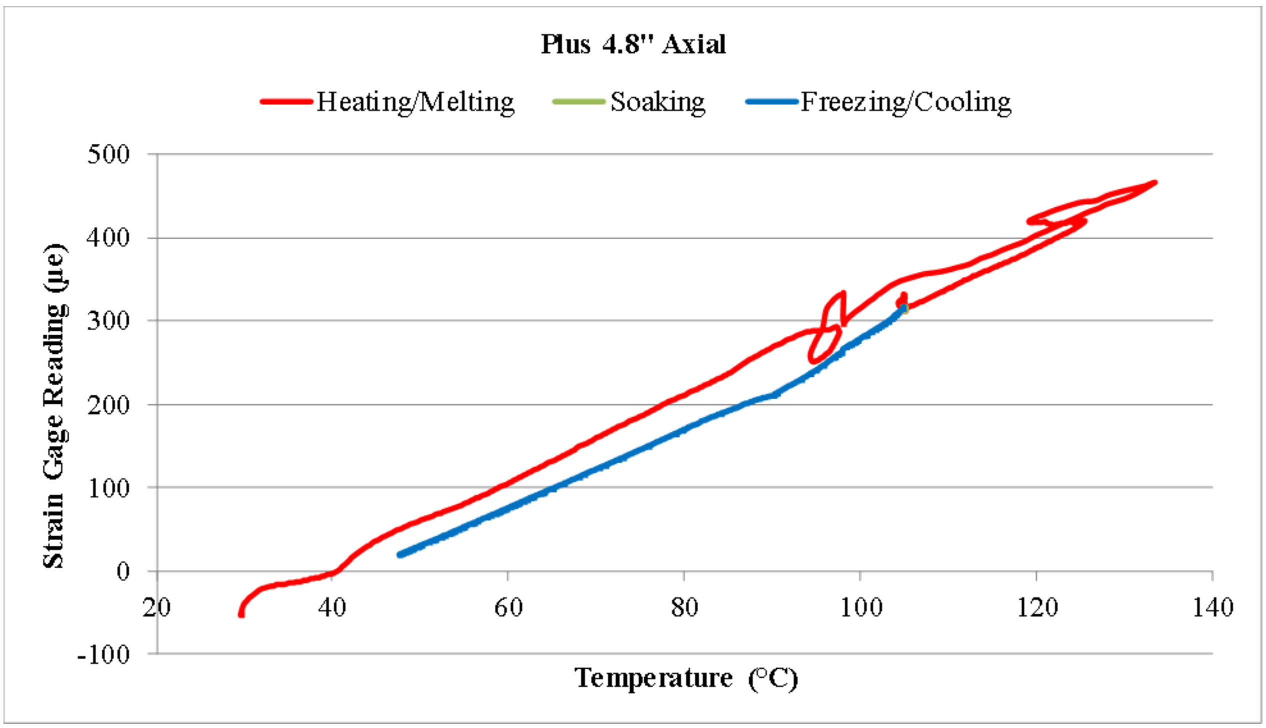

Figure 62. Entire axial strain history at +4.8" from the test section center in Test 6.

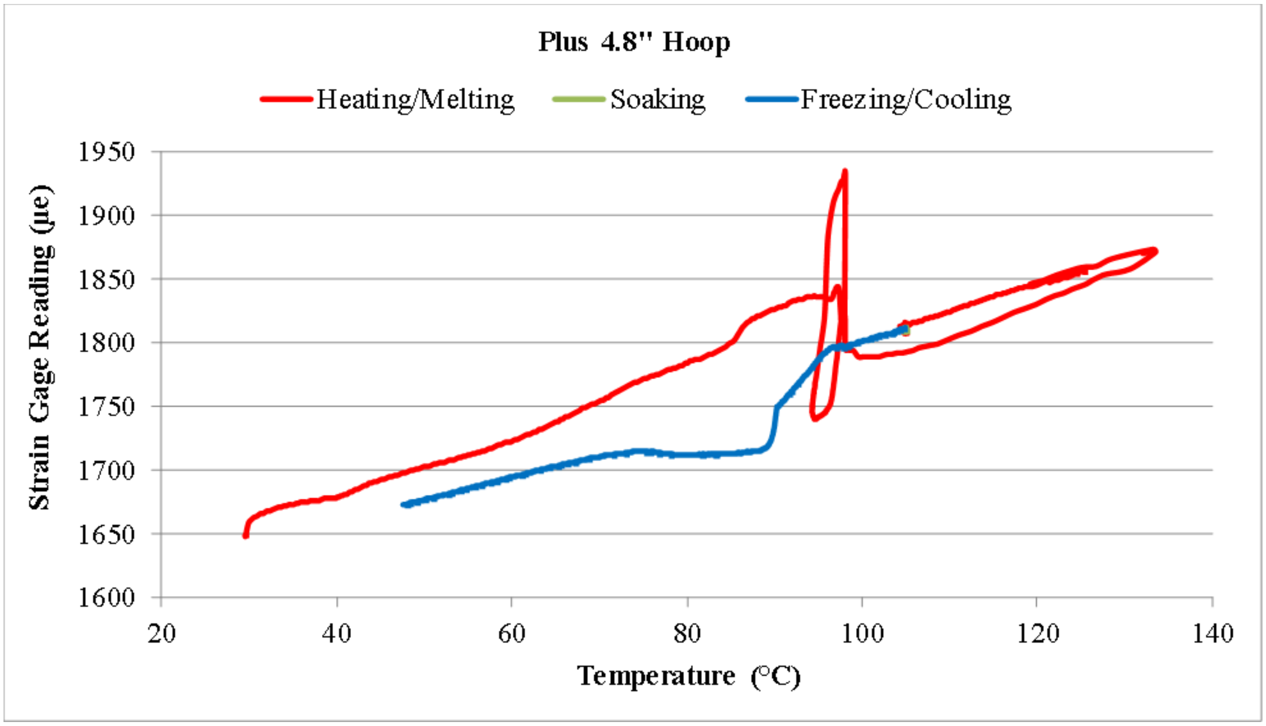

Figure 63. Entire hoop strain history at +4.8" from the test section center in Test 6.

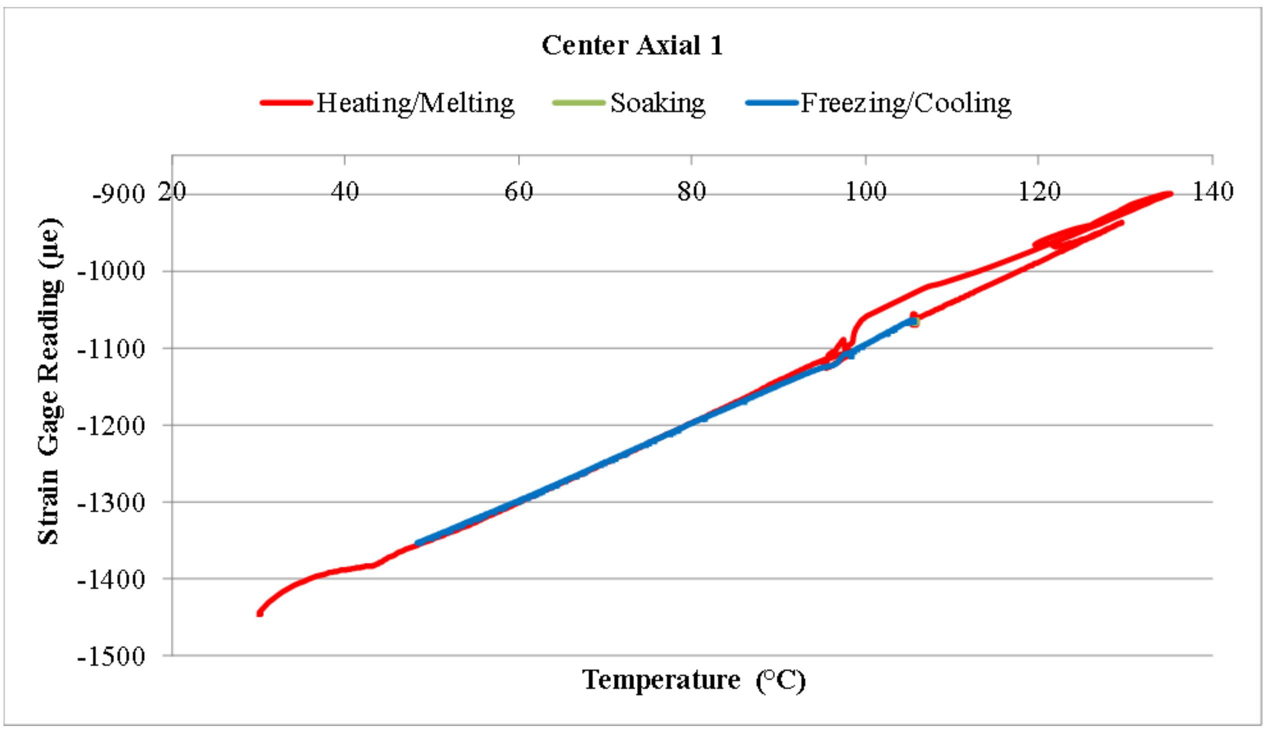

Figure 64. Entire axial strain 1 history at the test section center in Test 6.

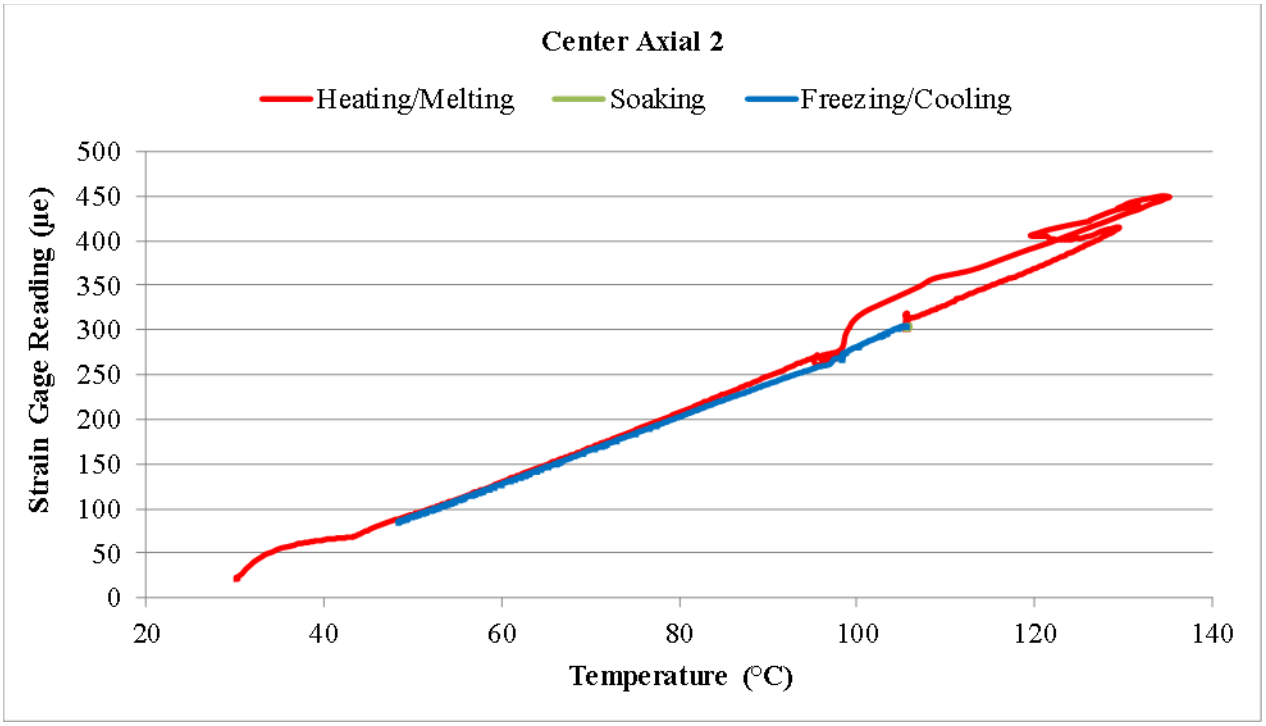

Figure 65. Entire axial strain 2 history at the test section center in Test 6.

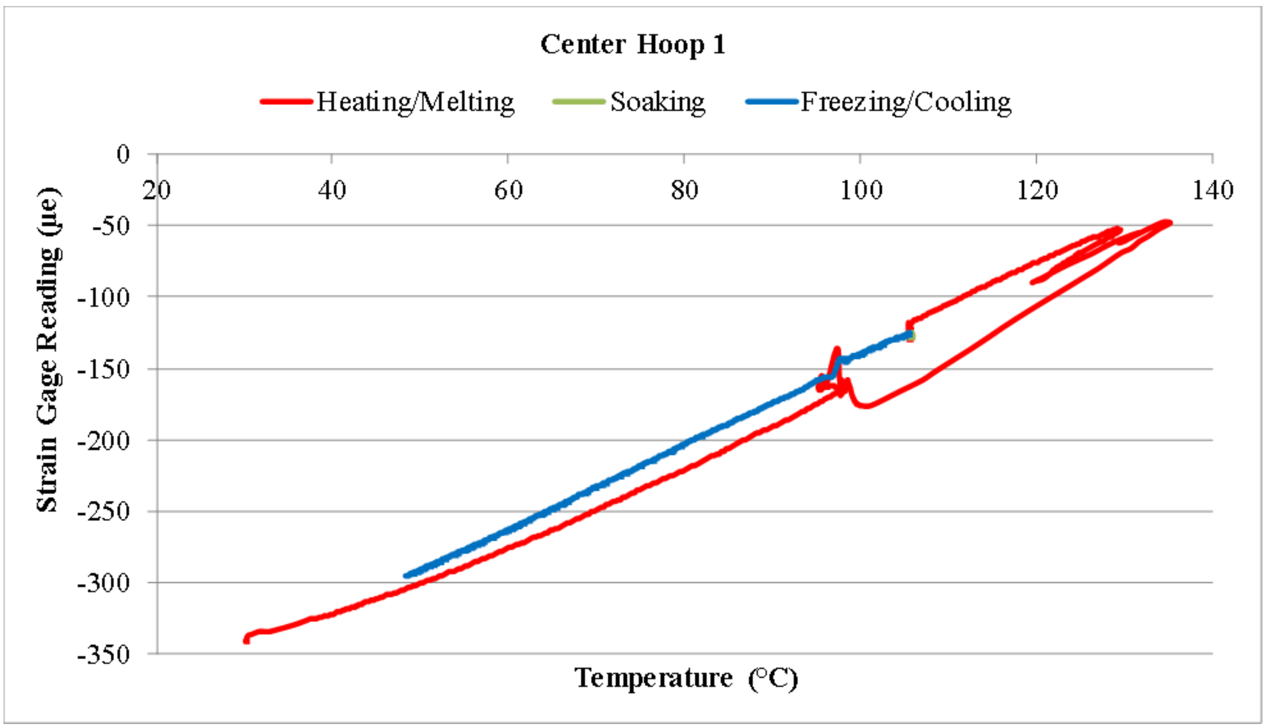

Figure 66. Entire hoop strain 1 history at the test section center in Test 6.

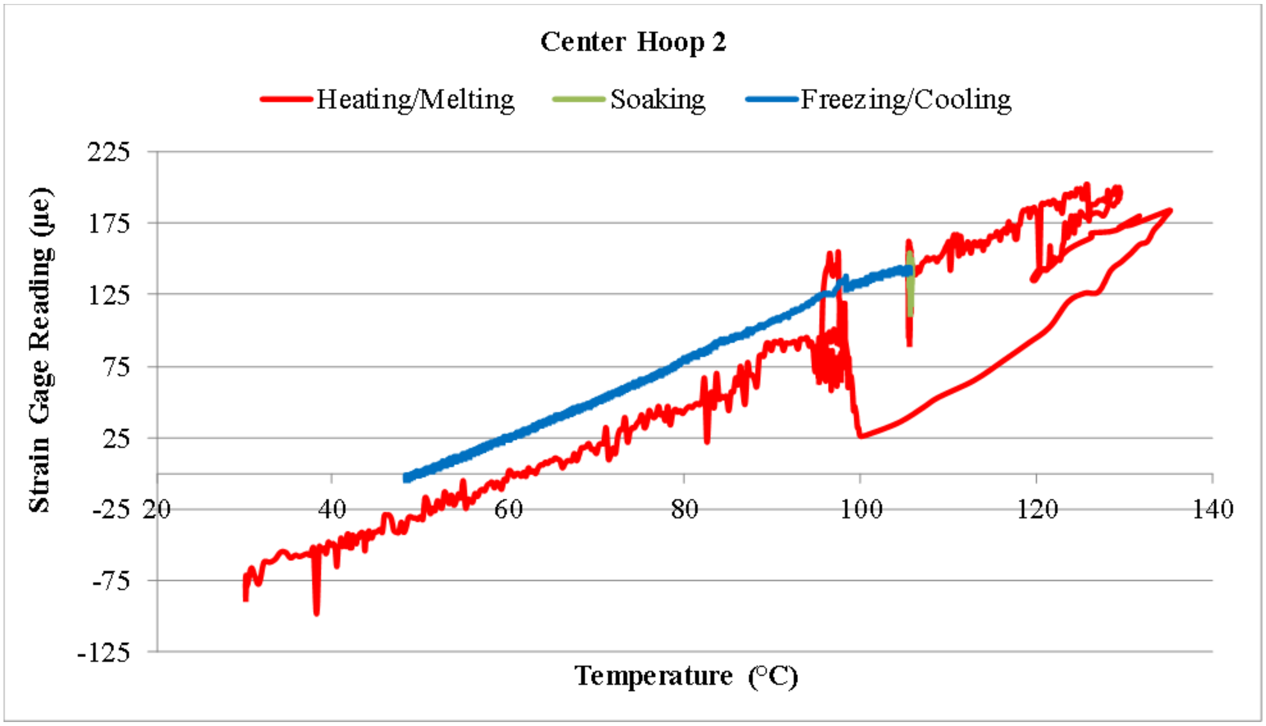

Figure 67. Entire hoop strain 2 history at the test section center in Test 6.

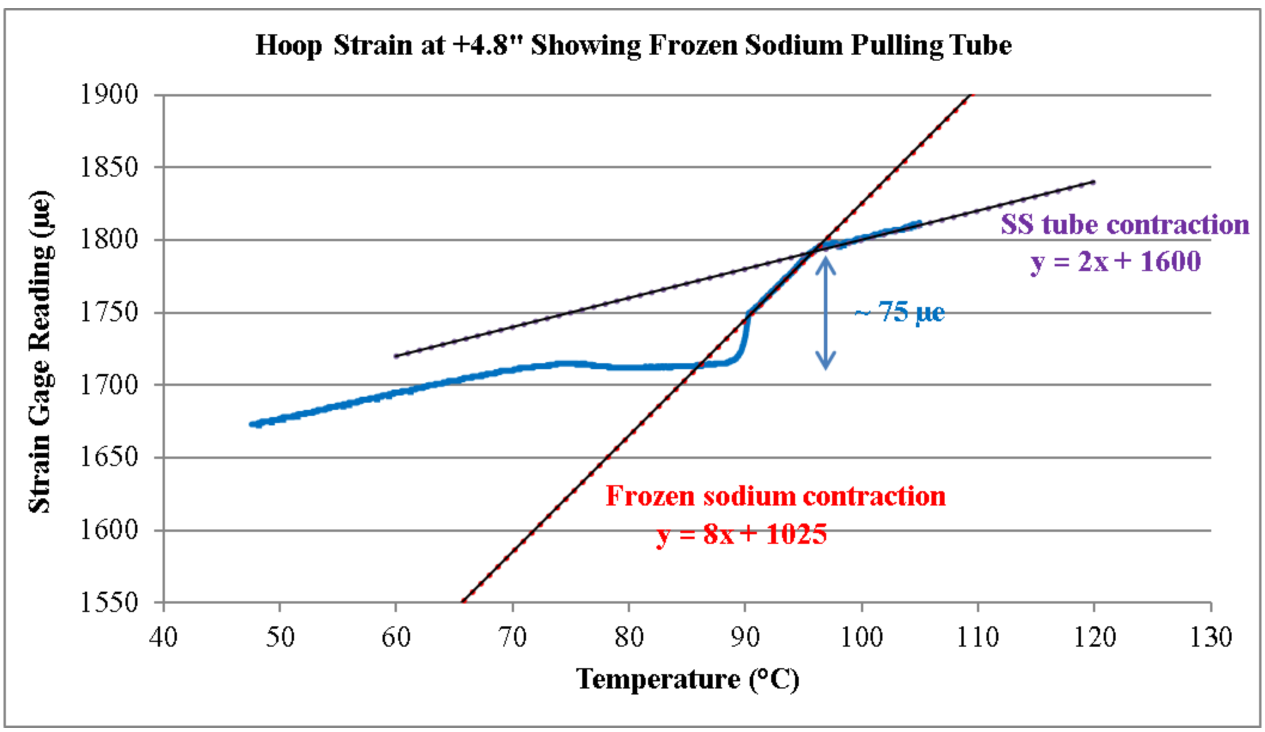

Figure 68. Hoop strain showing frozen sodium pulling the test section wall at the +4.8" location.

Since the potential physical phenomenon of solid sodium pulling the test section wall after freezing was observed in Test 6, it was decided to perform the same re-analysis of data for all the previous 5 tests. The measured strain histories for each previous test are shown in Figure 69 to Figure 108. As can be seen, the aforementioned physical phenomenon does not show in Test 1, shows in Test 2 but not prominently, and consistently shows in Test 3 to Test 6 after the 500°C wetting test. This is additional evidence of achievement of good wetting with the 500°C heating. However, it was also noticed that the phenomenon of solid sodium pulling the test section wall was only observed at the +4.8” location in the previous tests, which led to the question of what was special about the +4.8” location and why it did not occur at the center and -4.8” location. After some discussion and thinking, the authors came up with a hypothesis that might explain the observation. First of all, if the observed strain vs. temperature slope change does represent the physical phenomenon of solid sodium pulling the tube wall after freezing, the fact that it only occurred at the +4.8” location indicates that dense frozen sodium without voids had formed at this location while voids must have formed at the other two locations. In the previous freezing tests, when freezing was initiated from the two ends of the test section, due to the sodium contraction and associated negative pressure, breaking of frozen sodium and cavitation in liquid sodium could possibly occur. Because the +4.8” and -4.8” locations were able to communicate through the liquid sodium in between, they were competing and voids tended to form at the end with a weaker sodium frozen plug. Due to the larger diameter of the sodium reservoir, increased wetting along the test section, and possibly other reasons, the -4.8” lost the competition and voids formed there. As the freezing front propagated to the center, the voids also propagated to the center, which explained why the phenomenon of solid sodium pulling the tube wall only occurred at the +4.8” location.

To prove the above hypothesis and make sure that the phenomenon of solid sodium pulling the tube wall after freezing is not specific to the +4.8” location due to some intrinsic local features, a new test (Test 7) was performed, in which a new freezing pattern was employed to increase the strength of frozen plug on the reservoir side.

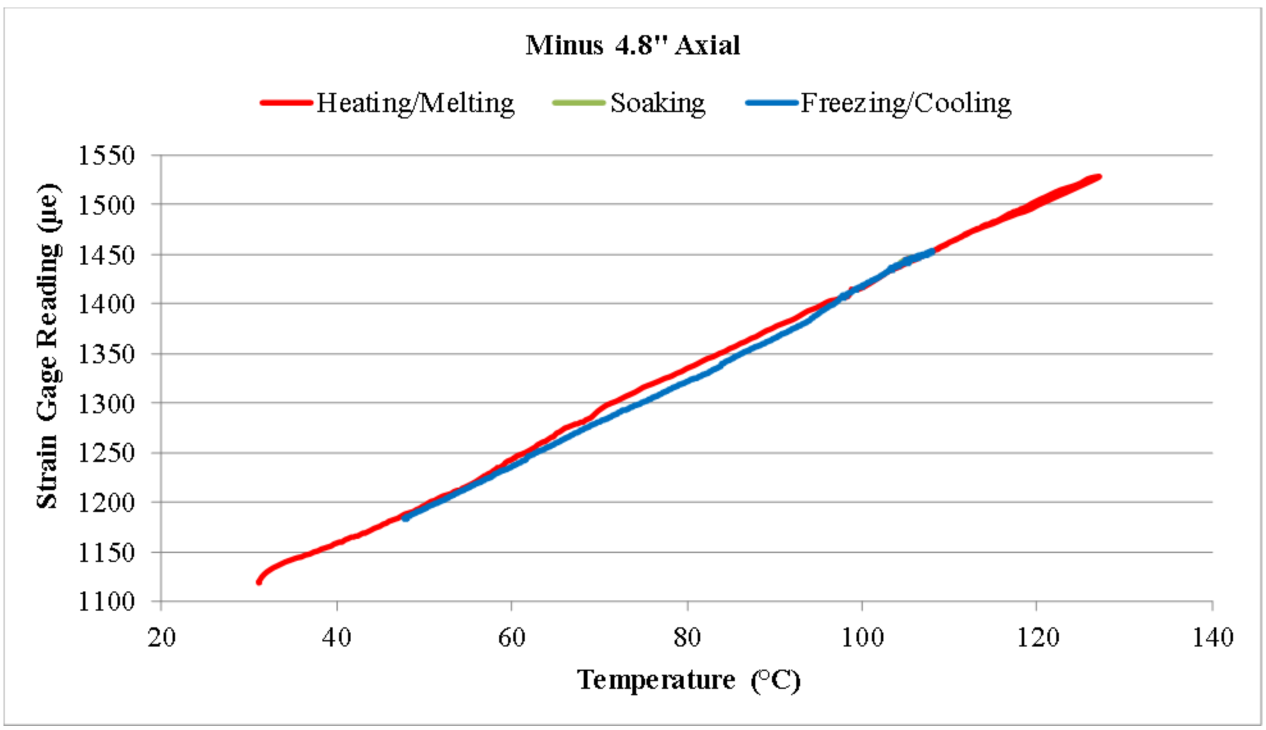

Figure 69. Entire axial strain history at –4.8” from the test section center in Test 5.

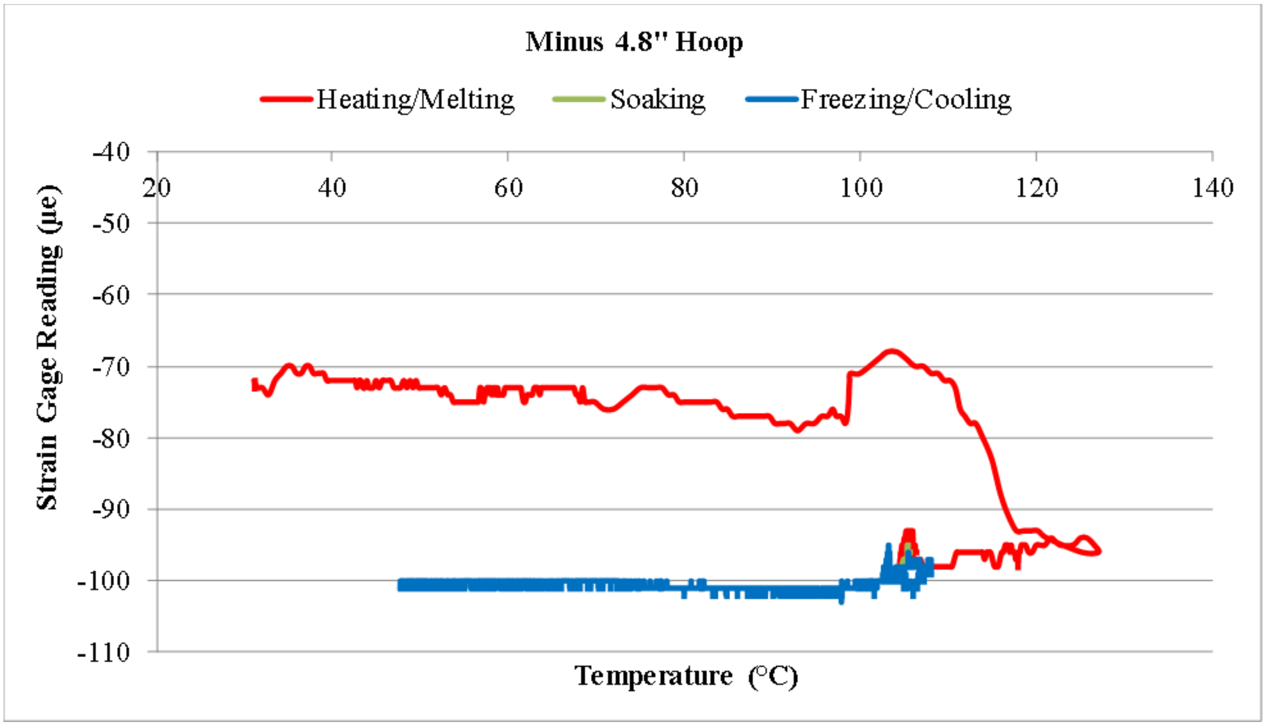

Figure 70. Entire hoop strain history at -4.8" from the test section center in Test 5.

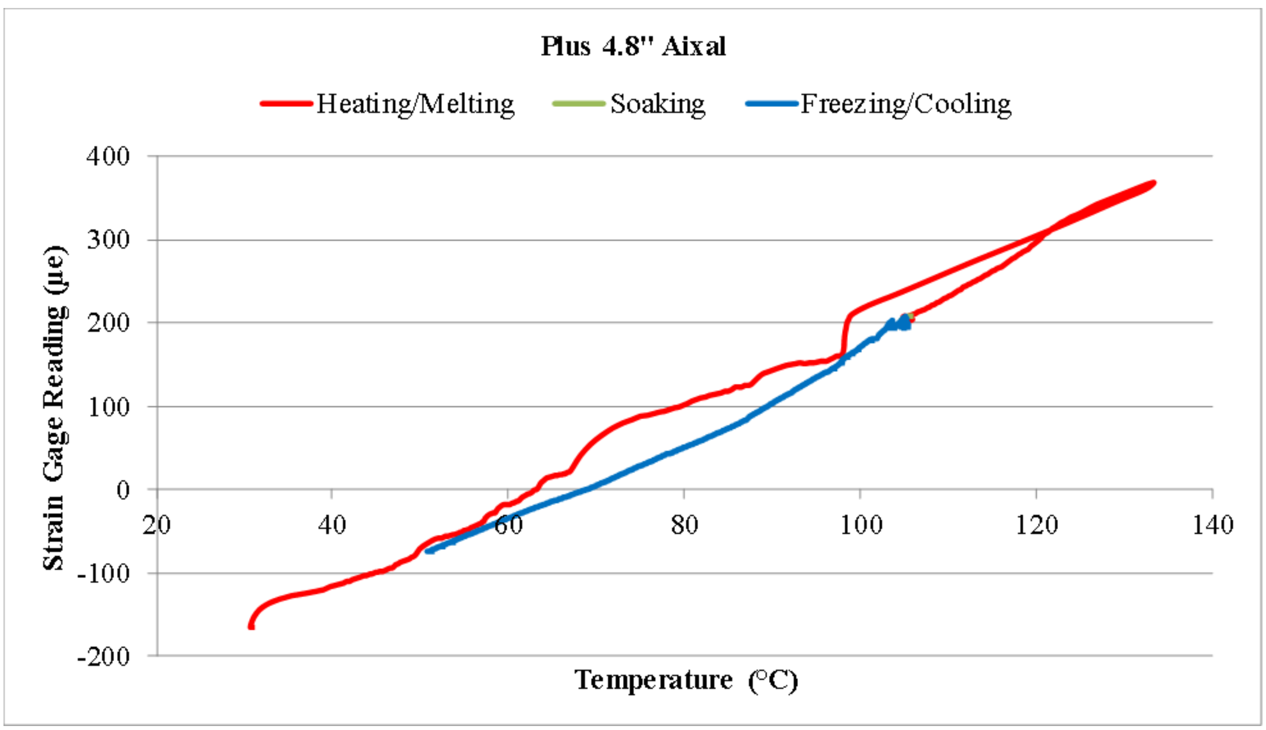

Figure 71. Entire axial strain history at +4.8" from the test section center in Test 5.

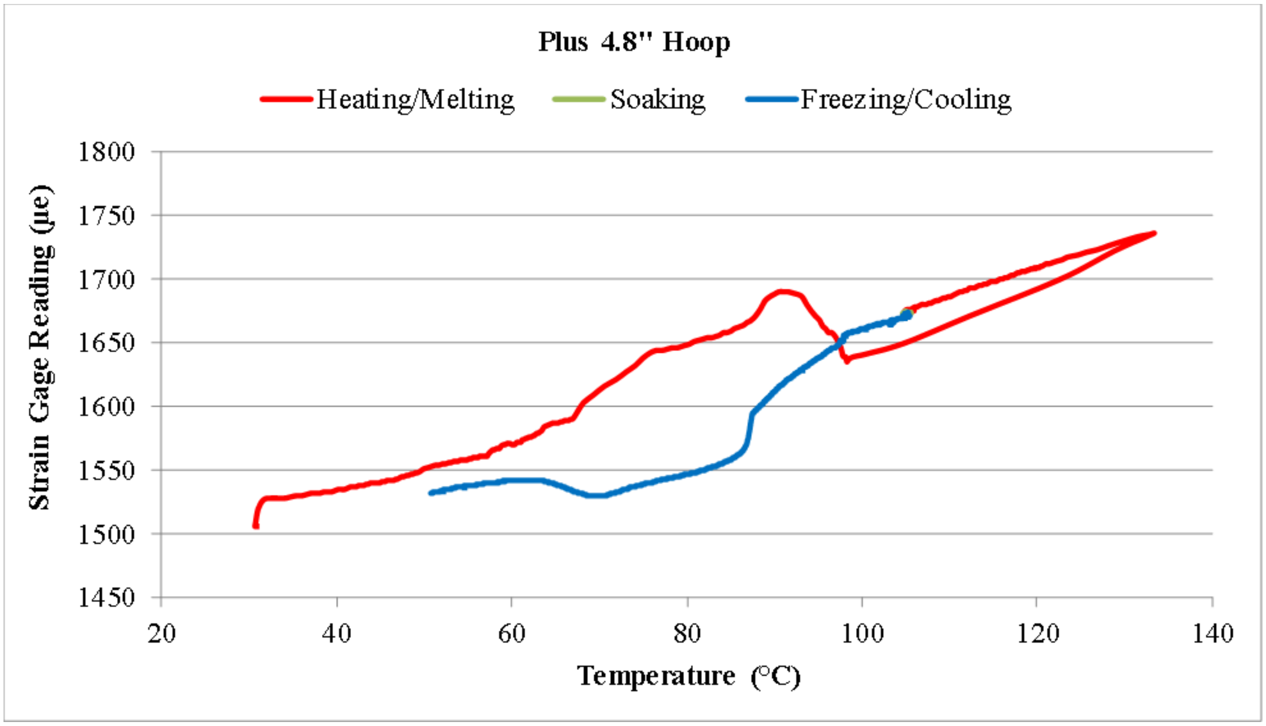

Figure 72. Entire hoop strain history at +4.8" from the test section center in Test 5.

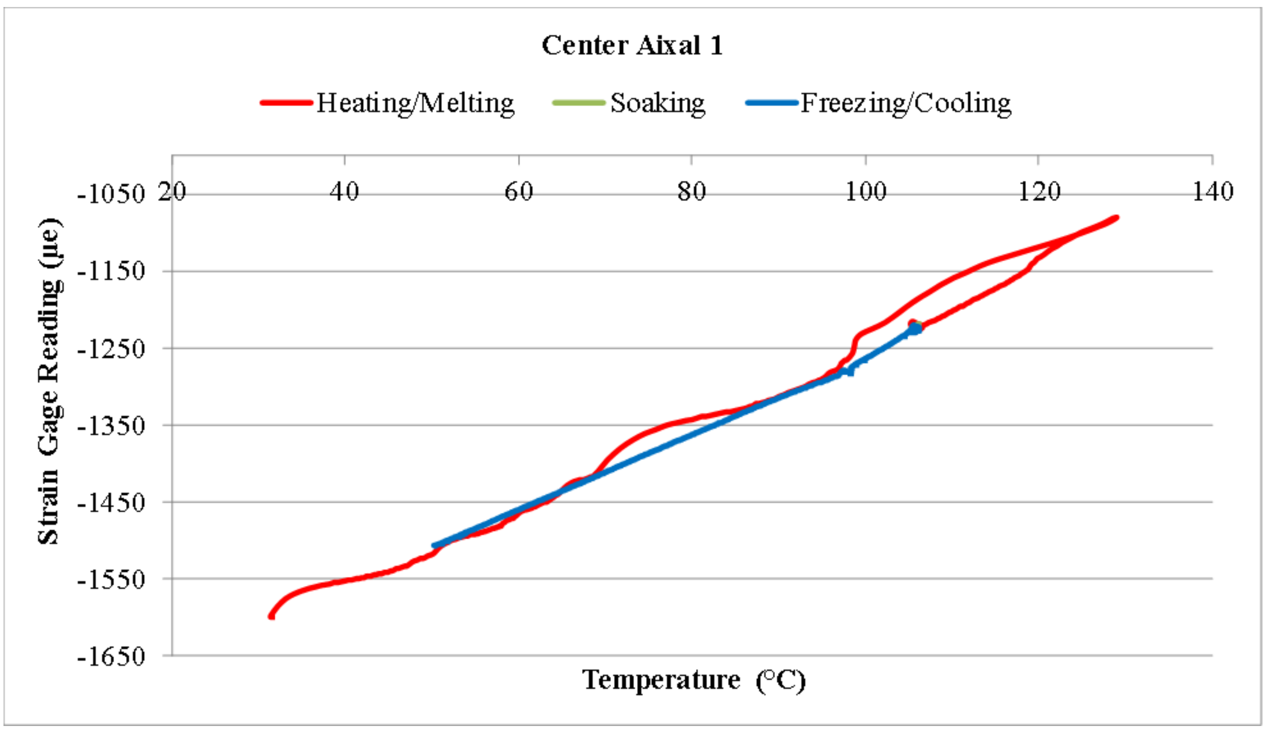

Figure 73. Entire axial strain 1 history at the test section center in Test 5.

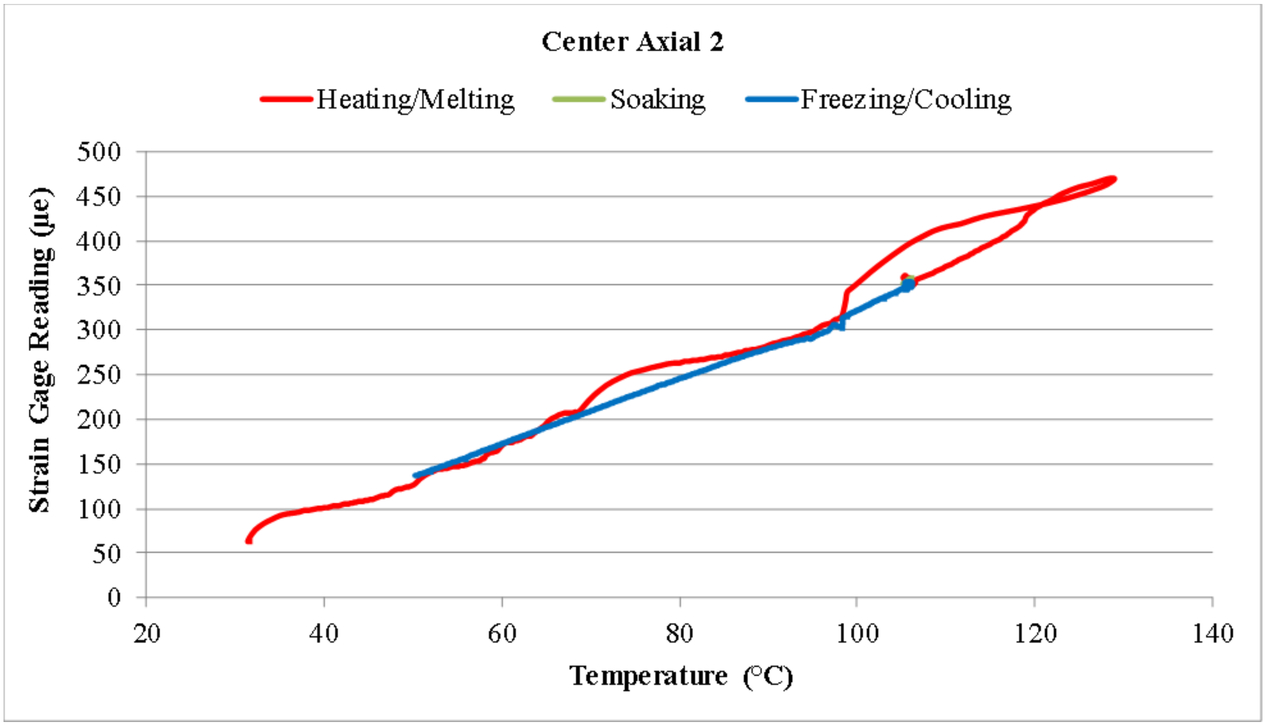

Figure 74. Entire axial strain 2 history at the test section center in Test 5.

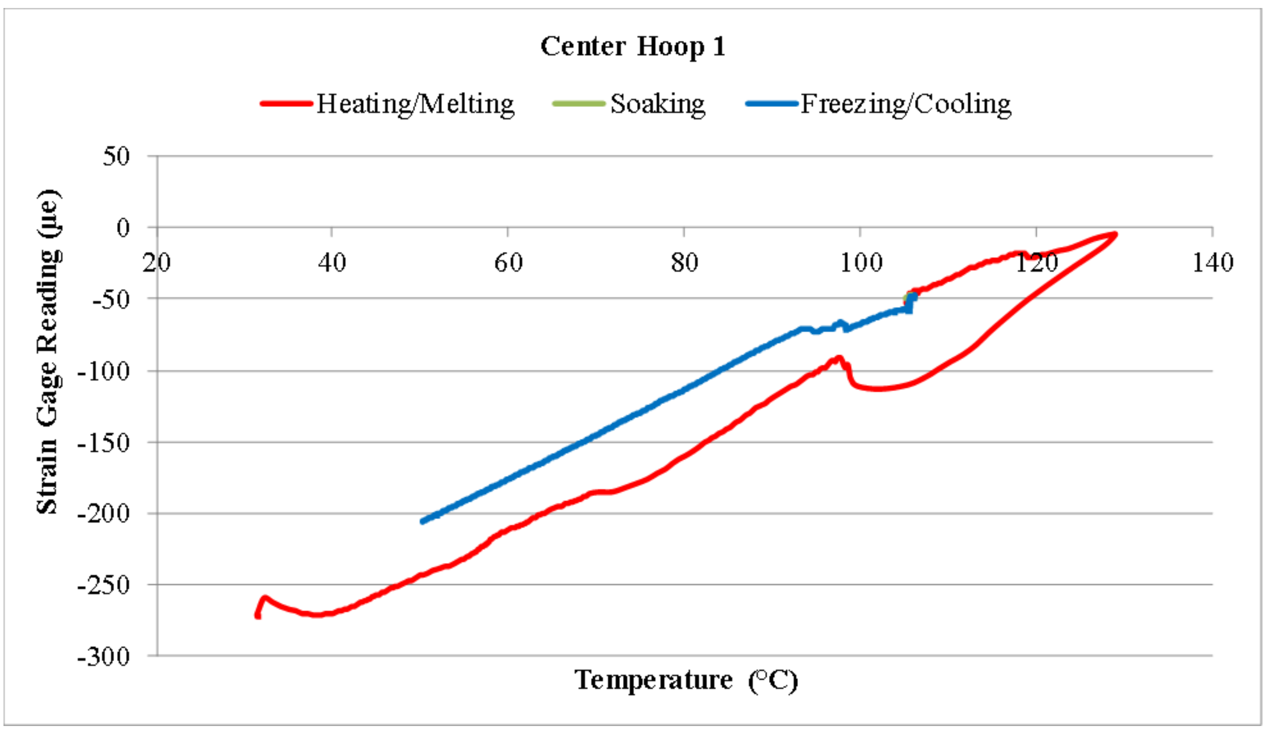

Figure 75. Entire hoop strain 1 history at the test section center in Test 5.

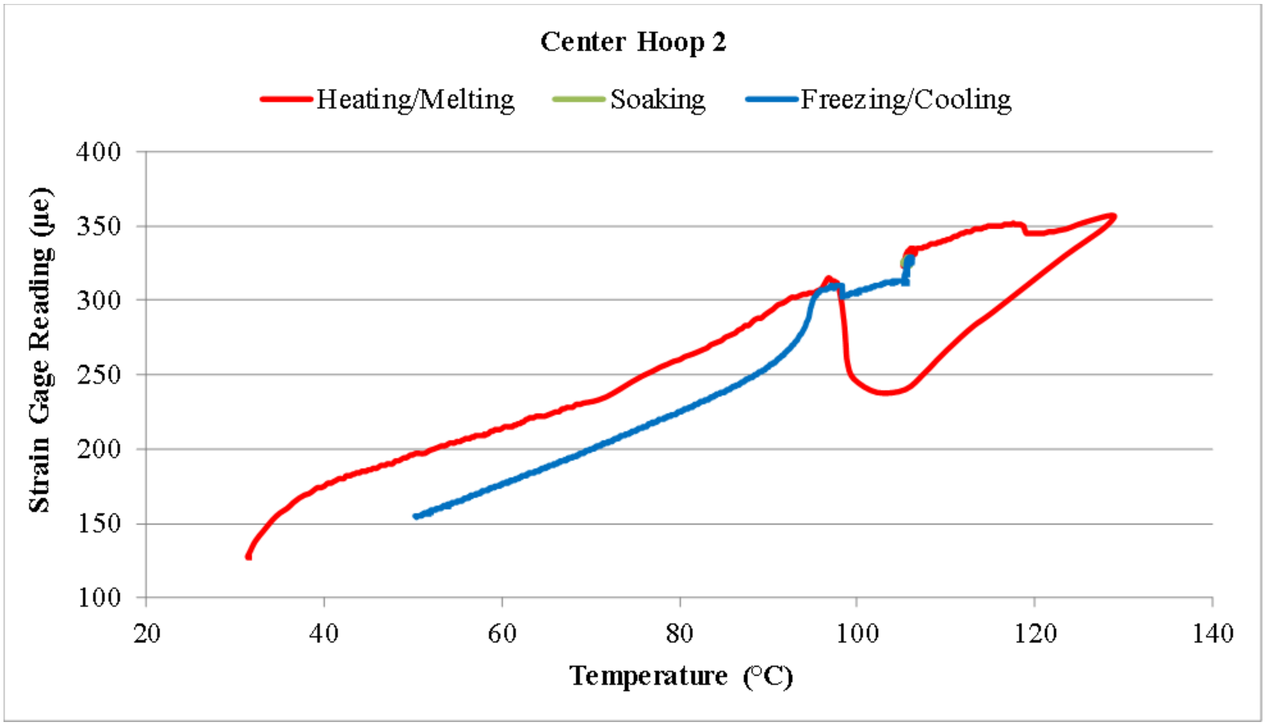

Figure 76. Entire hoop strain 2 history at the test section center in Test 5.

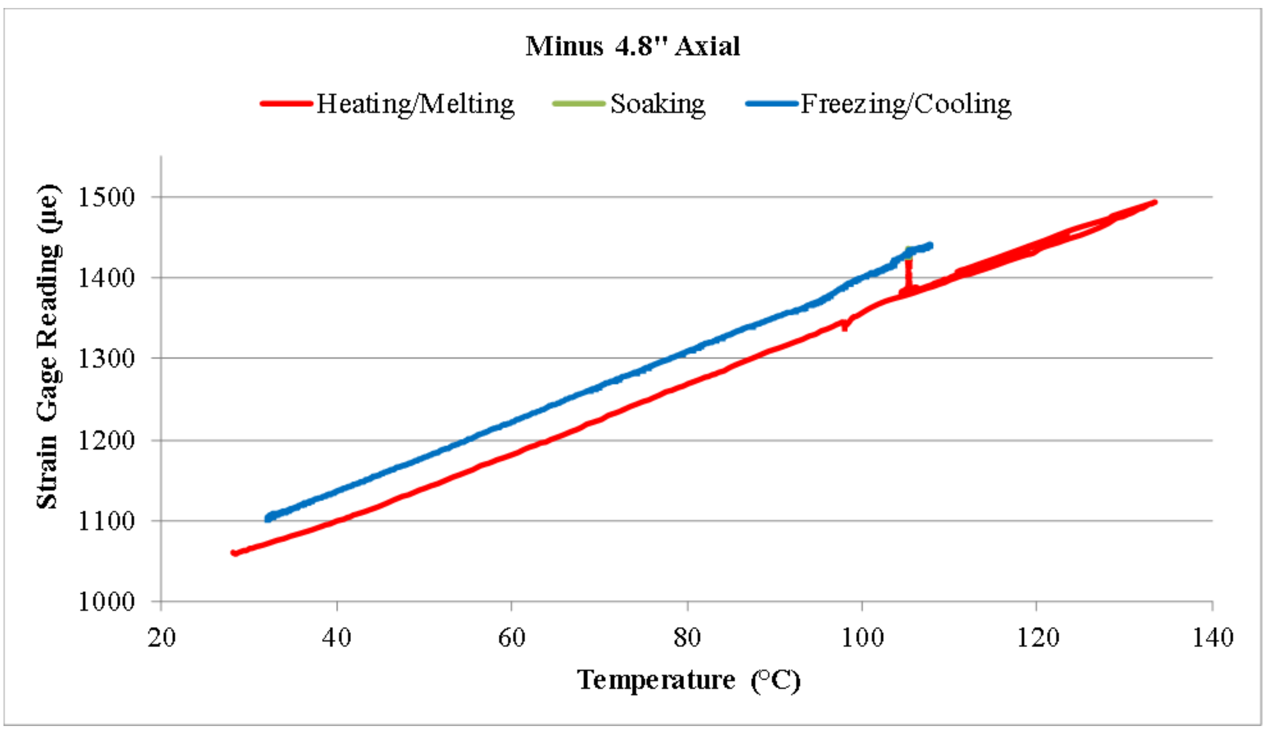

Figure 77. Entire axial strain history at –4.8” from the test section center in Test 4.

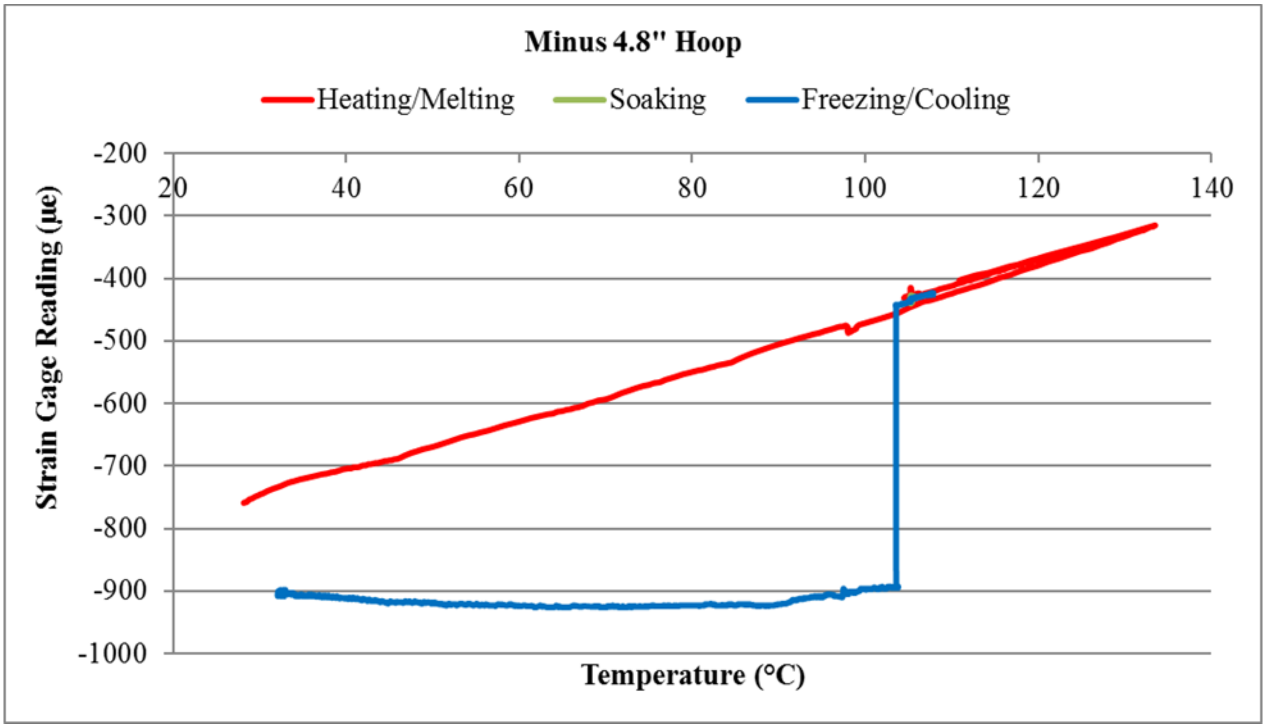

Figure 78. Entire hoop strain history at -4.8” from the test section center in Test 4.

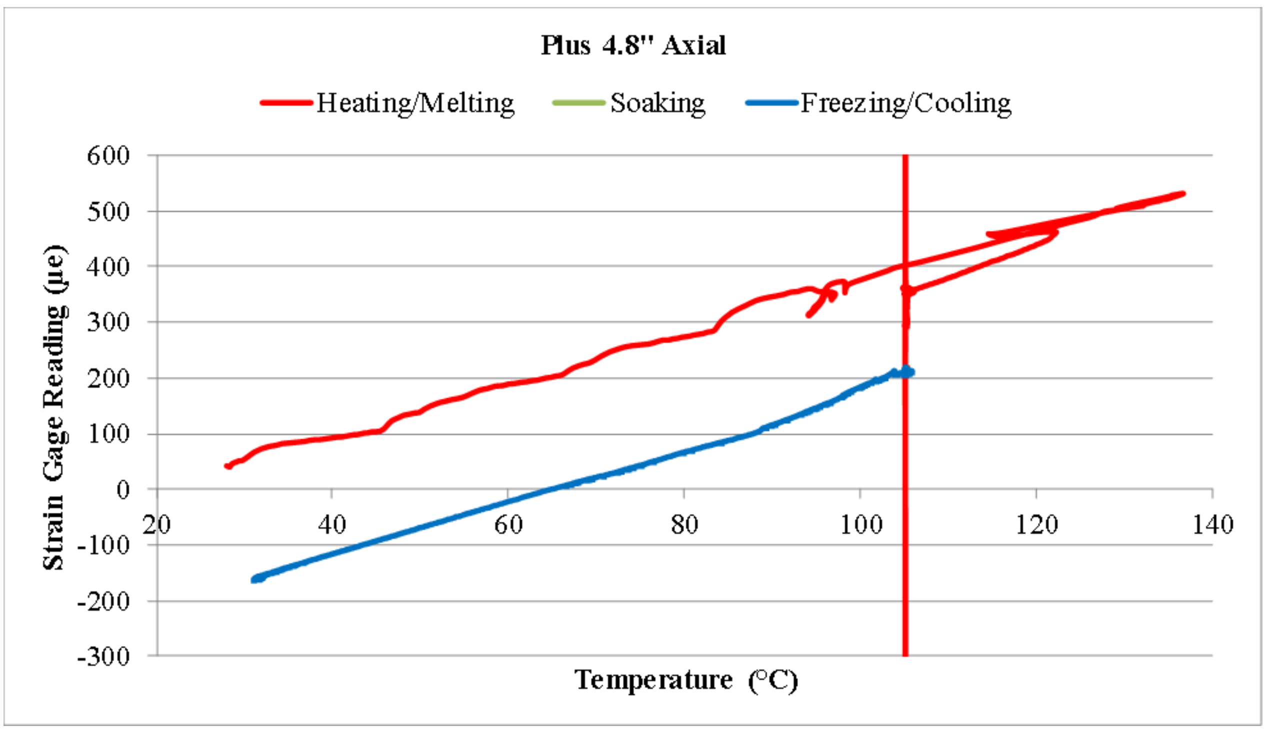

Figure 79. Entire axial strain history at +4.8” from the test section center in Test 4.

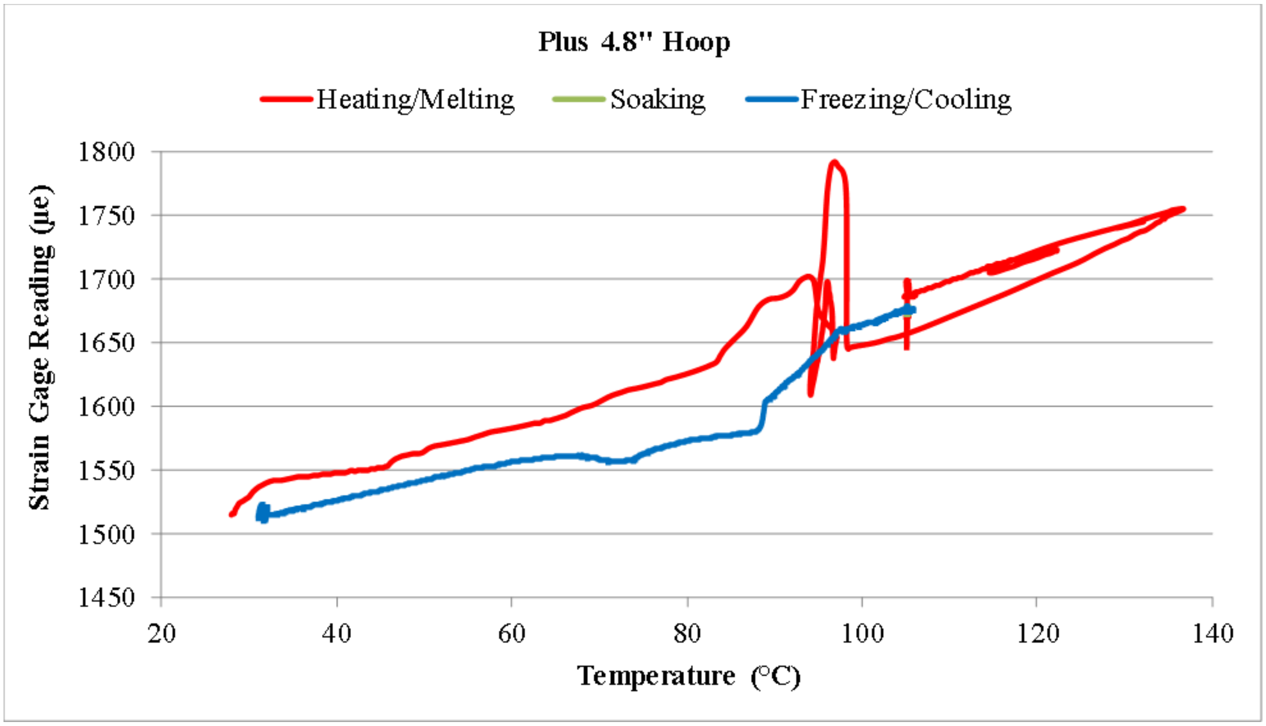

Figure 80. Entire hoop strain history at +4.8" from the test section center in Test 4.

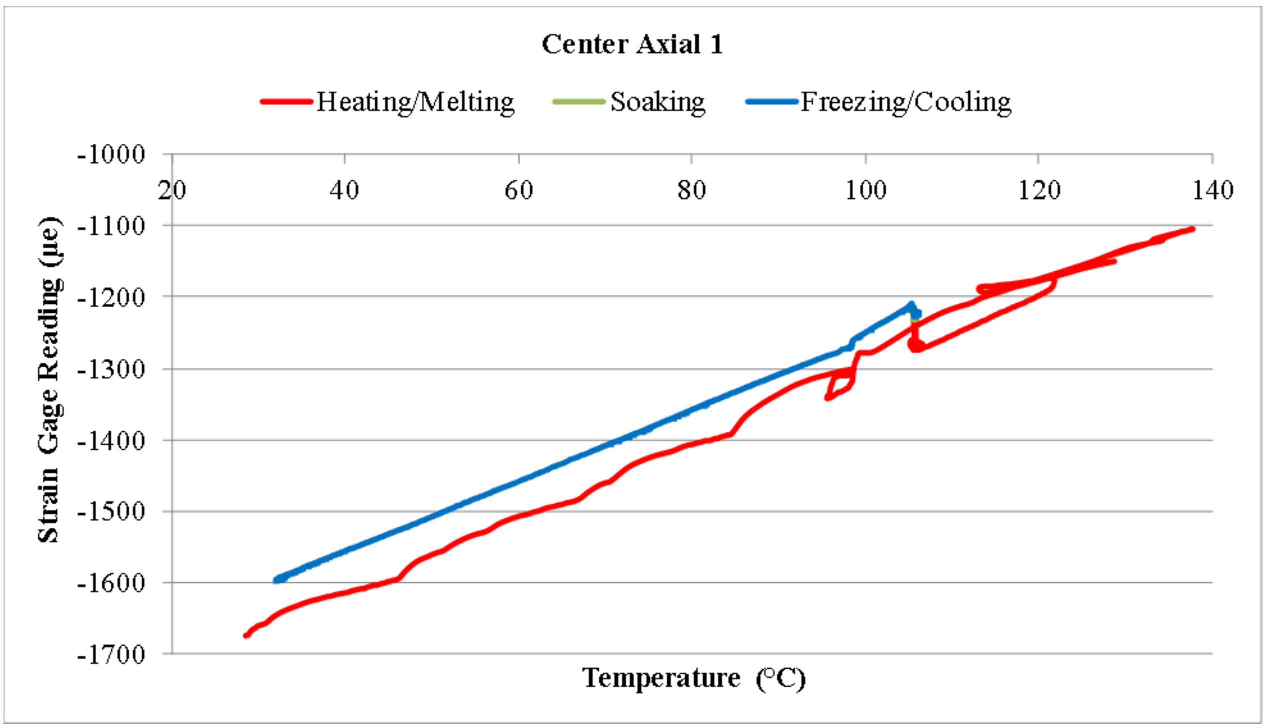

Figure 81. Entire axial strain 1 history at the test section center in Test 4.

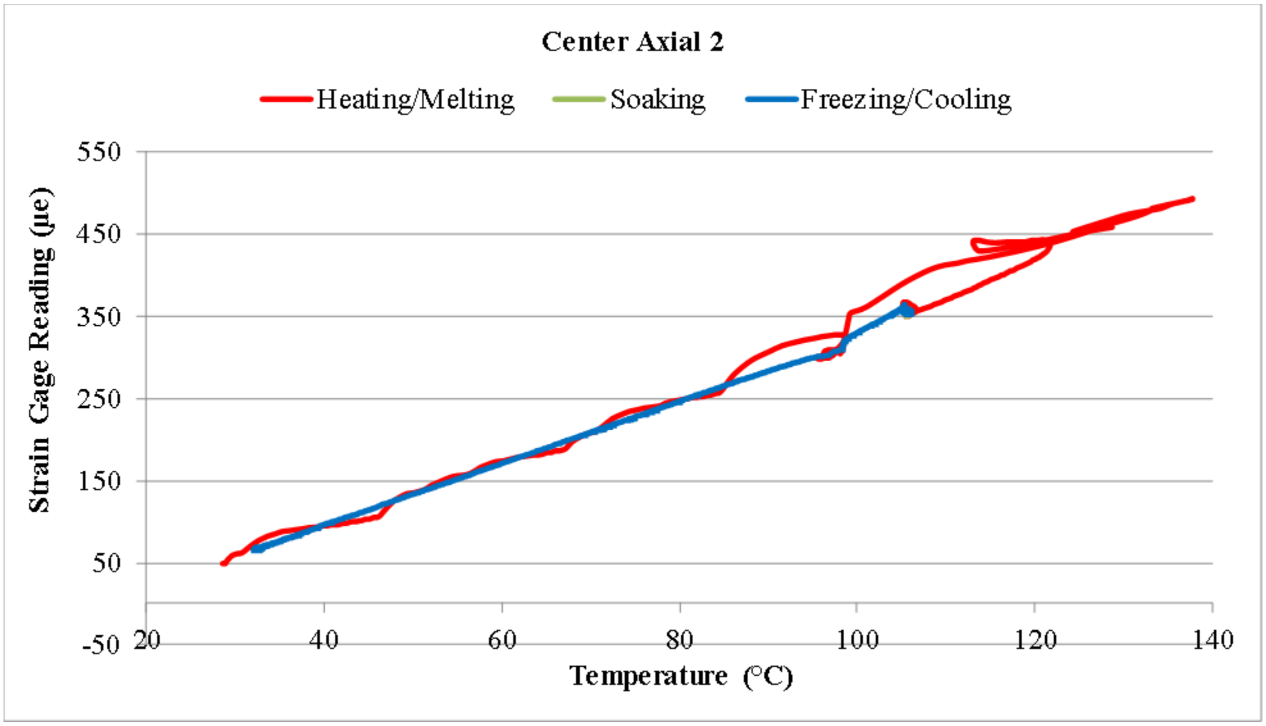

Figure 82. Entire axial strain 2 history at the test section center in Test 4.

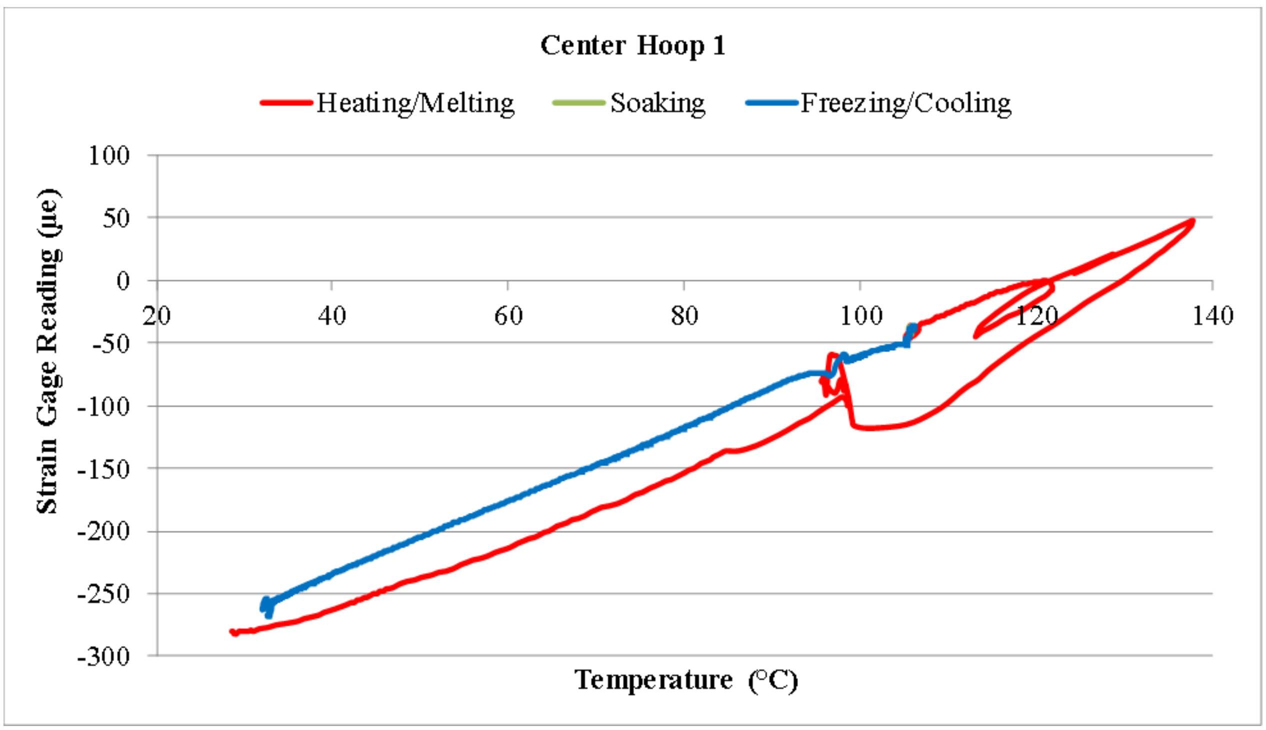

Figure 83. Entire hoop strain 1 history at the test section center in Test 4.

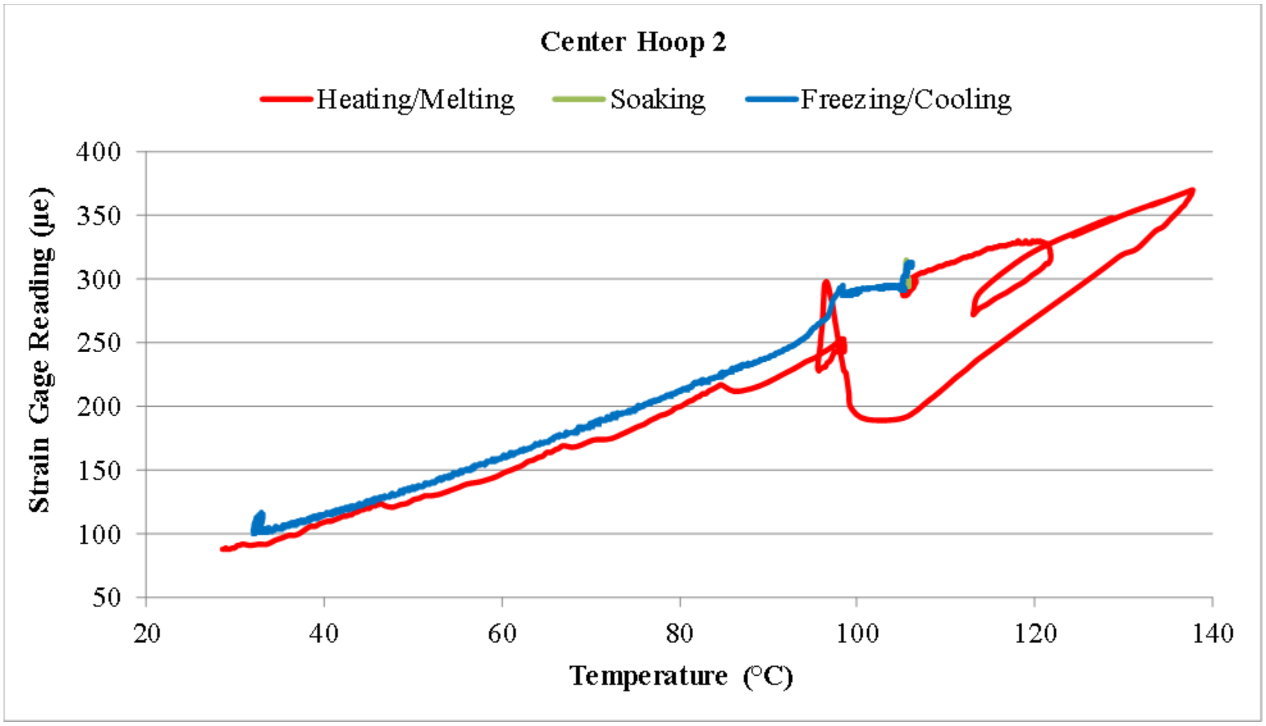

Figure 84. Entire hoop strain 2 history at the test section center in Test 4.

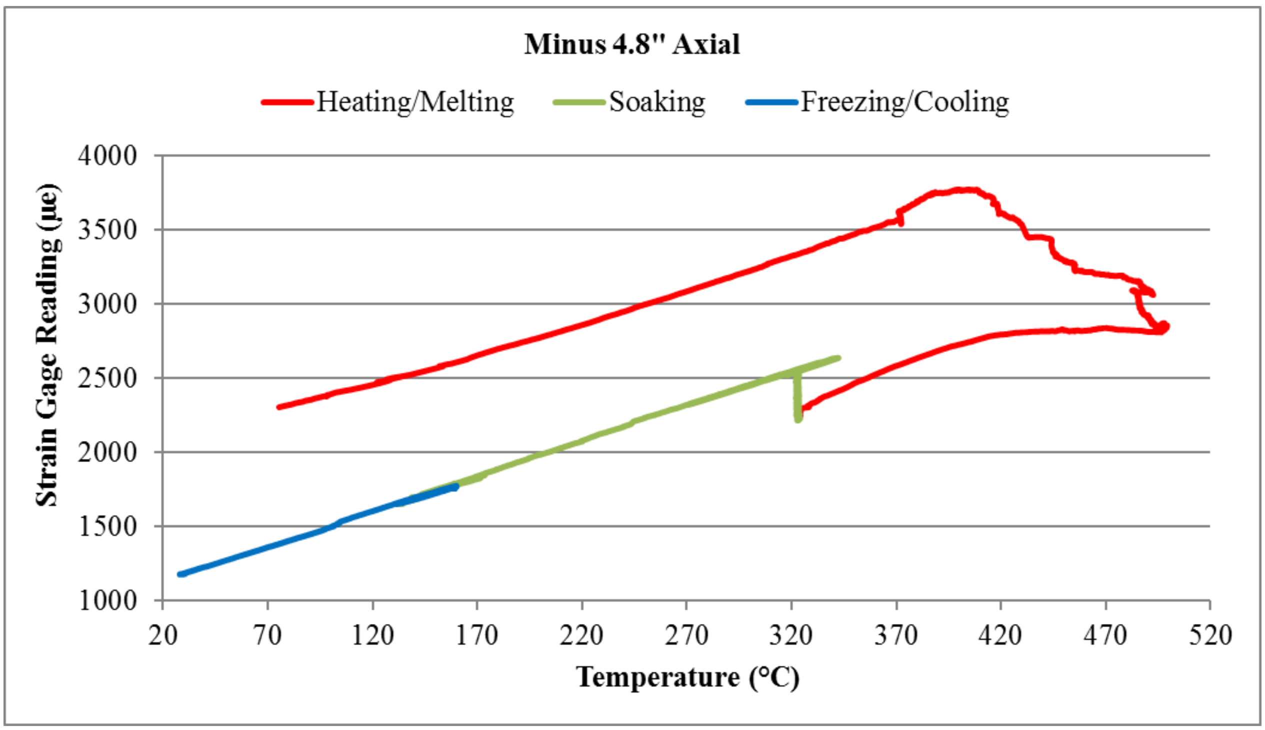

Figure 85. Entire axial strain history at –4.8” from the test section center in Test 3.

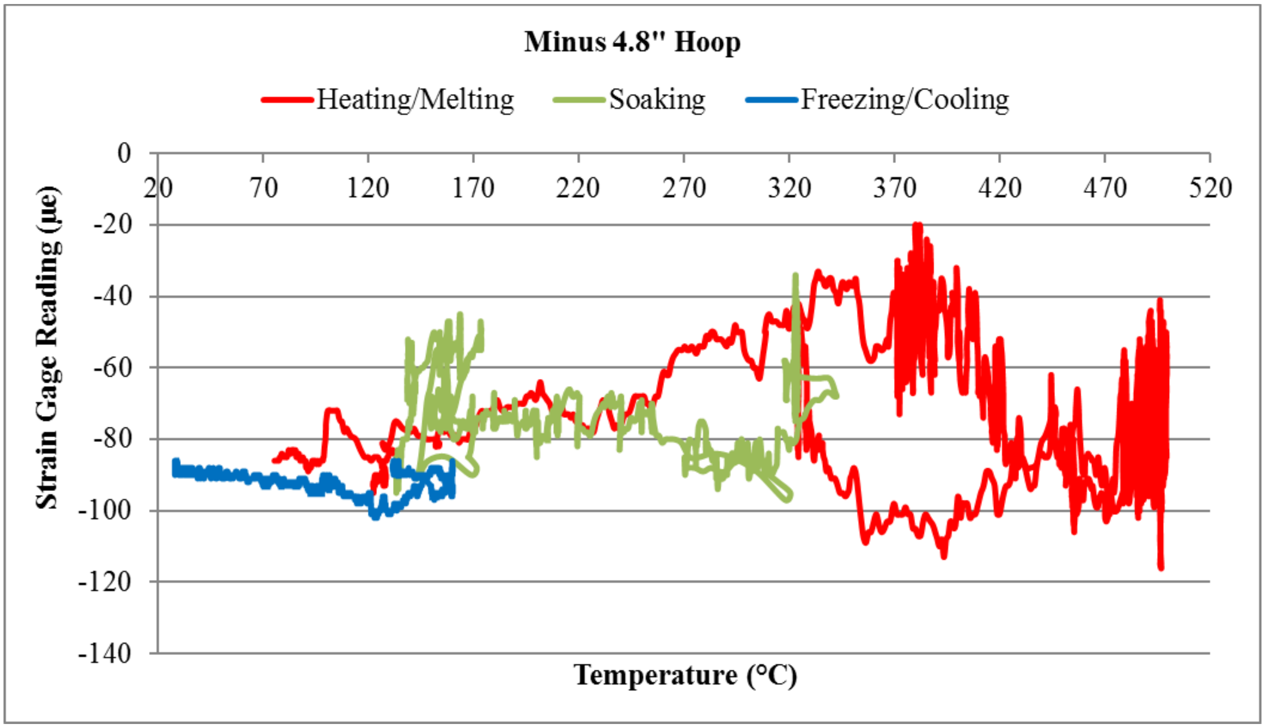

Figure 86. Entire hoop strain history at -4.8” from the test section center in Test 3.

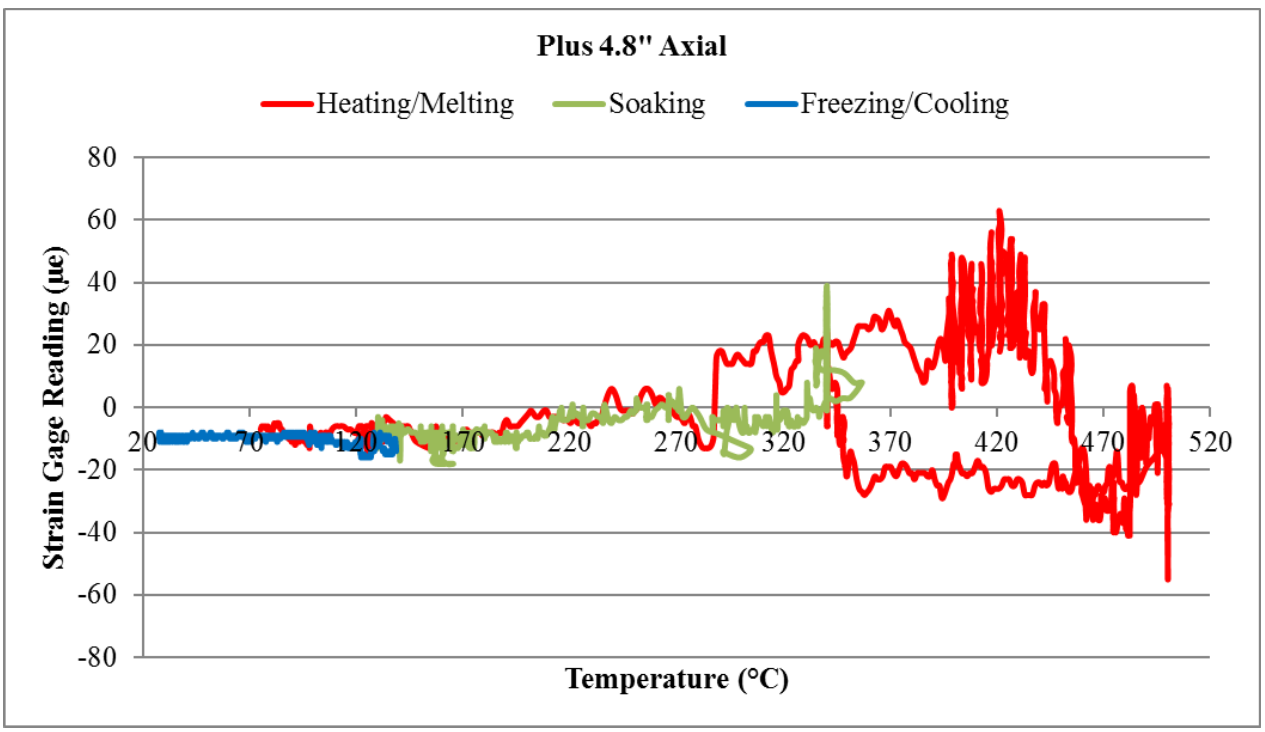

Figure 87. Entire axial strain history at +4.8” from the test section center in Test 3.

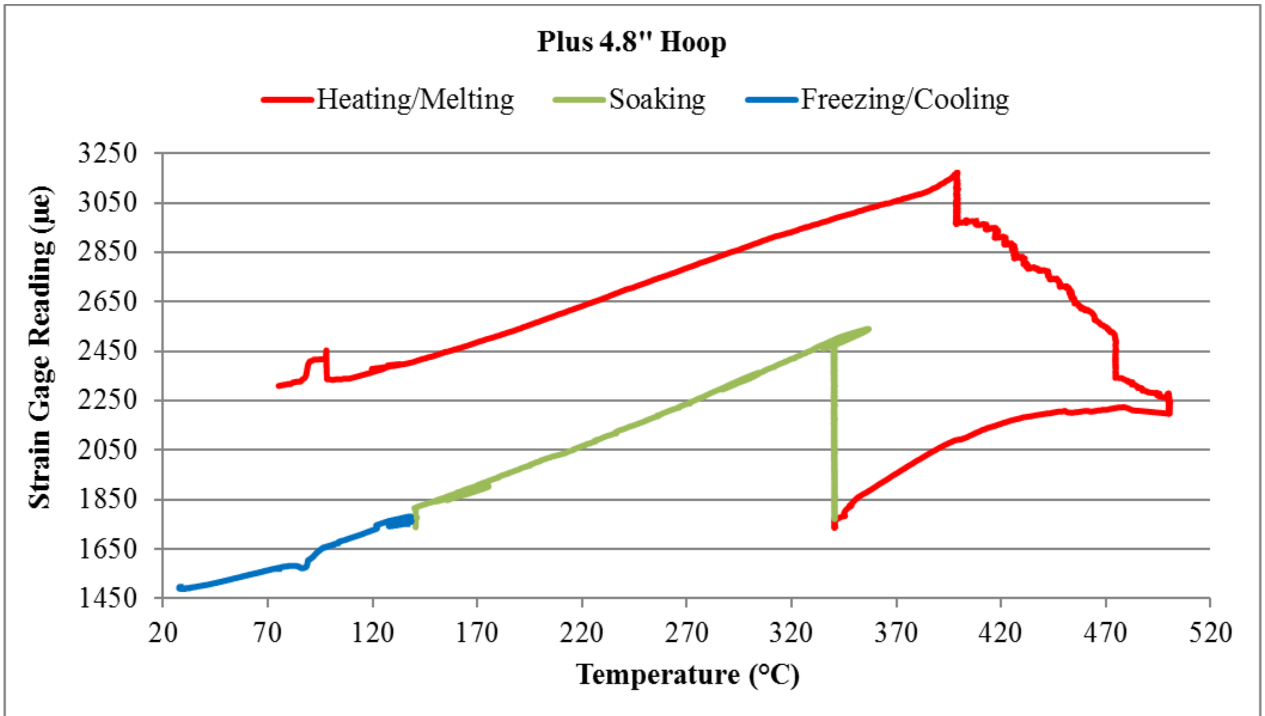

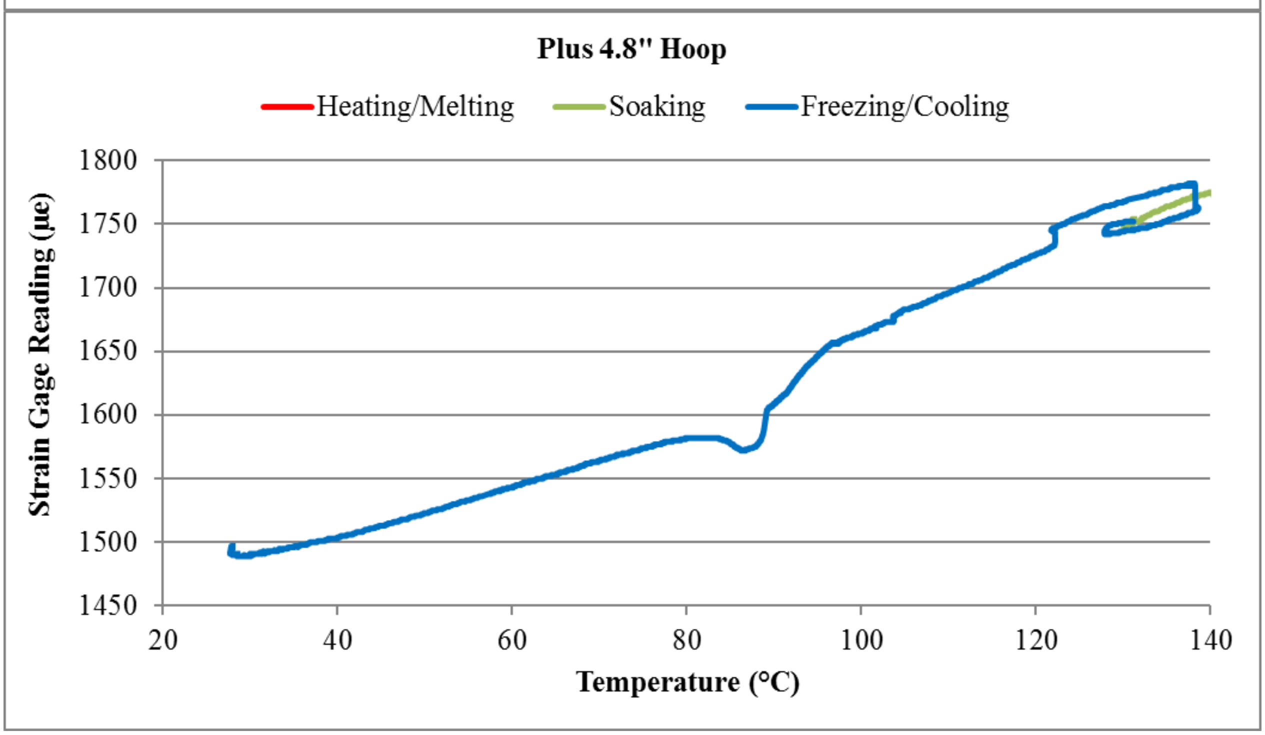

Figure 88. Entire hoop strain history (top) and zoom in of Freezing/Cooling phase (bottom) at +4.8" from the test section center in Test 3.

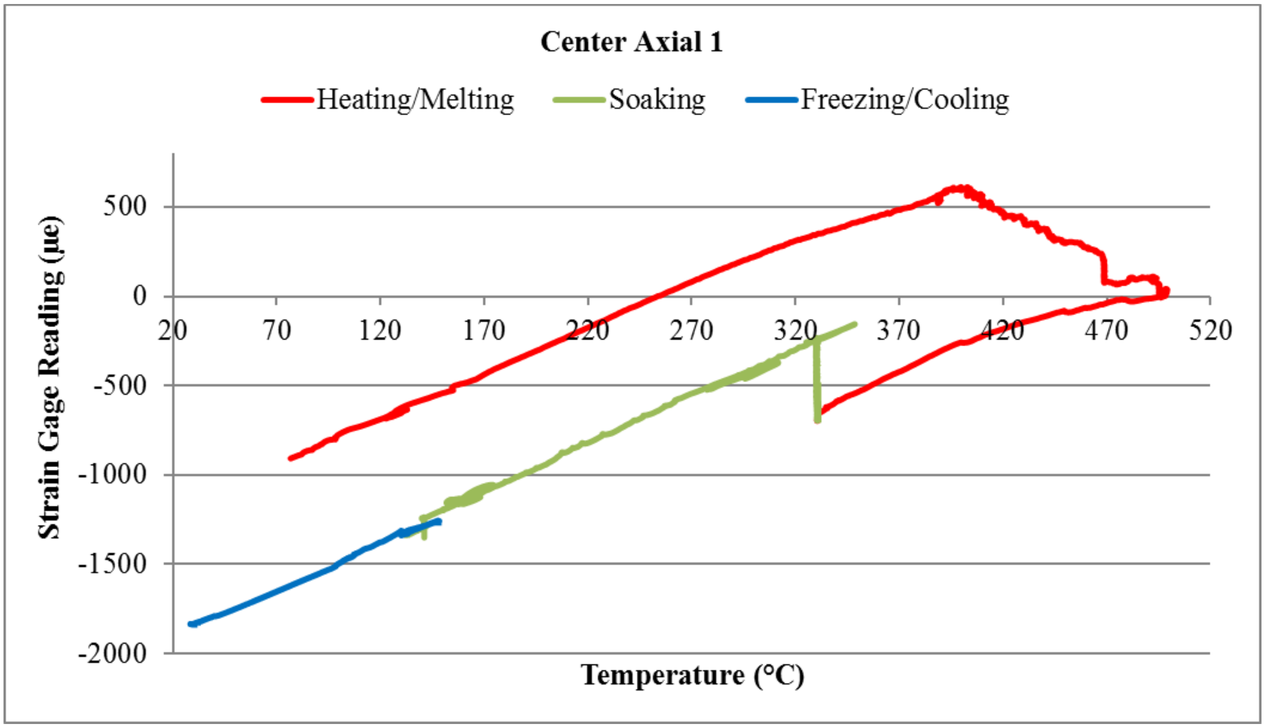

Figure 89. Entire axial strain 1 history at the test section center in Test 3.

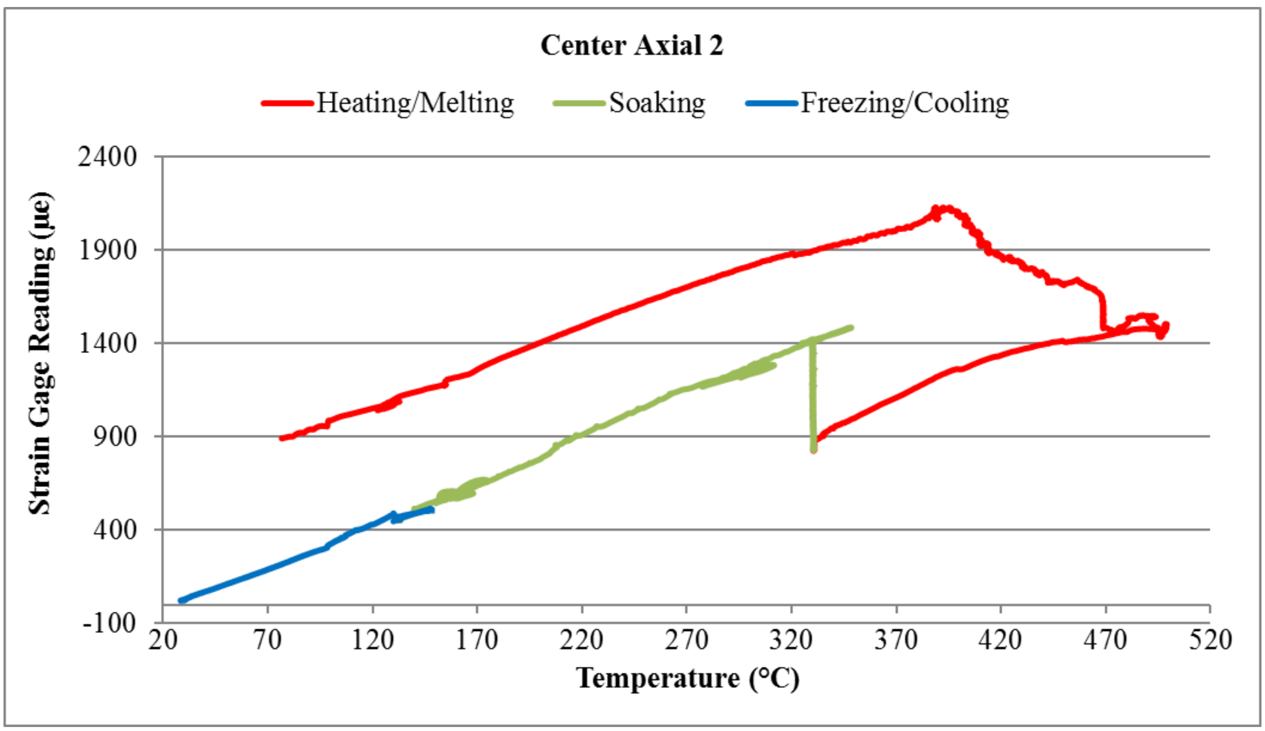

Figure 90. Entire axial strain 2 history at the test section center in Test 3.

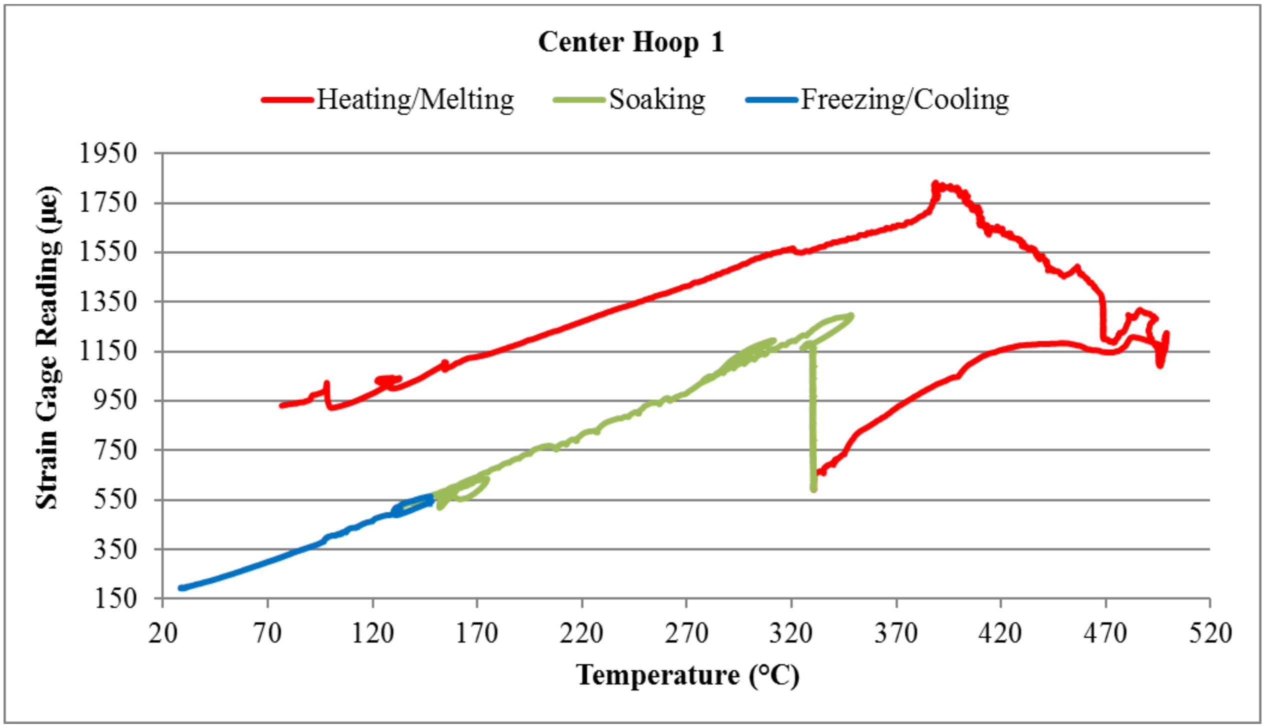

Figure 91. Entire hoop strain 1 history at the test section center in Test 3.

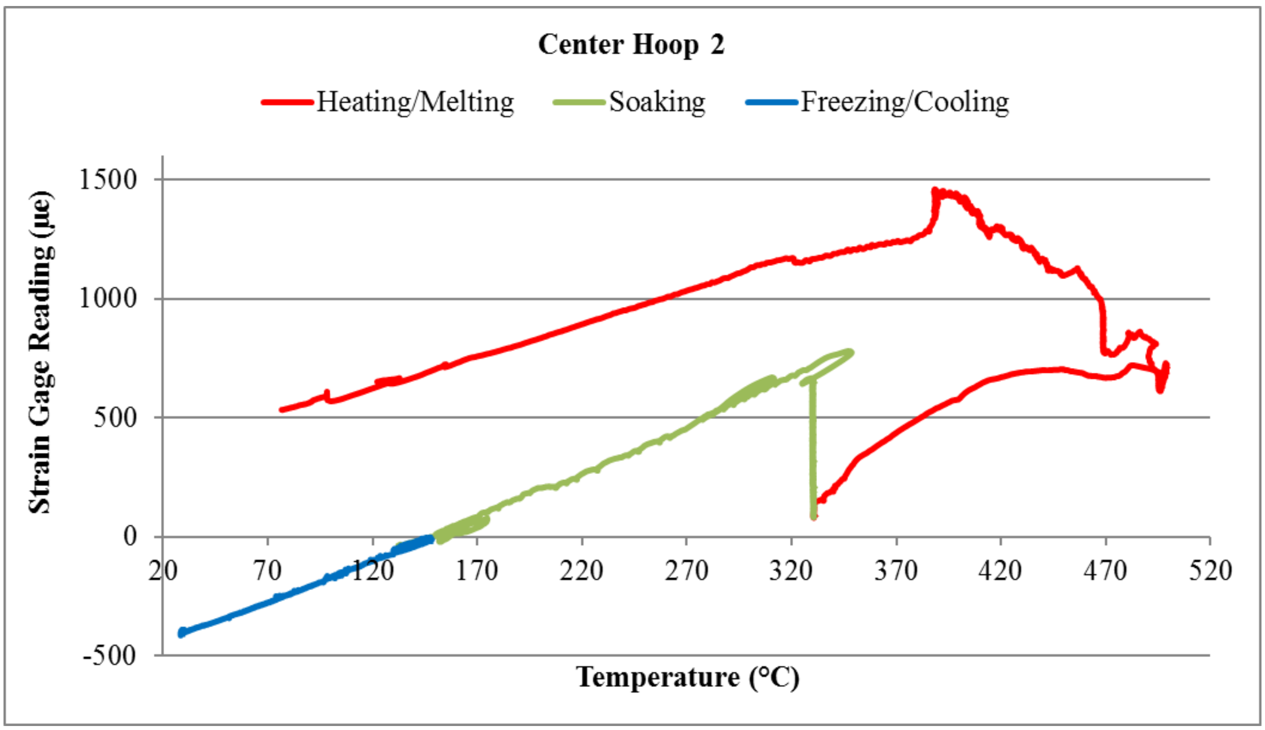

Figure 92. Entire hoop strain 2 history at the test section center in Test 3.

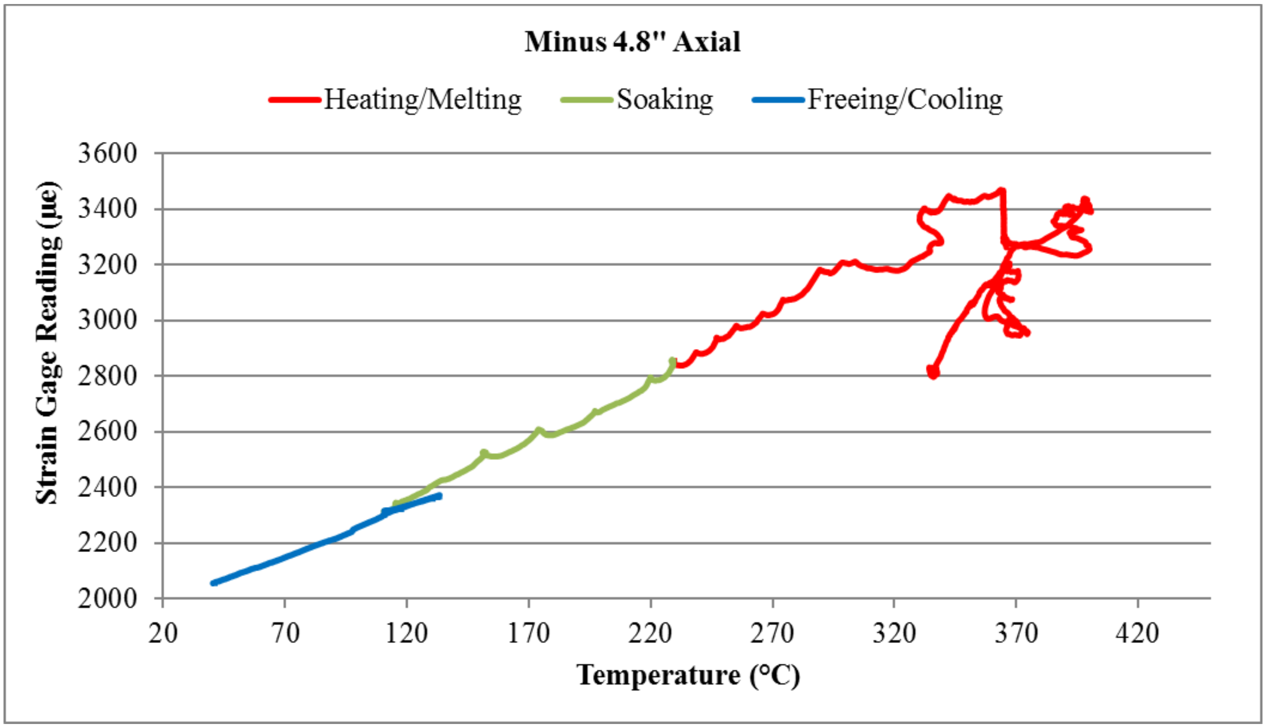

Figure 93. Entire axial strain history at –4.8" from the test section center in Test 2.

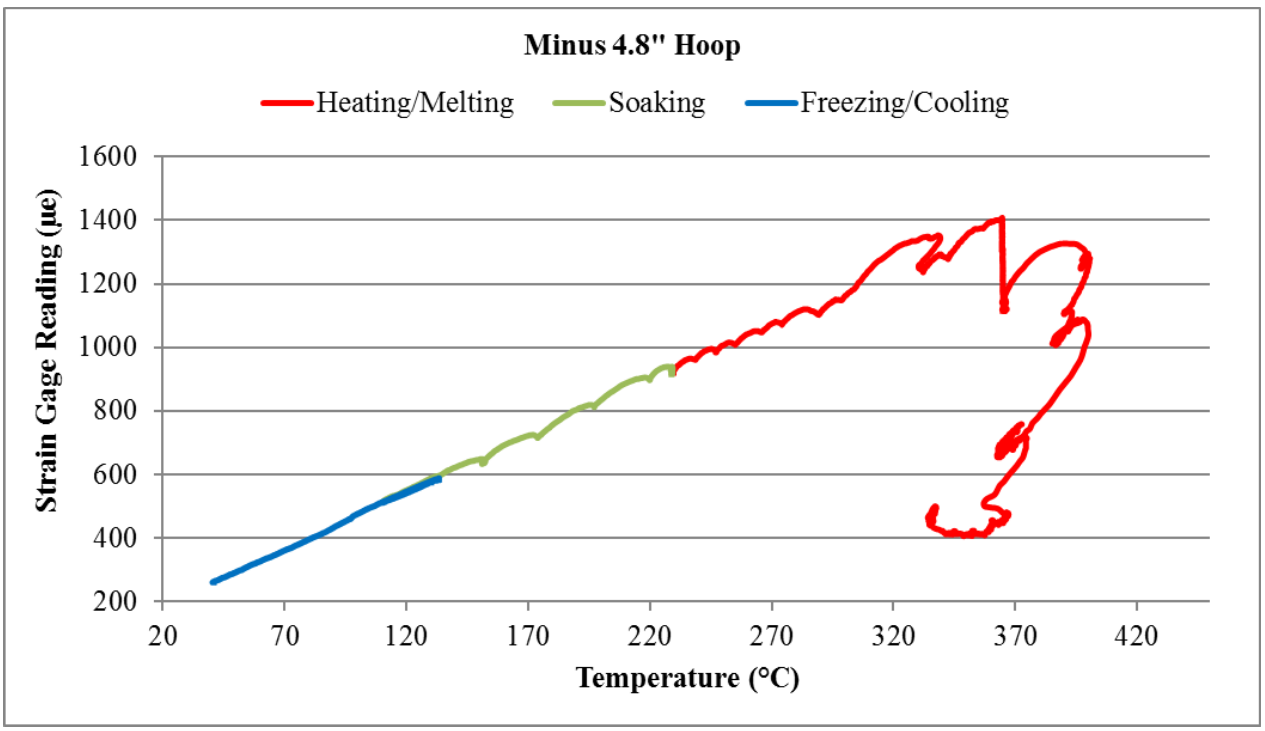

Figure 94. Entire hoop strain history at -4.8" from the test section center in Test 2.

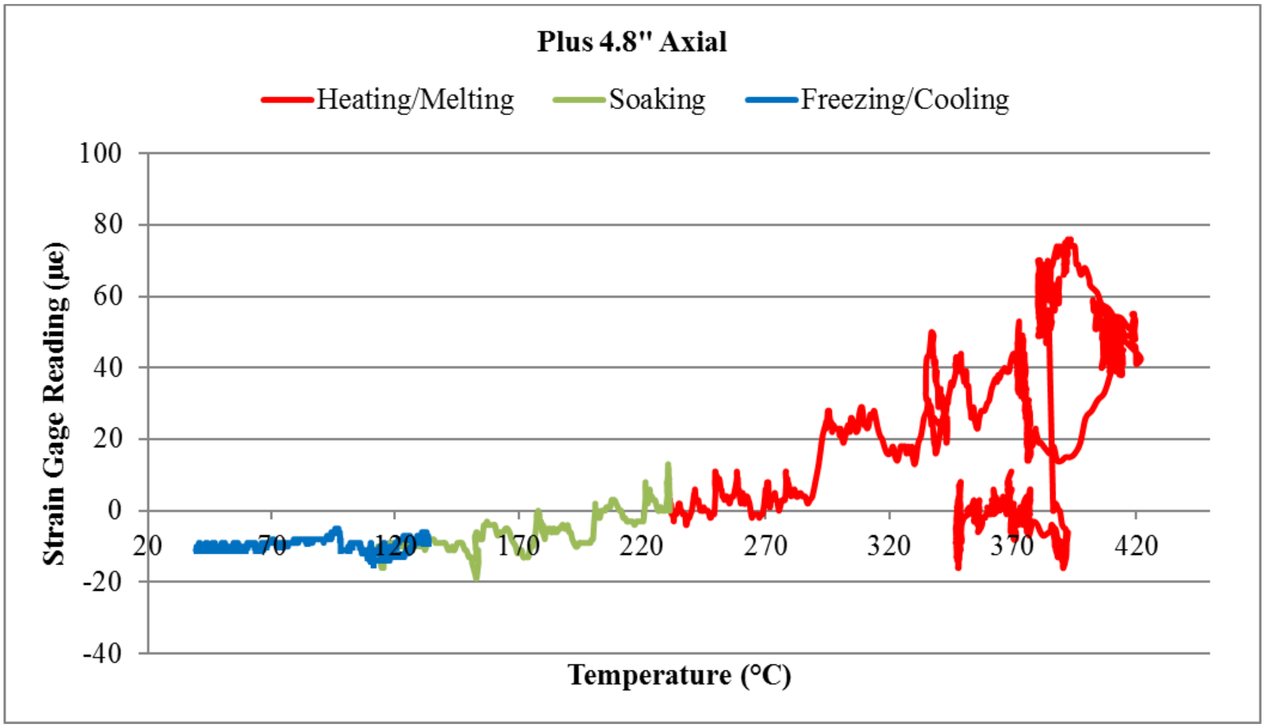

Figure 95. Entire axial strain history at +4.8" from the test section center in Test 2.

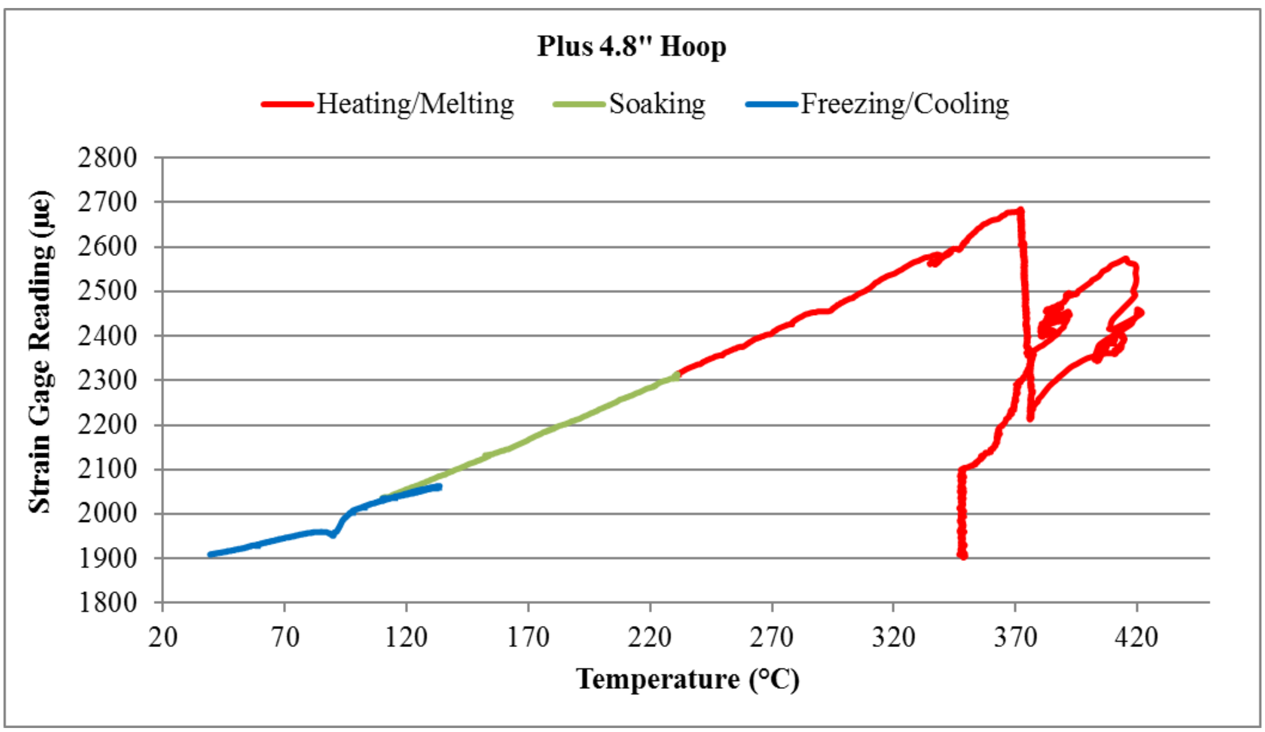

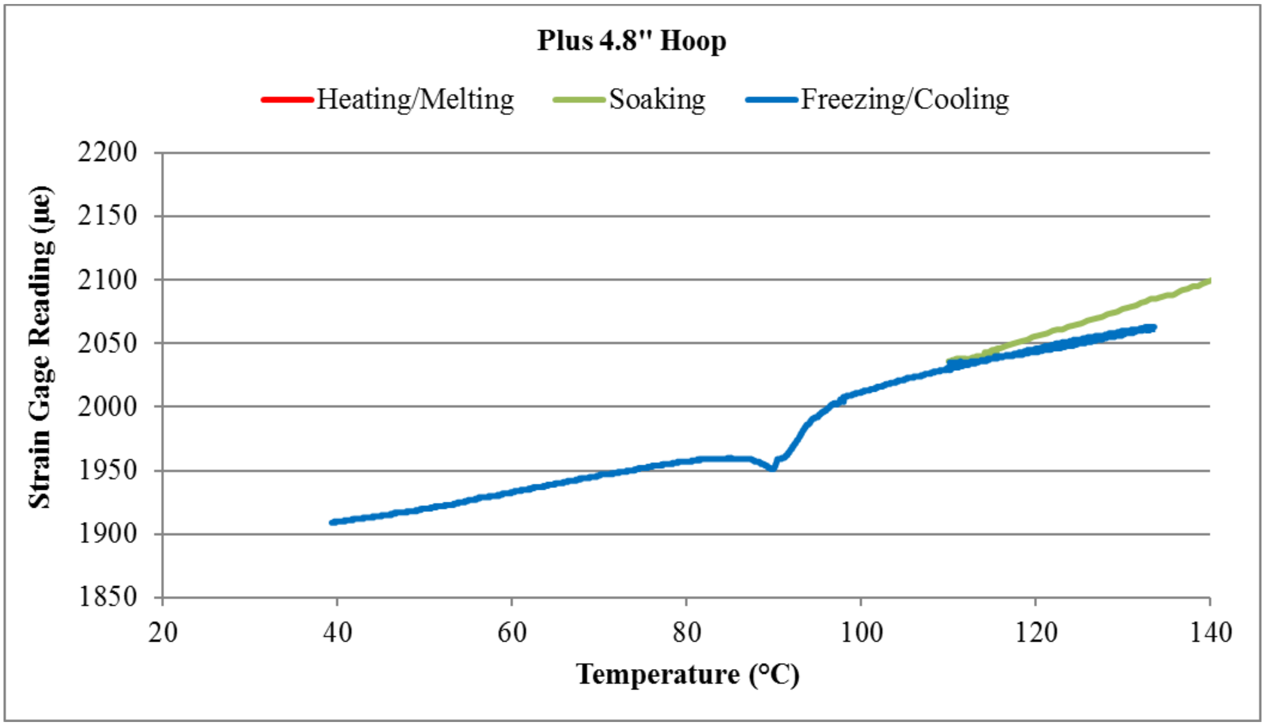

Figure 96. Entire hoop strain history (top) and zoom in of Freezing/Cooling phase (bottom) at +4.8" from the test section center in Test 2.

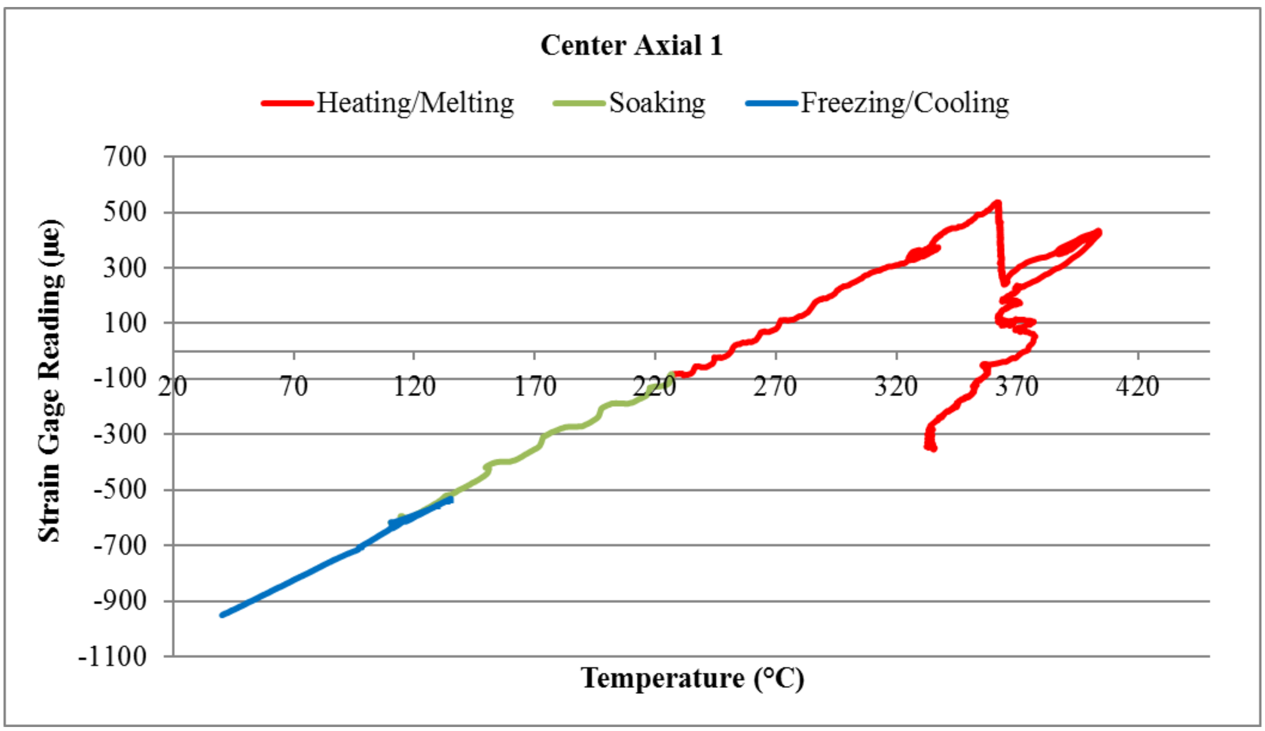

Figure 97. Entire axial strain 1 history at the test section center in Test 2.

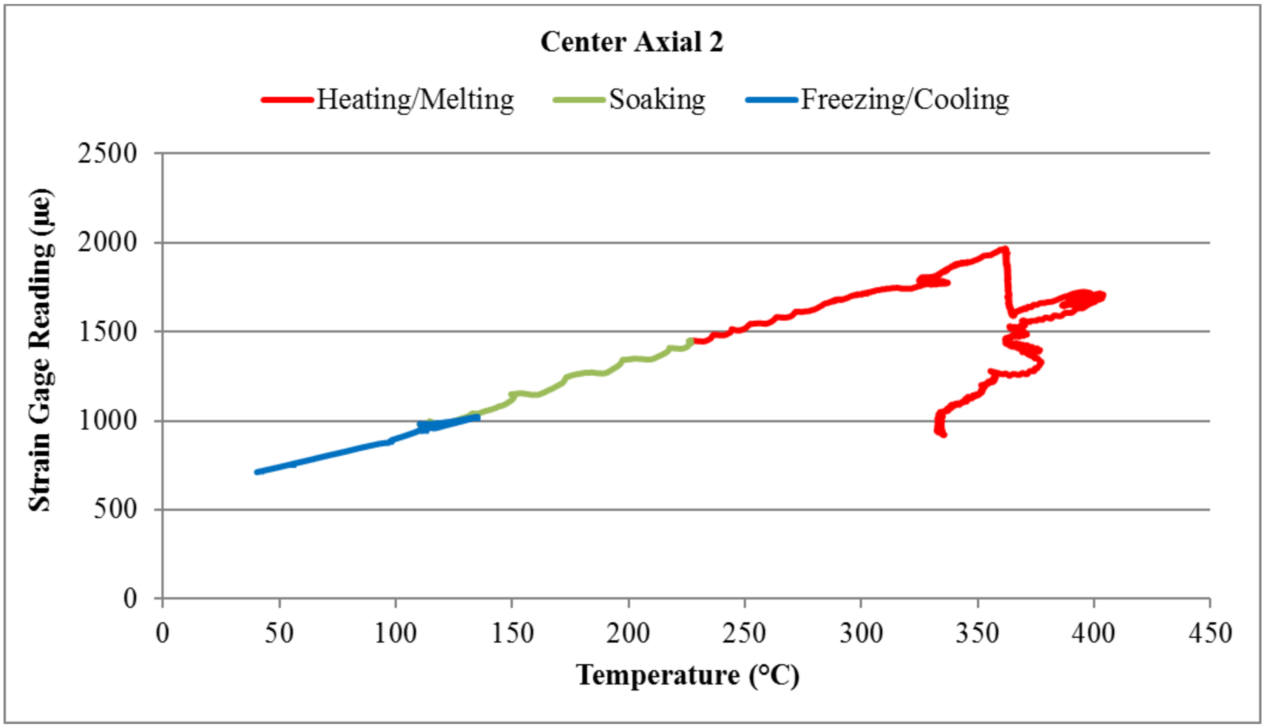

Figure 98. Entire axial strain 2 history at the test section center in Test 2.

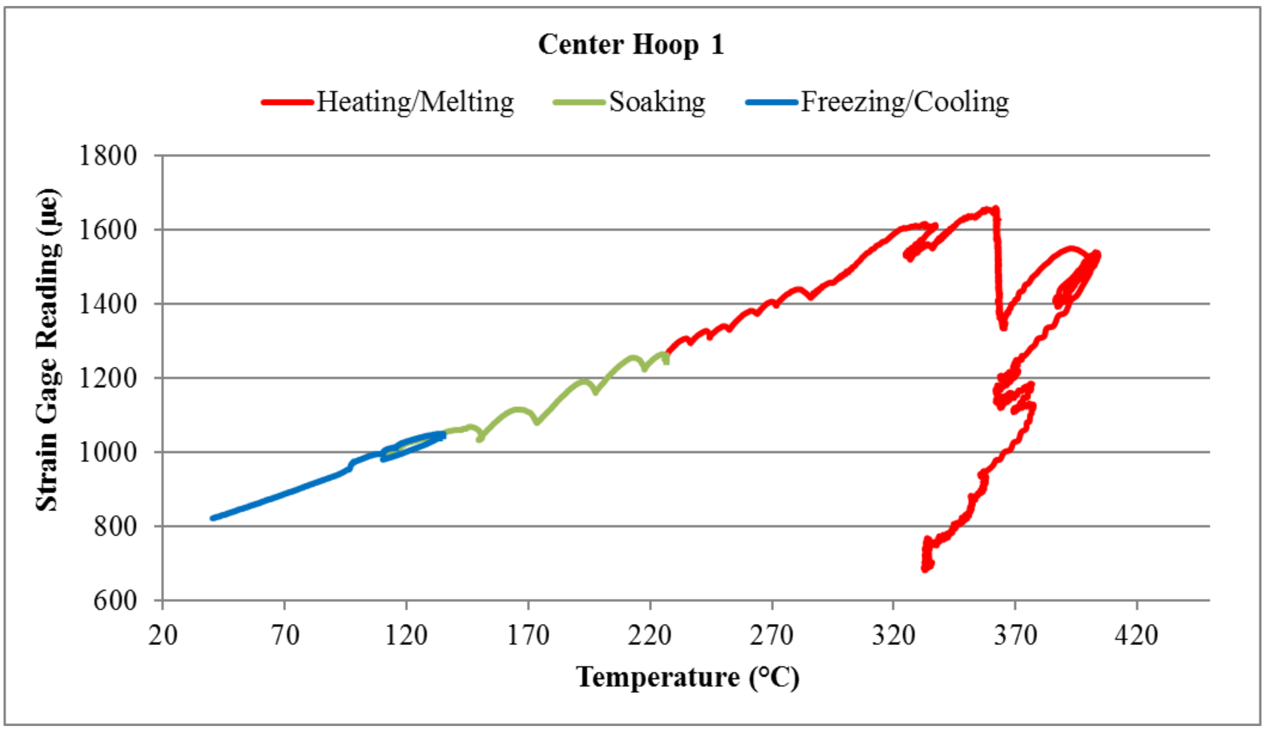

Figure 99. Entire hoop strain 1 history at the test section center in Test 2.

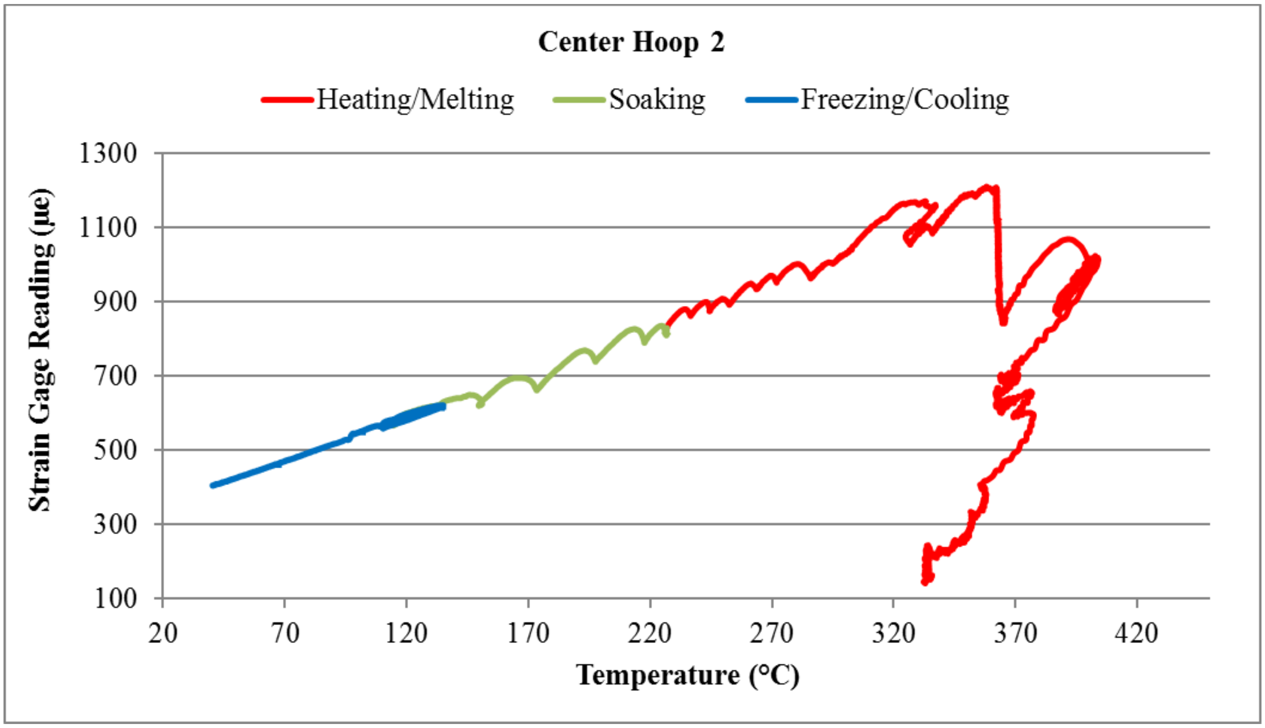

Figure 100. Entire hoop strain 2 history at the test section center in Test 2.

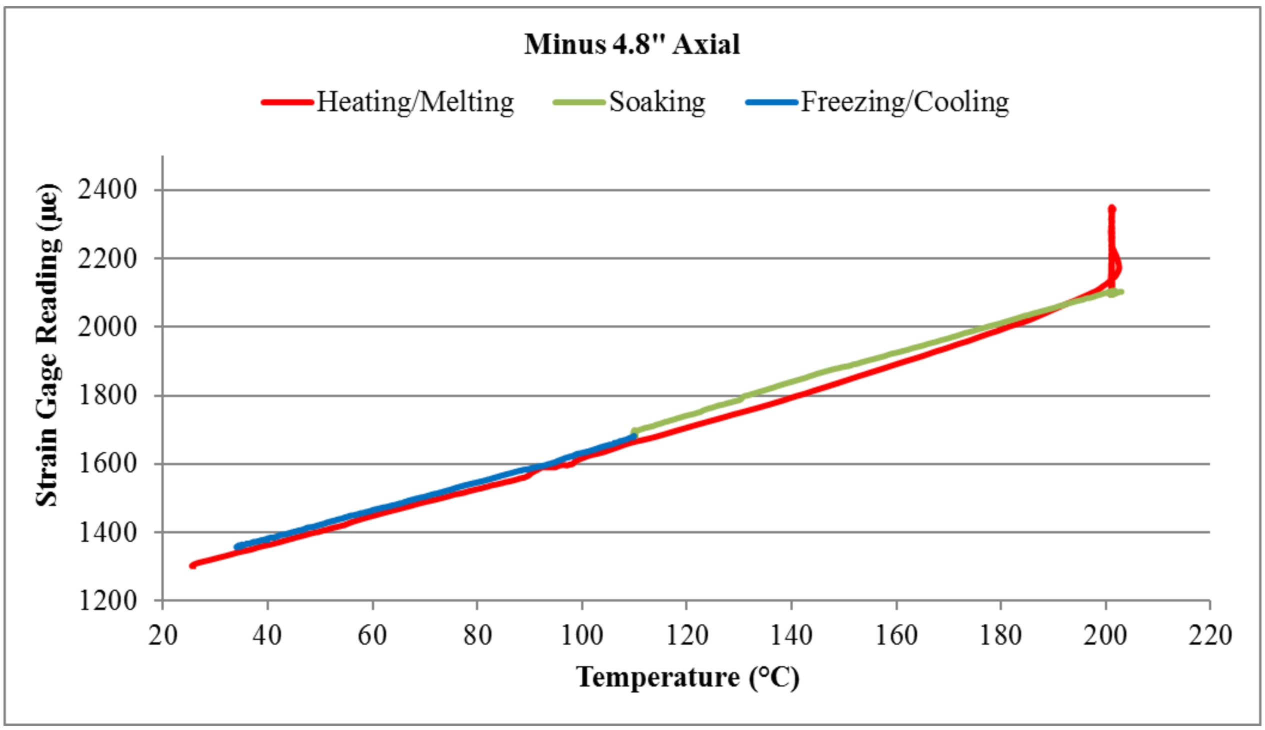

Figure 101. Entire axial strain history at –4.8” from the test section center in Test 1.

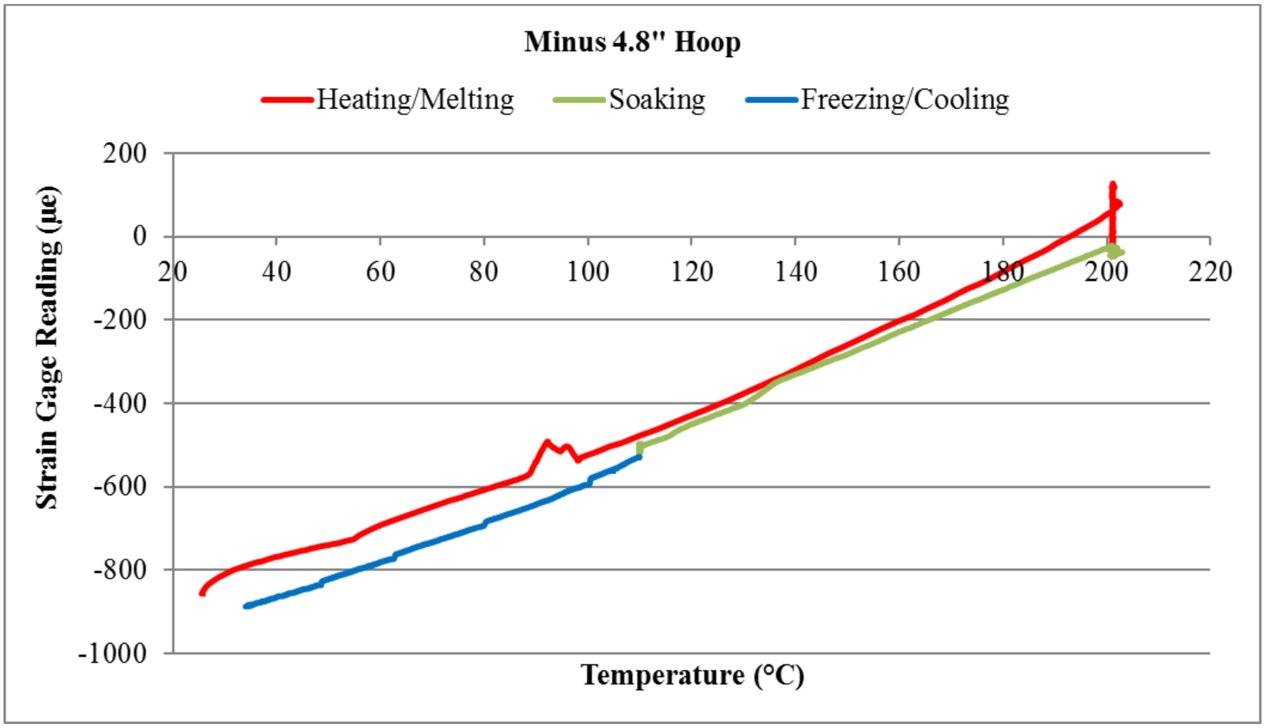

Figure 102. Entire hoop strain history at -4.8" from the test section center in Test 1.

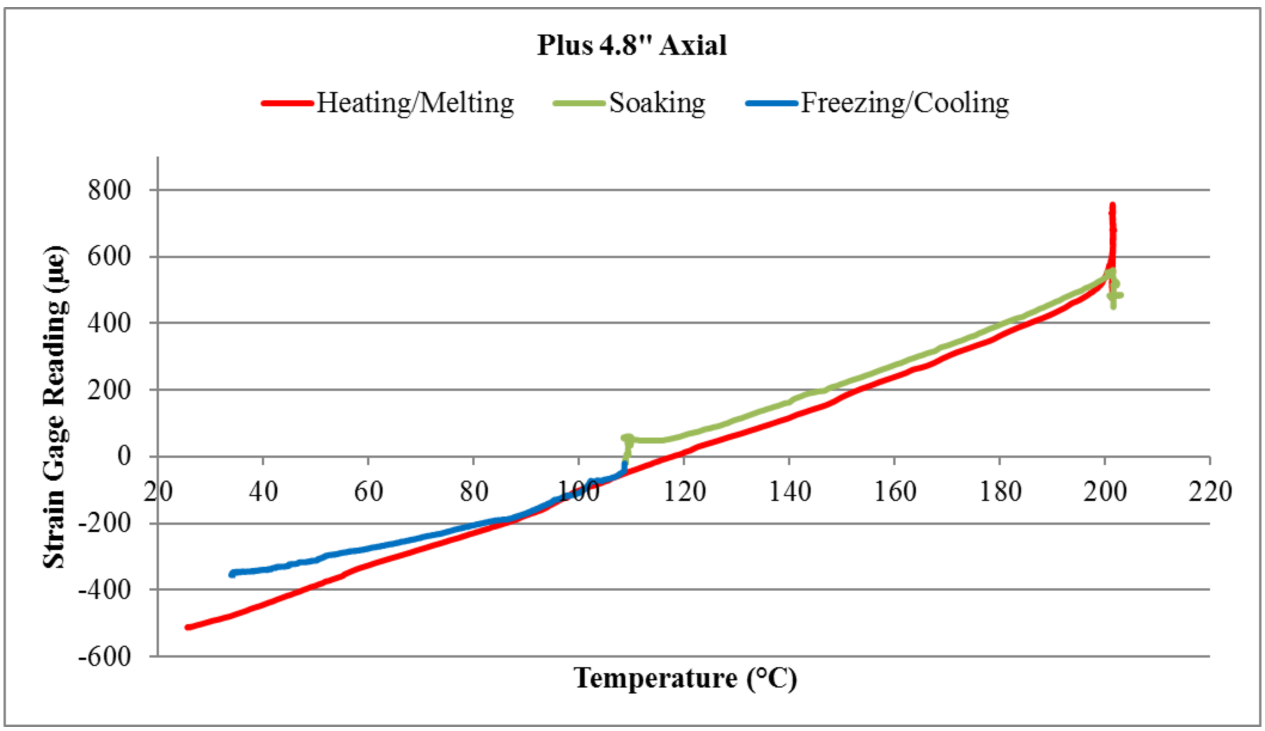

Figure 103. Entire axial strain history at +4.8" from the test section center in Test 1.

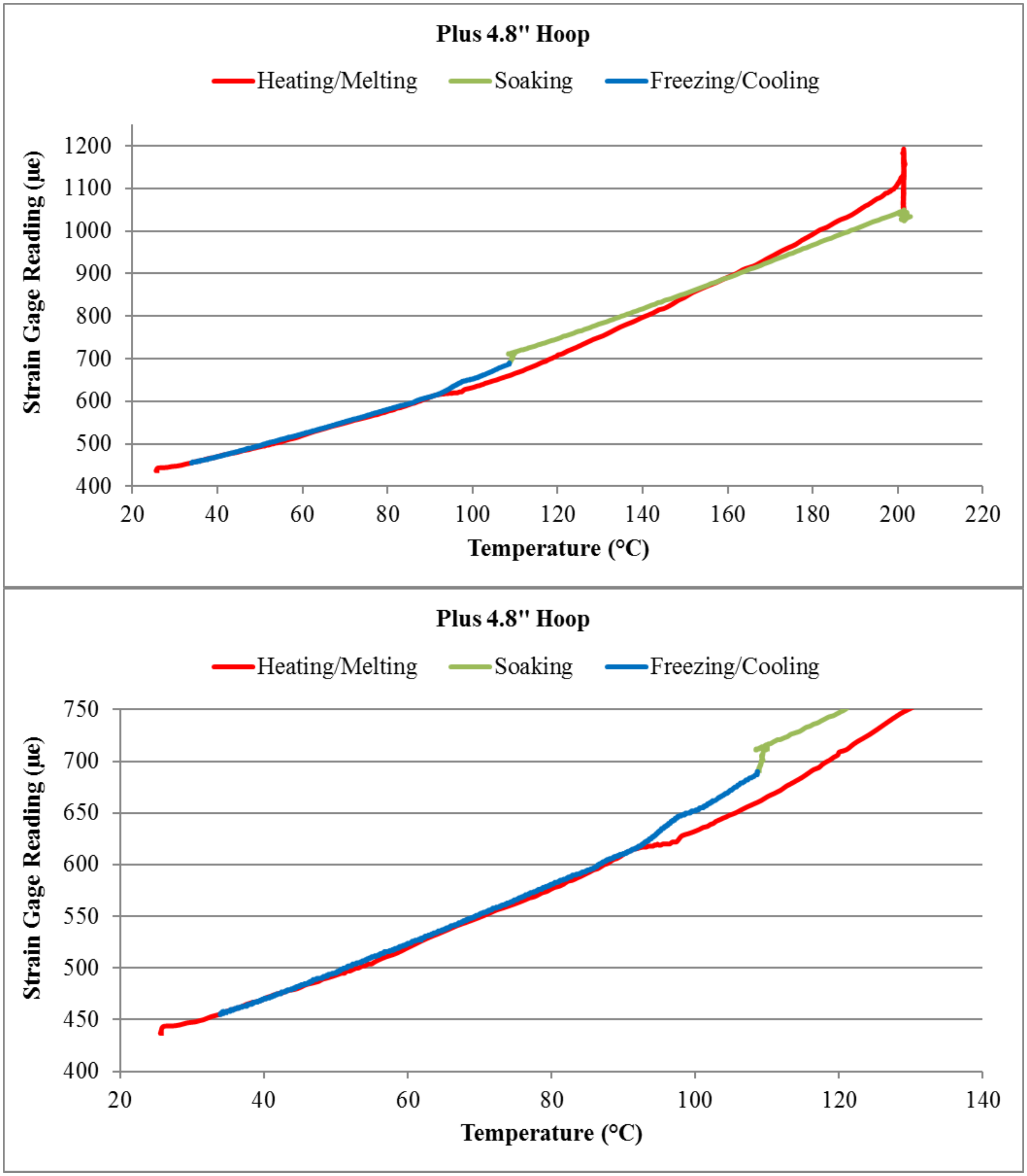

Figure 104. Entire hoop strain history (top) and zoom in of Freezing/Cooling phase (bottom) at +4.8" from the test section center in Test 1.

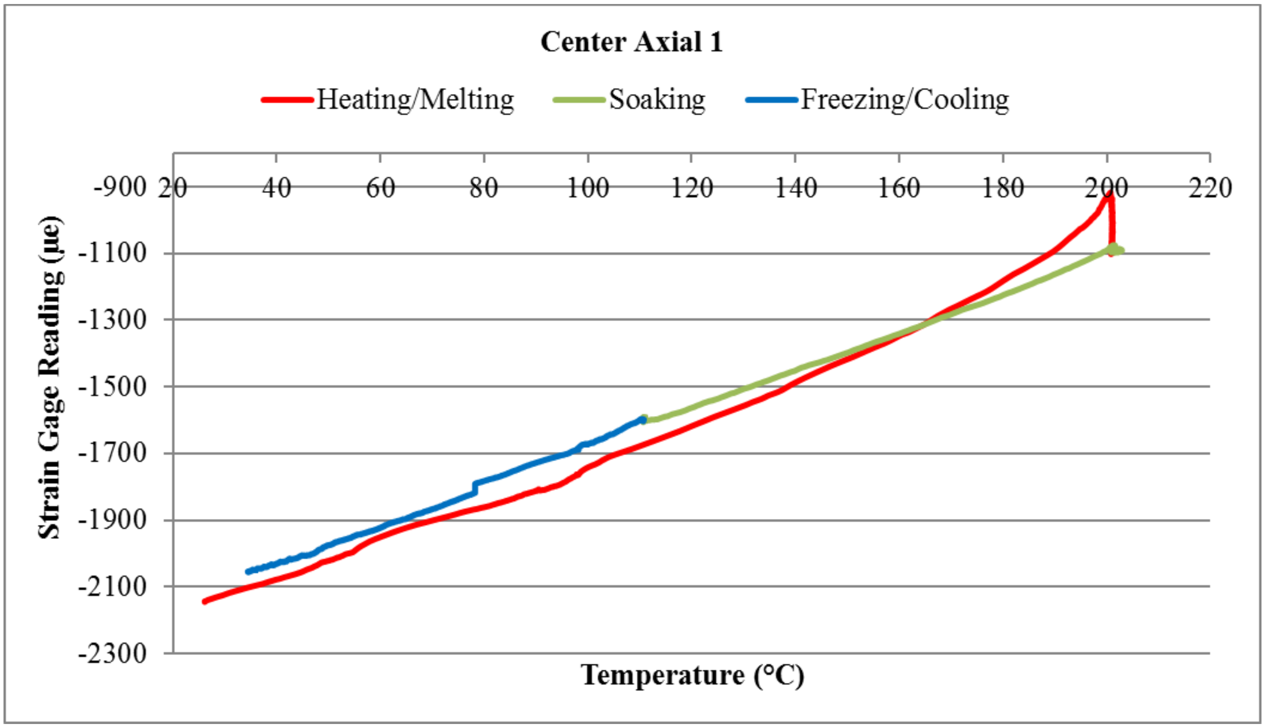

Figure 105. Entire axial strain 1 history at the test section center in Test 1.

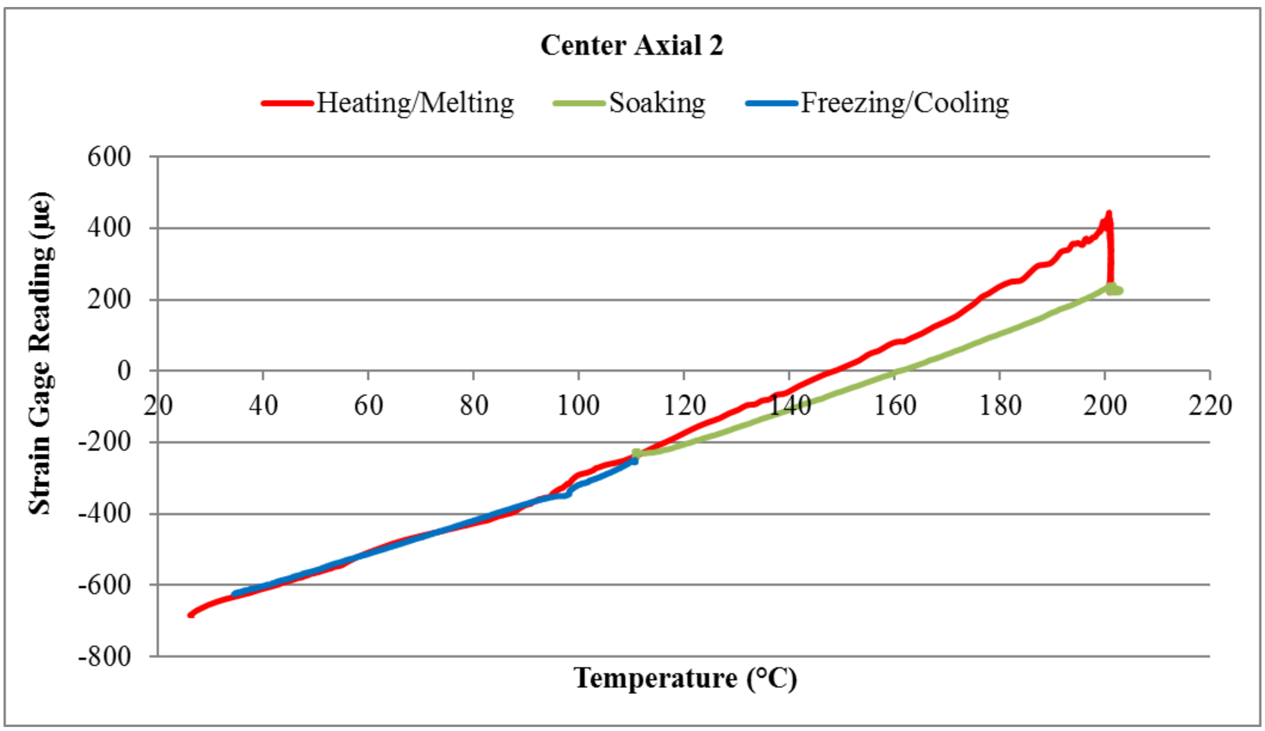

Figure 106. Entire axial strain 2 history at the test section center in Test 1.

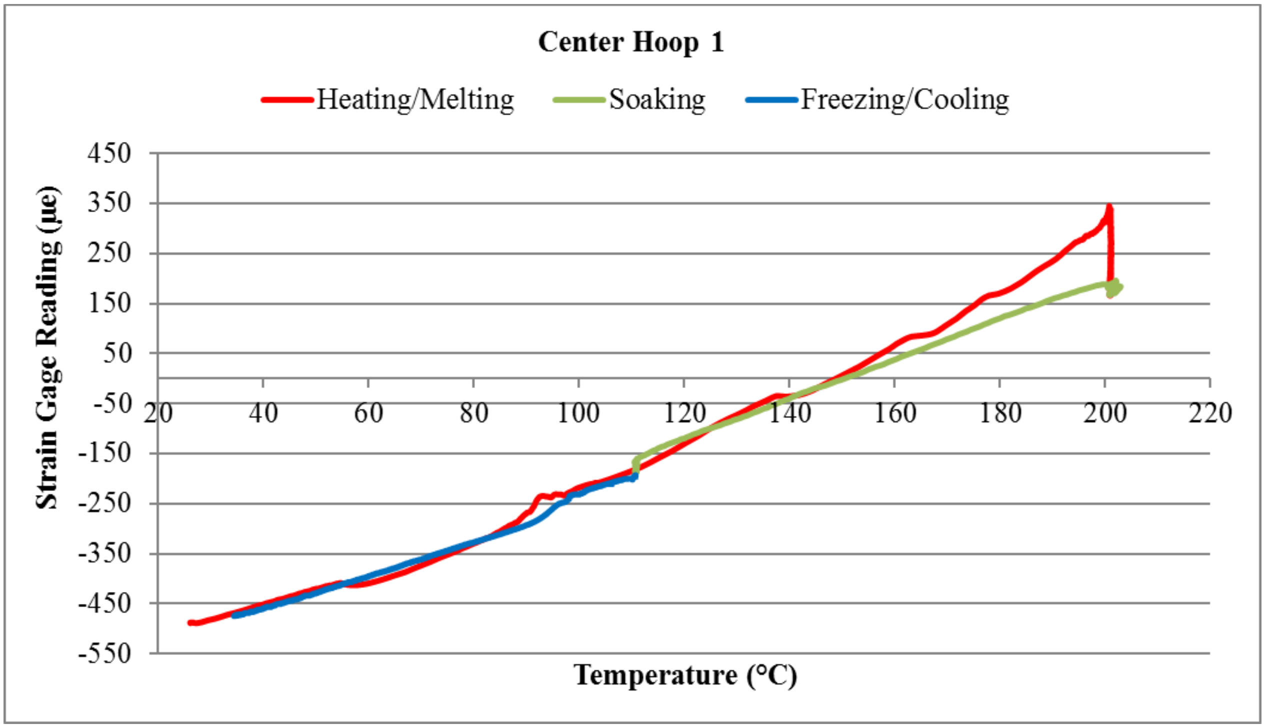

Figure 107. Entire hoop strain 1 history at the test section center in Test 1.

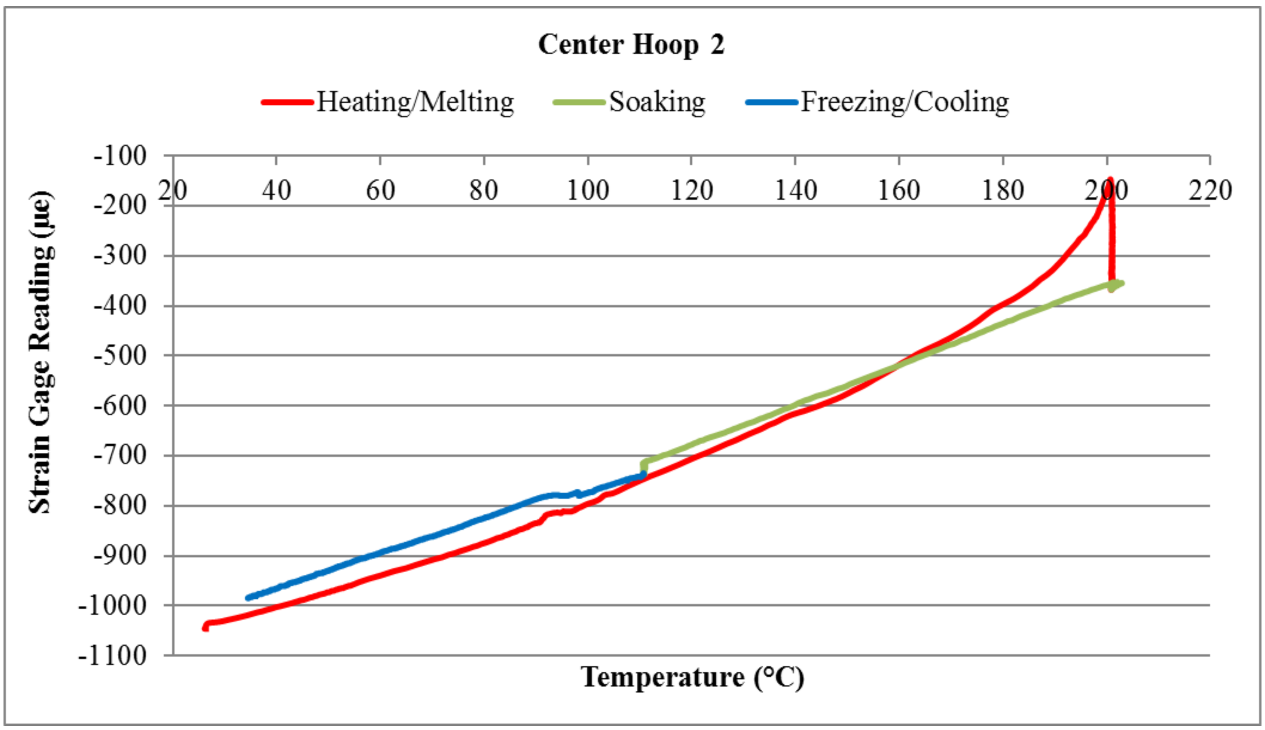

Figure 108. Entire hoop strain 2 history at the test section center in Test 1.

3.7 Test 7: Test with Freezing Pattern 3

Through the re-compiling of the results in all previous tests, it was noticed that the axial strain gage at the +4.8” location and the hoop strain gage at the -4.8” location behaved abnormally in some of the tests (see Figure 70, Figure 78, Figure 79, Figure 86, Figure 87, and Figure 95). After investigation, the issue was found to be due to loose electrical connections for these two strain gages. The issue was fixed before performing Test 7. As mentioned earlier, the main purpose of Test 7 is to prove the hypothesis proposed in Section 3.6 and demonstrate that the phenomenon of solid sodium pulling the tube wall after freezing is not specific to the +4.8” location due to some intrinsic local features. Test 7 was similar to Test 6 with the difference that the frozen plug on the reservoir side was extended beyond Zone 7 and all the way to Zone 3 to increase its strength. Because of the new freezing pattern, the -4.8” measurement location was sacrificed. The measured strain changes during sodium freezing at the other two locations are shown in Figure 109 to Figure 114. Due to potential cavitation, no prominent strain drop was measured by any of these strain gages during sodium freezing. The entire strain histories measured by the strain gages are shown in Figure 115 to Figure 122. As can be seen, with a strengthened frozen plug on the reservoir side, the physical phenomenon of solid sodium pulling the tube wall shifted from the +4.8” location to the center. In addition, the center hoop strain gage 2 was also measuring a ~ 75 µe drop before the solid sodium broke away from the tube wall. This finding is consistent with the previous hypothesis and demonstrates that the phenomenon of solid sodium pulling the tube wall after freezing is probably physical and not specific to the +4.8” location due to some intrinsic local features.

Another interesting finding from Test 7 is in the measured center hoop Strain 2. As shown in Figure 122, after the temperature drops below ~ 105°C, the strain vs temperature slope becomes steeper. After carefully checking the temperatures on the EM pump side, it was found that a frozen plug had not formed on that side yet. Therefore, the steeper slope could not be due to thermal contraction of liquid sodium. In addition, according to the previous discussion, cavitation would likely occur when confined liquid sodium contracts, compromising the measured thermal contraction rate. Therefore, the steeper slope can only be explained by external stress from the loop or the Poisson effect. According to the previous study [8], the current loop design is flexible enough with regard to the local thermal effect. In addition, as it shows on Figure 119 and Figure 120, over the same temperature range, the measured axial strains increase as temperature decreases. This indicates that the observed steeper slope of center hoop Strain 2 vs temperature below ~ 105°C is probably due to the Poisson effect. Actually the same effect has been observed during sodium freezing in previous tests. In Test 2 (see Figure 7 - Figure 14), a strain increase was observed during sodium freezing. Initially, this was considered to be due to breakaway of solid sodium from tube wall. However, based on the previous discussion, the breakaway is likely to occur over a larger temperature scale and the observed strain increase in Figure 7 - Figure 14 is more likely due to the Poisson effect.

The aforementioned Poisson effect in center hoop Strain 2 is, however, negligible in center hoop Strain 1. Since these two strain gages are located at the same axial location, but just different azimuthal angles, this finding indicates the non-uniformity of the test section wall and that hoop Strain Gage 2 is probably attached to a weak spot. This is likely true considering the thin wall of the test section. Actually, the measured center hoop Strain 2 has become more and noisier during the last few tests. This was initially considered as signal noise, which was however probably physical and due to weakening of the attachment spot of hoop Strain Gage 2. The weakening of this spot made it more susceptible to the Poisson effect and fluctuations caused by local thermal stresses.

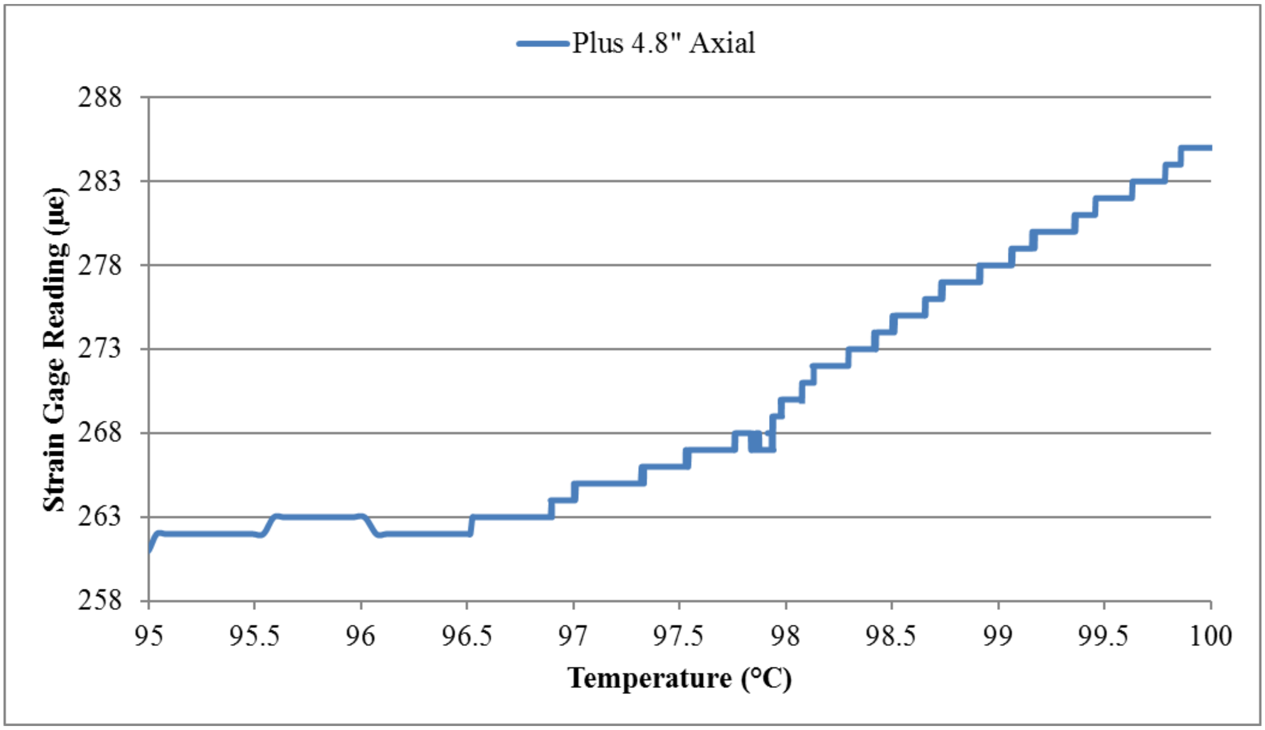

Figure 109. Axial strain vs temperature at +4.8" from the test section center in Test 7.

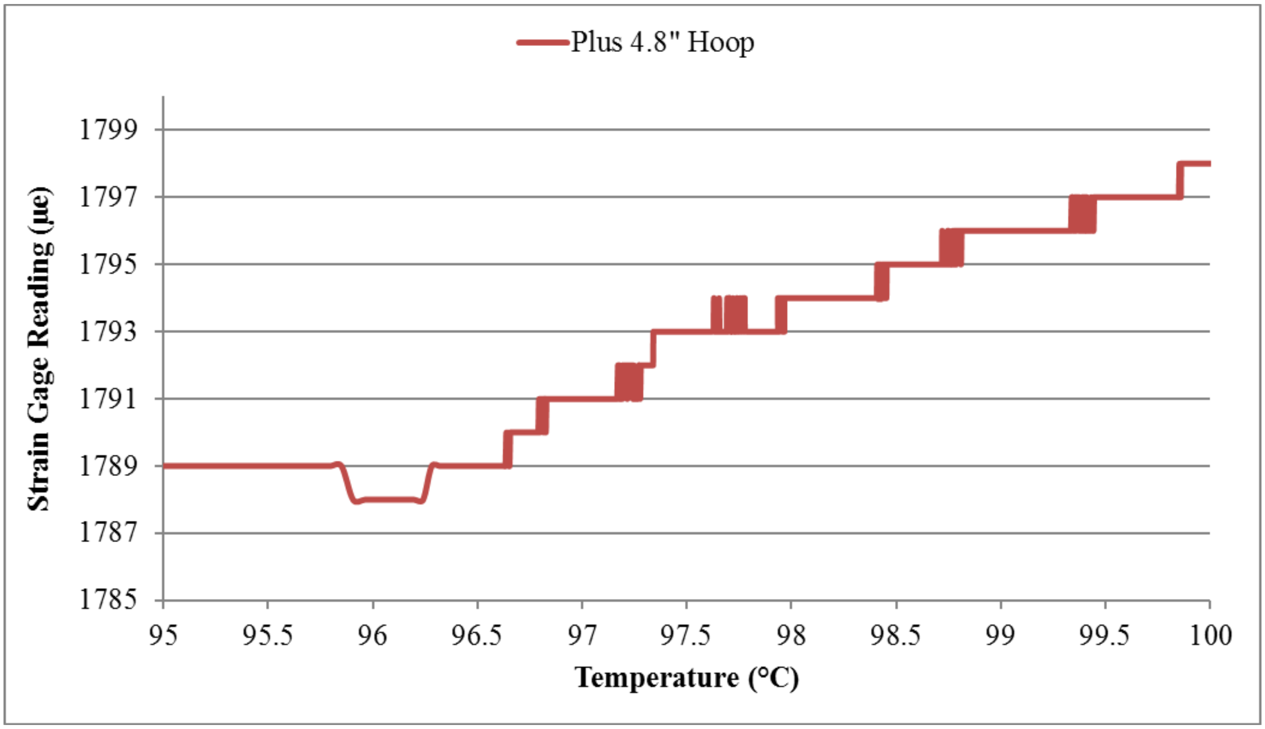

Figure 110. Hoop strain vs temperature at +4.8" from the test section center in Test 7.

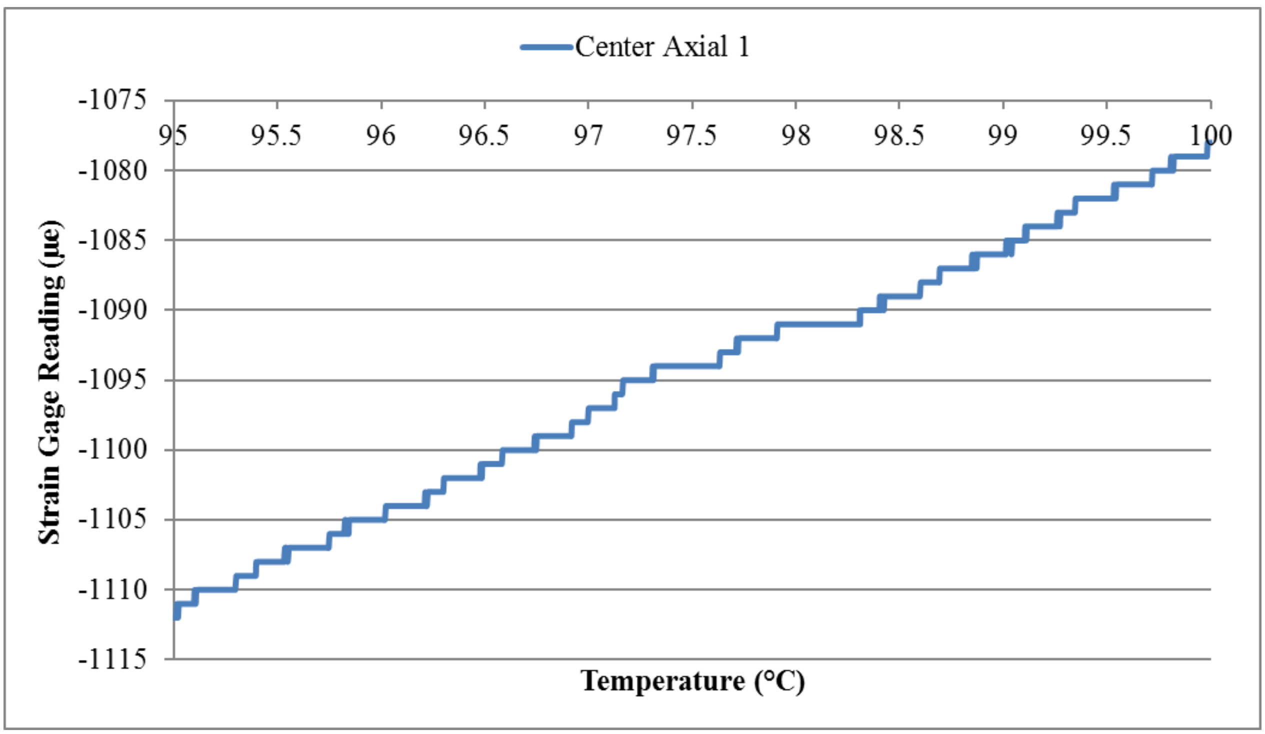

Figure 111. Axial Strain 1 vs temperature at the test section center in Test 7.

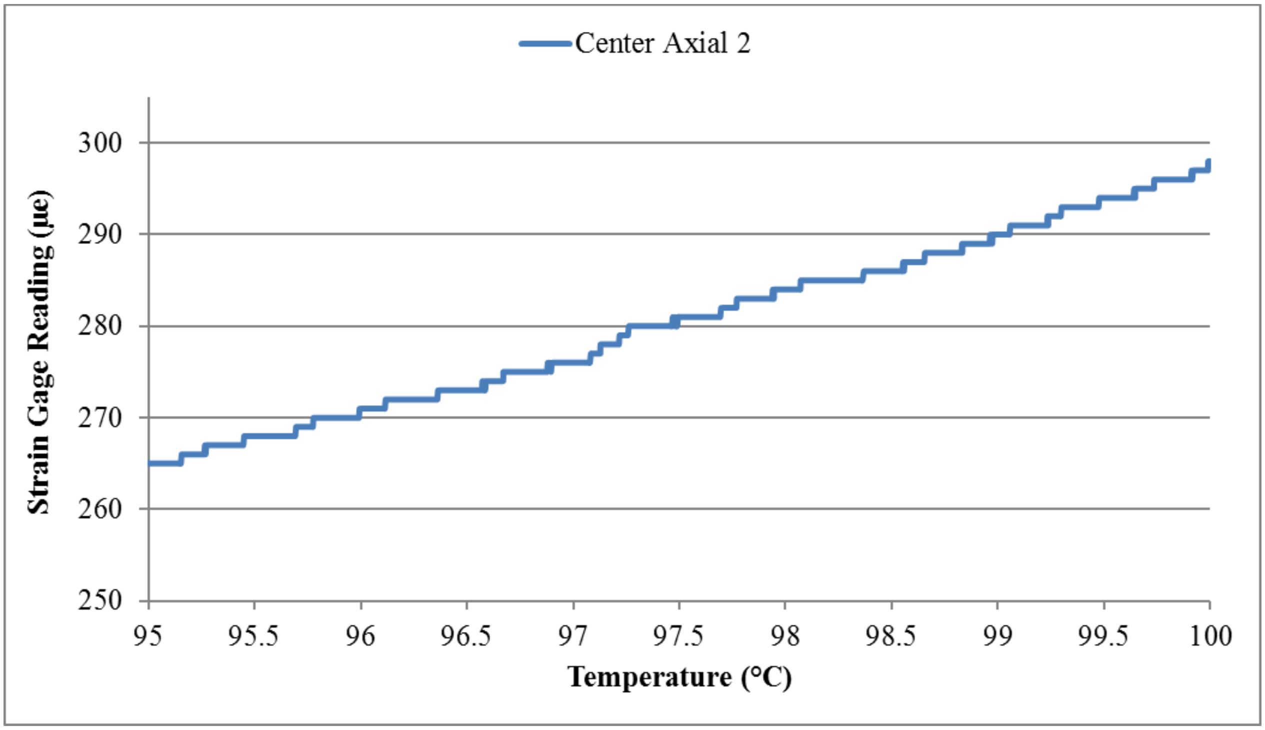

Figure 112. Axial Strain 2 vs temperature at the test section center in Test 7.

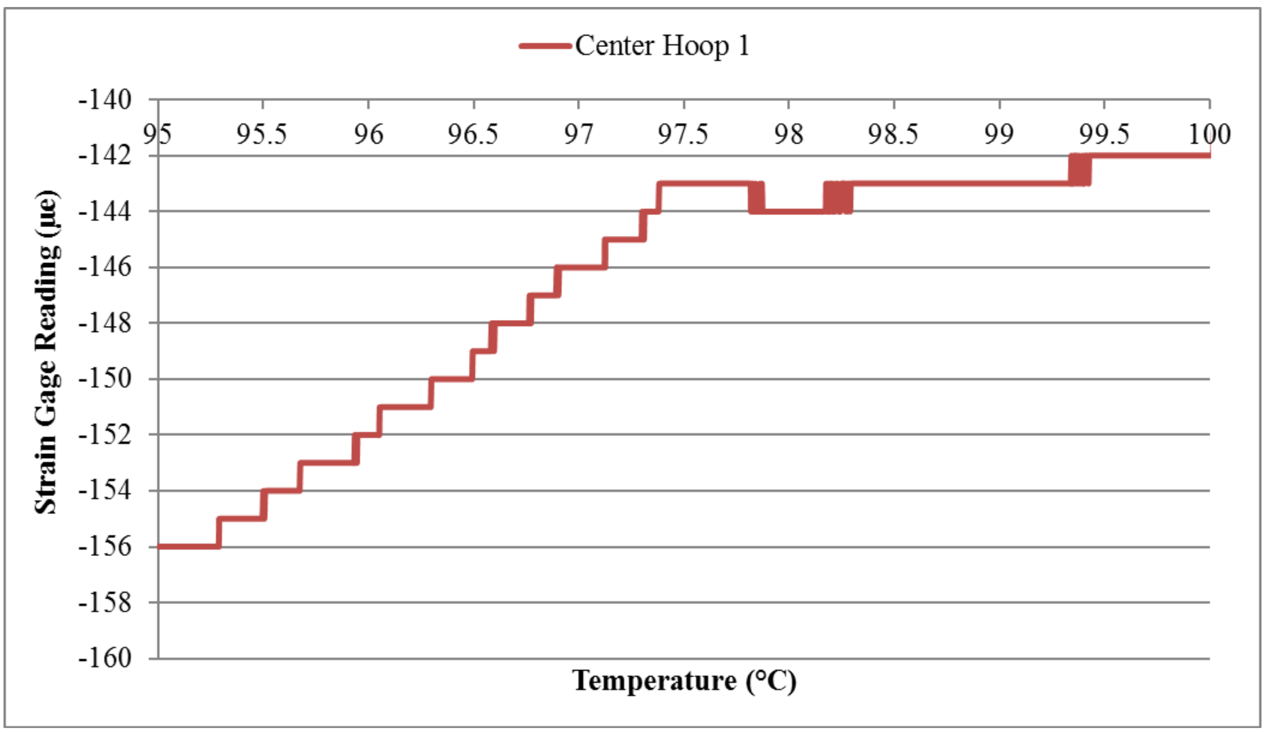

Figure 113. Hoop Strain 1 vs temperature at the test section center in Test 7.

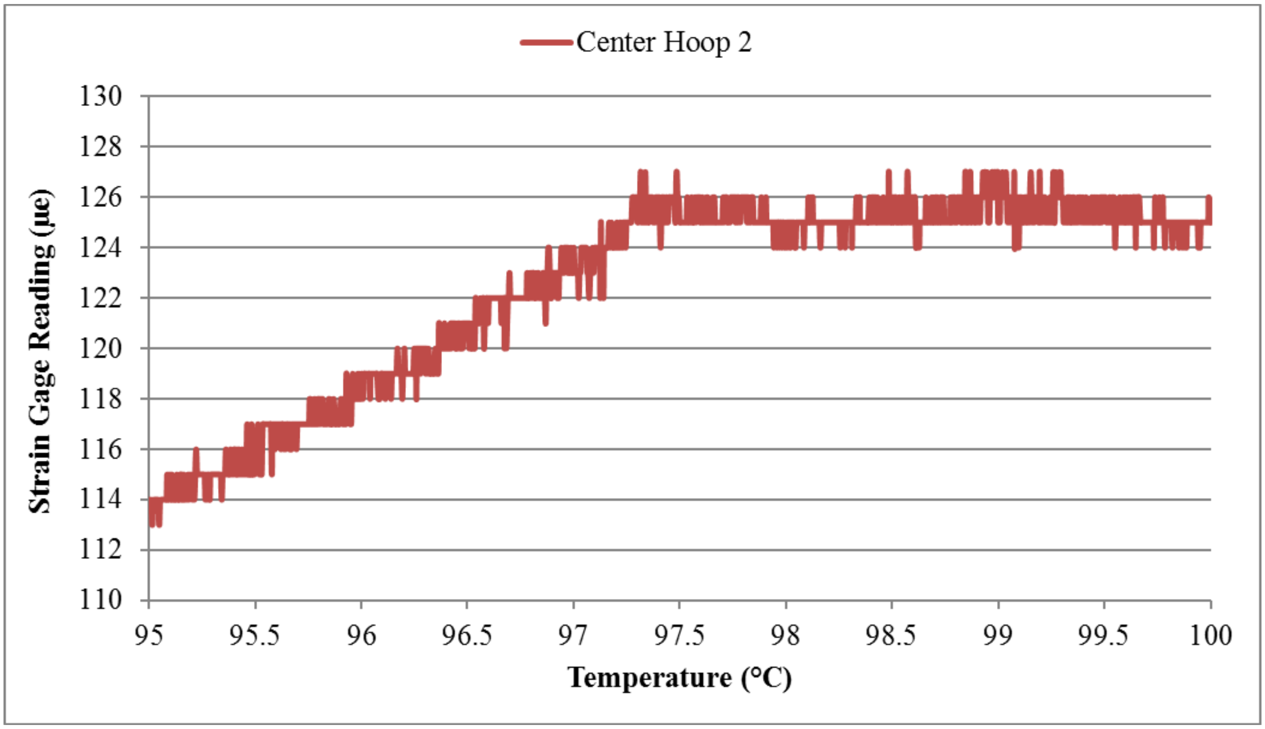

Figure 114. Hoop Strain 2 vs temperature at the test section center in Test 7.

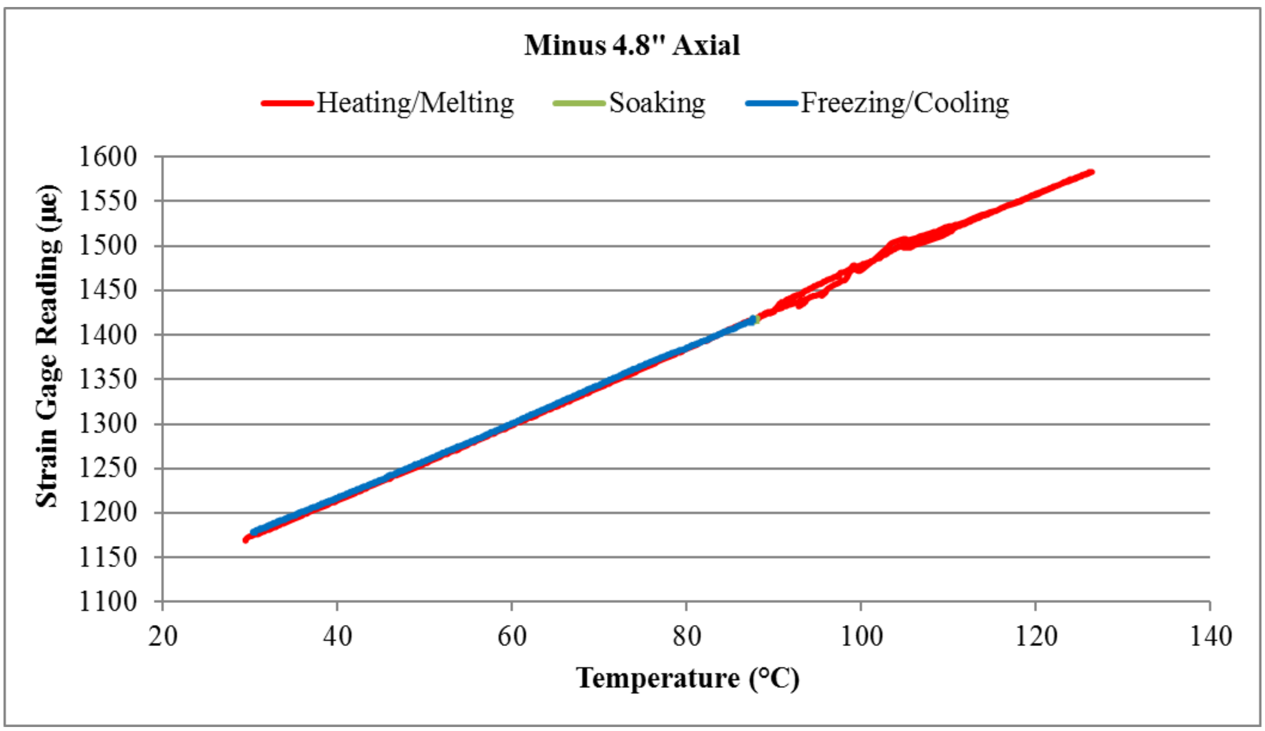

Figure 115. Entire axial strain history at –4.8" from the test section center in Test 7.

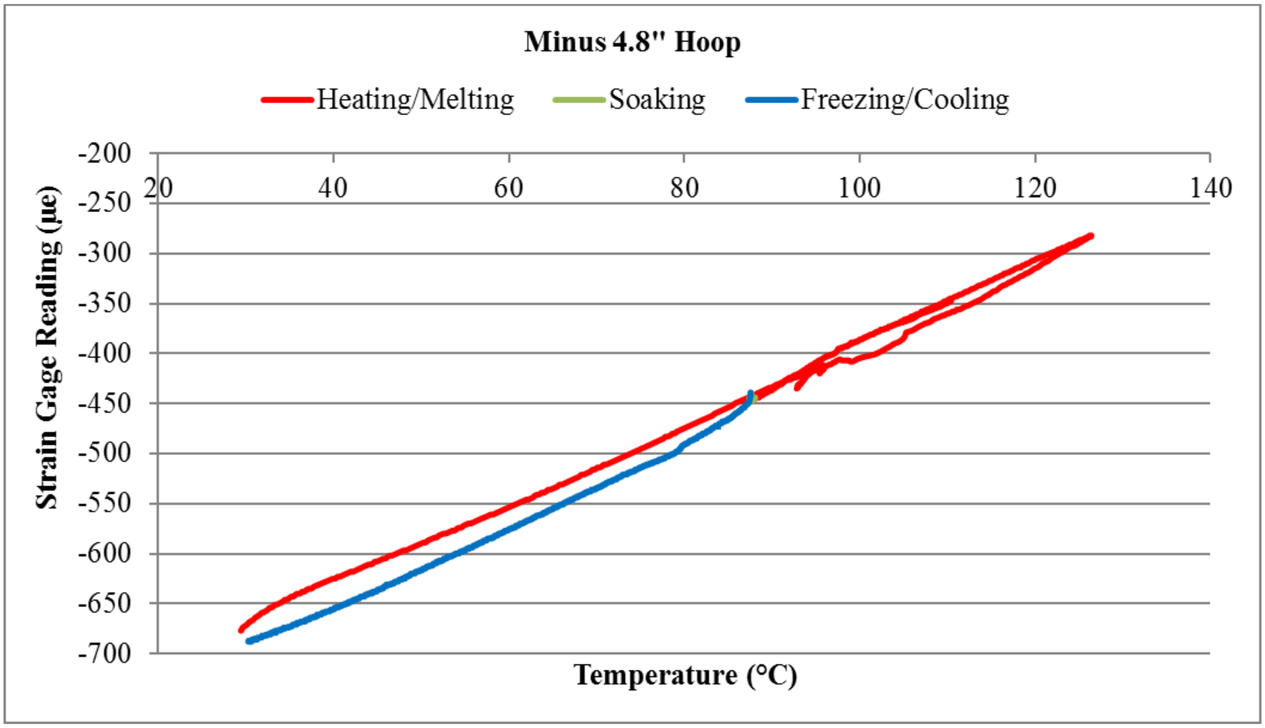

Figure 116. Entire hoop strain history at -4.8” from the test section center in Test 7.

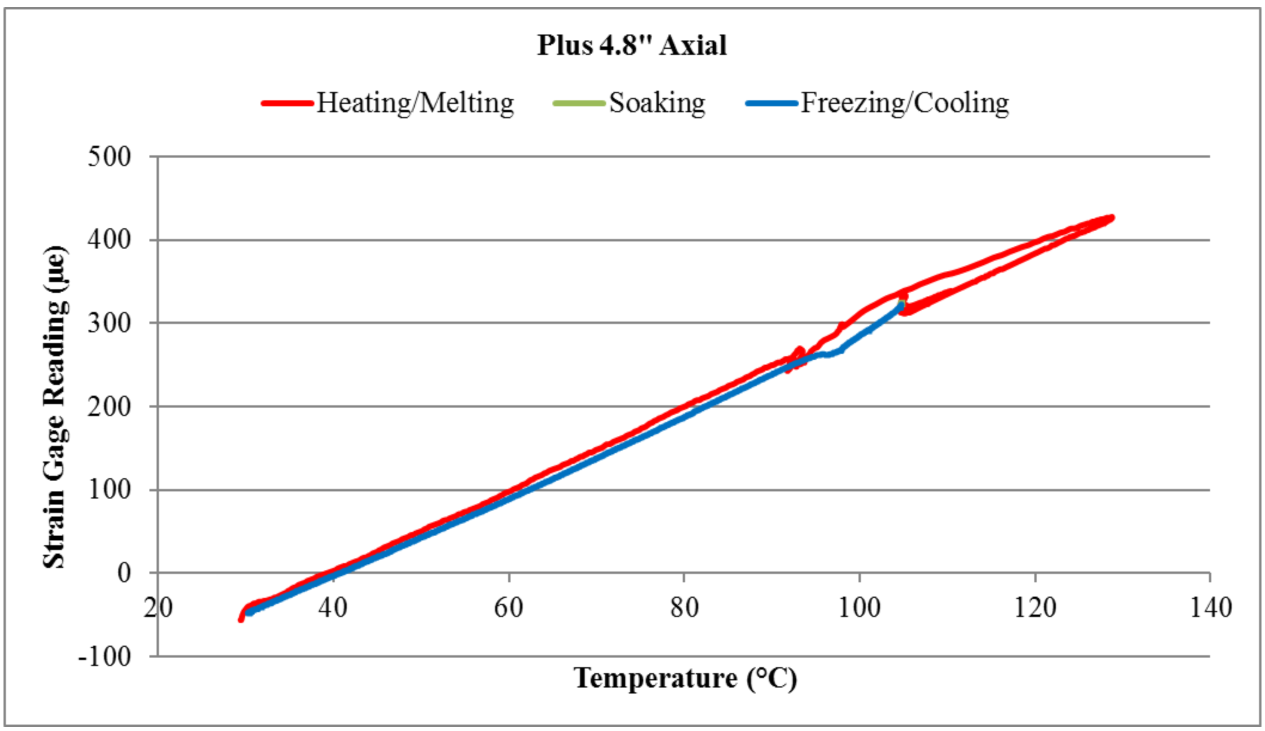

Figure 117. Entire axial strain history at +4.8” from the test section center in Test 7.

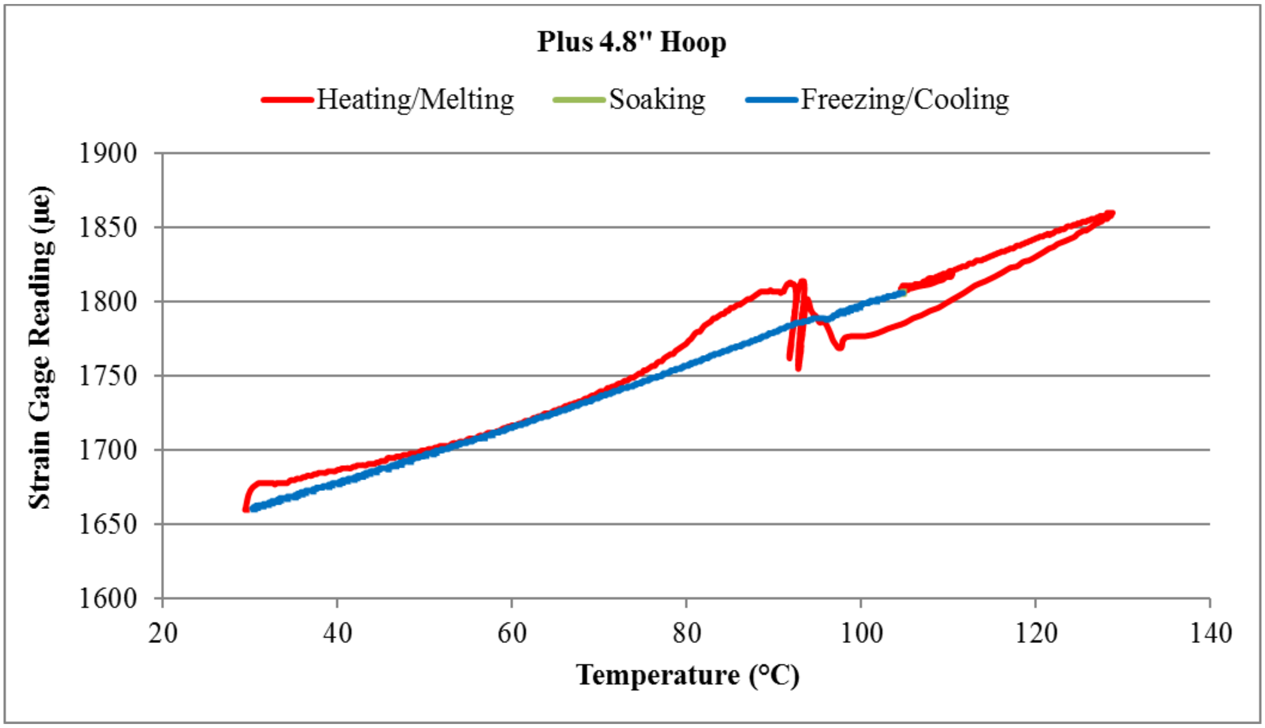

Figure 118. Entire hoop strain history at +4.8" from the test section center in Test 7.

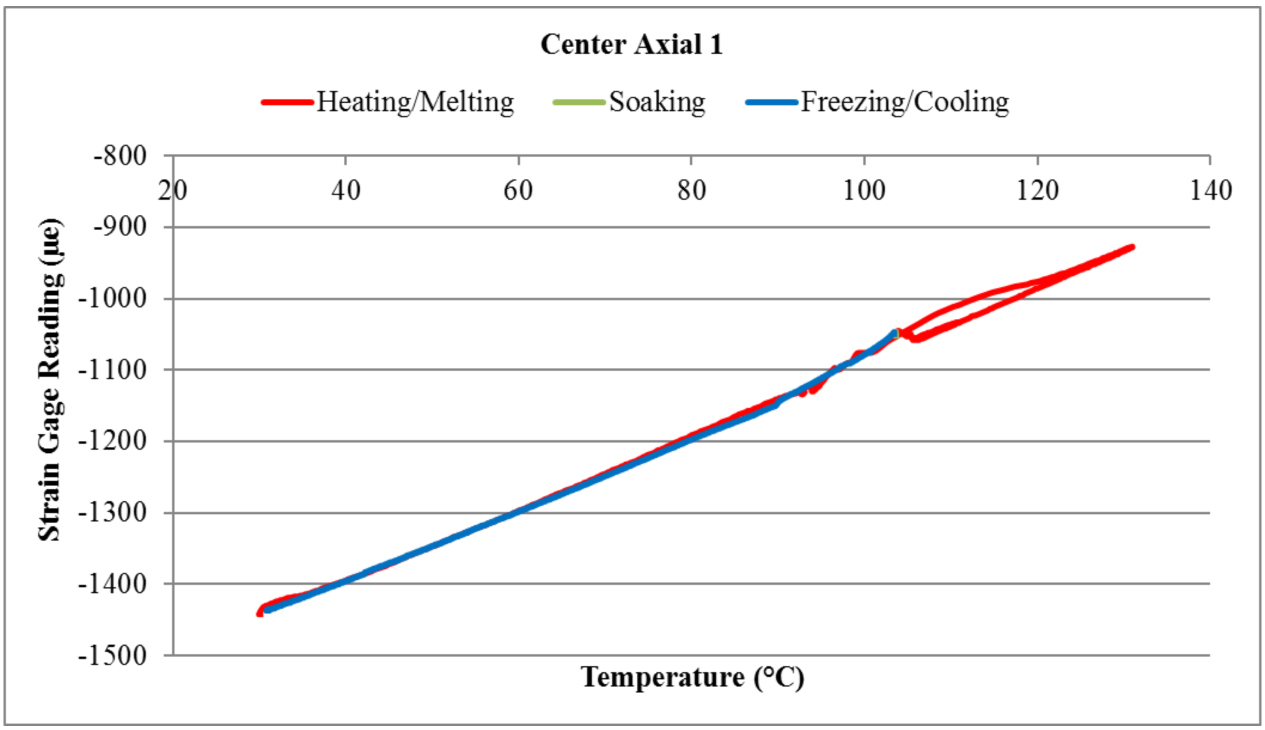

Figure 119. Entire axial strain 1 history at the test section center in Test 7.

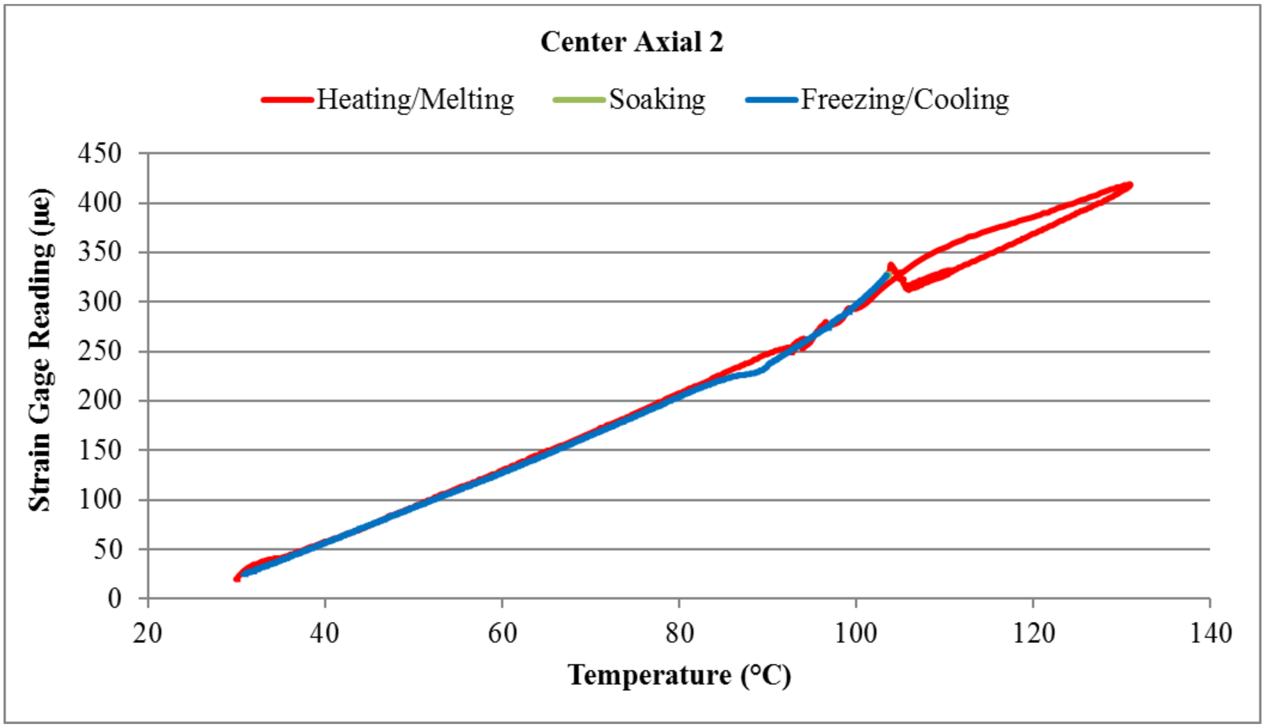

Figure 120. Entire axial strain 2 history at the test section center in Test 7.

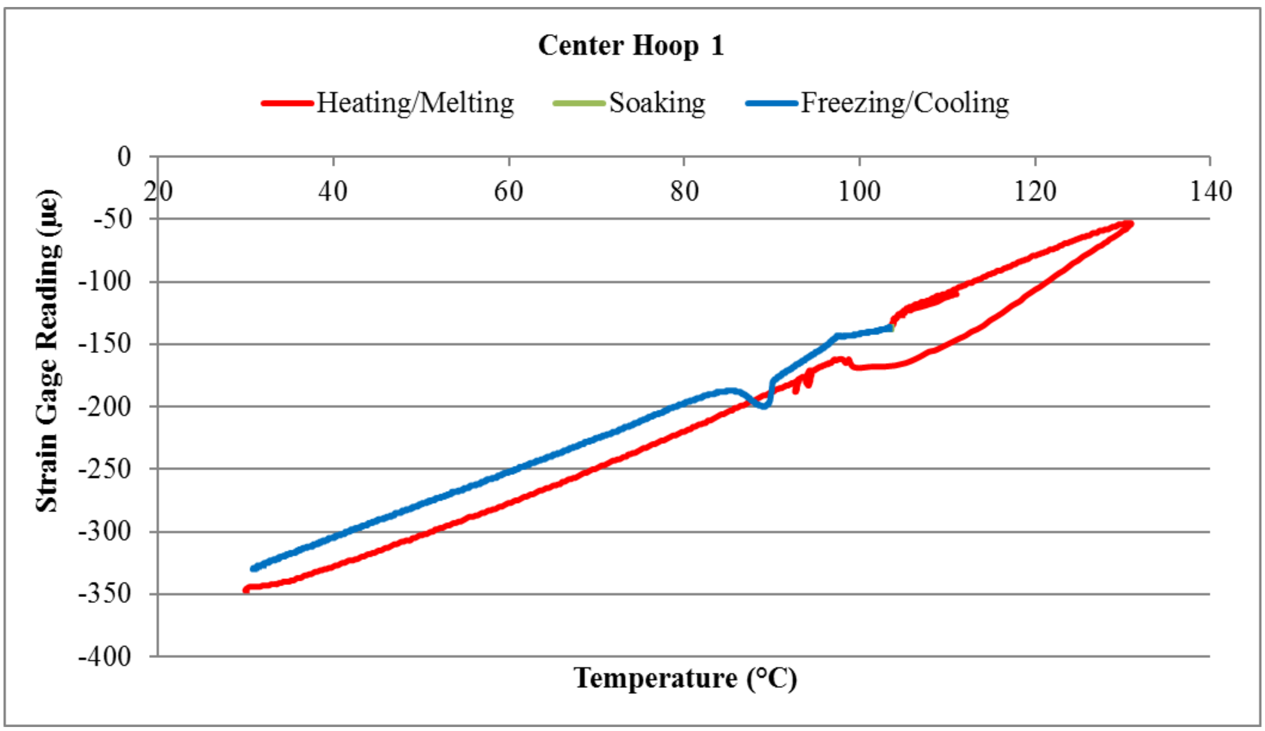

Figure 121. Entire hoop strain 1 history at the test section center in Test 7.

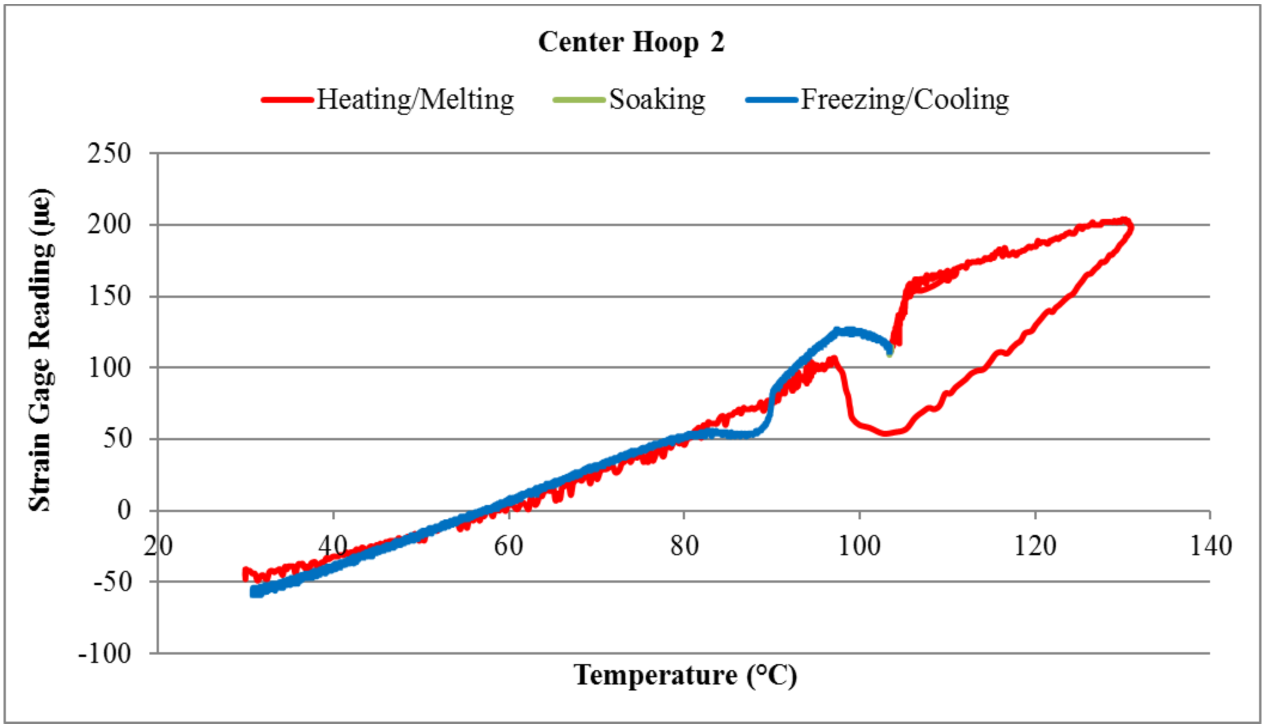

Figure 122. Entire hoop strain 2 history at the test section center in Test 7.

3.8 Test 8: Test with Freezing Pattern 4

To further investigate the previous hypothesis about solid sodium pulling the tube wall after freezing, Test 8 was performed. Test 8 was similar to Test 4 in the procedure with the difference that freezing was started from the center of the test section and toward the free surfaces. The measured strain changes during sodium freezing are shown in Figure 123 to Figure 130. As expected, with the frozen sodium still being able to communicate with the free surfaces during the freezing process in this test, there was no sharp strain drop observed, especially at the center axial Strain Gage 2 where a strain drop during sodium freezing was consistently observed in Test 2 to Test 6. The entire strain histories during this test are shown in Figure 131 to Figure 138. With the present freezing pattern, dense solid sodium is supposed to form at all three measurement locations, resulting in prominent phenomena of solid sodium pulling the tube wall after freezing. However, except for the slight improvement of this phenomenon at the -4.8” location compared to previous test (see Figure 132 vs Figure 61), there is negligible improvement for the center location, and for the +4.8” location there is even a decrease in the measured strain drop due to solid sodium pulling effect (~ 35 vs 75 micro strains). The only possible explanation for this finding is that, first of all, because the test section is horizontally oriented and the present freezing test was performed under vacuum, voids due to cavitation were still formed during sodium freezing. Because of the present freezing pattern, voids were formed homogeneously as the freezing front propagated from the test section center toward the free surfaces. This is why the phenomenon of solid sodium pulling the tube wall appears at all three measurement locations but less prominently. However, in all the previous tests, because of the frozen plugs, liquid sodium was freezing in a confined space. Because of that, cavitation was heterogeneous and tended to occur at the side with weaker frozen plug. With the sacrificial side to accommodate the voids, dense solid sodium could be formed on the other side, leading to more prominent phenomenon of solid sodium pulling the tube wall after freezing.

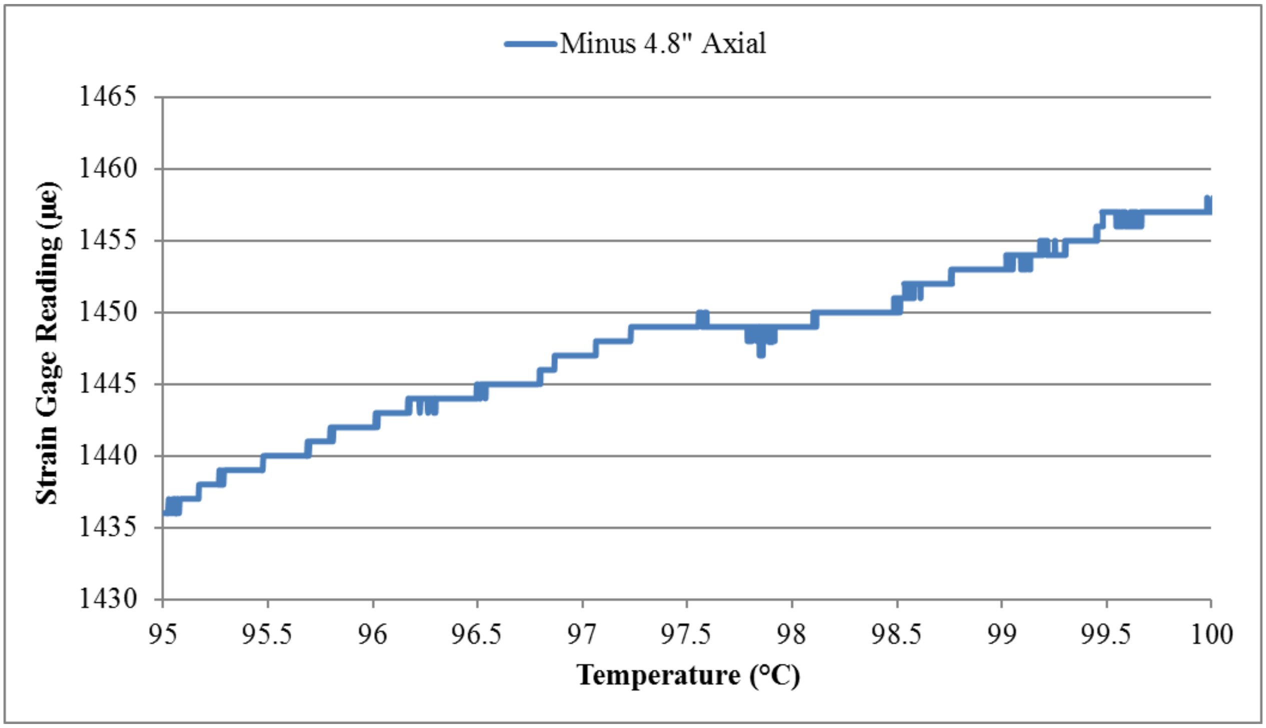

Figure 123. Axial strain vs temperature at –4.8" from the test section center in Test 8.

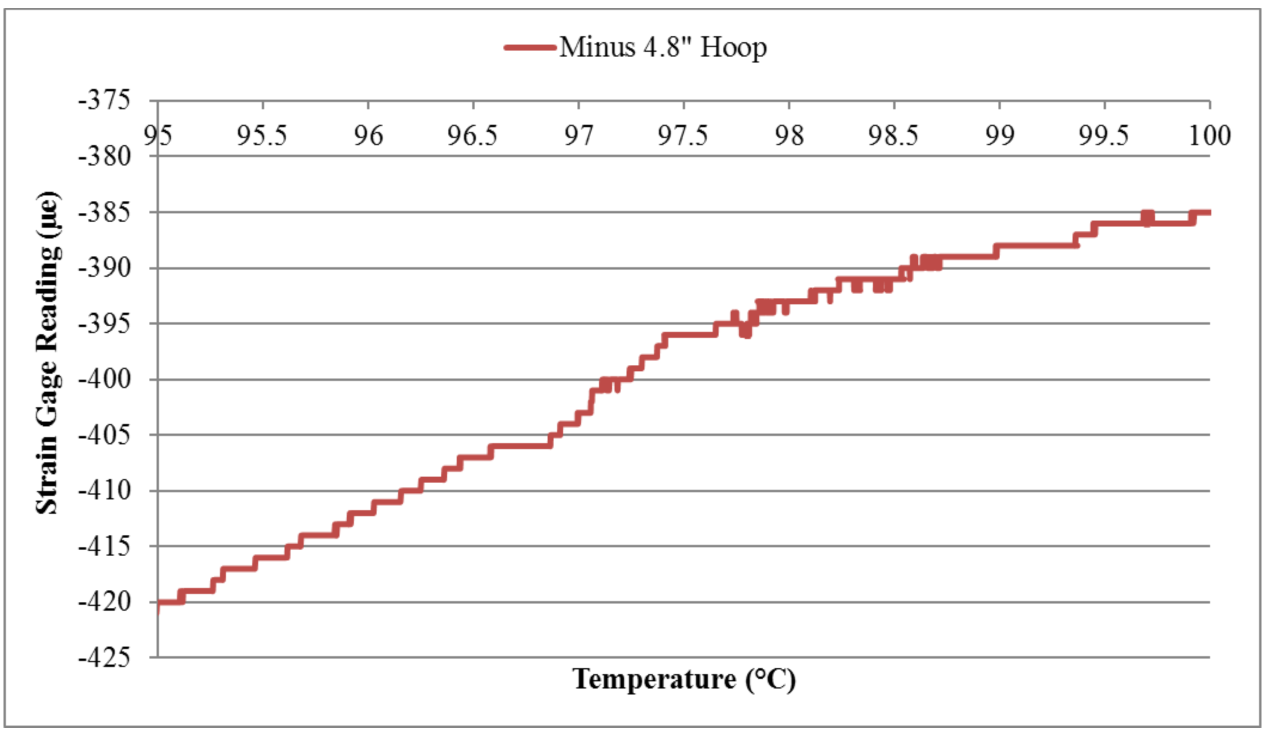

Figure 124. Hoop strain vs temperature at -4.8" from the test section center in Test 8.

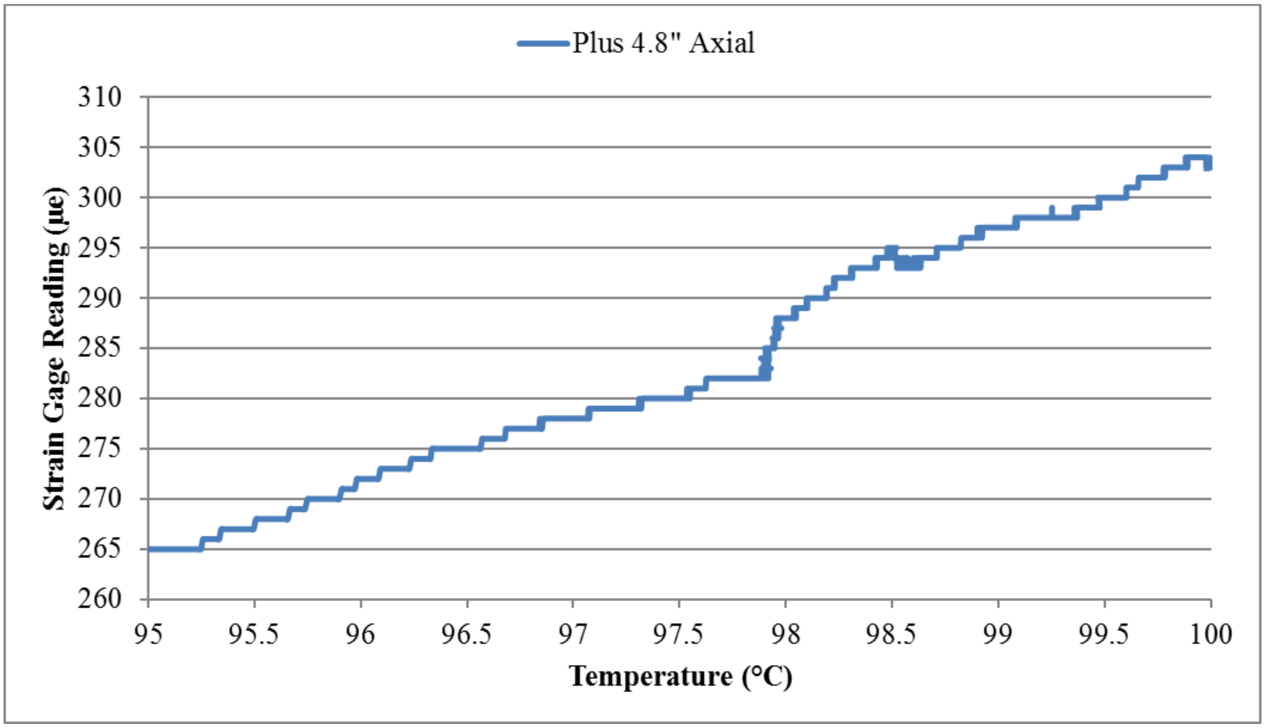

Figure 125. Axial strain vs temperature at +4.8" from the test section center in Test 8.

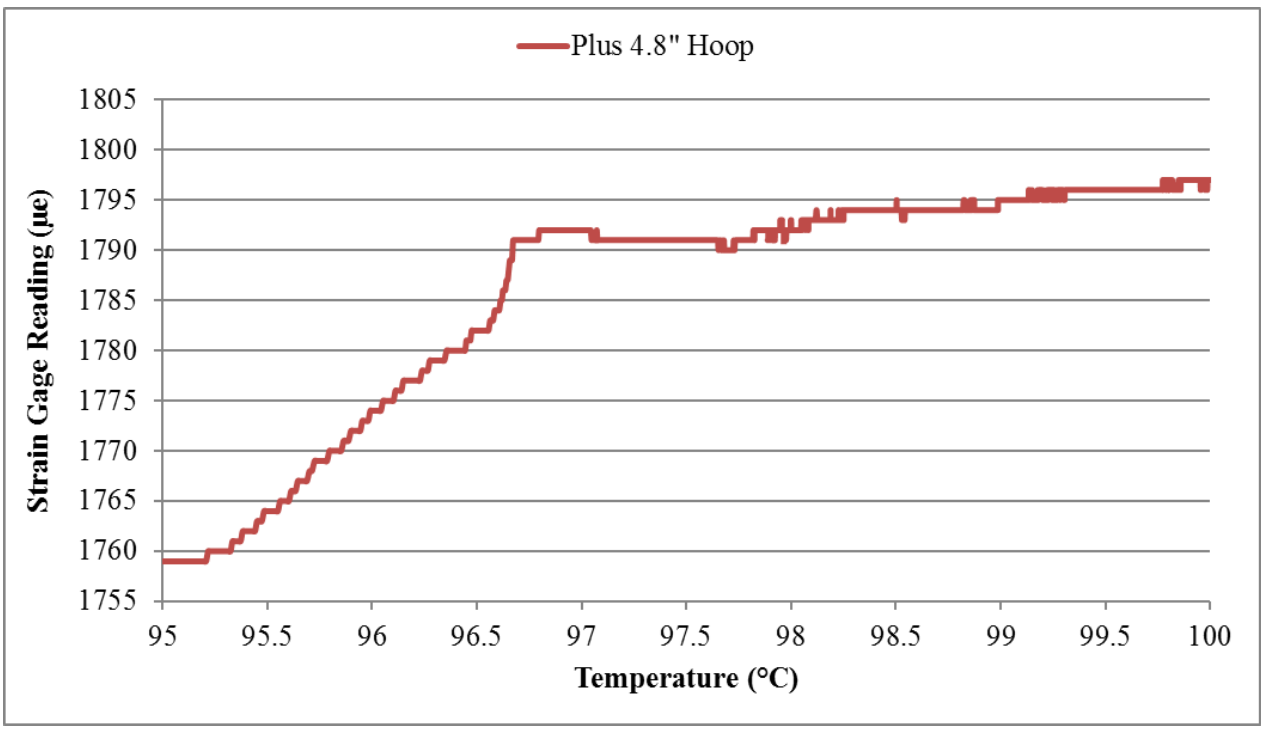

Figure 126. Hoop strain vs temperature at +4.8" from the test section center in Test 8.

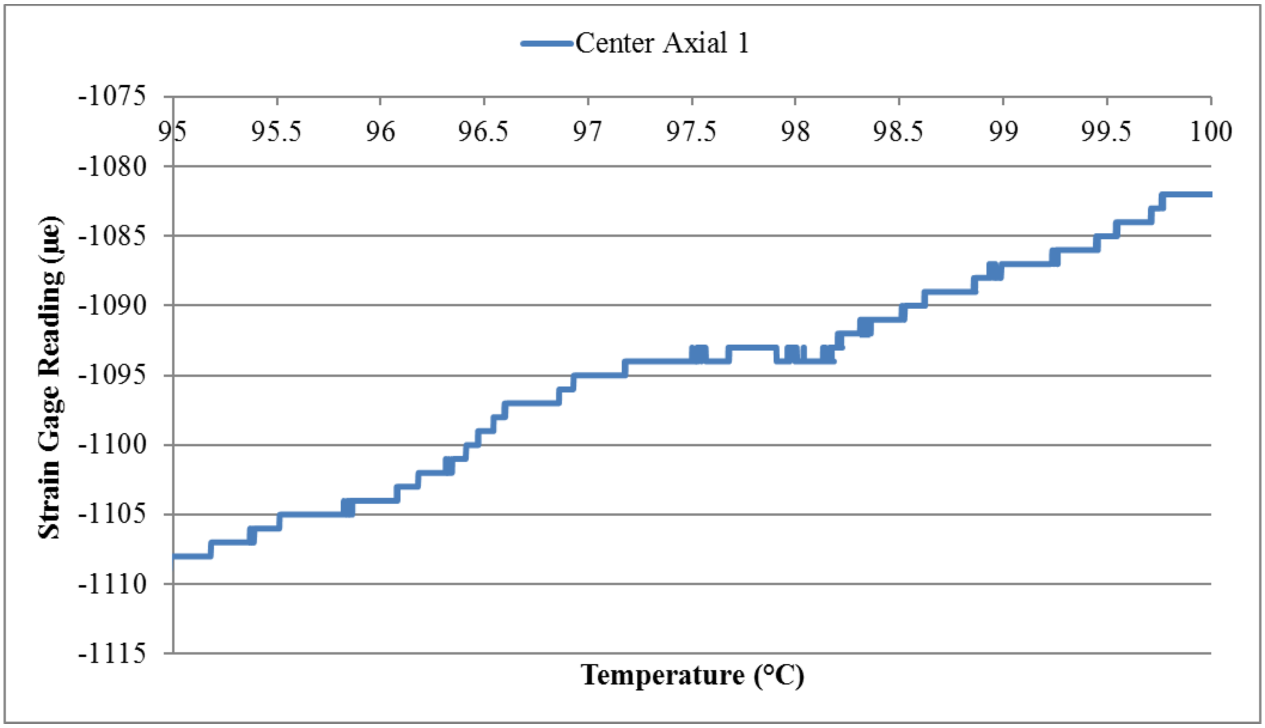

Figure 127. Axial Strain 1 vs temperature at the test section center in Test 8.

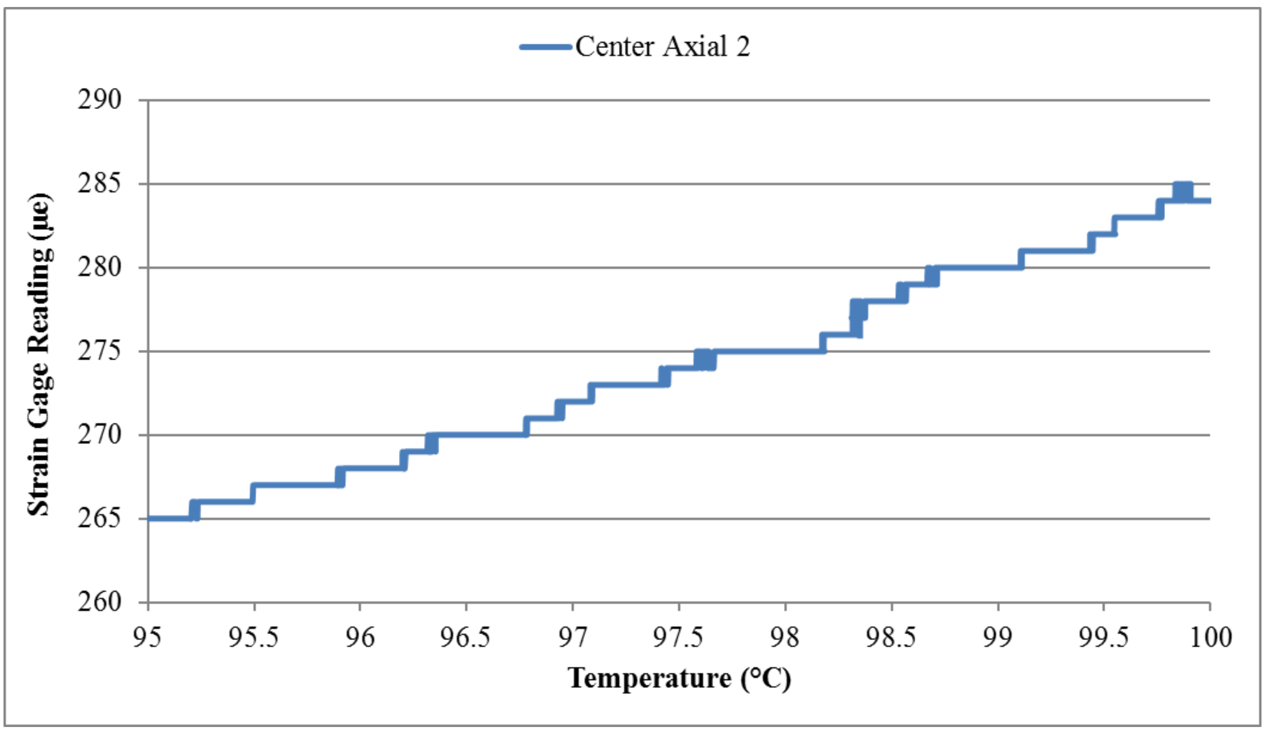

Figure 128. Axial Strain 2 vs temperature at the test section center in Test 8.

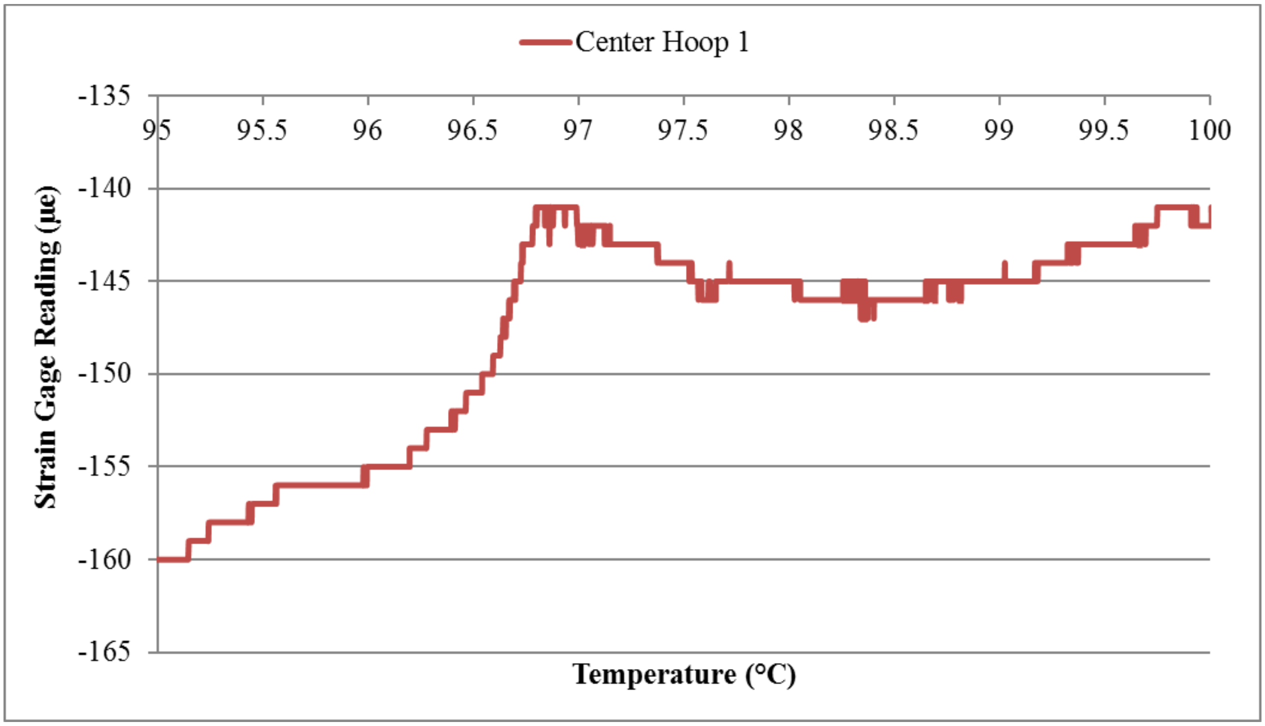

Figure 129. Hoop Strain 1 vs temperature at the test section center in Test 8.

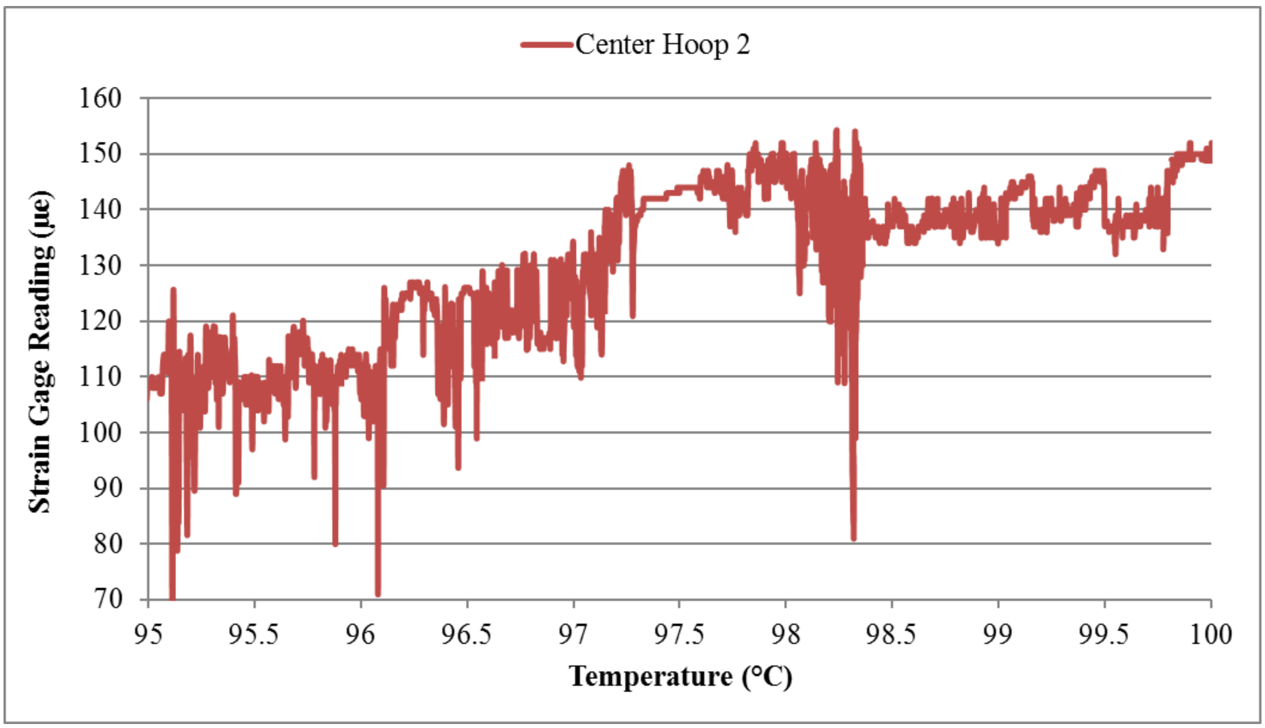

Figure 130. Hoop Strain 2 vs temperature at the test section center in Test 8.

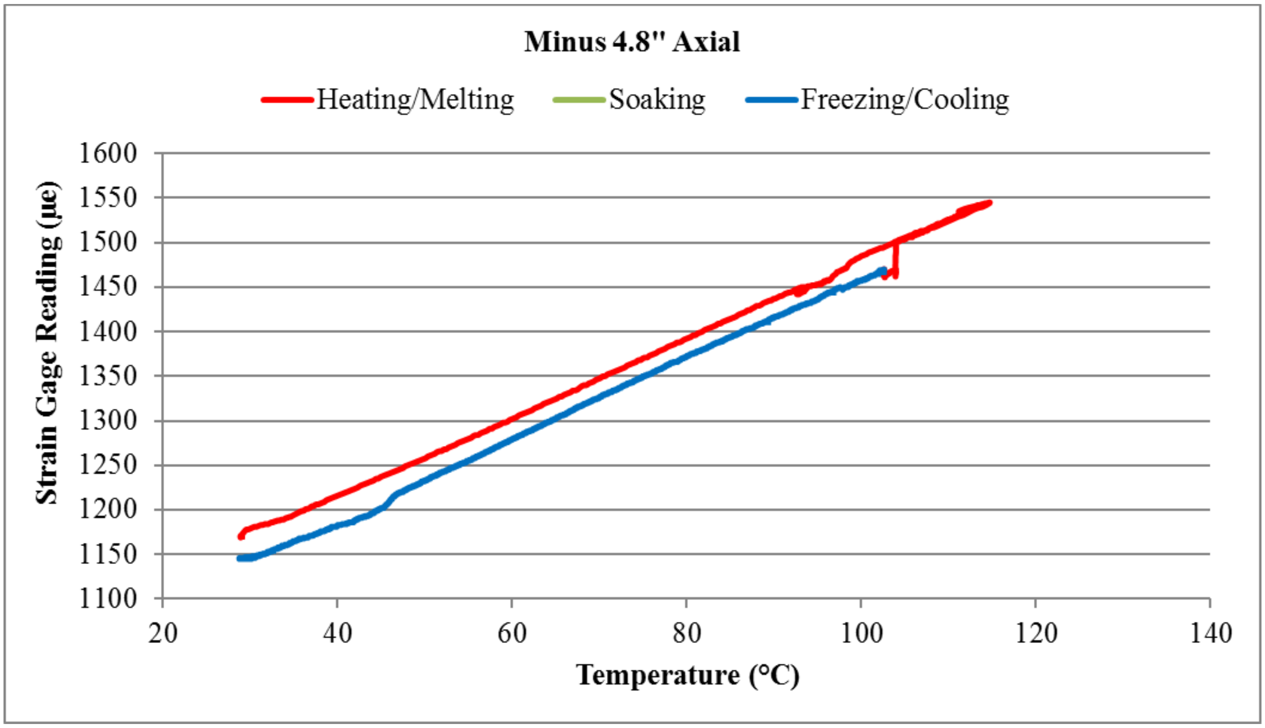

Figure 131. Entire axial strain history at –4.8” from the test section center in Test 8.

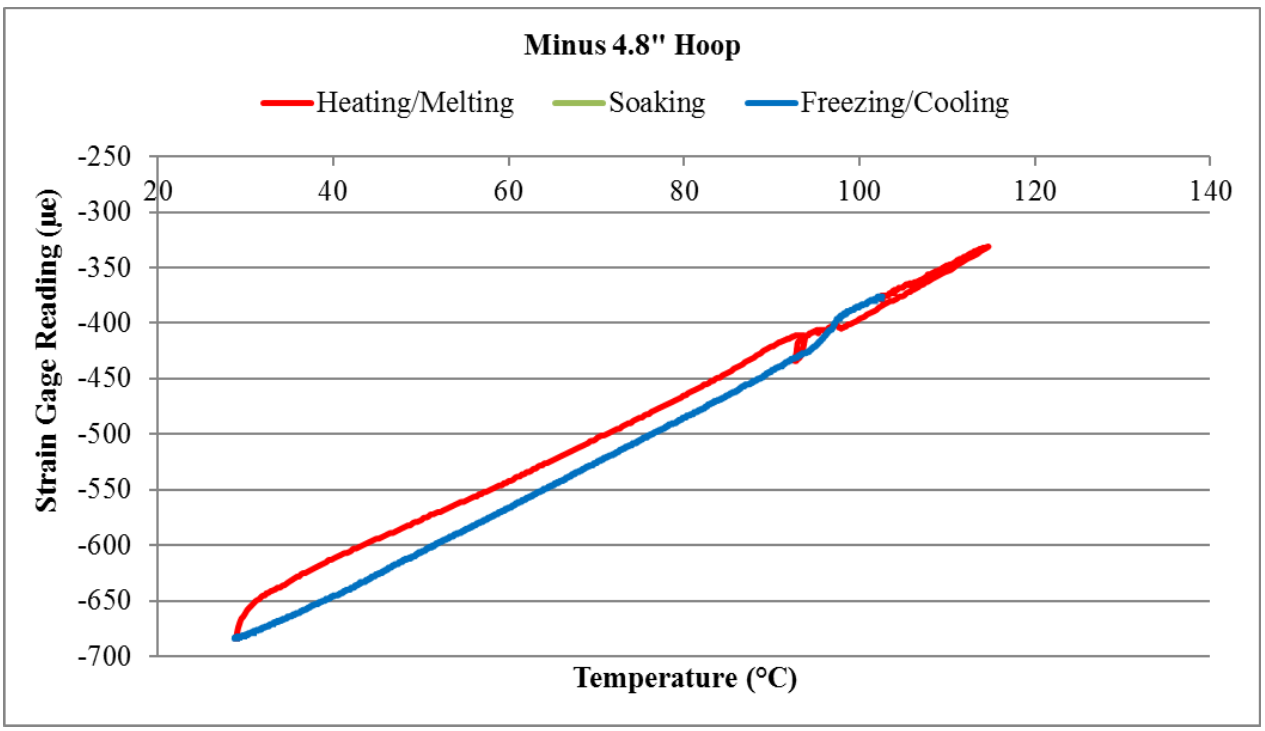

Figure 132. Entire hoop strain history at -4.8” from the test section center in Test 8.

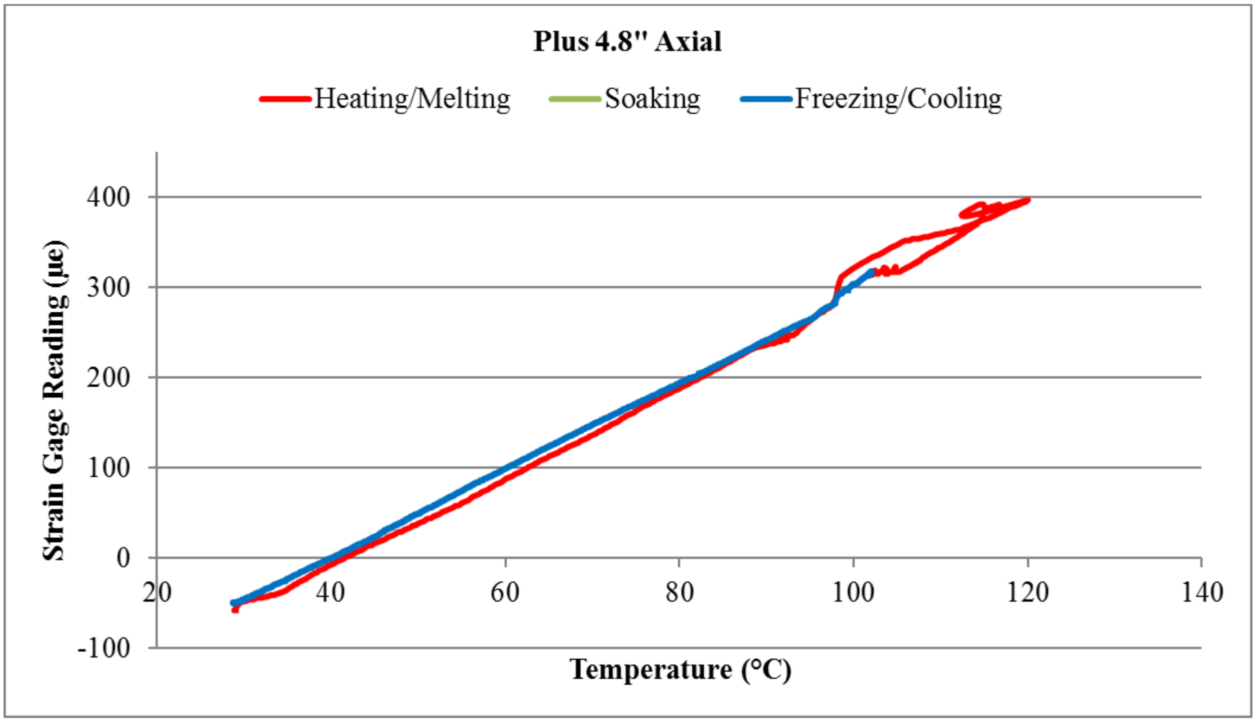

Figure 133. Entire axial strain history at +4.8” from the test section center in Test 8.

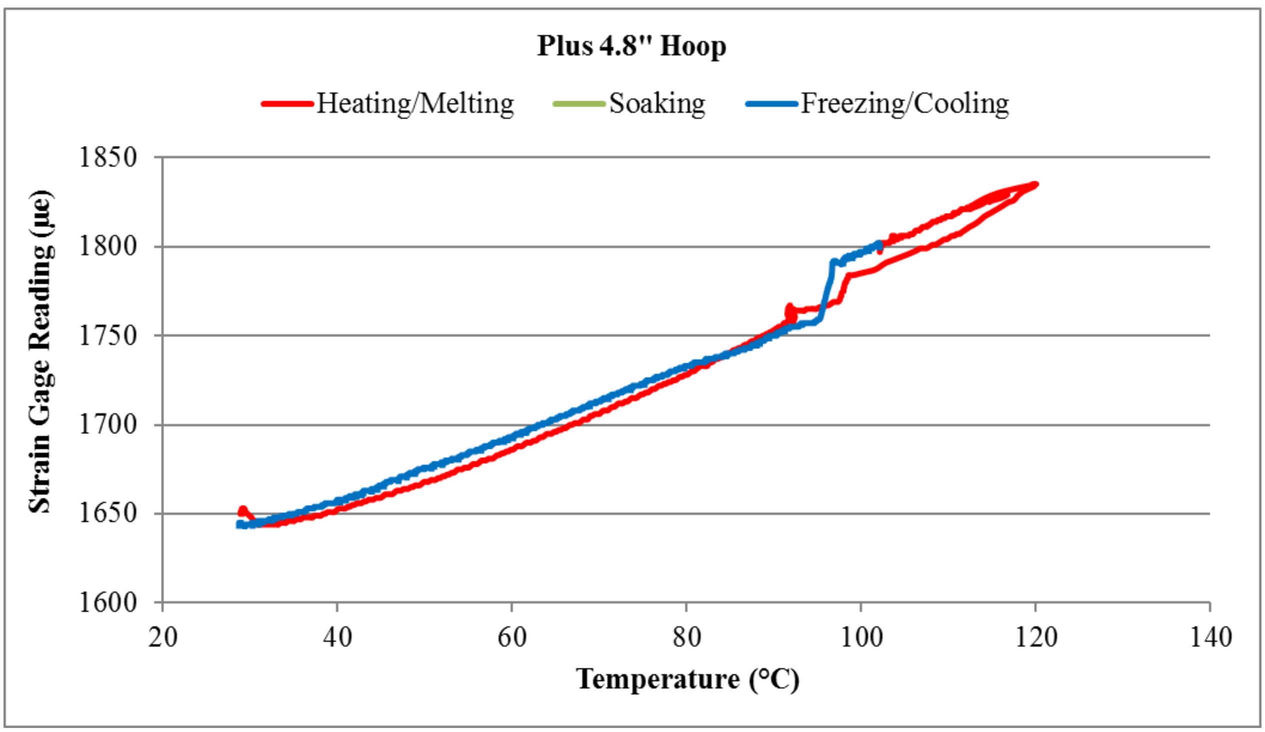

Figure 134. Entire hoop strain history at +4.8” from the test section center in Test 8.

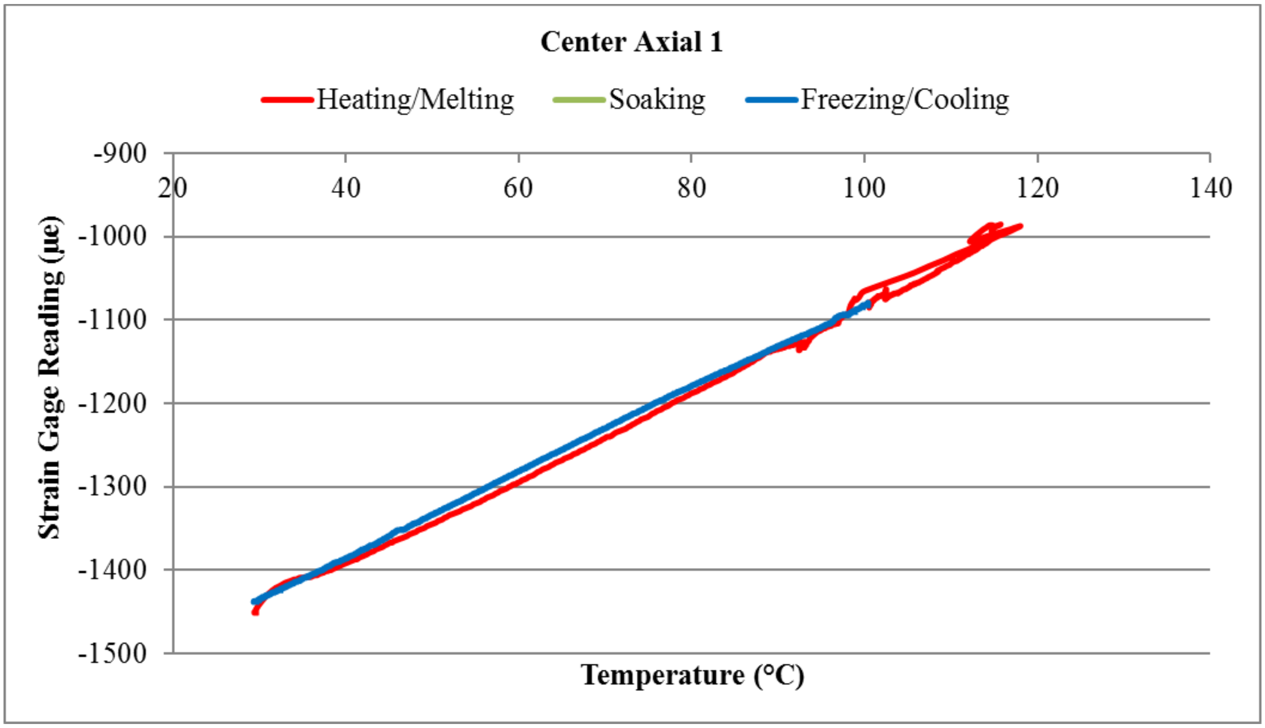

Figure 135. Entire axial strain 1 history at the test section center in Test 8.

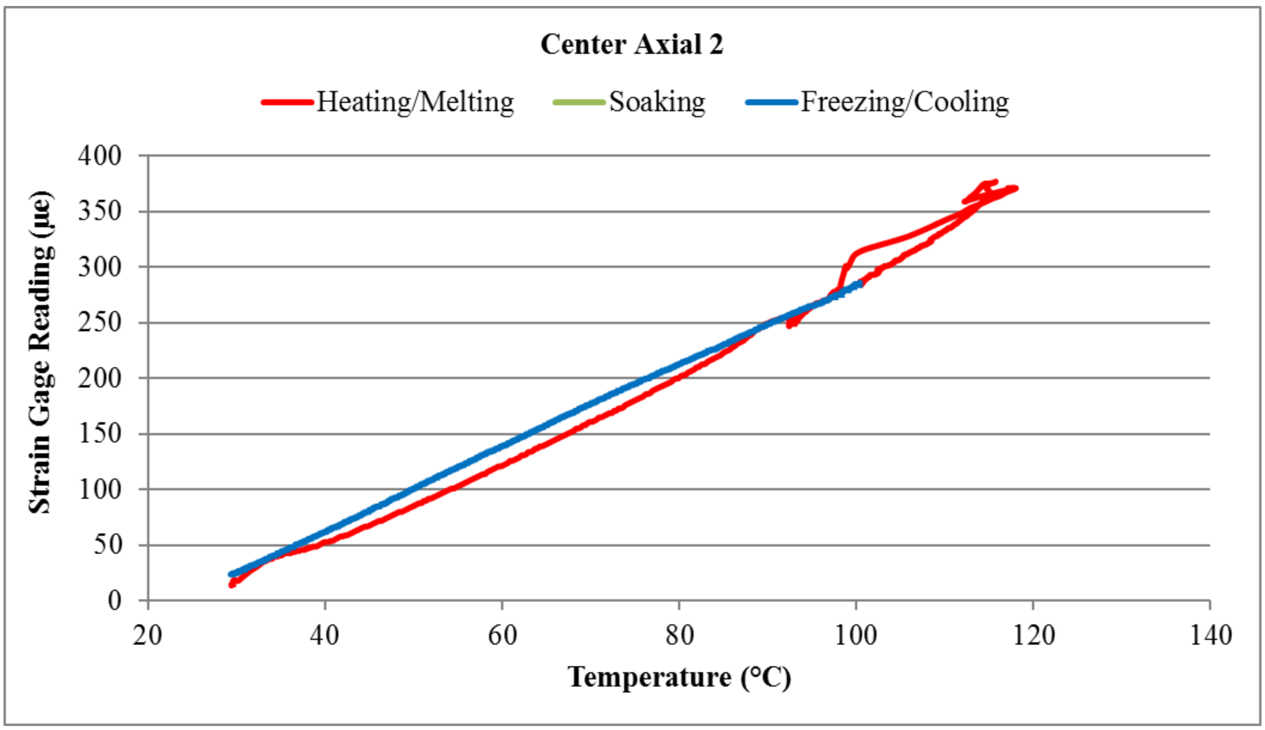

Figure 136. Entire axial strain 2 history at the test section center in Test 8.

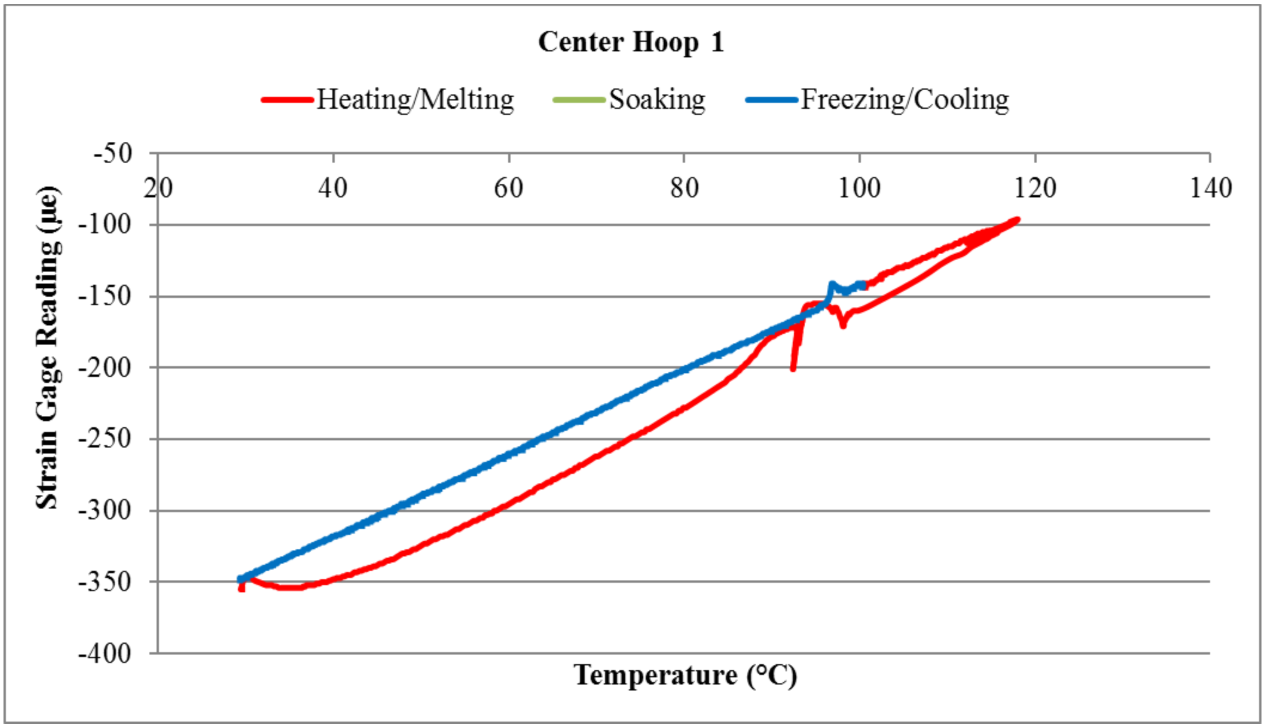

Figure 137. Entire hoop strain 1 history at the test section center in Test 8.

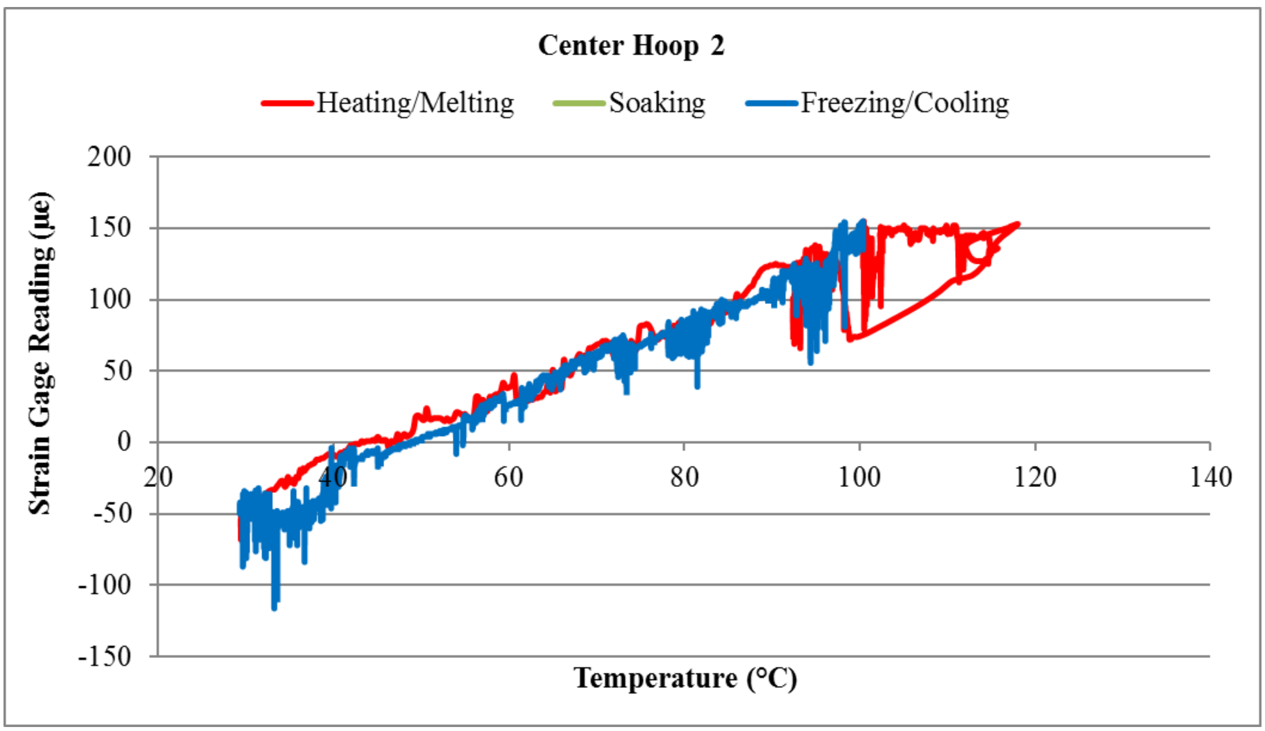

Figure 138. Entire hoop strain 2 history at the test section center in Test 8.

3.9 Test 9: Test with Freezing Pattern 5

Before performing the ultimate 30 psig test, it was decided to perform one last test under vacuum to test a few new ideas. First, in the previous tests, although efforts were made to form frozen plugs as solid as possible, significant strain changes due to sodium freezing were never observed. In addition, as advised by the lead experimenter of the previous liquid lithium experiment [4], there was no intentional control of cooling in the liquid lithium experiment in which deformation of the rectilinear EM pump duct due to lithium freezing was observed. Therefore, it was decided to rely on the natural heat loss in the loop to form the freezing plugs. In this test, after all the sodium was melted, the test section center temperature was (Zone 1) at 115°C while turning off all the other heaters. Second, after freezing plugs were formed and further solidified overnight, the temperature of the test section center was manipulated, trying to eliminate voids (if any) formed in the frozen plugs. The test section center temperature was first lowered to 102°C and then increased to 137°C with a controlled cooling and heating rate of 1°C per 4 minutes. Third, after the test section center temperature stabilized at 137°C, the heater set temperature was lowered to room temperature at a constant rate of 1°C per 4 minutes.

There was a noticeable finding in this test. As shown in Figure 139, a constant temperature corresponding to sodium freezing point was not observed in this test, which was however observed in all previous tests. The controlled cooling was first ruled out as the possible reason. When sodium freezes, it is supposed to maintain at a constant temperature for a while. However, the heater set temperature continues to ramp down. As long as the set temperature is lower than the measured temperature, the heater is equivalent to being completely off. The effect of pressure on the sodium melting temperature as a possible reason was also investigated. According to [13], the rate of melting point change with pressure for sodium is ~ 7E-8 K/Pa, which is too small to cause any appreciable change in the sodium melting point with pressure change that could be experienced in this test.

The entire strain histories in this test are shown in Figure 140 to Figure 147. The phenomenon of solid sodium pulling the tube wall after freezing again shows at the +4.8” location in the hoop strain. Another noticeable finding is the sharp drop of ~ 50 micro strains right after freezing observed at the center location (hoop strain 2), which was never observed in previous tests.

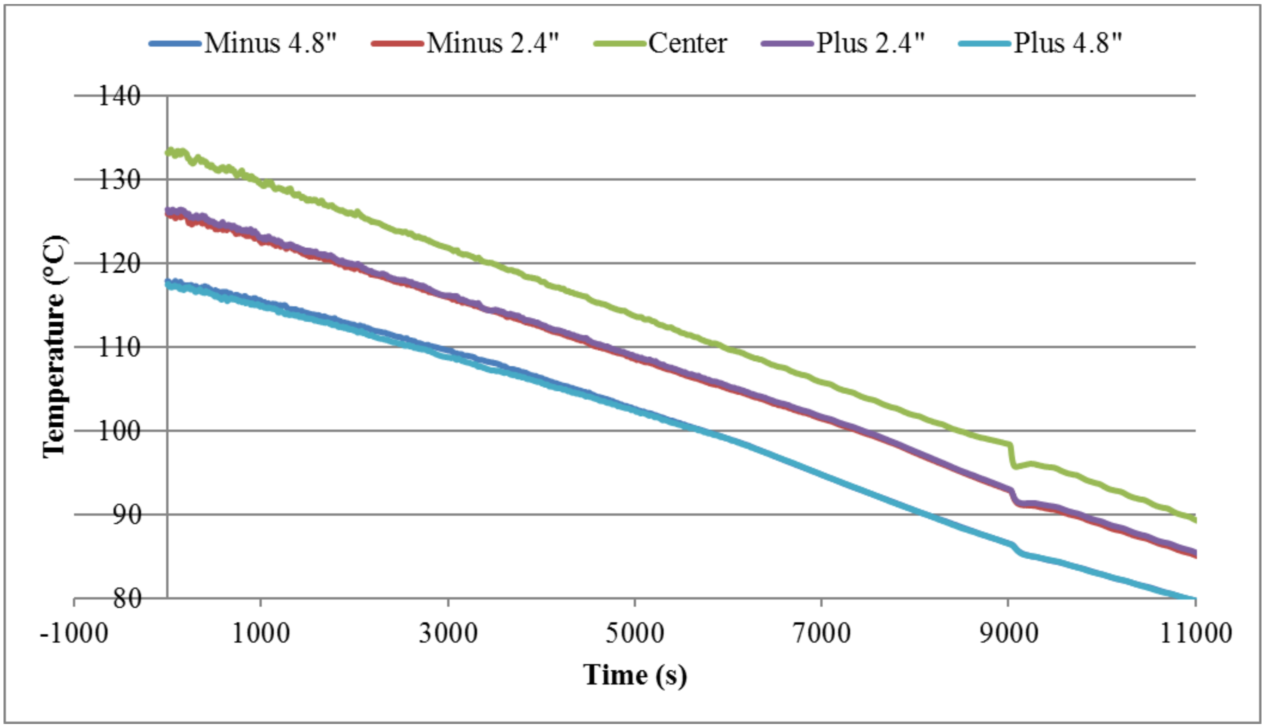

Figure 139. No constant temperatures shown during sodium freezing in the test section in Test 9.

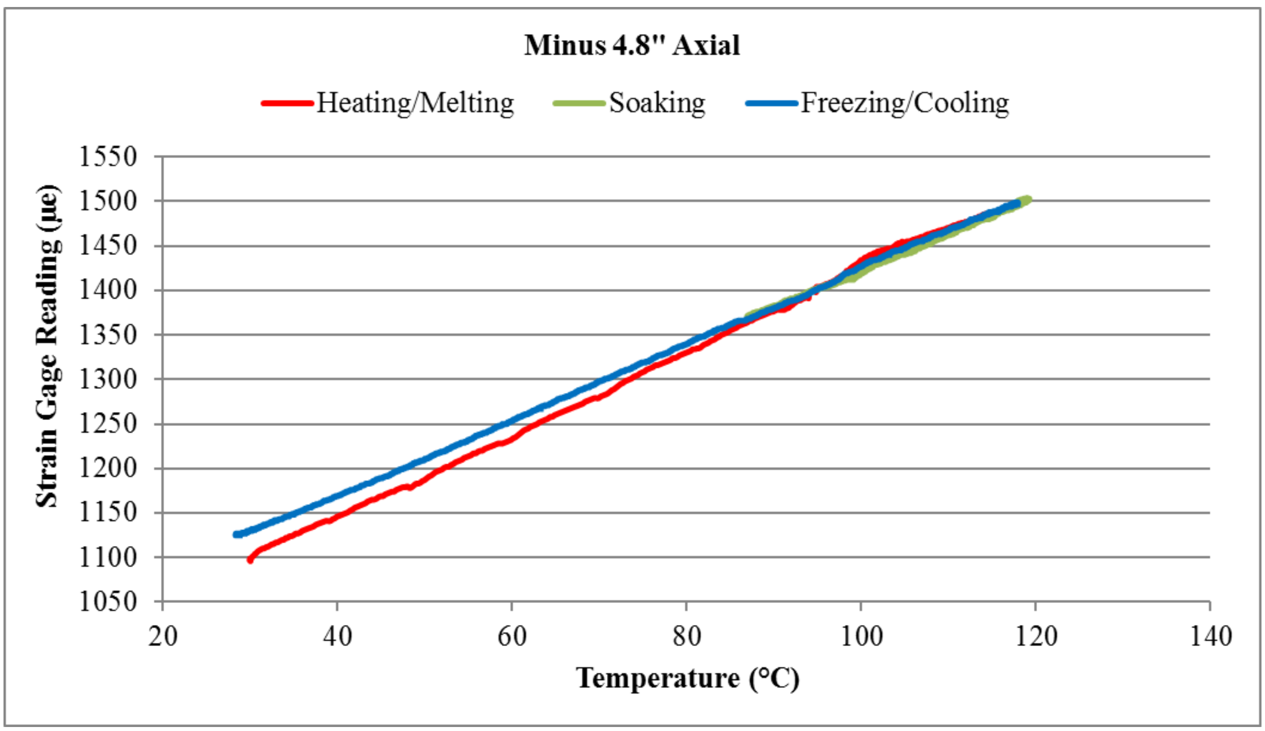

Figure 140. Entire axial strain history at –4.8” from the test section center in Test 9.

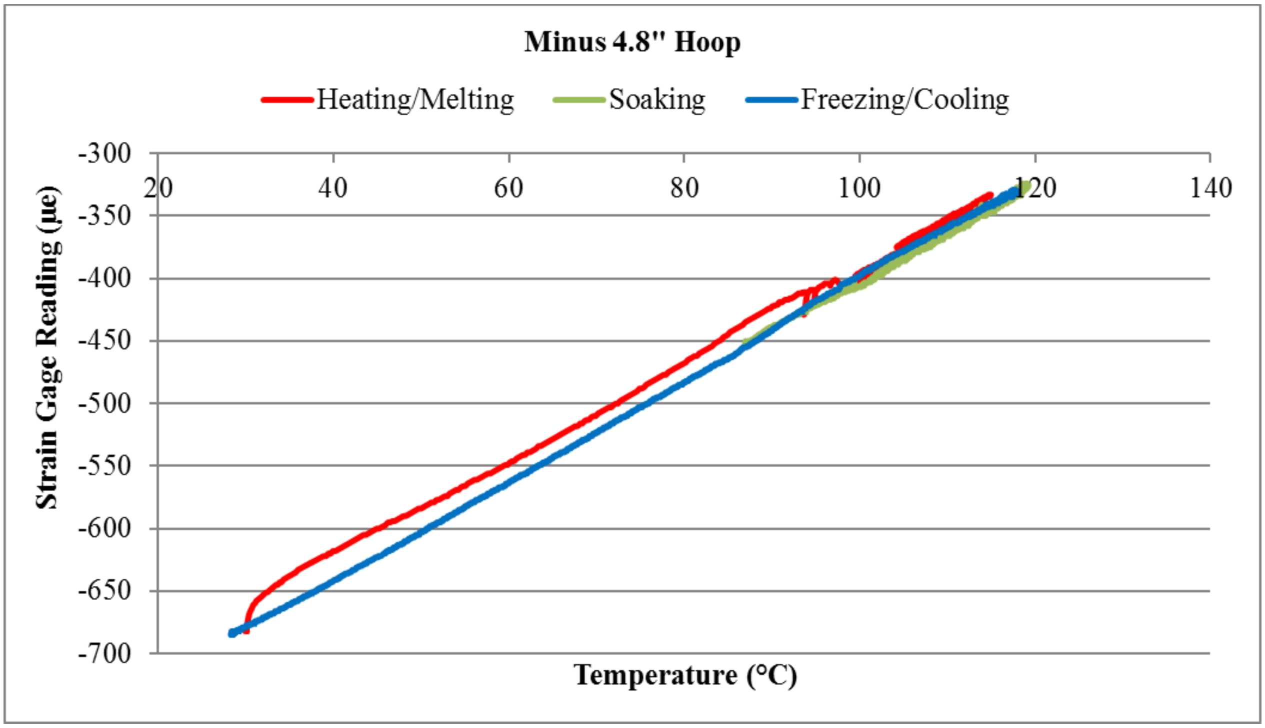

Figure 141. Entire hoop strain history at -4.8" from the test section center in Test 9.

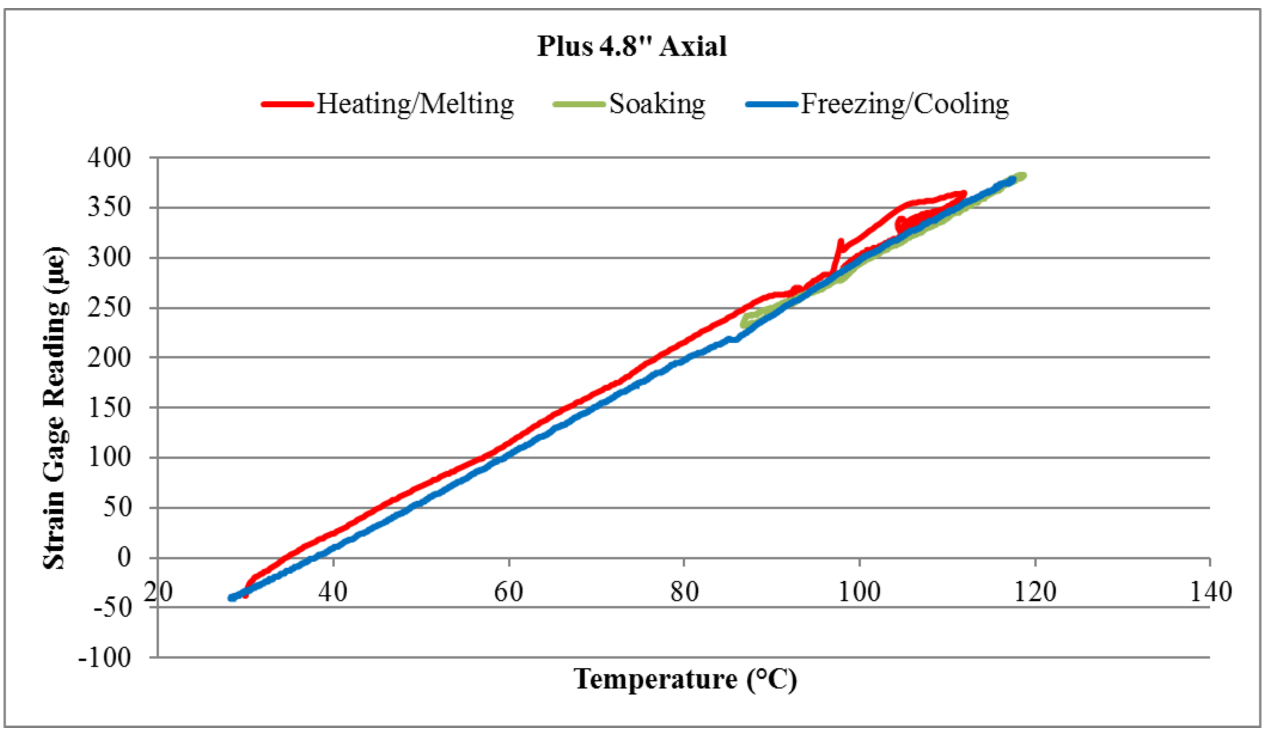

Figure 142. Entire axial strain history at +4.8" from the test section center in Test 9.

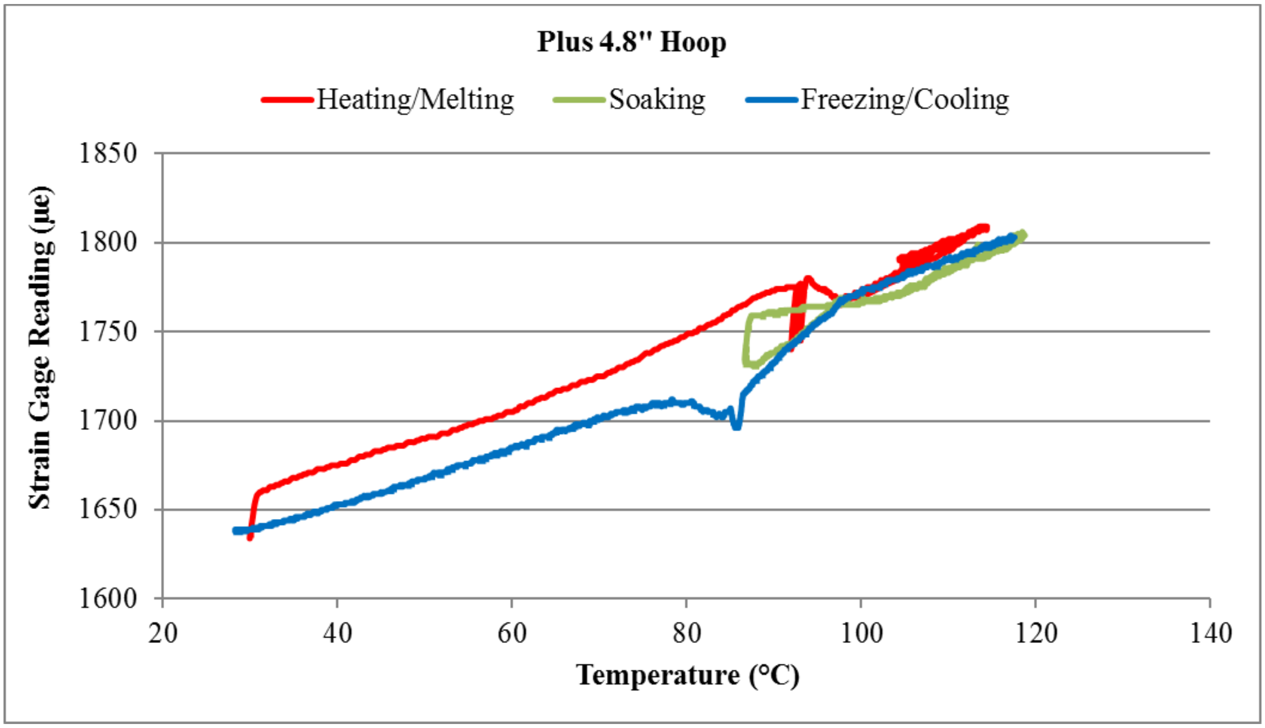

Figure 143. Entire hoop strain history at +4.8" from the test section center in Test 9.

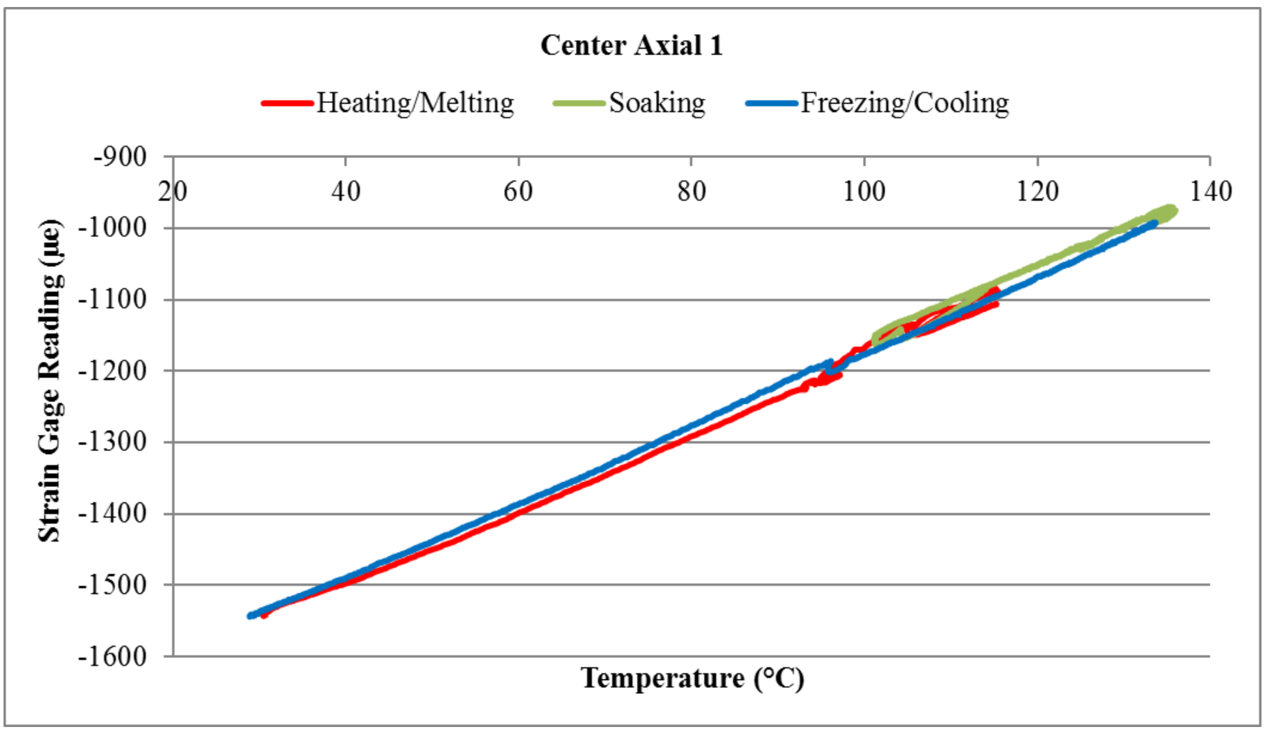

Figure 144. Entire axial strain 1 history at the test section center in Test 9.

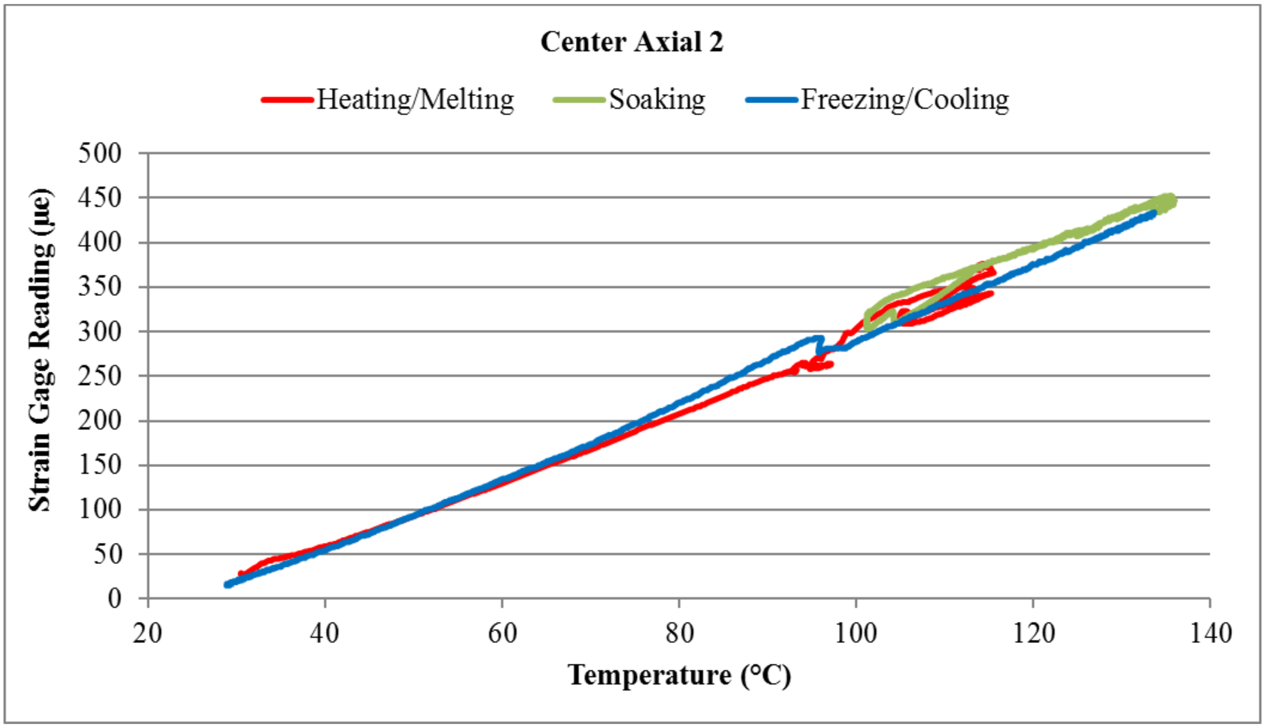

Figure 145. Entire axial strain 2 history at the test section center in Test 9.

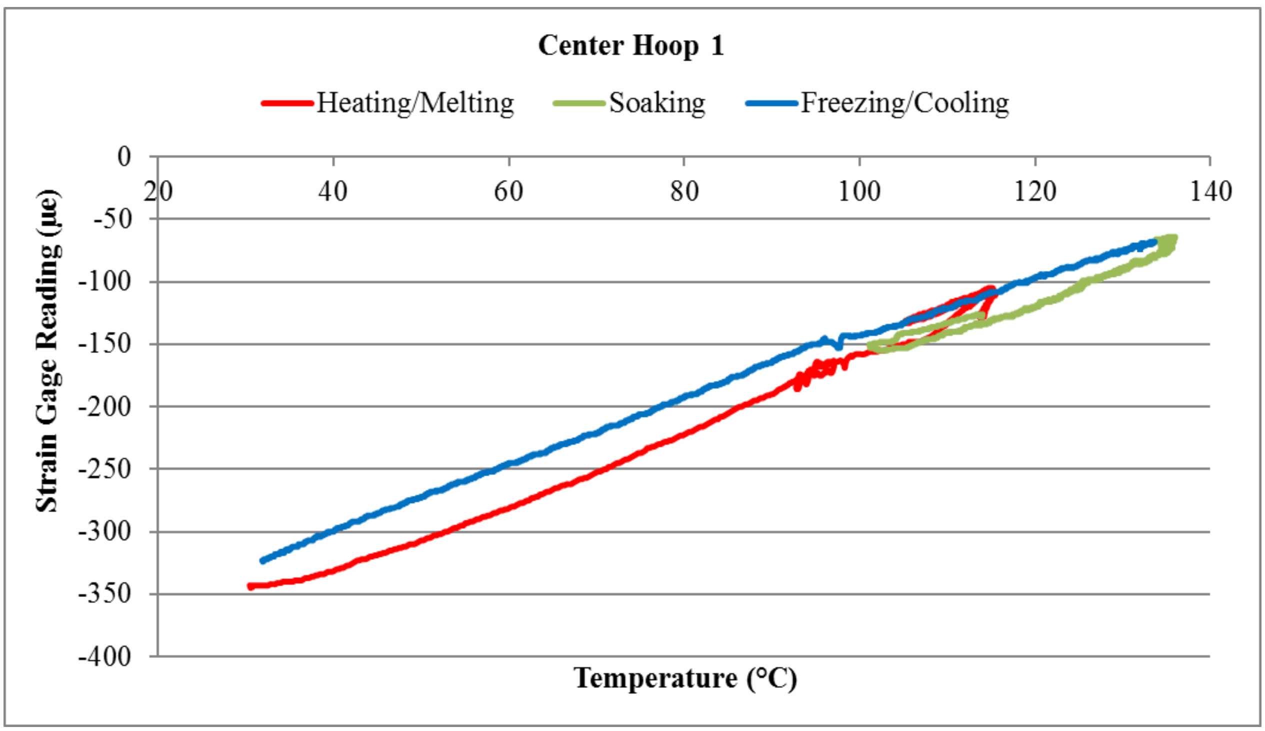

Figure 146. Entire hoop strain 1 history at the test section center in Test 9.

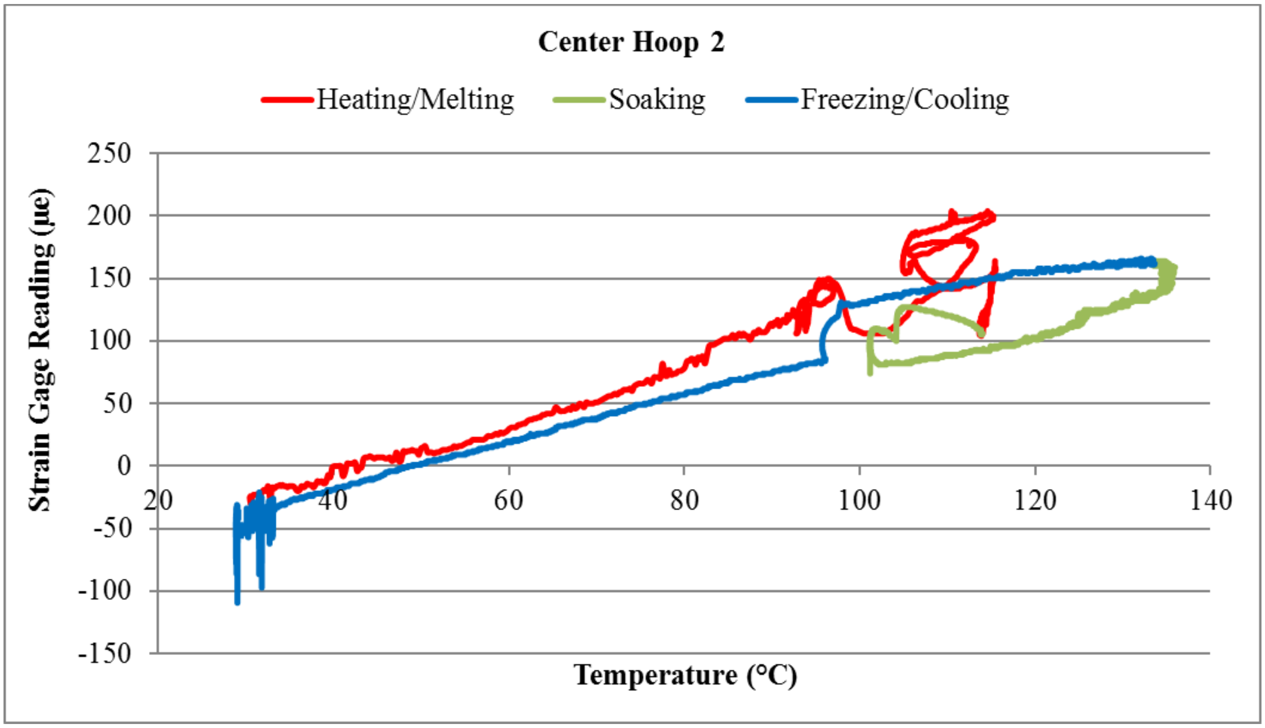

Figure 147. Entire hoop strain 2 history at the test section center in Test 9.

3.10 Test 10: 30 psig Test

As discussed earlier, the main purpose of this test is to indirectly prove the previous hypothesis of Ar cavitation during sodium freezing. In addition, the pressure response of the strain gages was tested before freezing was initiated. The pressure response information of the strain gages is necessary to properly translate the previously measured strain drops due to sodium freezing and solid sodium pulling the tube wall after freezing to negative pressures. In this test, after all the sodium was melted and the test section temperature stabilized at ~ 105°C, the strain gage pressure response test was performed by injecting Ar and increasing the cover gas pressure gradually from vacuum to 30 psig. The pressure response results of the 8 strain gages are shown in Figure 148 to Figure 155. With this information, the previously measured maximum strain change during sodium freezing (10 micro strains at center axial Strain Gage 2) is equivalent to a negative pressure of approximately 55 psi, and the maximum strain change due to solid sodium pulling the tube wall after freezing (60 micro strains at +4.8" hoop) is equivalent to a negative pressure of approximately 77 psi. The latter negative pressure may represent the yield strength of solid sodium. Considering that the yield strength of solid lithium is approximately 81 psi [14], this speculation seems reasonable.

After the pressure response test, the freezing test was started by forming frozen plugs first in Zones 6 and 7. After that, the frozen plugs were extended to the free surfaces and further cooled down over night. The test section was frozen by turning off all the heaters on the second day. The entire strain histories in this test are shown in Figure 156 to Figure 163. The initial purpose of this test was to prove the hypothesis of Ar cavitation during sodium freezing. If cavitation does occur during sodium freezing (say at 0 psia), the strain drop due to the initial cover gas pressure should be first registered, causing a more significant drop at the sodium melting point. This, however, did not occur as expected. A strain drop due to the initial cover gas pressure was indeed observed at all strain measurement locations, as shown in Figure 156 to Figure 163. However, it occurred before the test section was frozen. A closer examination of the data showed that it occurred after frozen plugs were formed in Zones 6 and 7, and was probably caused by the growth of the frozen plugs into the test section and the subsequent cooling down. In addition, all the measured strains were found to drop to values corresponding to 0 psia. This indicates that the frozen plugs were able to withstand a pressure difference of 45 psi, which is consistent with the previous speculation about the yield strength of solid sodium.

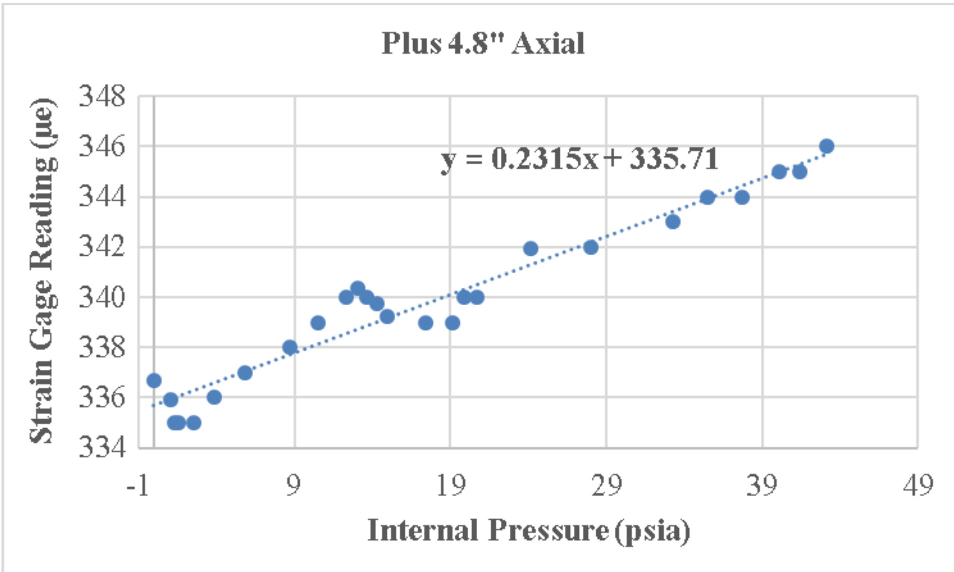

Figure 148. Pressure response of the axial strain gage at +4.8" in Test 10.

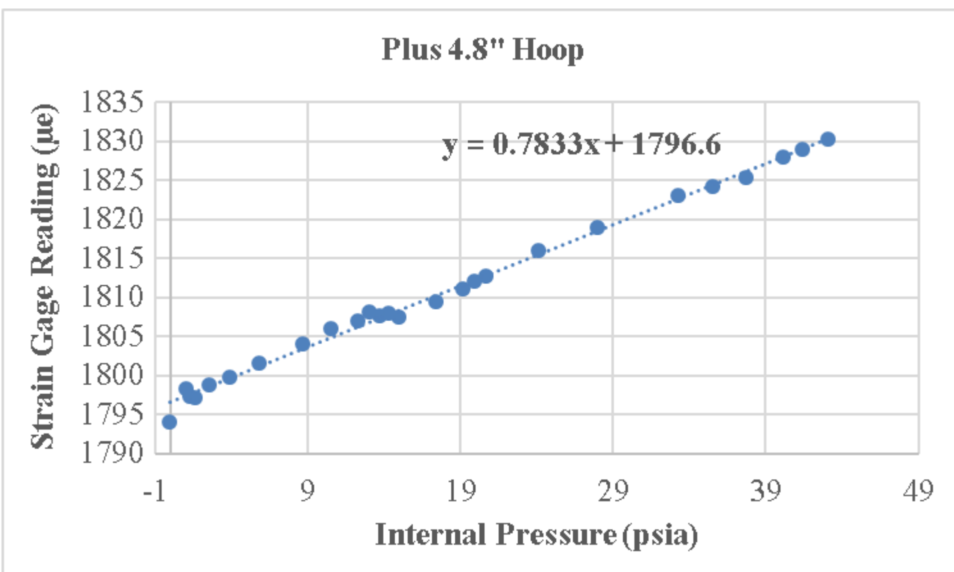

Figure 149. Pressure response of the hoop strain gage at +4.8" in Test 10.

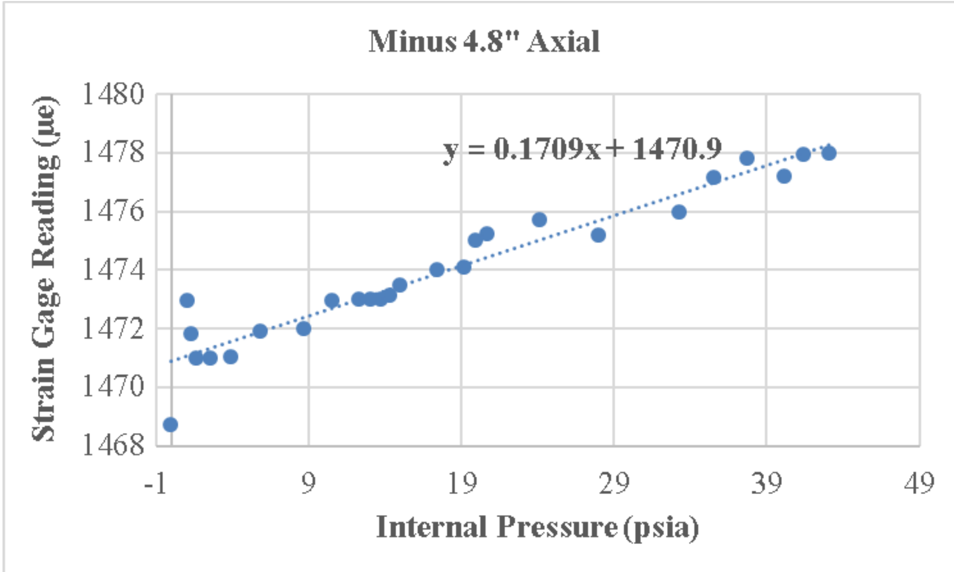

Figure 150. Pressure response of the axial strain gage at -4.8" in Test 10.

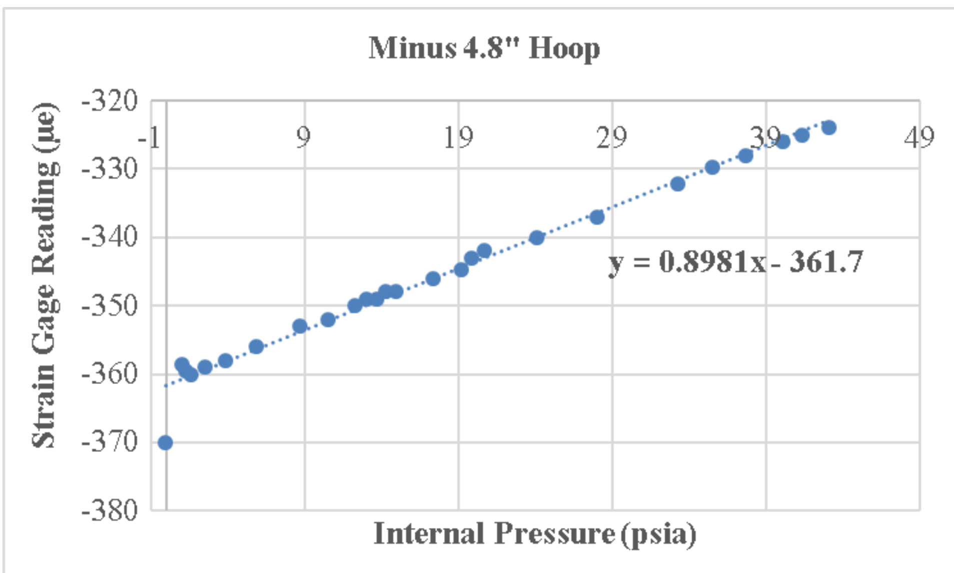

Figure 151. Pressure response of the hoop strain gage at -4.8" in Test 10.

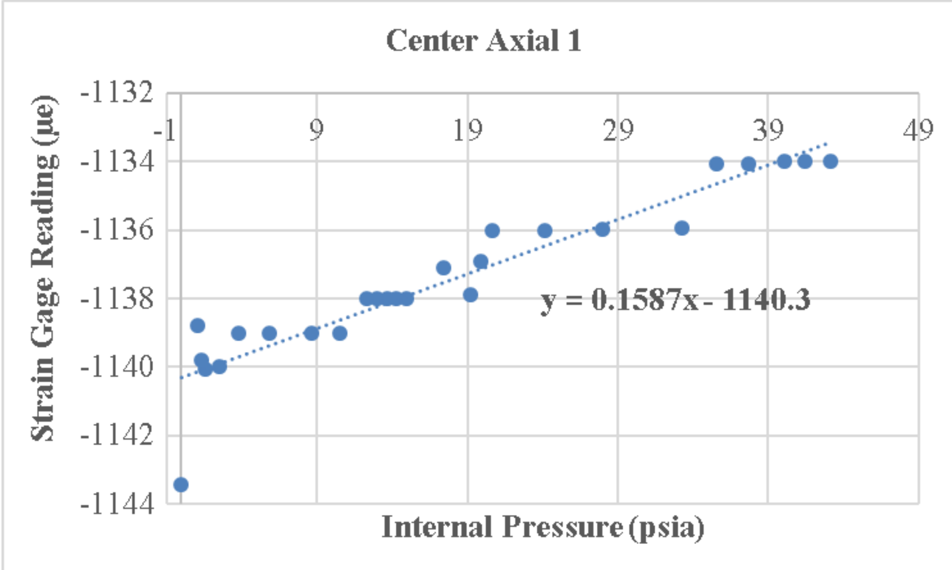

Figure 152. Pressure response of the axial strain gage 1 at center in Test 10.

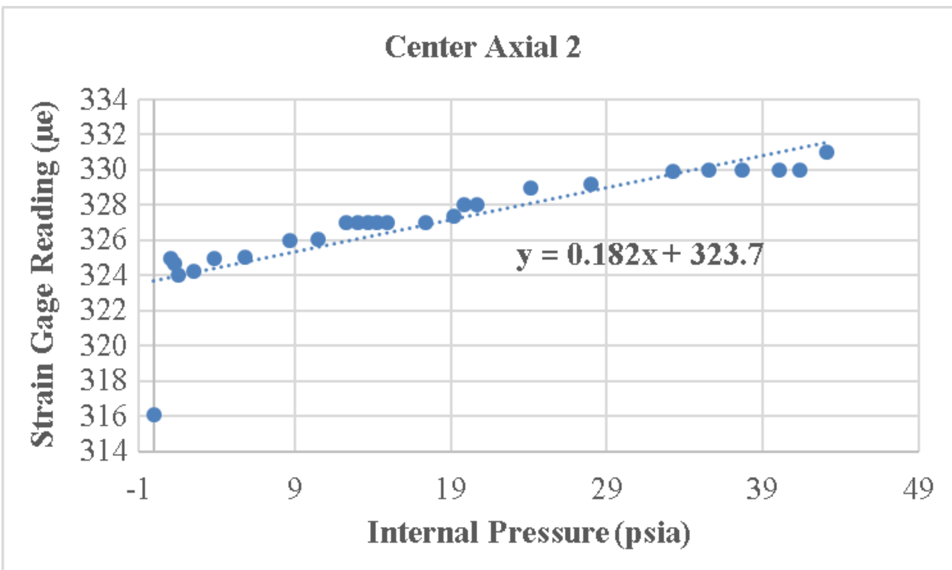

Figure 153. Pressure response of the axial strain gage 2 at center in Test 10.

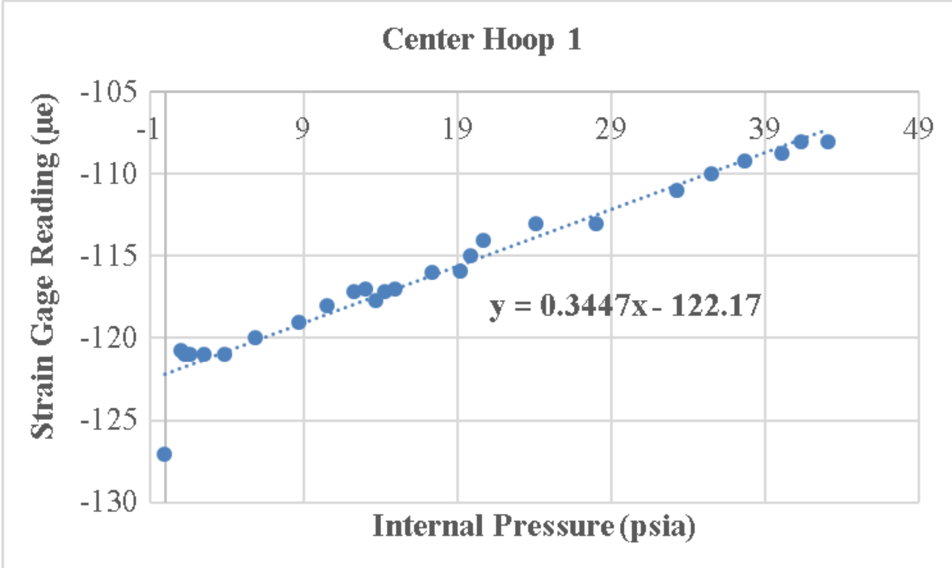

Figure 154. Pressure response of the hoop strain gage 1 at center in Test 10.

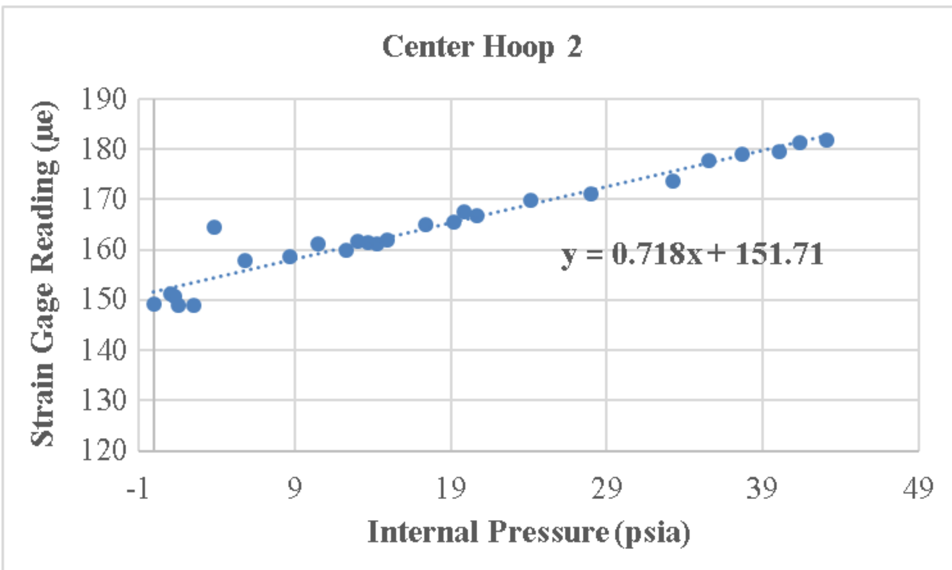

Figure 155. Pressure response of the hoop strain gage 2 at center in Test 10.

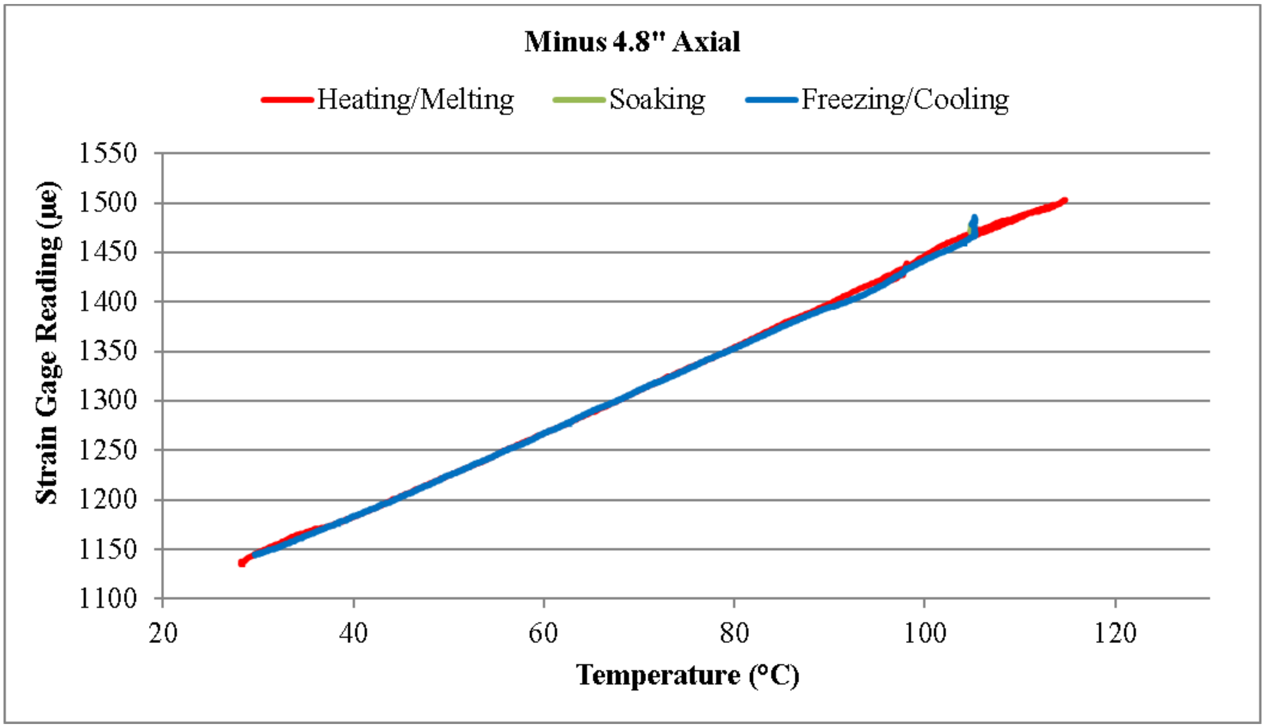

Figure 156. Entire axial strain history at –4.8" from the test section center in Test 10.

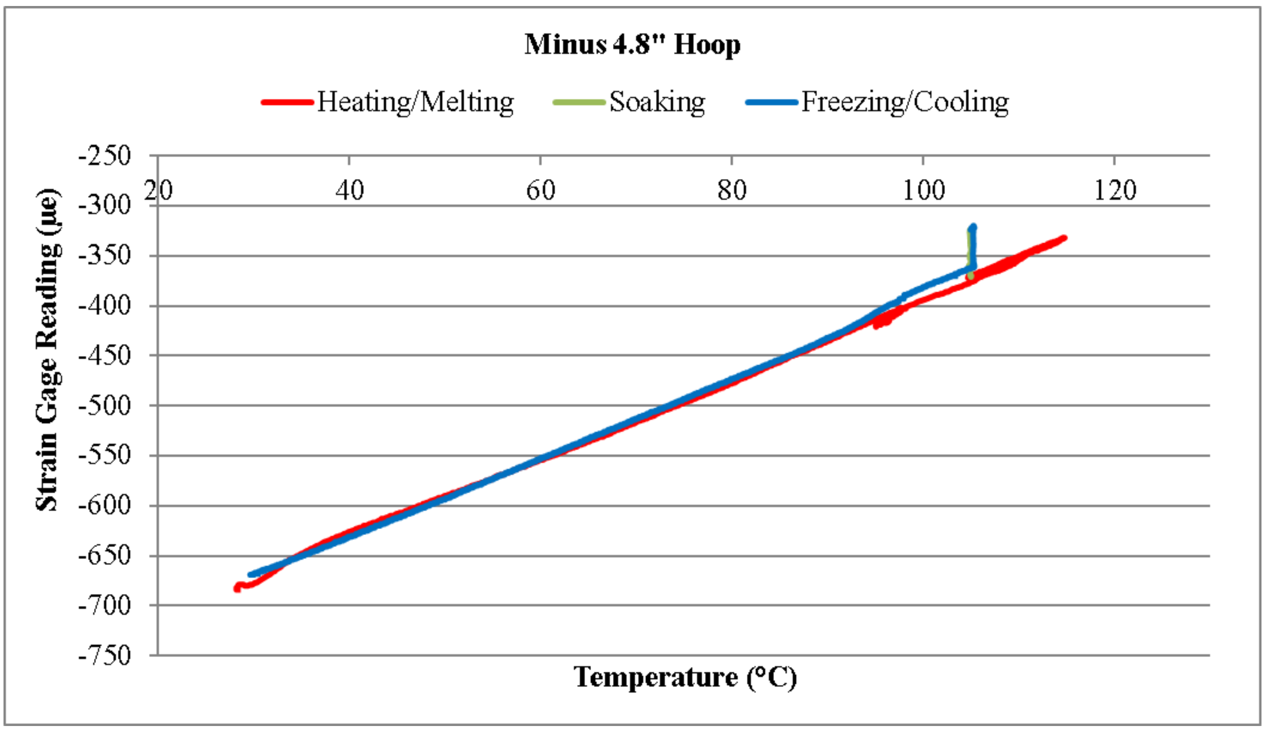

Figure 157. Entire hoop strain history at -4.8" from the test section center in Test 10.

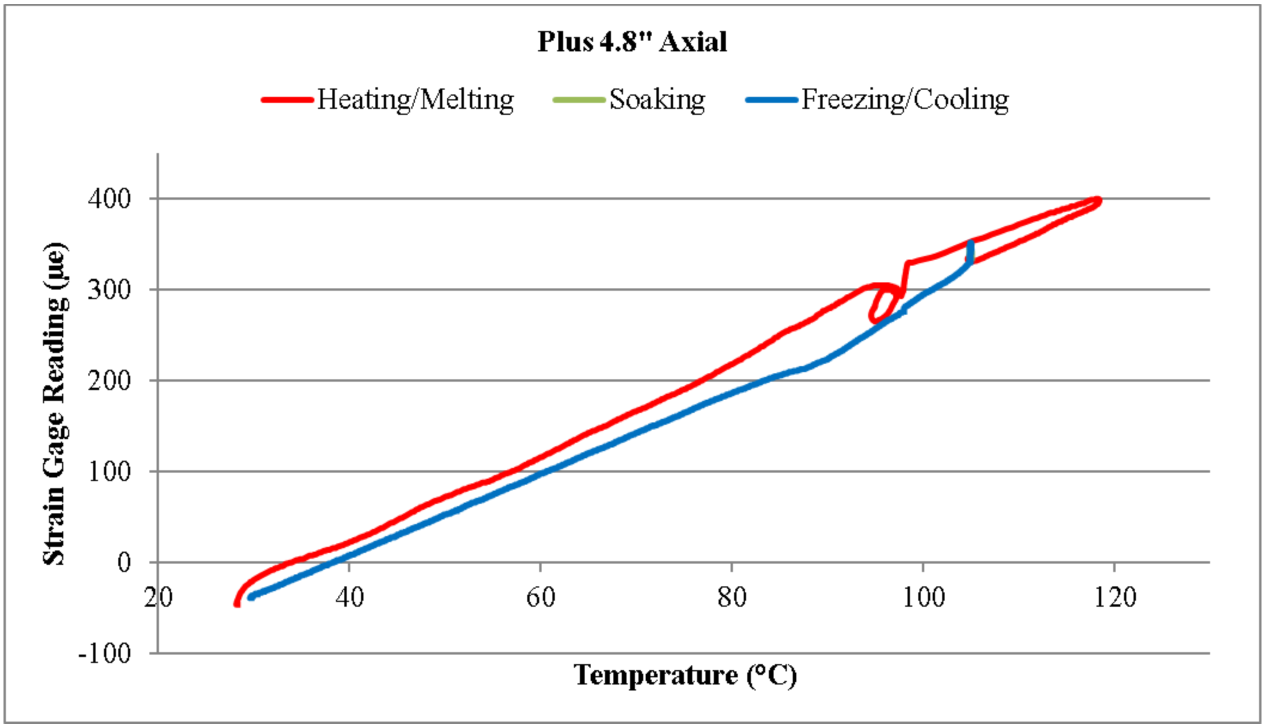

Figure 158. Entire axial strain history at +4.8” from the test section center in Test 10.

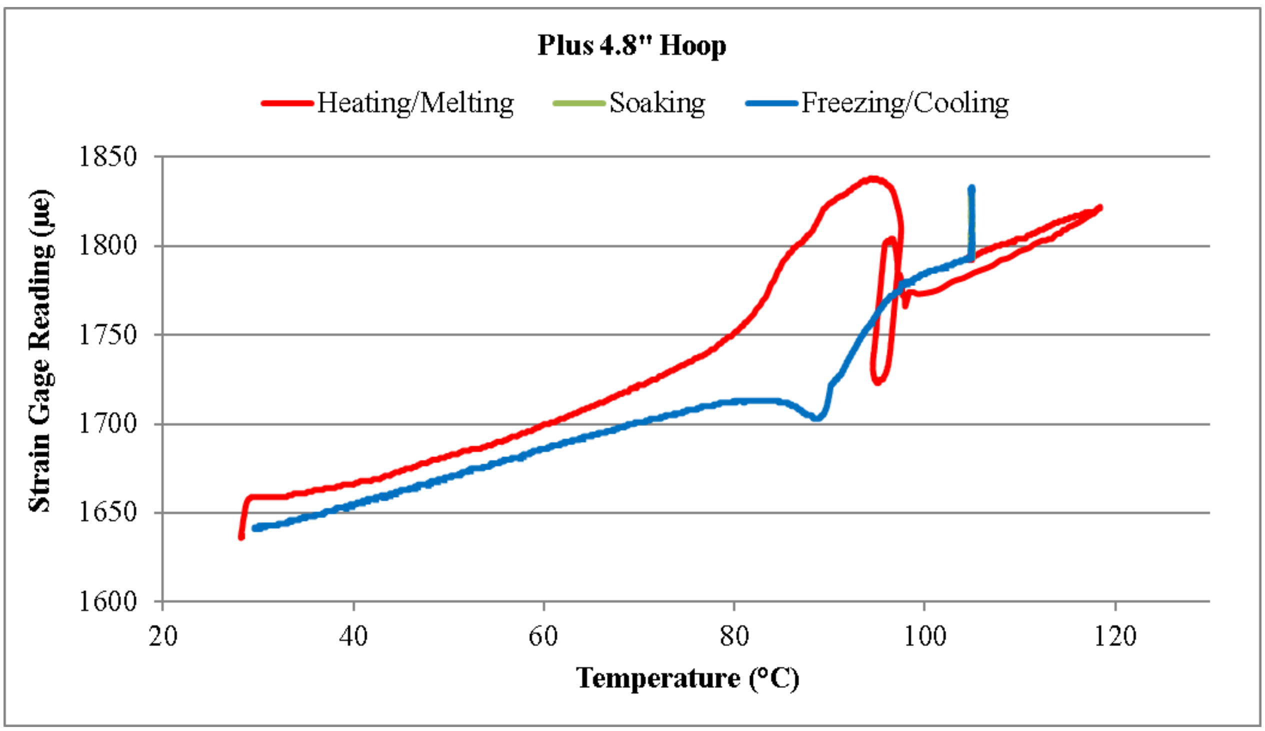

Figure 159. Entire hoop strain history at +4.8” from the test section center in Test 10.

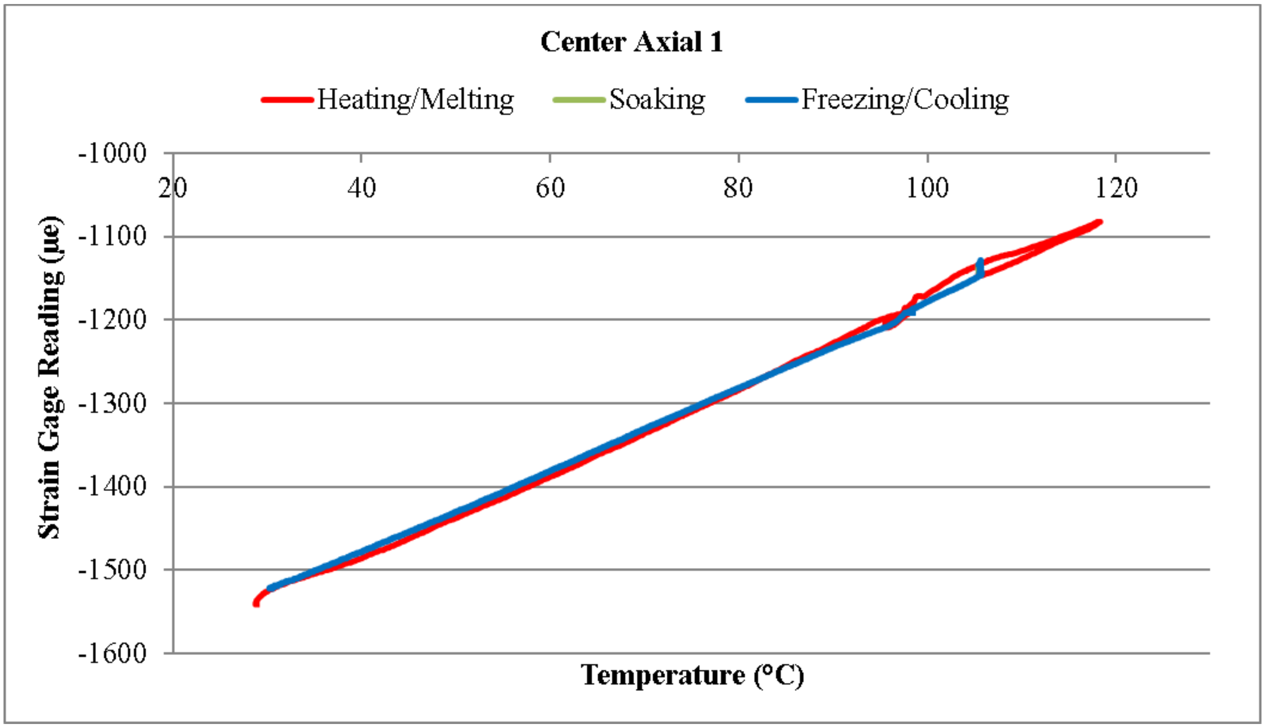

Figure 160. Entire axial strain 1 history at the test section center in Test 10.

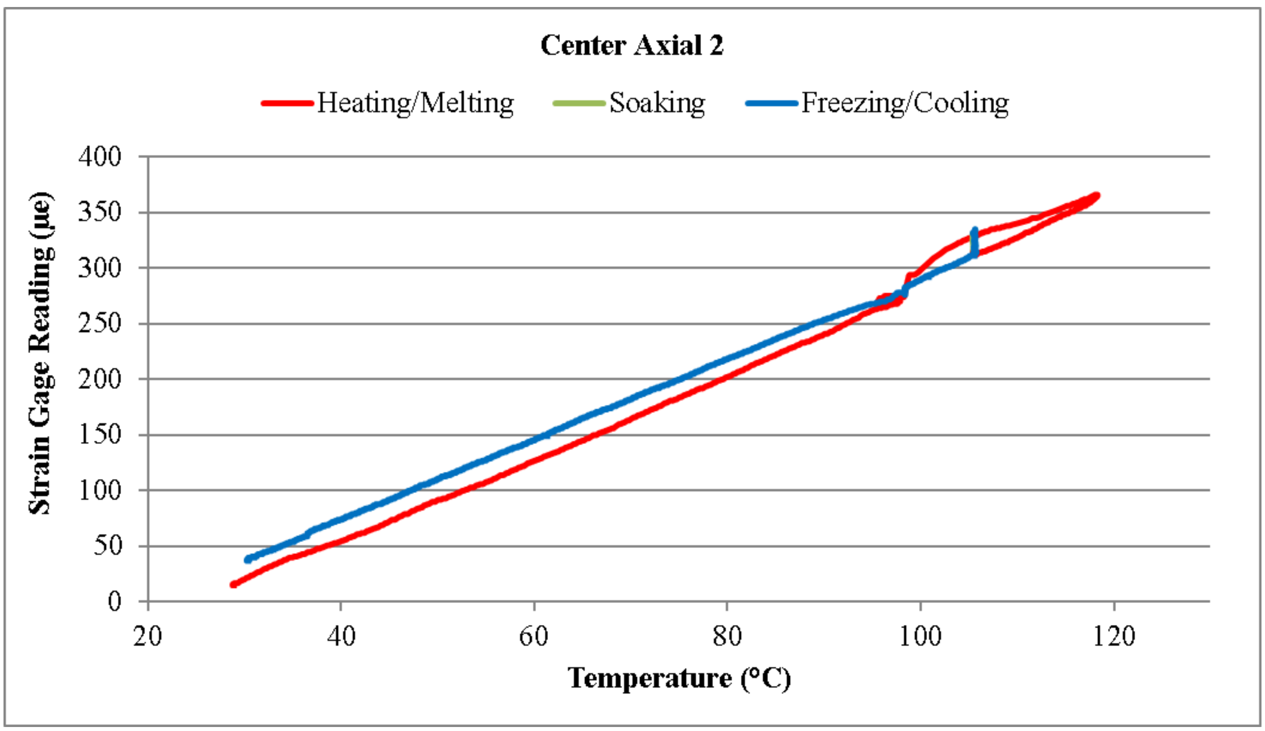

Figure 161. Entire axial strain 2 history at the test section center in Test 10.

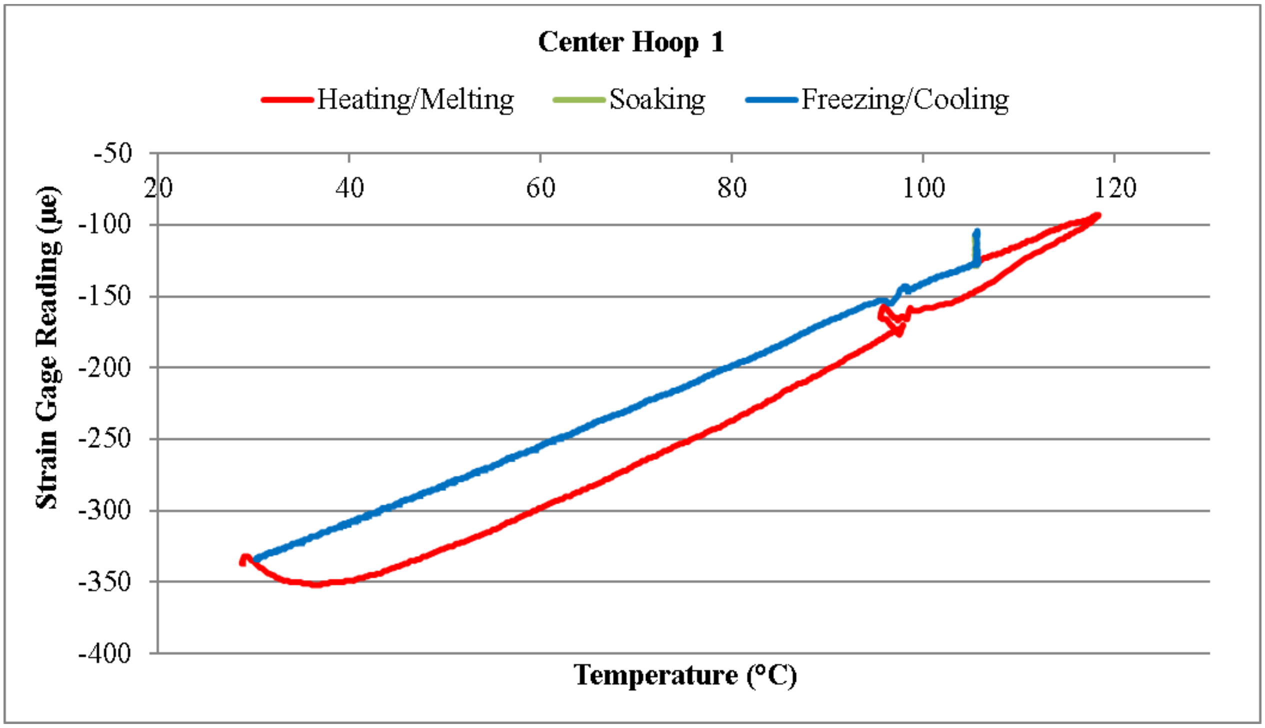

Figure 162. Entire hoop strain 1 history at the test section center in Test 10.

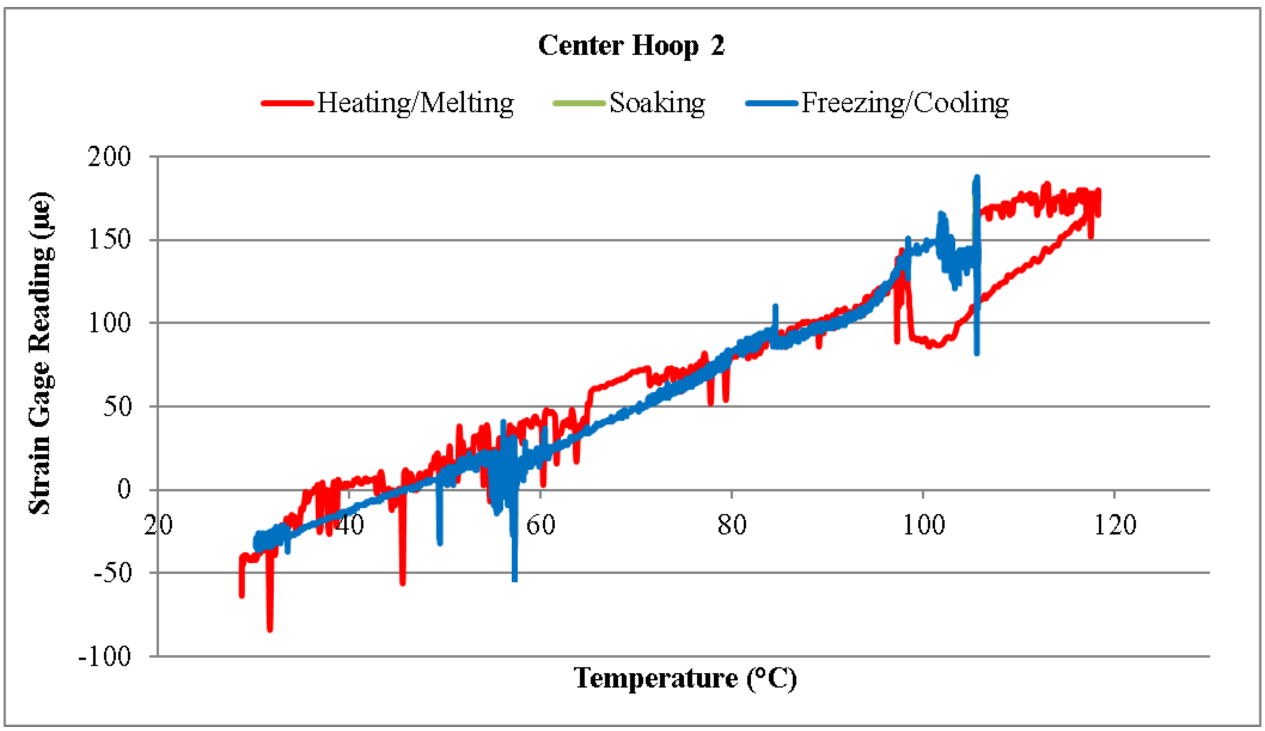

Figure 163. Entire hoop strain 2 history at the test section center in Test 10.

3.11 Test 11: Test with Freezing Pattern 4 and 10 psig Ar

This test is quite similar to Test 8, with the difference that the new test was performed under an Ar cover gas of ~ 10 psig instead of a vacuum. As discussed previously, a prominent phenomenon of solid sodium pulling the tube wall after freezing was not observed at all three measurement locations in Test 8. It was suspected that cavitation still occurred in the test section during freezing, mainly due to the vacuum environment in Test 8, despite freezing being started from the center of the test section. Therefore, it was decided to introduce Ar cover gas (at ~ 10 psig) before initiating freezing in Test 11, to suppress the cavitation process. With Ar cover gas and freezing started from the center of the test section, cavitation is not likely to occur, and dense solid sodium should form at all three measurement locations. Therefore, a prominent phenomenon of solid sodium pulling the tube wall after freezing should be observed at all three measurement locations in this new test. The full strain histories in Test 11 are shown in Figure 164 to Figure 171. Indeed, hoop strain drops due to the pulling from the solid sodium are clearly observed at all three measurement locations, as shown in Figure 165, Figure 167, Figure 170, and Figure 171. In addition, compared to Test 8, this phenomenon in Test 11 is more prominent (Figure 165 vs Figure 132, Figure 167 vs Figure 134, Figure 170 vs Figure 137, and Figure 171 vs Figure 138). These findings corroborate the previous postulate about what occurred in Test 8, and further prove the hypothesis of solid sodium pulling the tube wall after freezing.

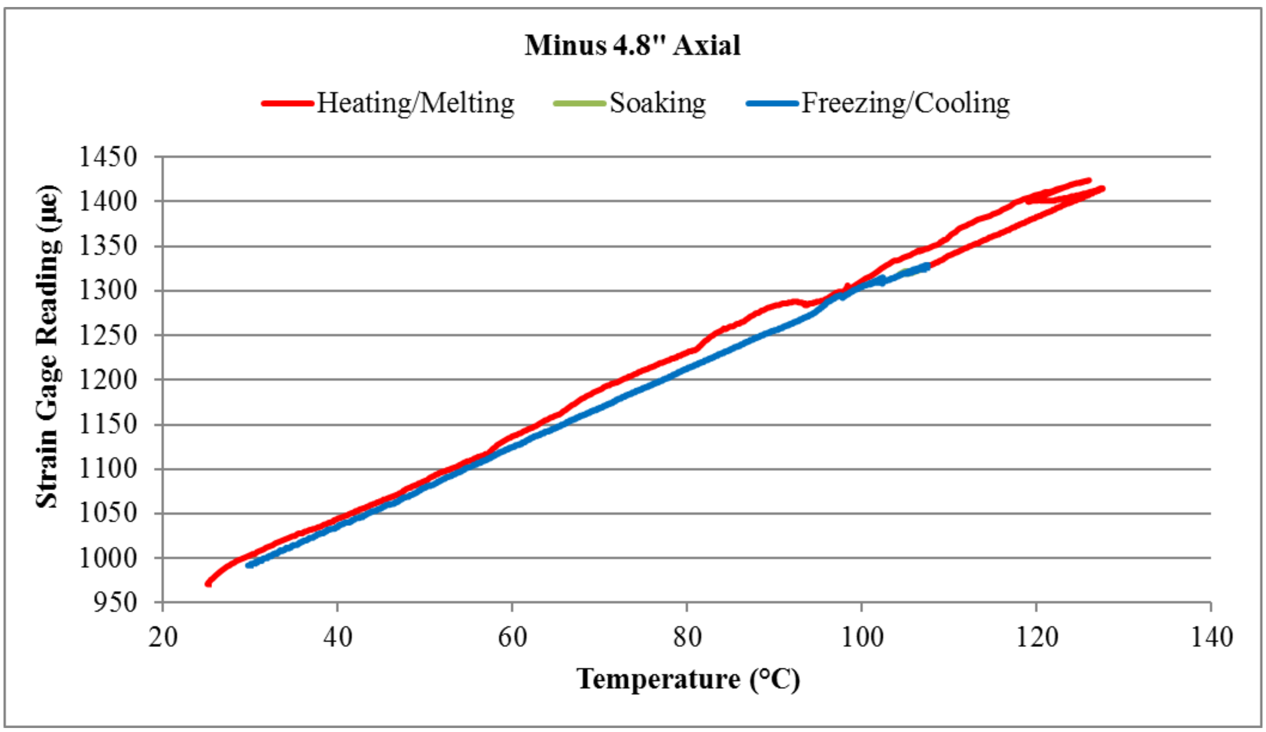

Figure 164. Entire axial strain history at –4.8” from the test section center in Test 11.

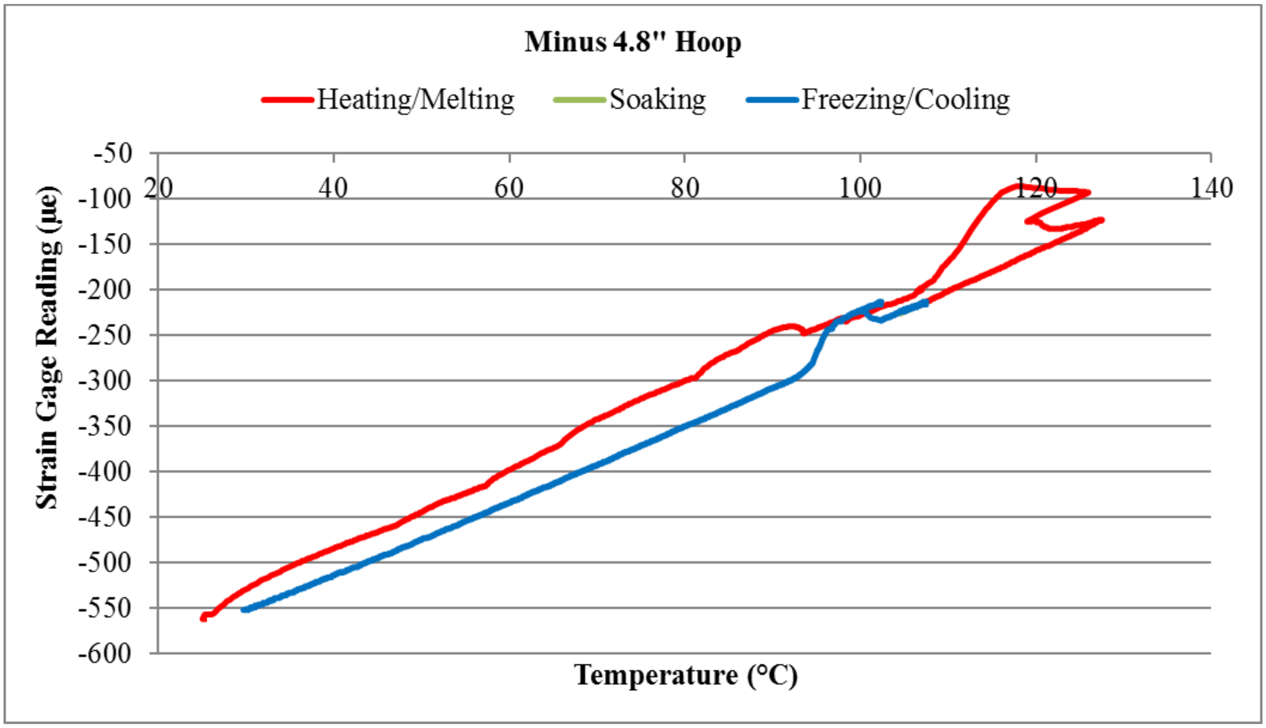

Figure 165. Entire hoop strain history at -4.8" from the test section center in Test 11.

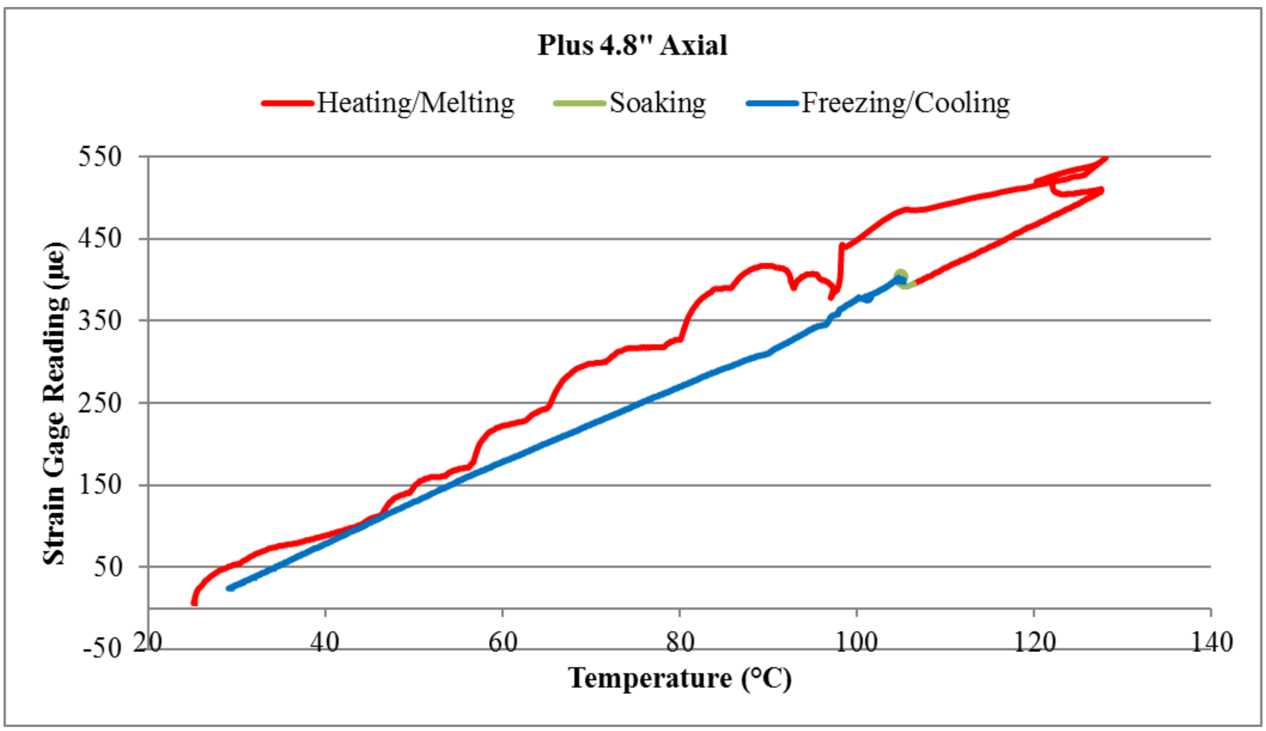

Figure 166. Entire axial strain history at +4.8" from the test section center in Test 11.

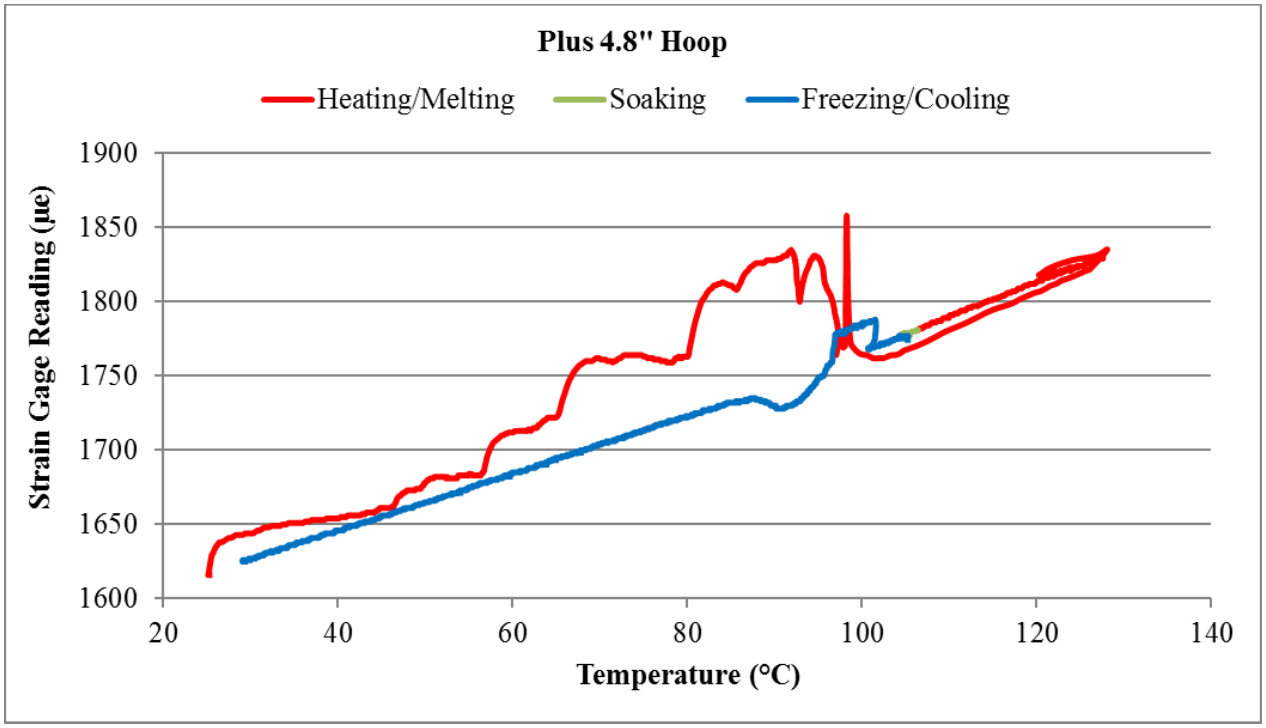

Figure 167. Entire hoop strain history at +4.8" from the test section center in Test 11.

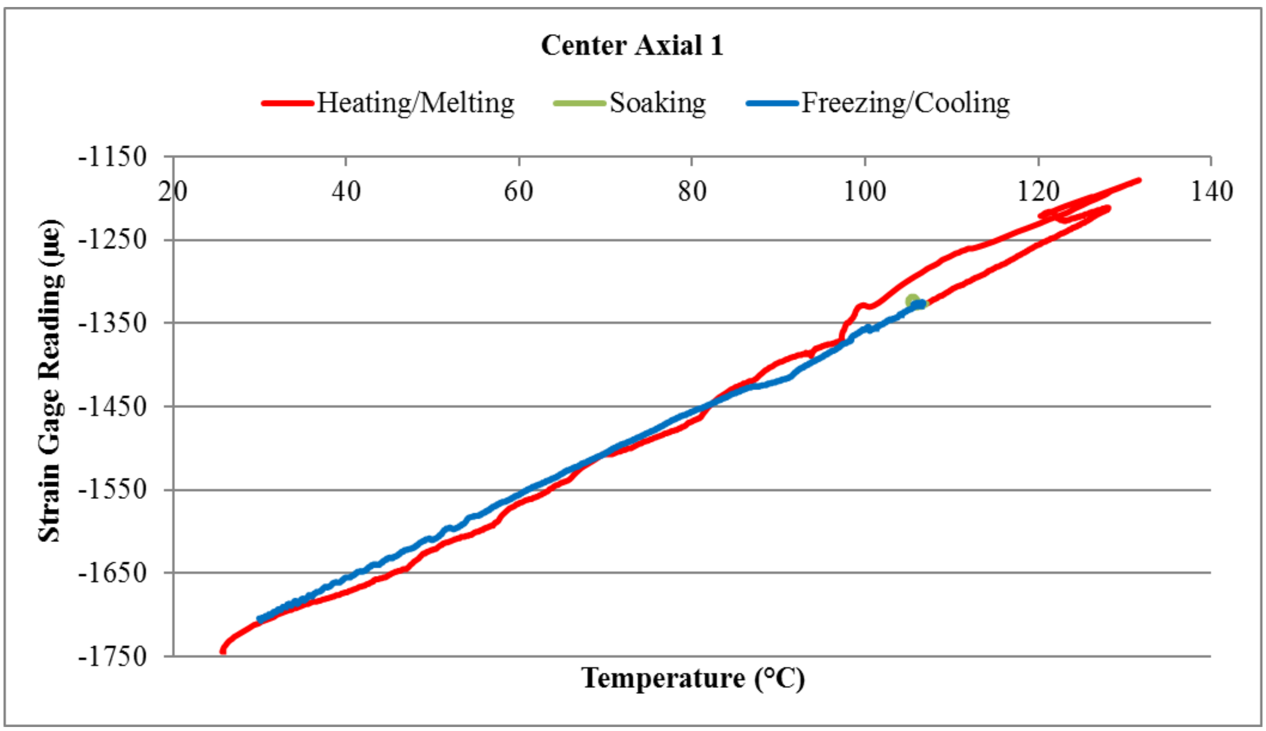

Figure 168. Entire axial strain 1 history at the test section center in Test 11.

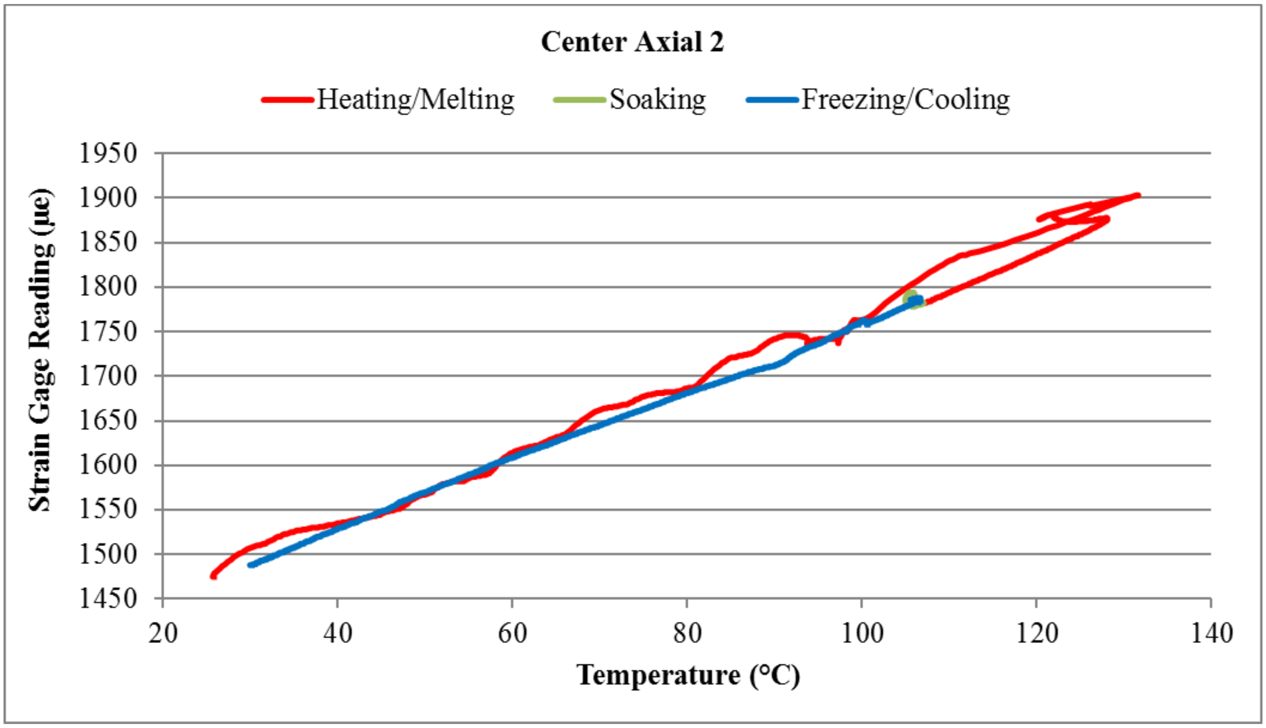

Figure 169. Entire axial strain 2 history at the test section center in Test 11.

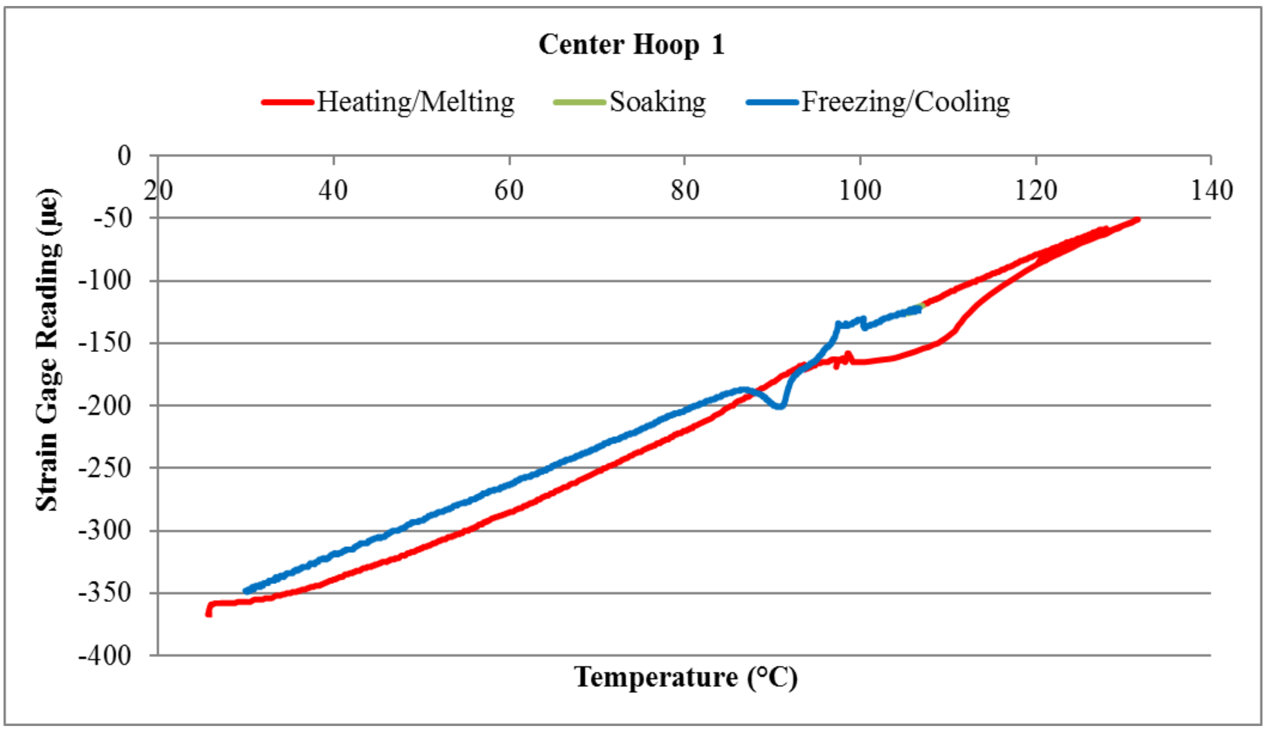

Figure 170. Entire hoop strain 1 history at the test section center in Test 11.

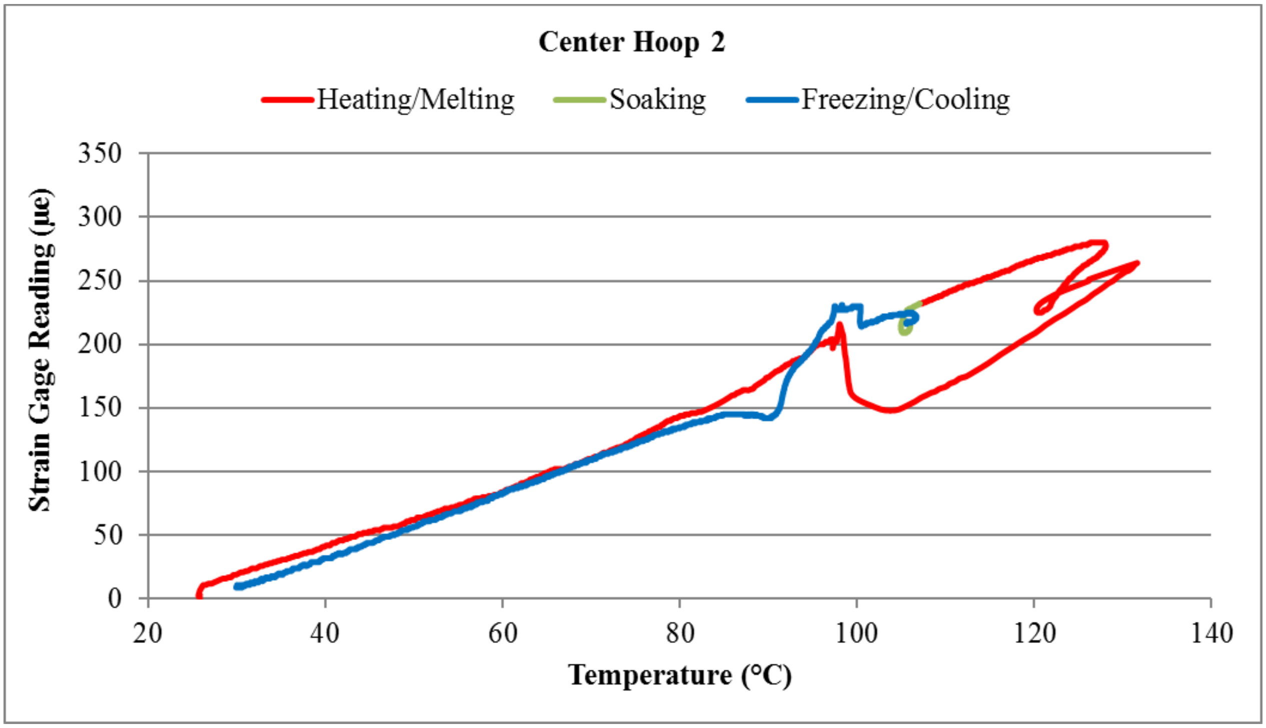

Figure 171. Entire hoop strain 2 history at the test section center in Test 11.

3.12 Test 12: 2nd 500°C Wetting Test

In the first 500°C wetting test, a heating time of ~ 24 hours (at 500°C) was selected based on two factors. First, there was no previous experience of operating the Freezing and Remelting Test Facility at 500°C prior to the first 500°C wetting test. Therefore, it was decided to adopt a proper heating time that is long enough to wet the test section while not unnecessarily long to cause potential tube failure. Second, based on existing information on wetting rate vs temperature [9], 24 hours were deemed sufficient to wet the test section at 500°C. Considering the uncertainty in the literature data, a second 500°C wetting test was proposed and performed to affirm the achievement of wetting in the test section, as well as to investigate the effect of extended heating time (at 500°C) on the freezing behavior. The procedure of melting the sodium and heating the test section to 500°C is similar to that in the first wetting test. However, the previous experience with the first wetting test has helped to shorten the ramping up process significantly, as shown in Figure 172 (vs Figure 20). The test section was maintained at ~ 500°C for approximately 24.5 hours in the second wetting test. The monitored test section voltage with a constant current of 4 A is shown in Figure 173. As can be seen, over the duration of 500°C heating, the test section electrical resistance decreases slightly. In addition, compared to that in the first wetting test (Figure 21), the test section electrical resistance in the new wetting test is also reduced slightly. This could indicate improvement of wetting in the test section, but not by a significant amount. Its effect on the freezing behavior, however, is yet to be determined and will be discussed in the following sections.

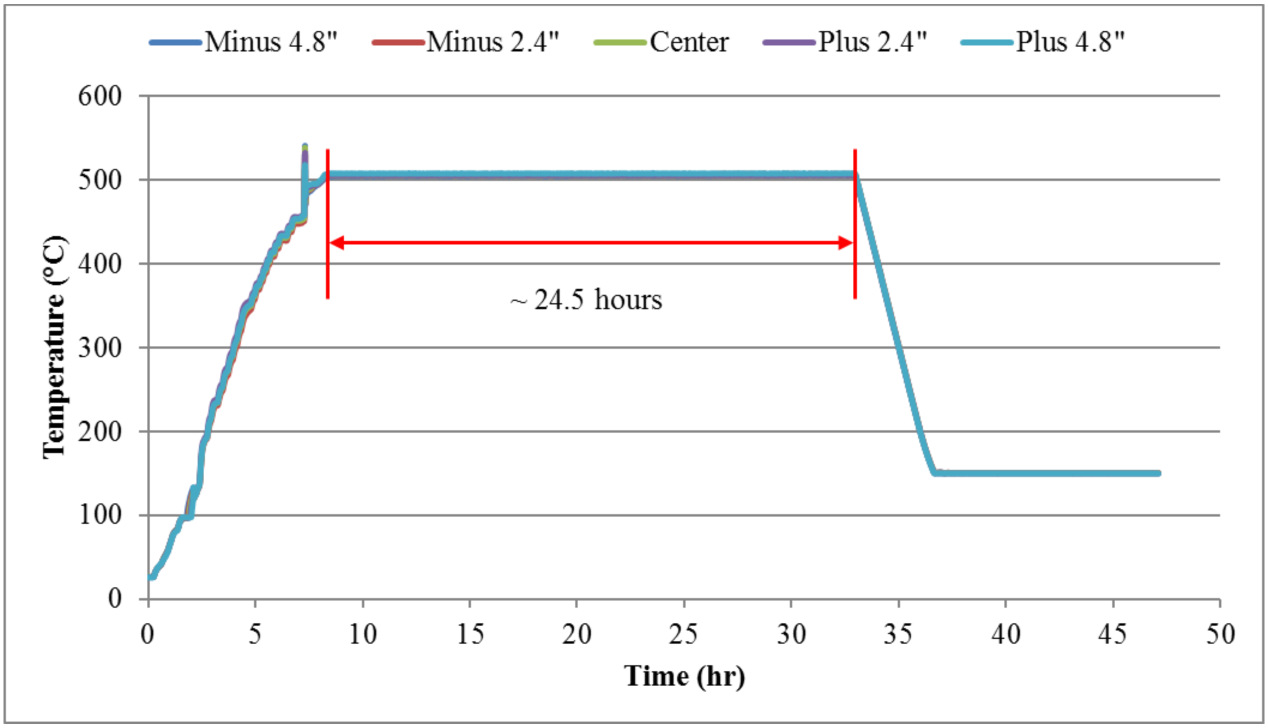

Figure 172. Heating history of the test section in Test 12.

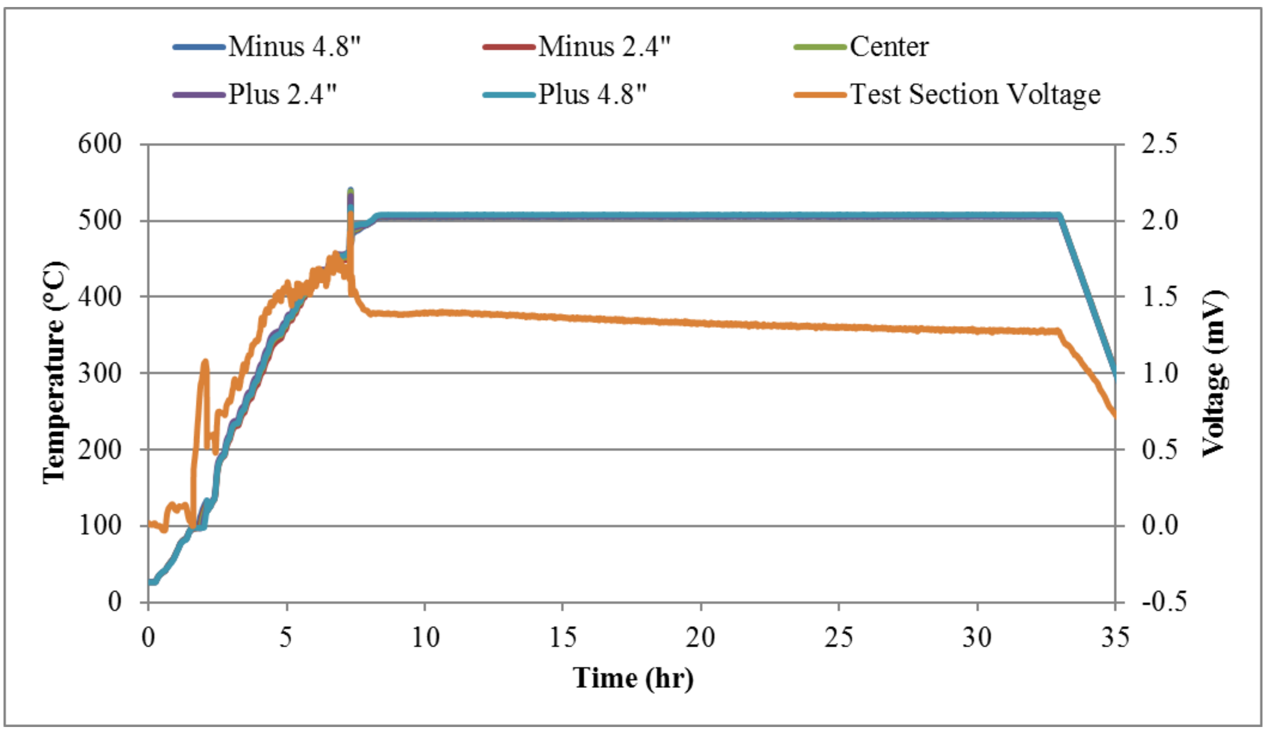

Figure 173. Test section electrical voltage/resistance monitoring in Test 12.

Following the 500°C heating of the test section, the loop temperature was lowered and a freezing test was performed. In this freezing test, Freezing Pattern 2 was adopted. Freezing plugs were first formed in the zones upstream and downstream of the test section (Zones 7 and 6), and then extended toward the free surfaces. With the freezing plugs cooled to reach their lowest temperatures, freezing was initiated in the test section, from the ends toward the center. The measured strain changes during sodium freezing are shown in Figure 174 to Figure 181. Compared to the first wetting test, no improvement was observed in the measured strain changes during sodium freezing in the new test. This is understandable since the freezing behavior is dominated by the cavitation process, as has been found in previous tests. In addition, the above finding indicates that good wetting had been achieved in the first wetting test. Otherwise, the freezing behavior in the first wetting test would have been dominated by the wetting characteristics of the test section and shown a significant difference from that in the second wetting test. The entire strain histories in this test are shown in Figure 182 to Figure 189. As expected, the new test results are similar to the previous ones.

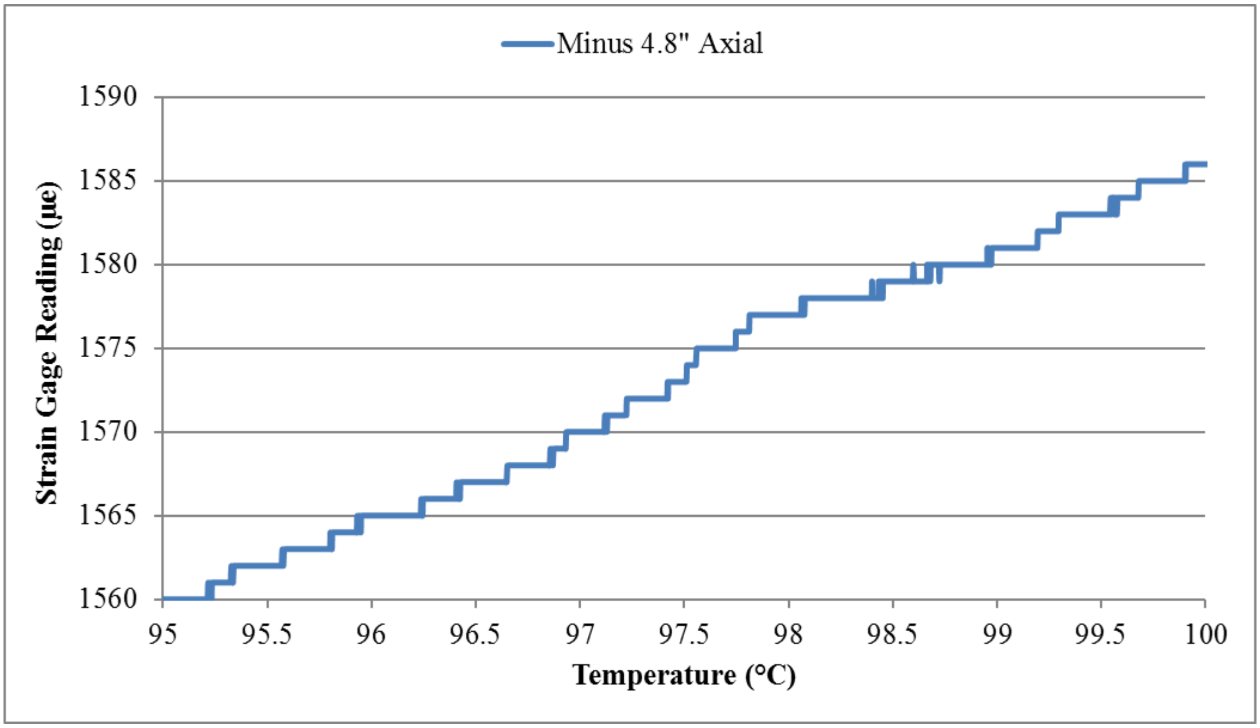

Figure 174. Axial strain vs temperature at –4.8” from the test section center in Test 12.

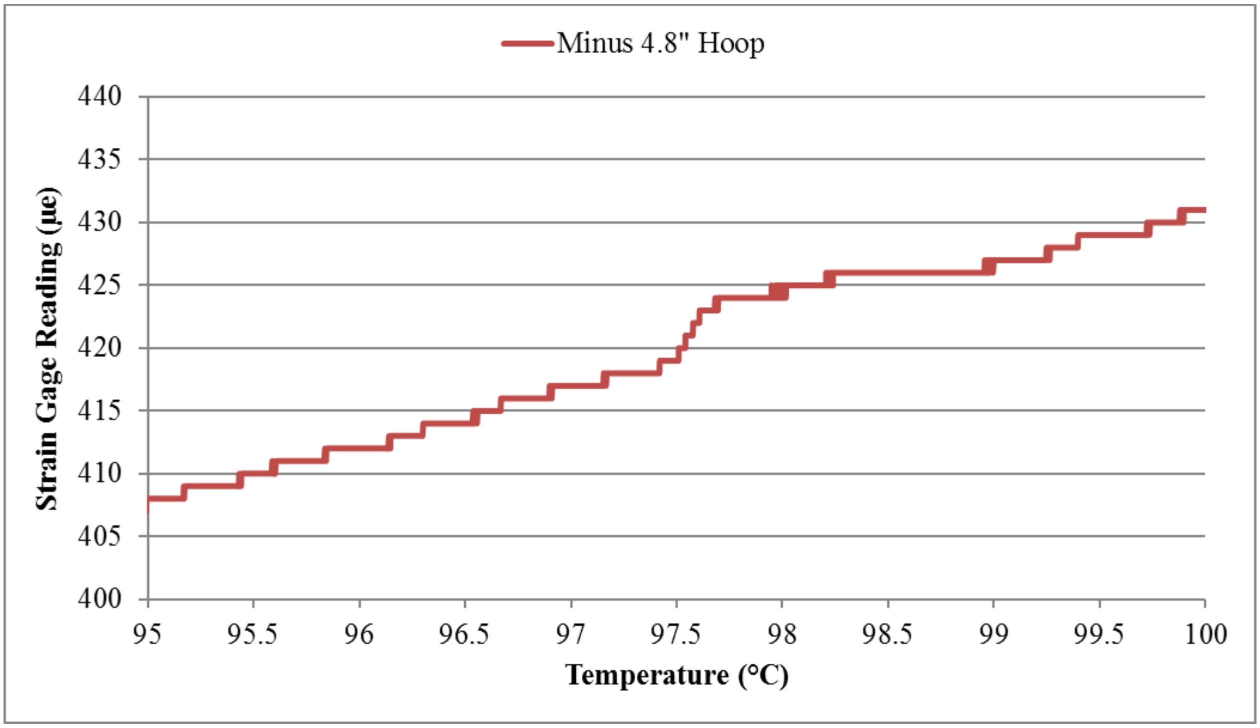

Figure 175. Hoop strain vs temperature at -4.8" from the test section center in Test 12.

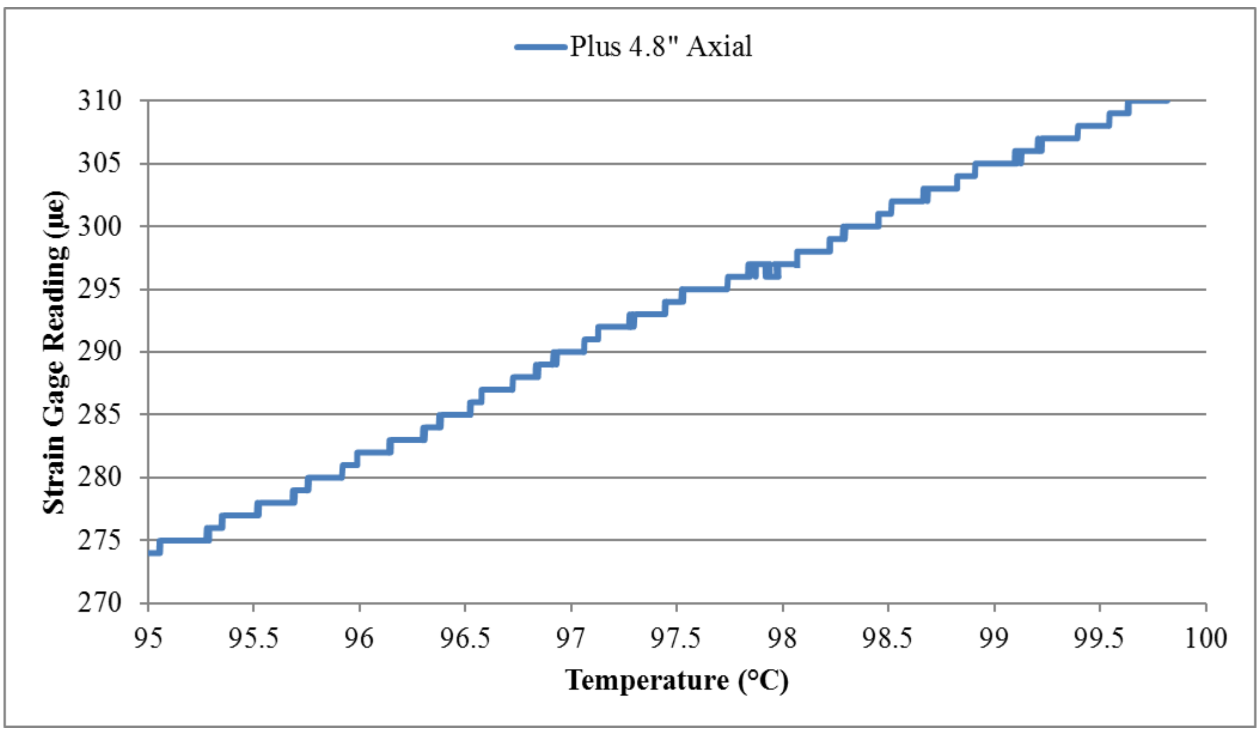

Figure 176. Axial strain vs temperature at +4.8" from the test section center in Test 12.

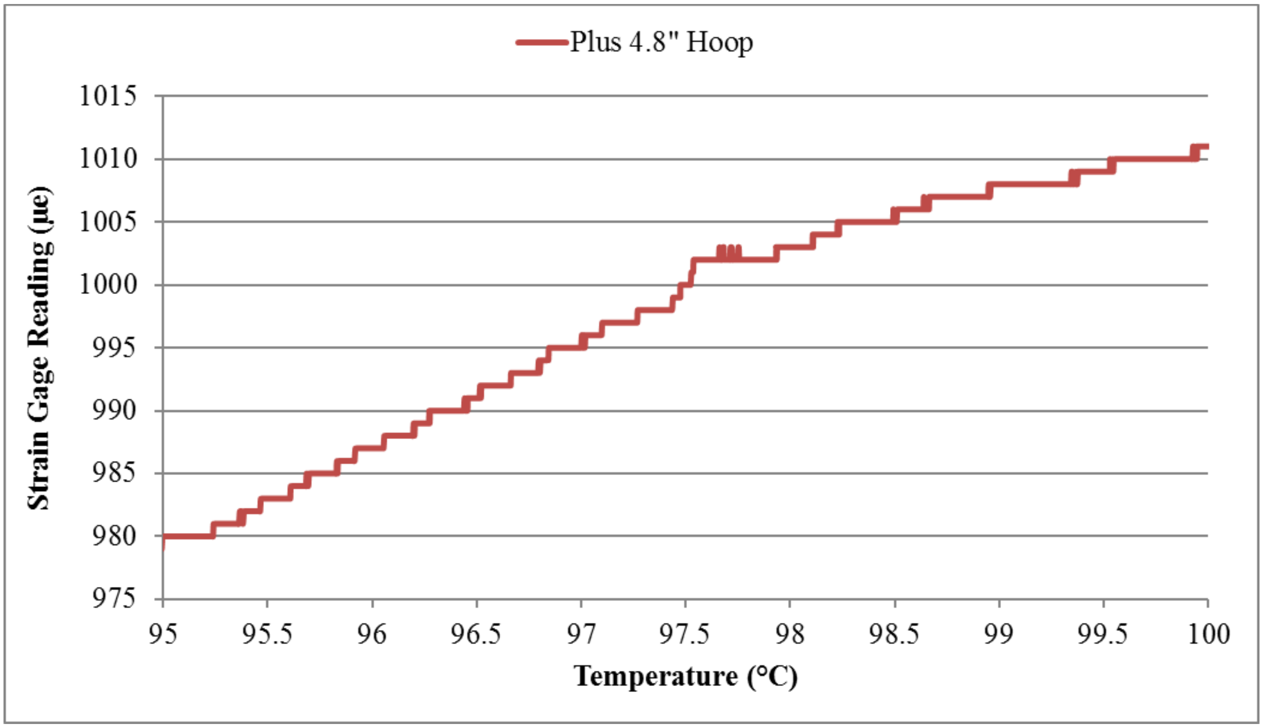

Figure 177. Hoop strain vs temperature at +4.8” from the test section center in Test 12.

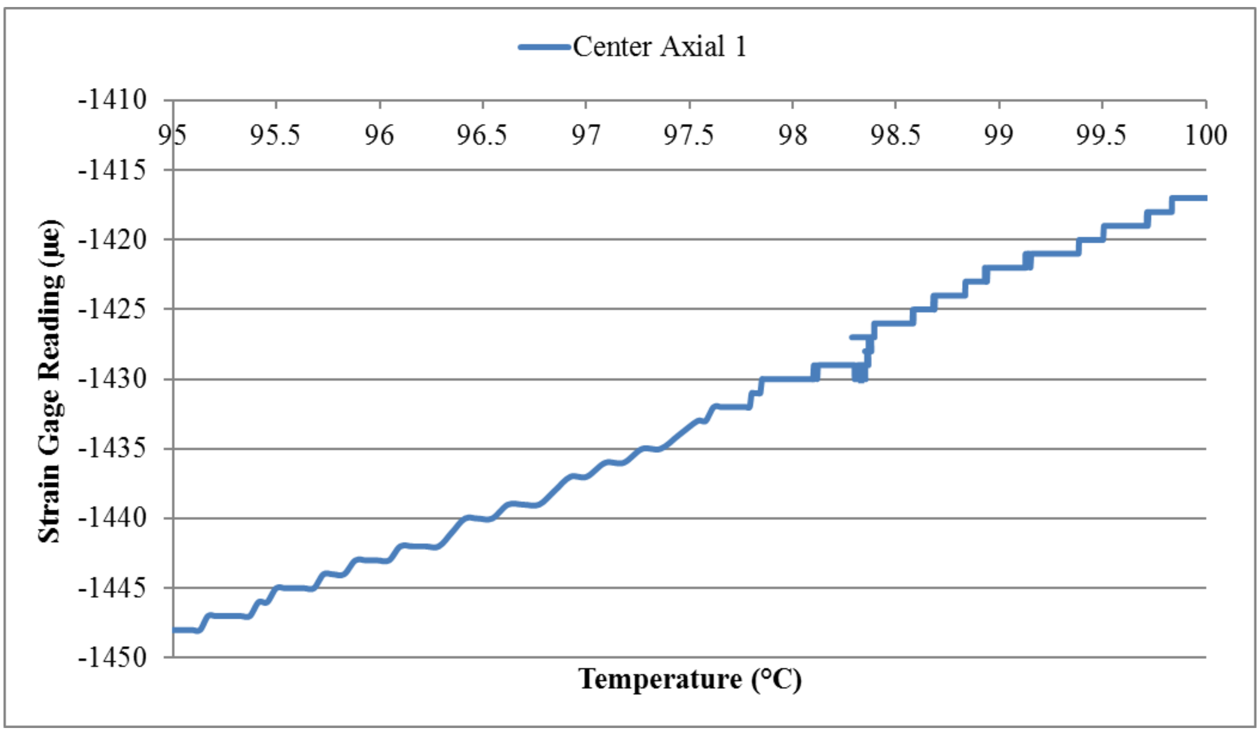

Figure 178. Axial Strain 1 vs temperature at the test section center in Test 12.

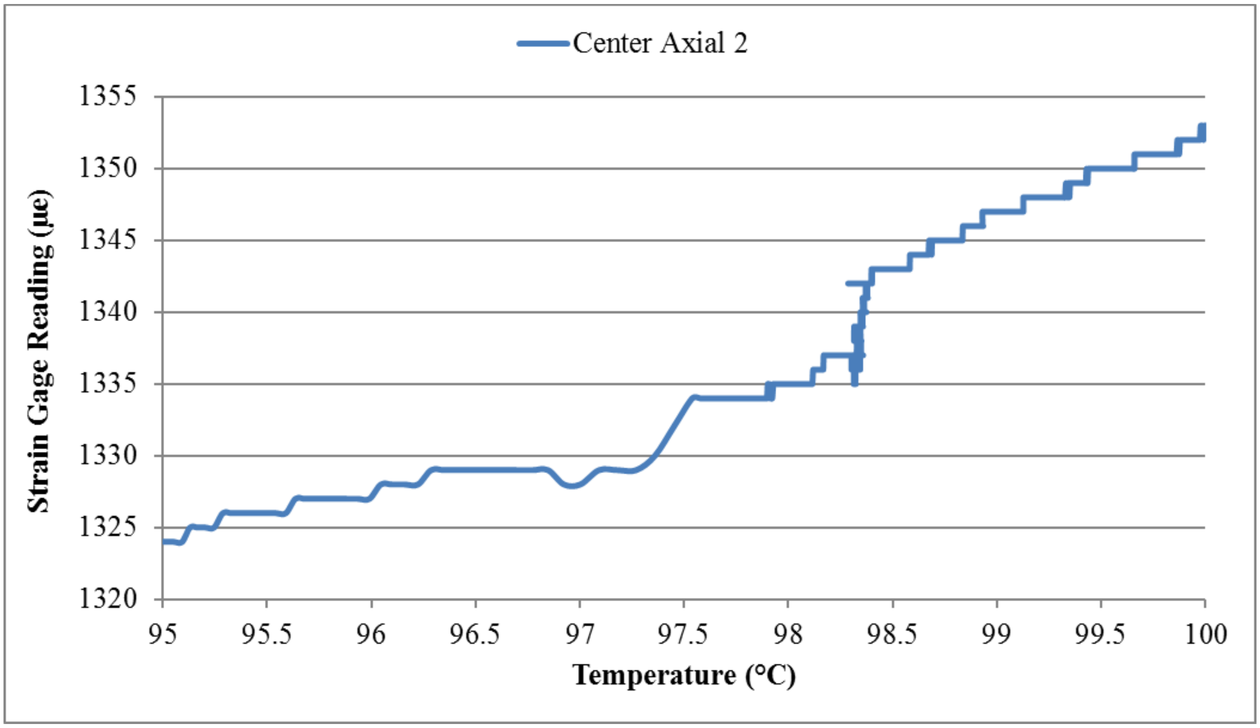

Figure 179. Axial Strain 2 vs temperature at the test section center in Test 12.

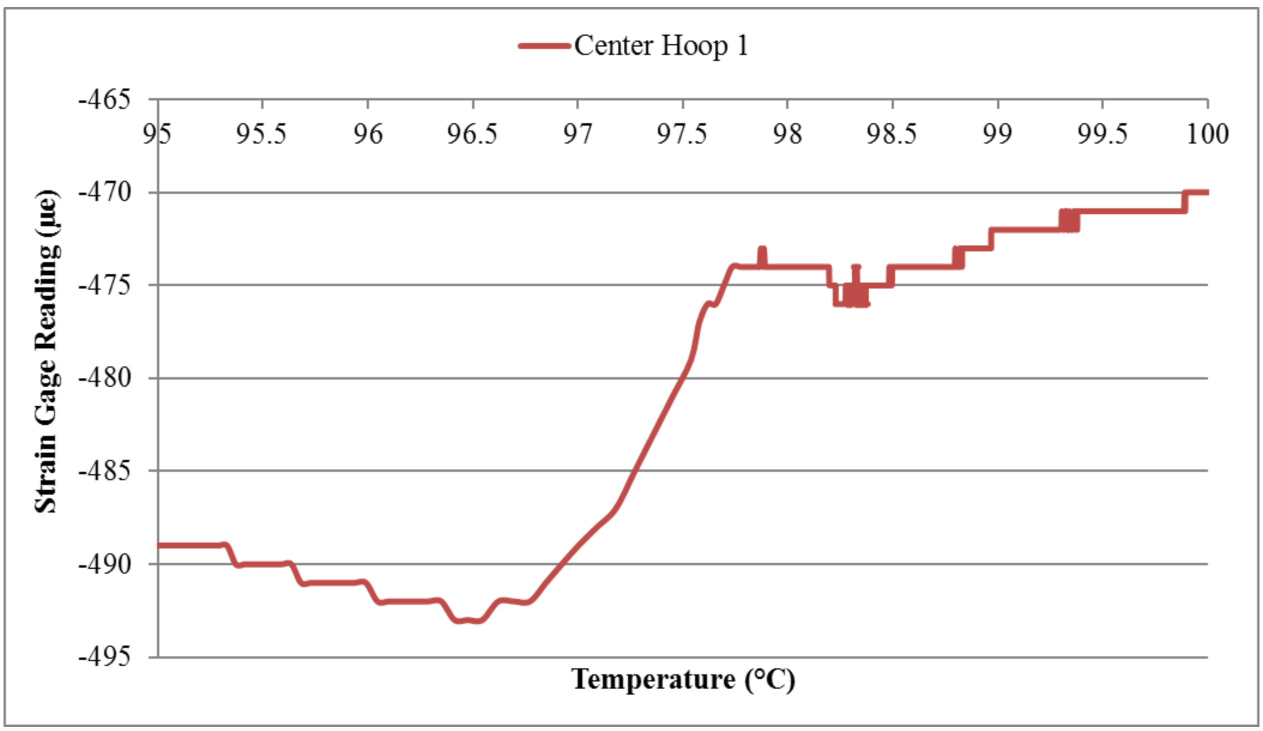

Figure 180. Hoop Strain 1 vs temperature at the test section center in Test 12.

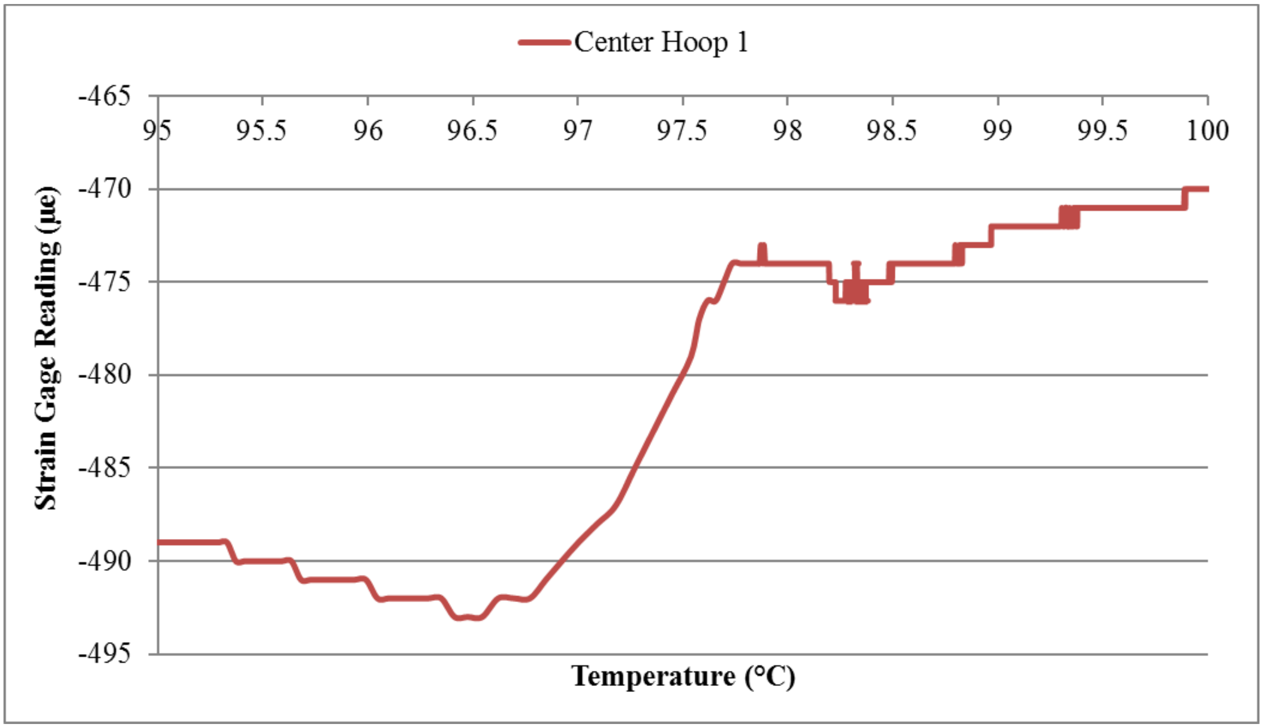

Figure 181. Hoop Strain 2 vs temperature at the test section center in Test 12.

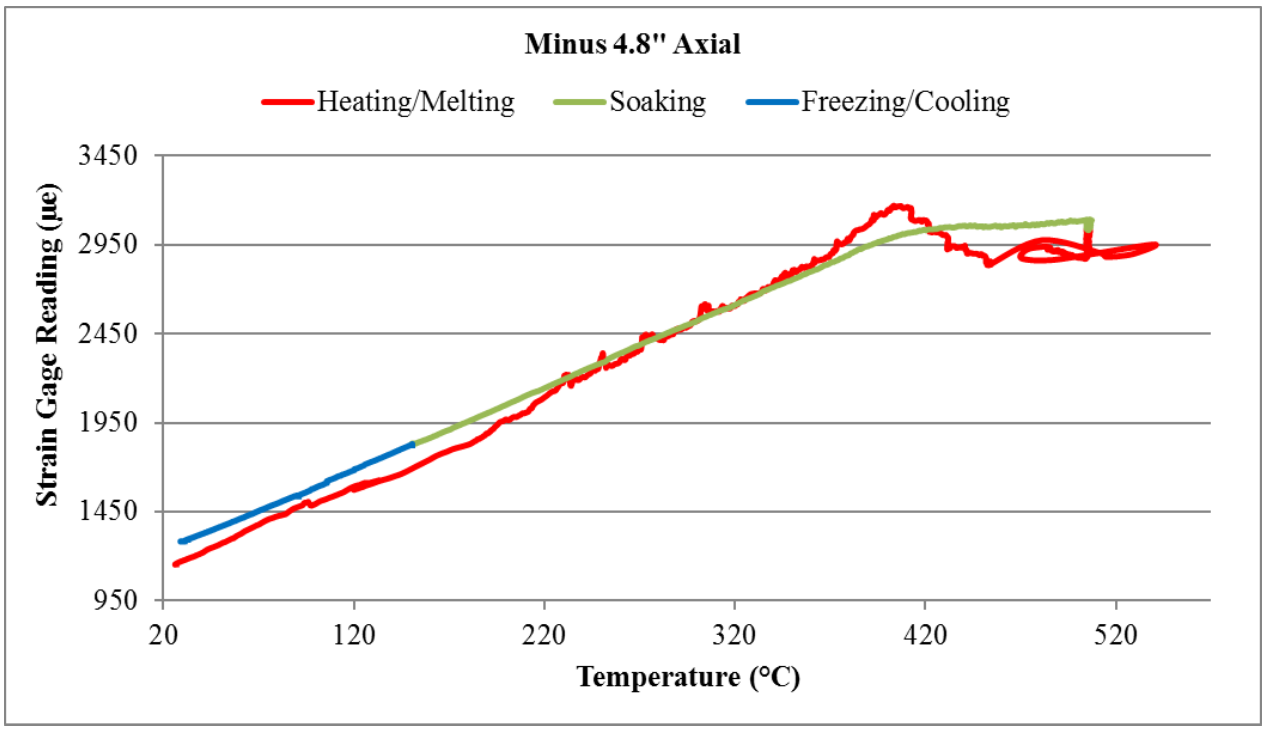

Figure 182. Entire axial strain history at –4.8" from the test section center in Test 12.

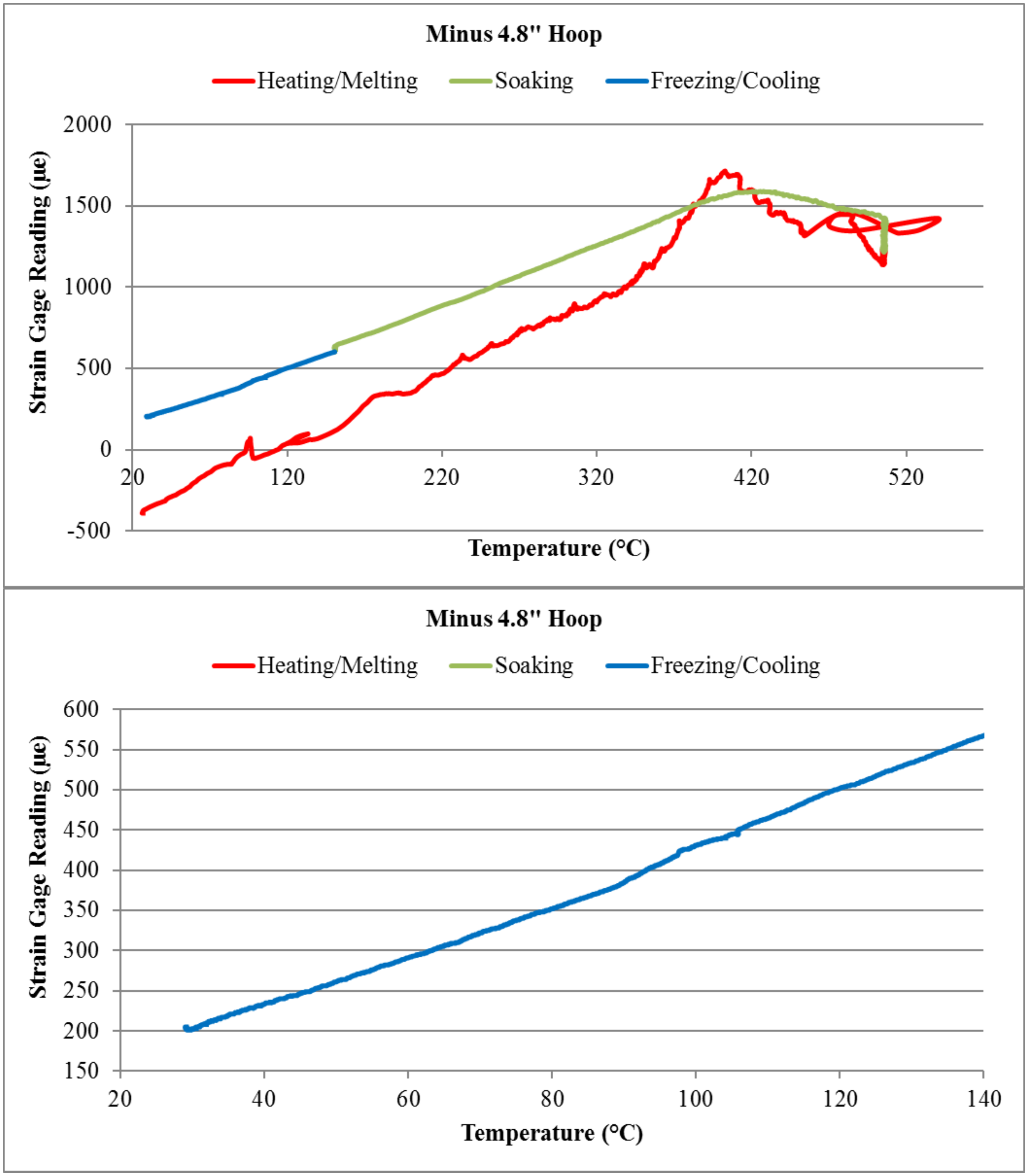

Figure 183. Entire hoop strain history (top) and zoom in of Freezing/Cooling phase (bottom) at -4.8" from the test section center in Test 12.

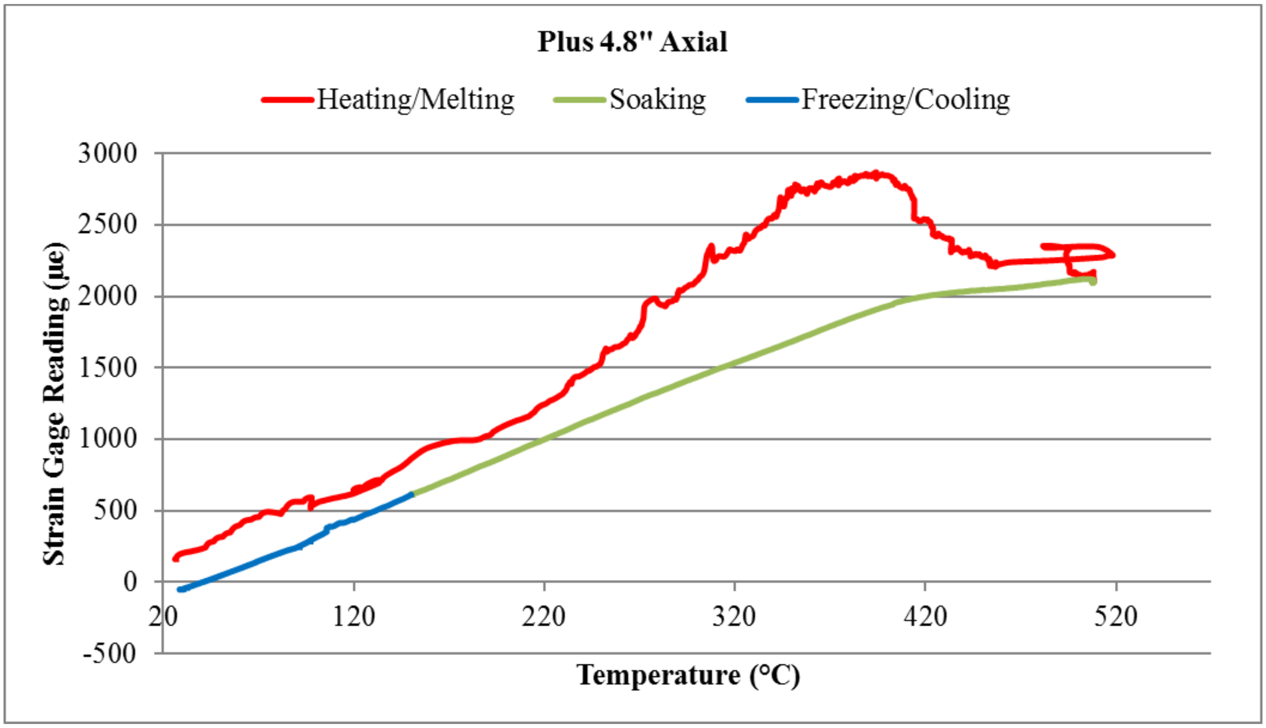

Figure 184. Entire axial strain history at +4.8” from the test section center in Test 12.

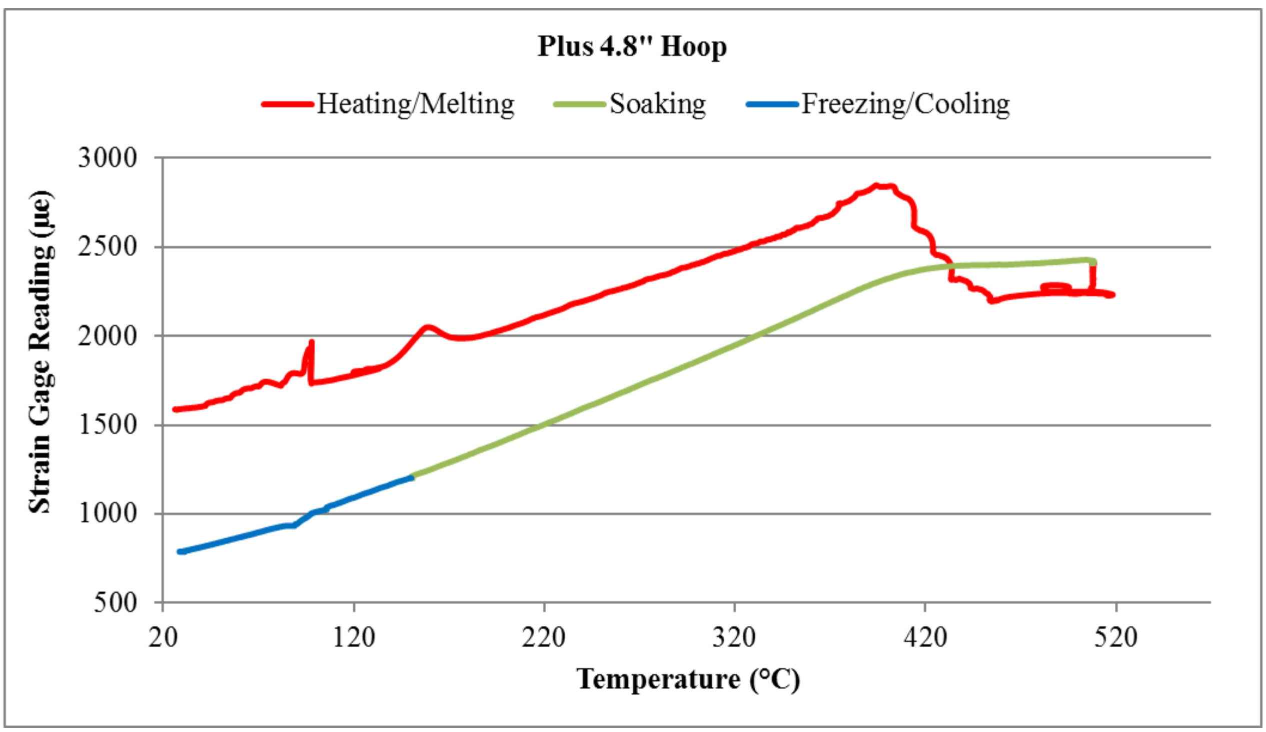

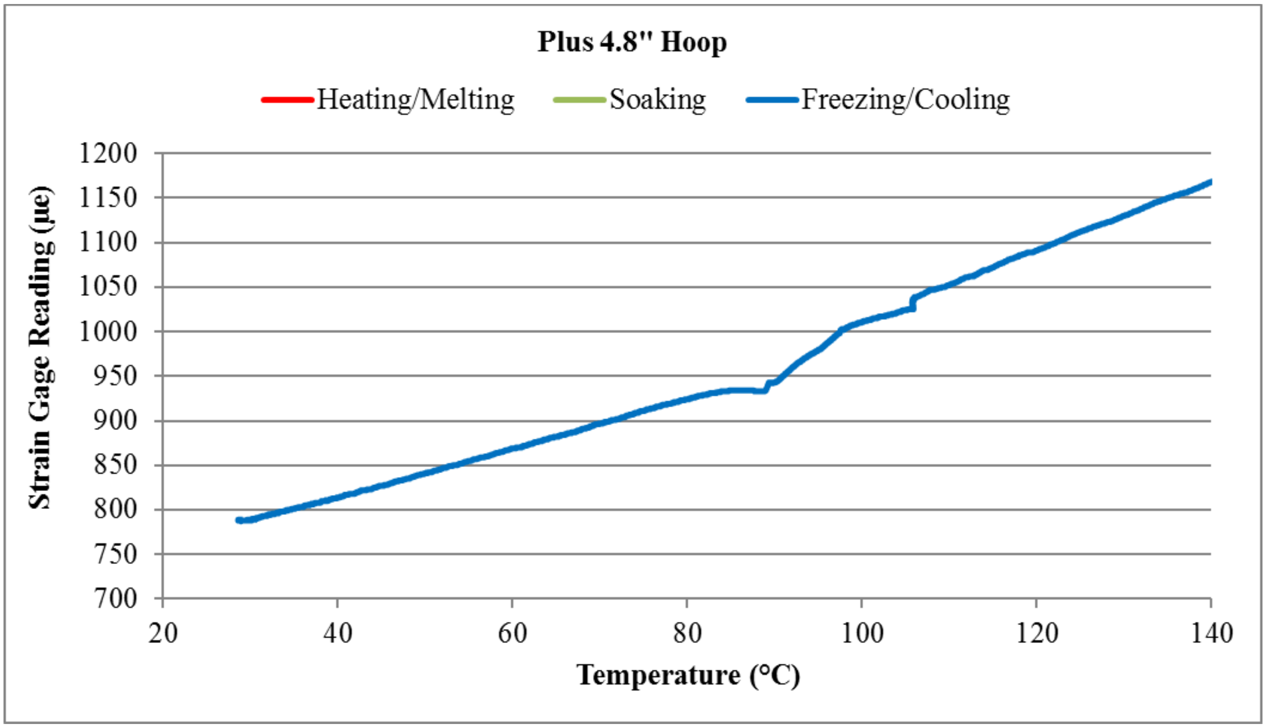

Figure 185. Entire hoop strain history (top) and zoom in of Freezing/Cooling phase (bottom) at +4.8" from the test section center in Test 12.

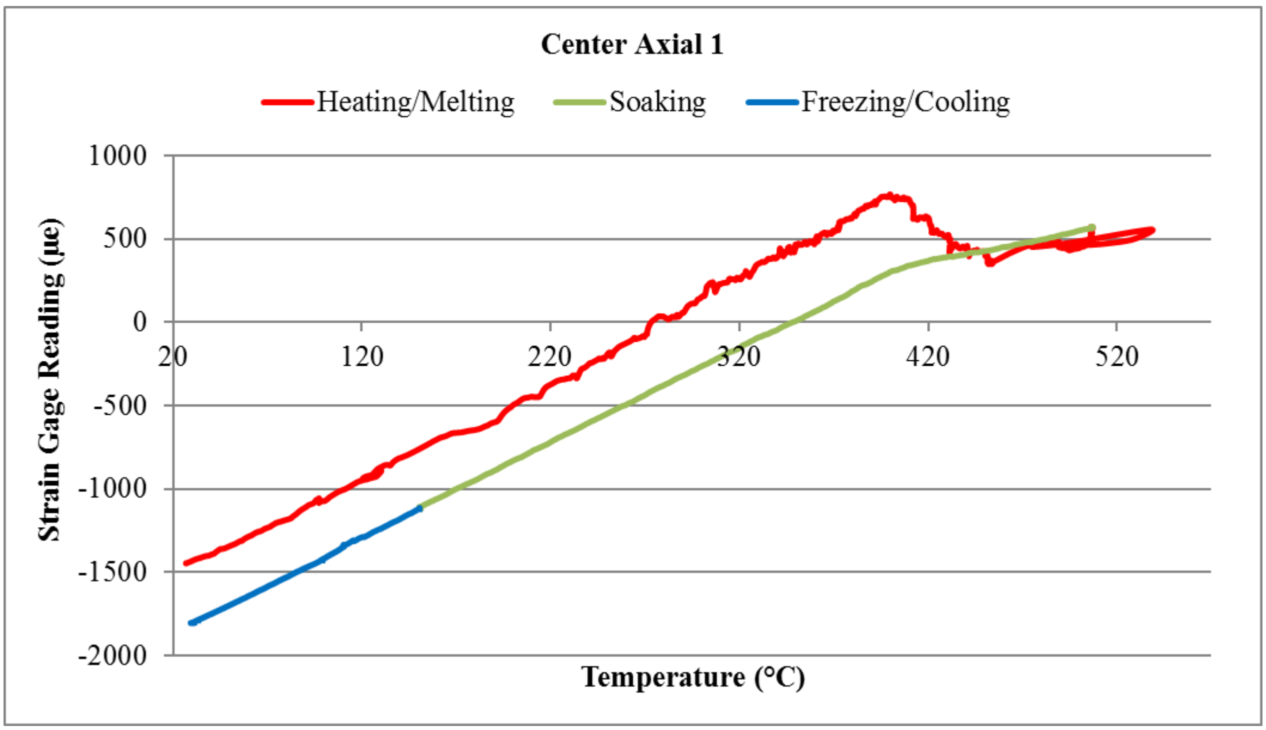

Figure 186. Entire axial strain 1 history at the test section center in Test 12.

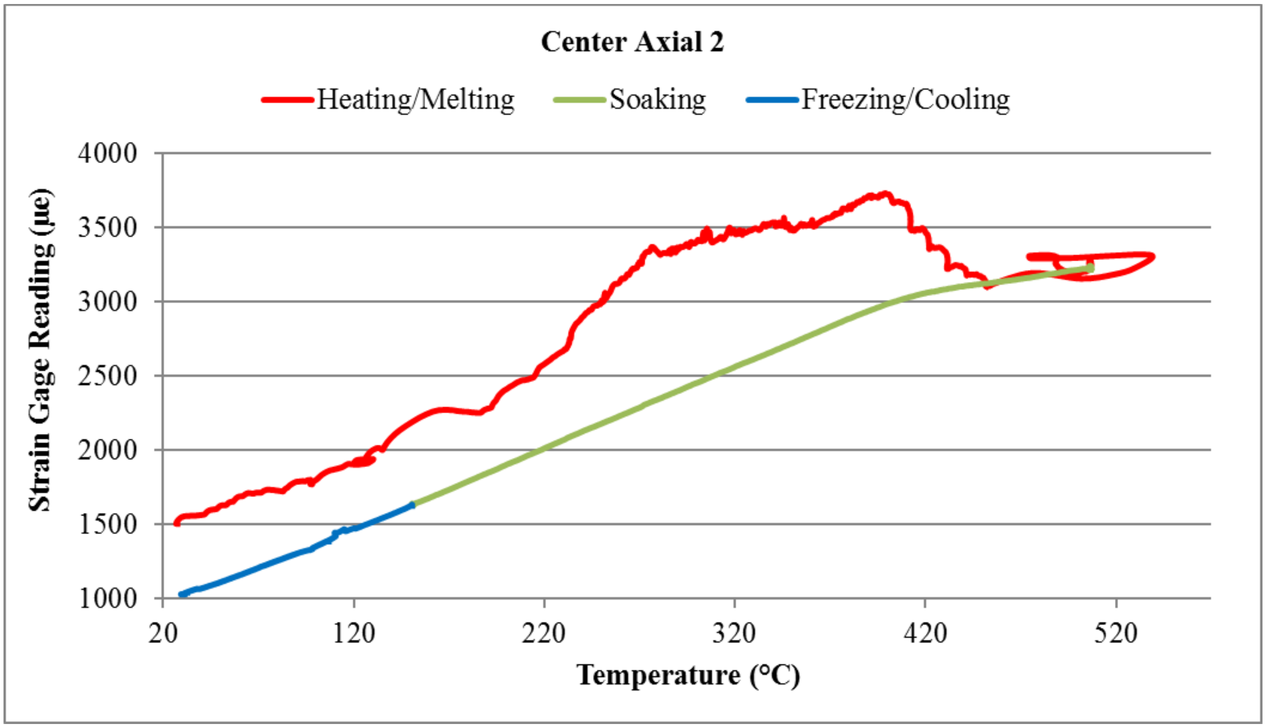

Figure 187. Entire axial strain 2 history at the test section center in Test 12.

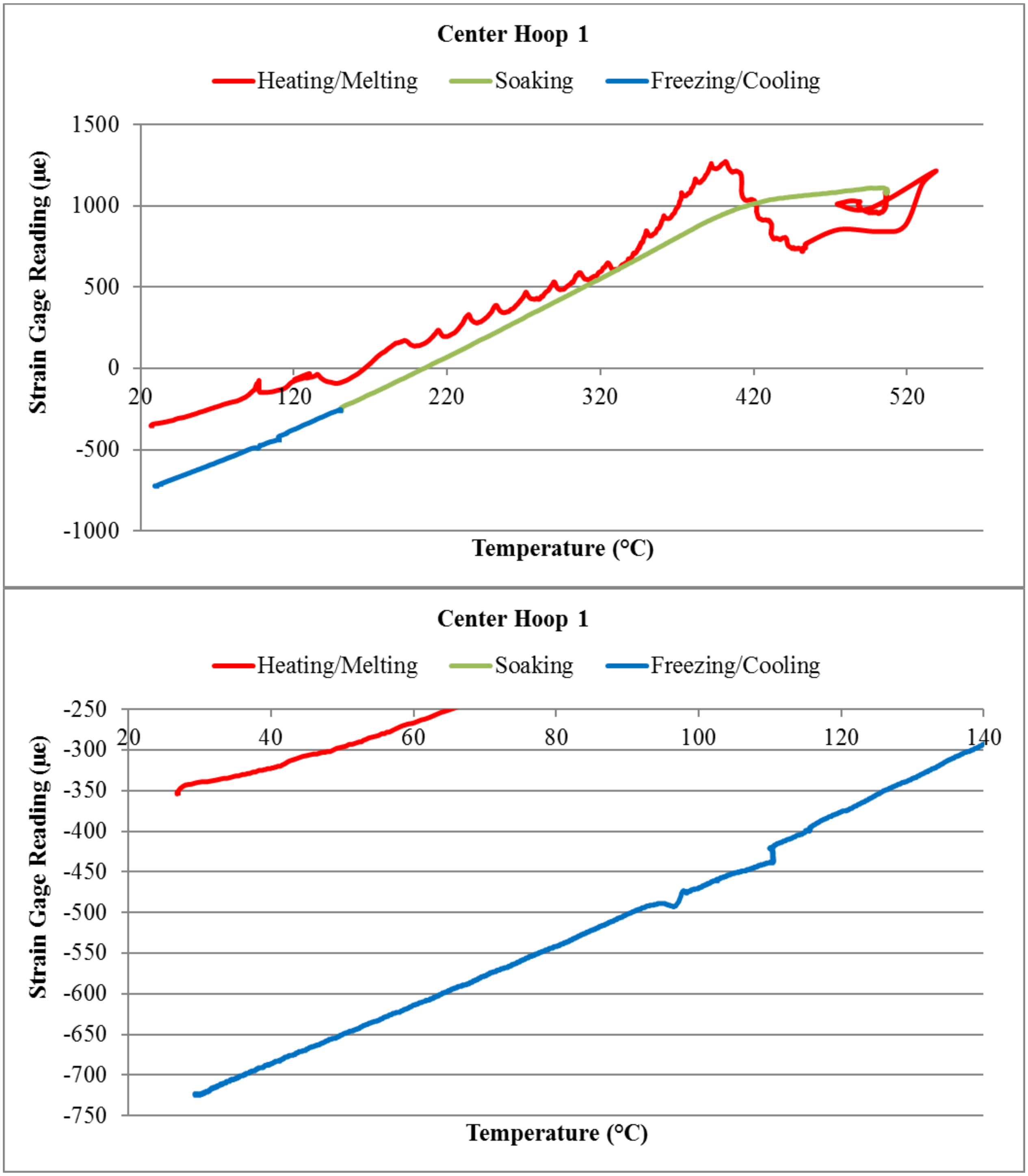

Figure 188. Entire hoop strain 1 history (top) and zoom in of Freezing/Cooling phase (bottom) at the test section center in Test 12.

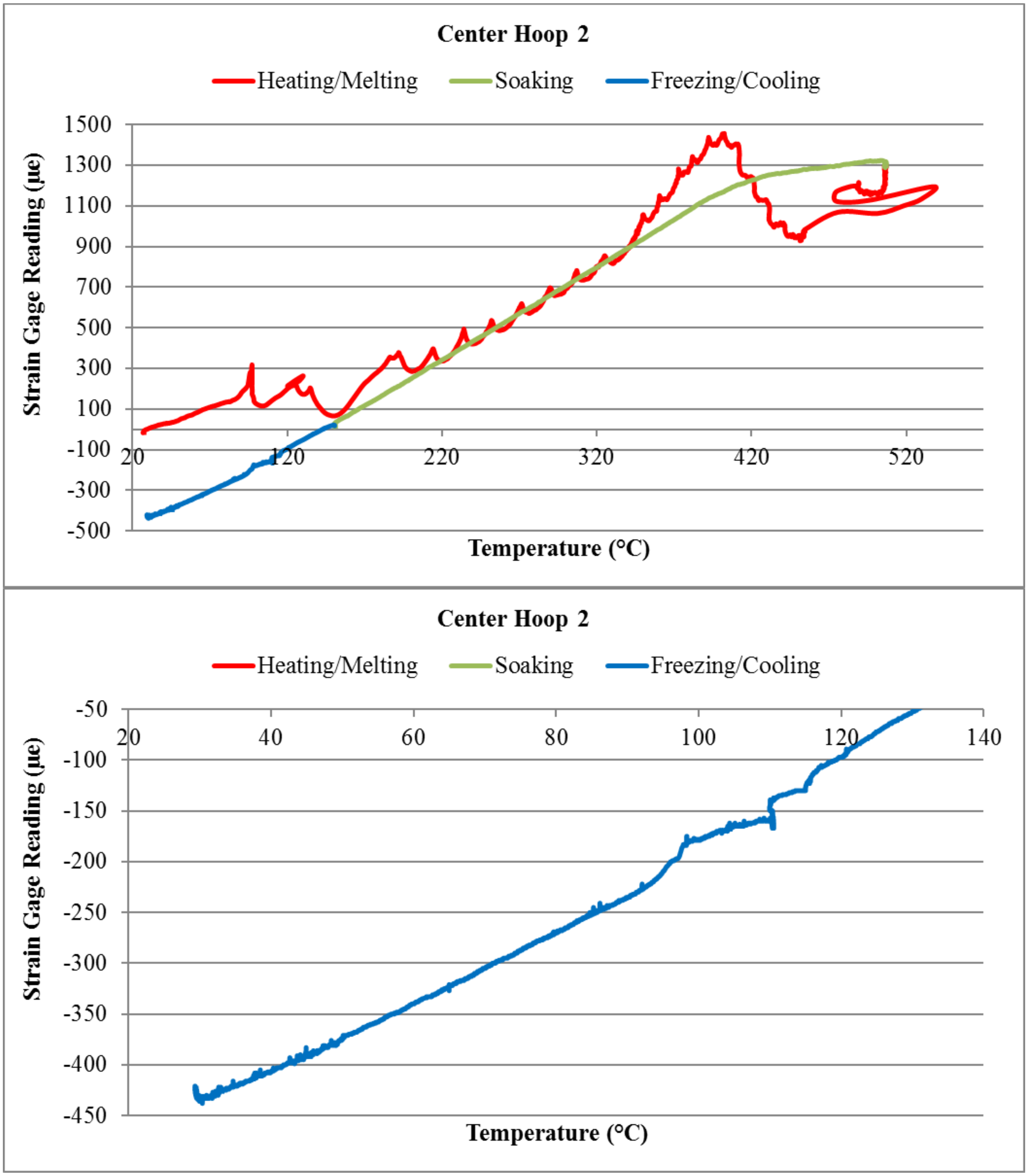

Figure 189. Entire hoop strain 2 history (top) and zoom in of Freezing/Cooling phase (bottom) at the test section center in Test 12.

3.13 Test 13: Repeat of Test 11 Following 2nd 500°C Wetting Test

This test is a repeat of Test 11 following the second 500°C wetting test. The main purpose of this test was to investigate the effect of the additional 500°C heating of the test section on the phenomenon of solid sodium pulling the test section wall after freezing. The test results are shown in Figure 190 to Figure 197. The new results are similar to those in Test 11, indicating that good wetting of the test section was already achieved after the first 500°C wetting test. In addition, the prominent phenomenon of solid sodium pulling the test section wall is observed at all three measurement locations again proving the previous hypothesis about the freezing process.

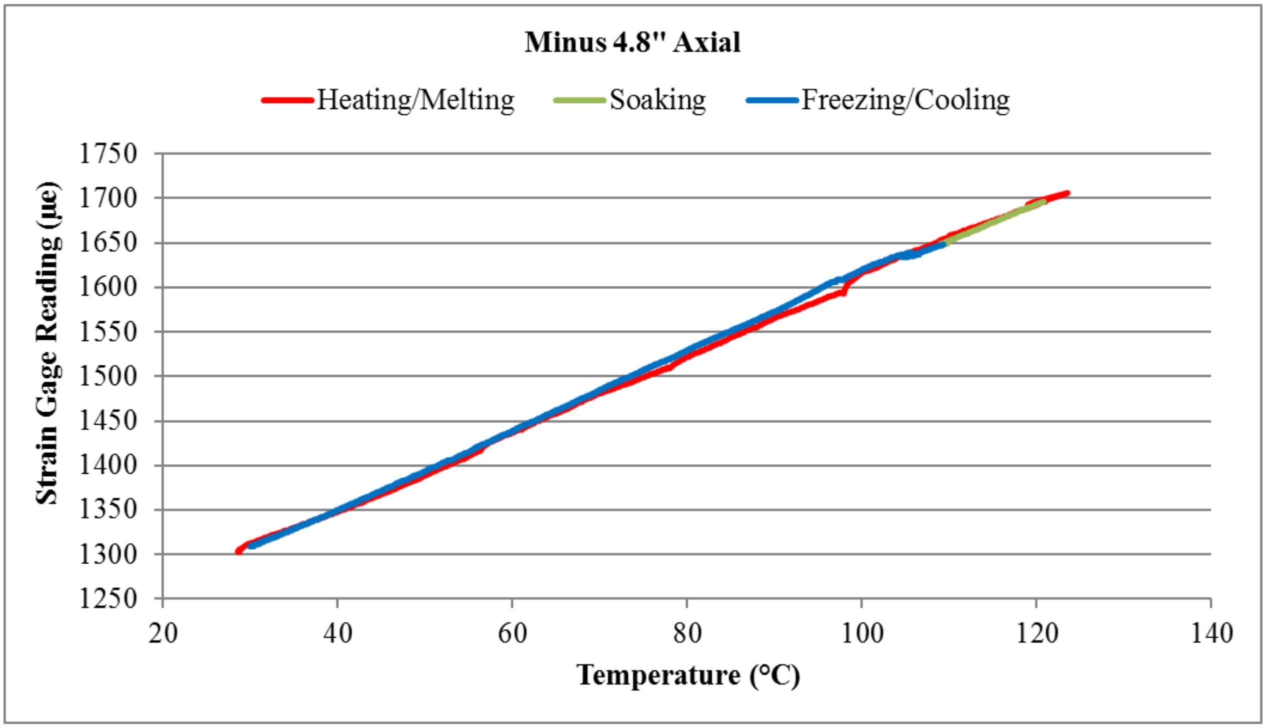

Figure 190. Entire axial strain history at –4.8" from the test section center in Test 13.

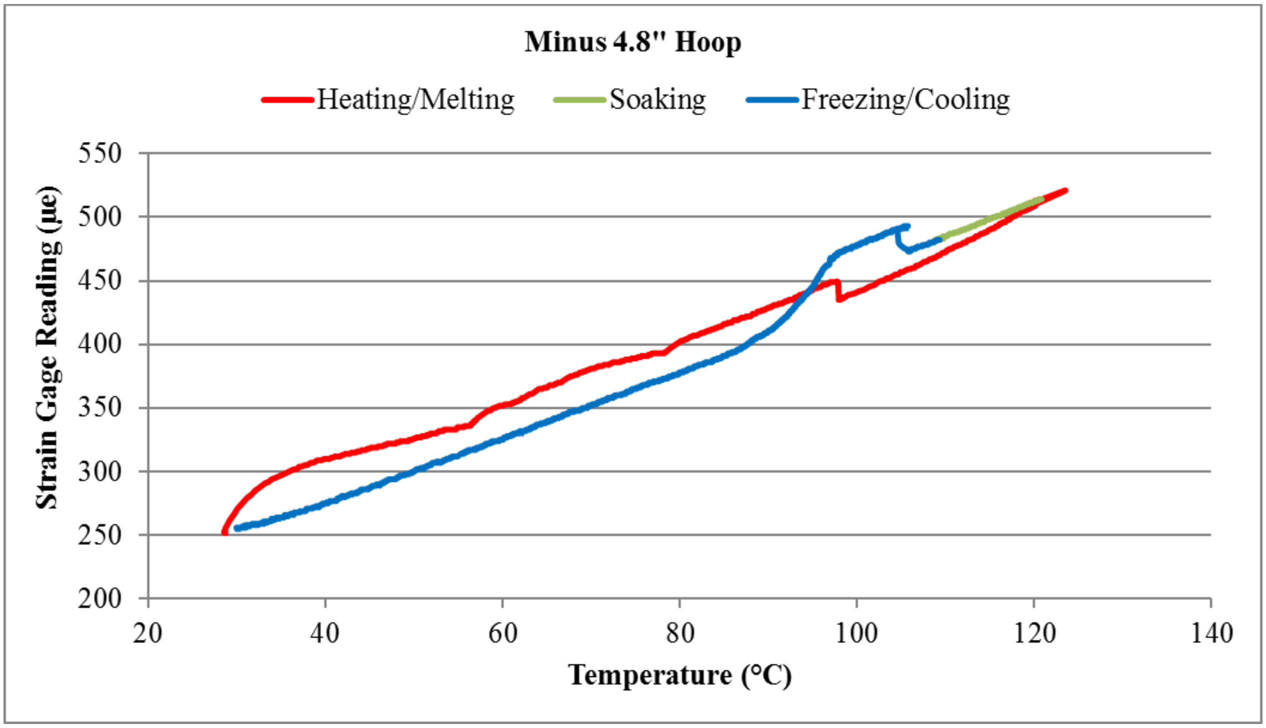

Figure 191. Entire hoop strain history at -4.8" from the test section center in Test 13.

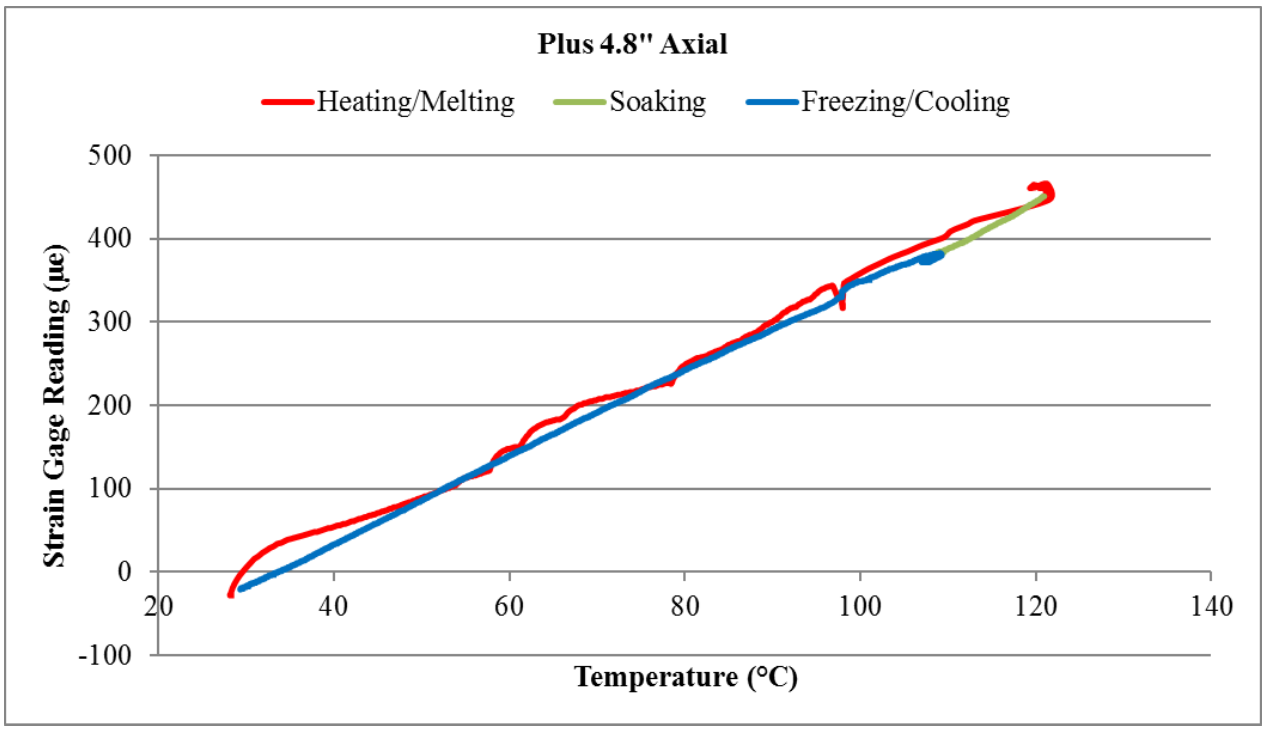

Figure 192. Entire axial strain history at +4.8" from the test section center in Test 13.

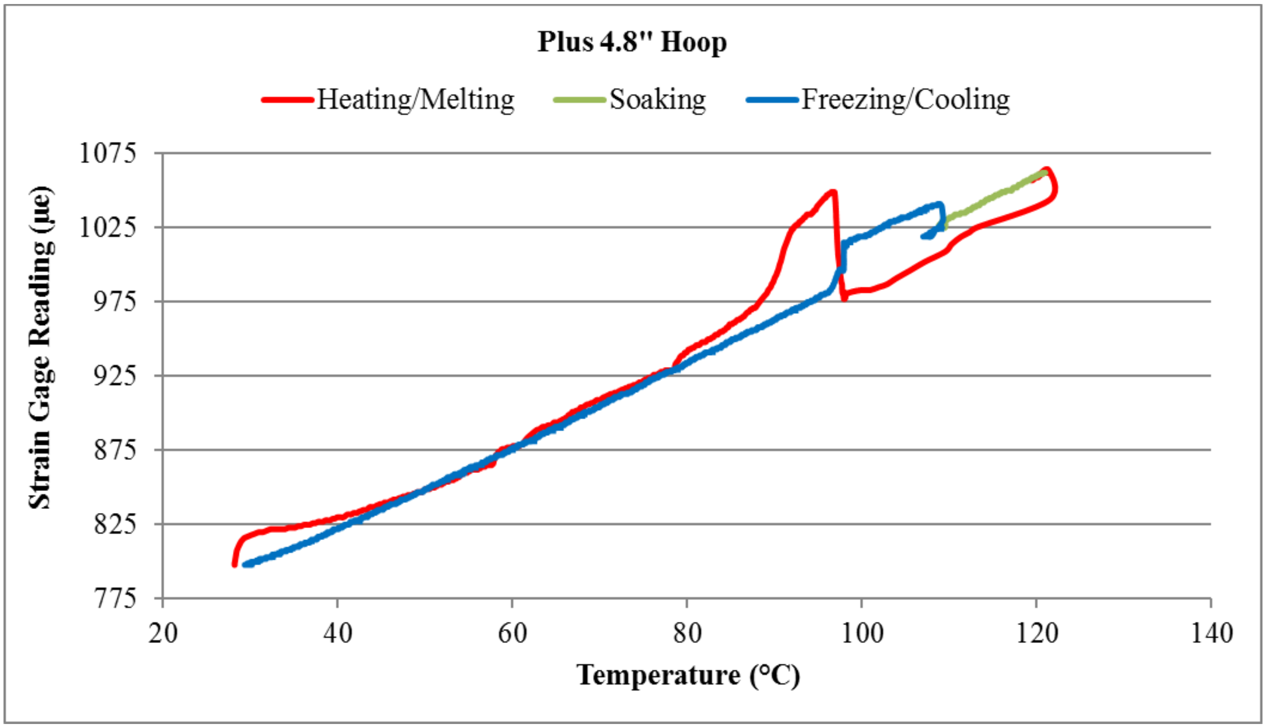

Figure 193. Entire hoop strain history at +4.8" from the test section center in Test 13.

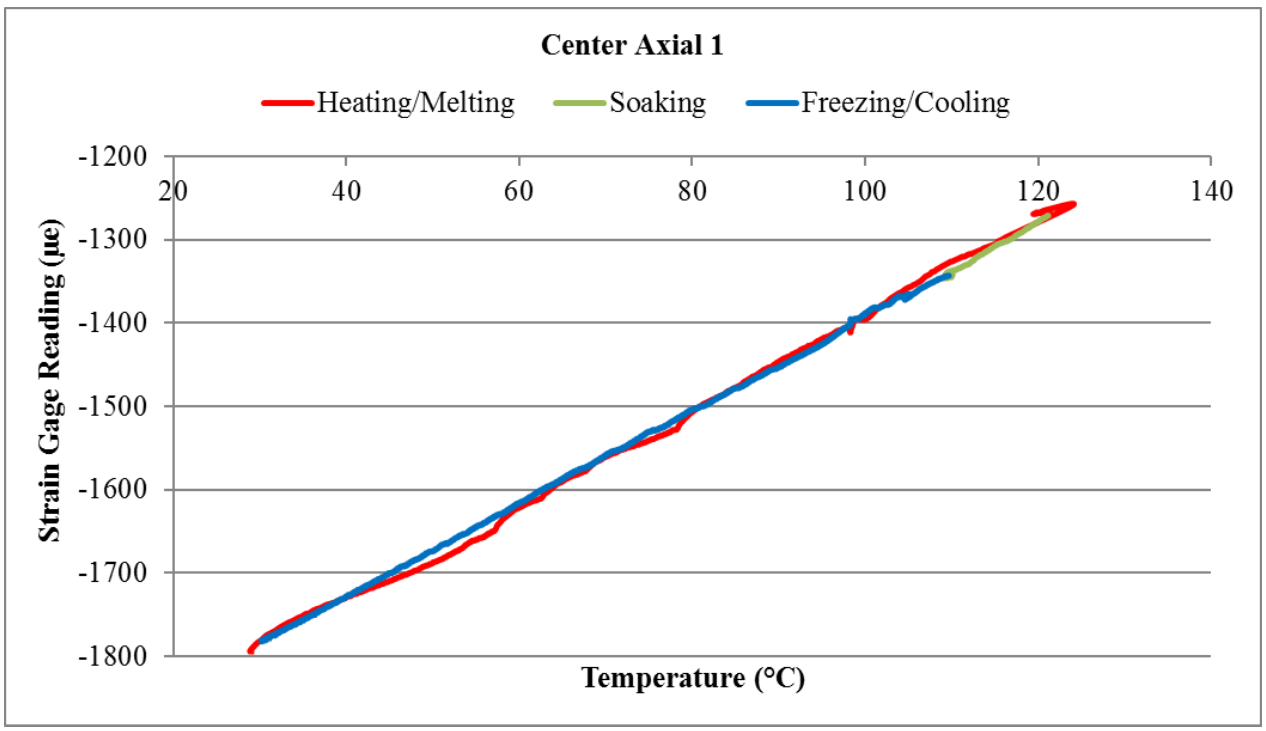

Figure 194. Entire axial strain 1 history at the test section center in Test 13.

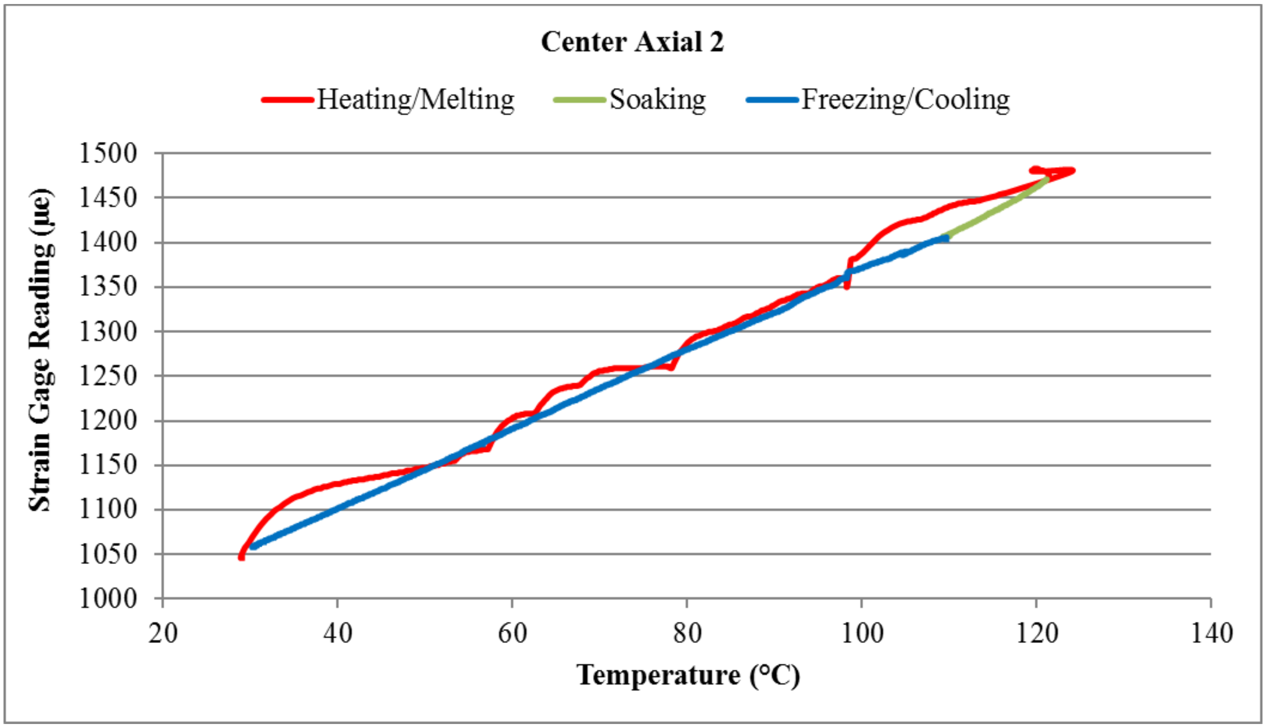

Figure 195. Entire axial strain 2 history at the test section center in Test 13.

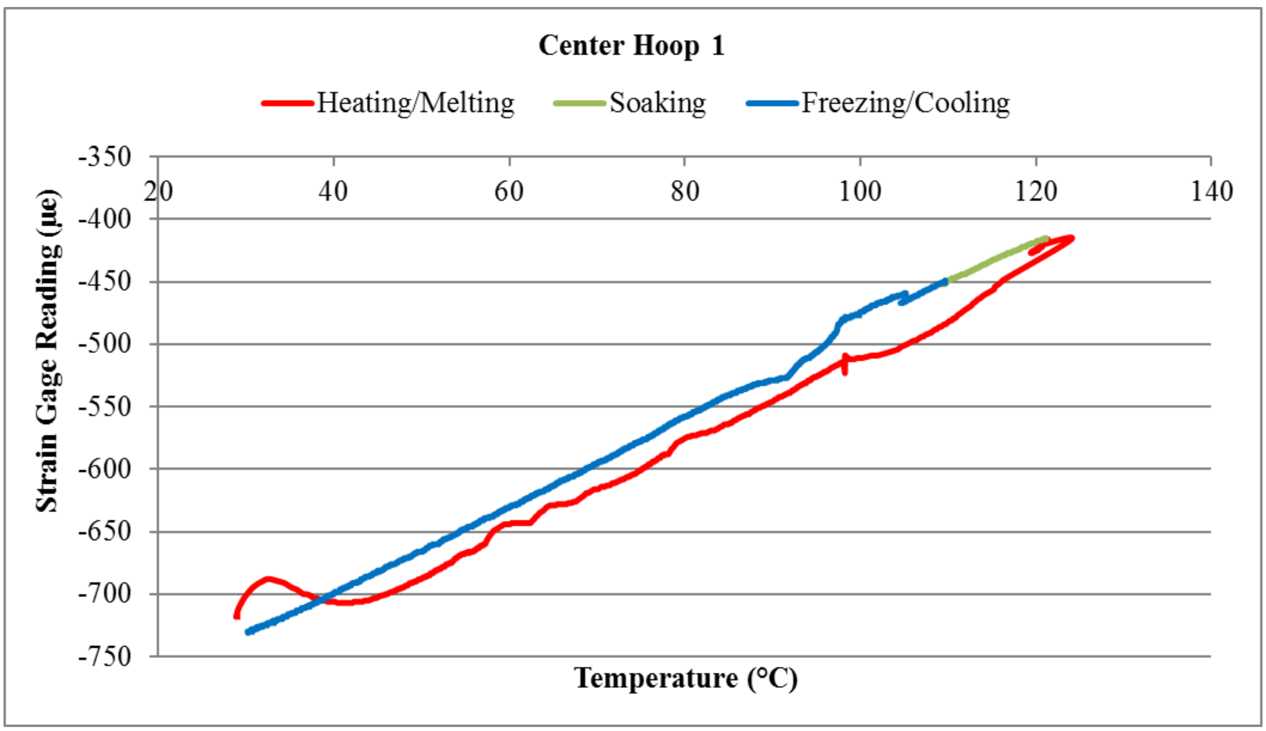

Figure 196. Entire hoop strain 1 history at the test section center in Test 13.

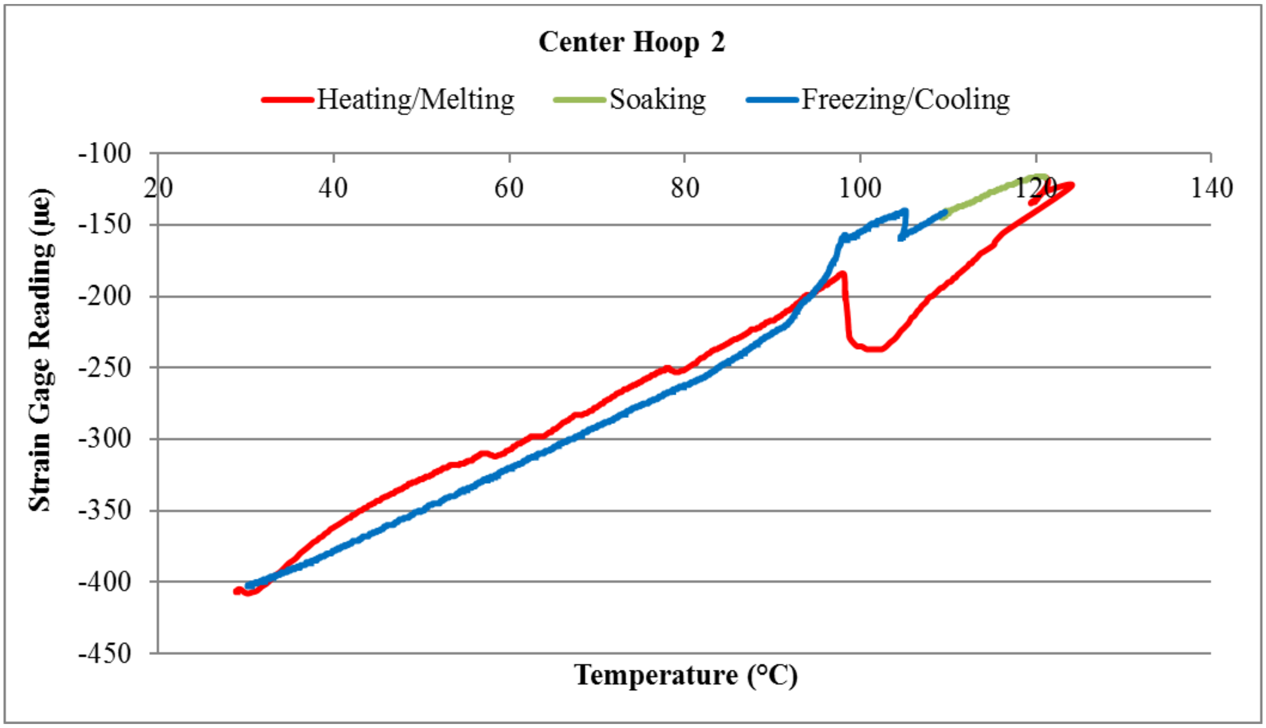

Figure 197. Entire hoop strain 2 history at the test section center in Test 13.

4 Summary

In FY 2017 and FY 2018, a total of thirteen tests were successfully performed in the Sodium Freezing and Remelting test facility. Each new test was carefully designed based upon the results and findings of the previous test to investigate the effects of different factors on the sodium freezing phenomena, including dissolved Ar cover gas versus vacuum, test section cooling rate during freezing, different freezing patterns (e.g., from the free surfaces inward toward the center versus from the center toward the free surfaces), and Ar cover gas pressure. The freezing results were found to depend upon a combination of phenomena. As more tests were conducted and lessons learned, the conduct of the tests improved. In particular, the last three experiments, Tests 11 through 13, may be singled out as providing representative data under well controlled conditions. A brief summary of the test conditions and results for the thirteen tests is provided in Table 2.

Table 2. Summary of all Sodium Freezing and Remelting Tests

Test No.	Test Conditions	Test Results
1	Shakedown test, ~ 200°C at TS, ~ 10 psig, Freezing Pattern 1.	Confirmed the functionality of the test loop. No significant strain drop observed following sodium freezing.
2	400°C wetting test, ~ 400°C at TS for ~ 2 hours, vacuum, Freezing Pattern 1.	Strain drop of 10 axial micro strains observed during sodium freezing. Solid sodium pulling the wall following sodium freezing observed, but not prominently (strain drop of 48 radial micro strains).
3	500°C wetting test, ~ 500°C at TS for ~ 24 hours, ~ 10 psig, Freezing Pattern 1.	Good wetting of TS achieved. Strain drop of 10 axial micro strains observed during sodium freezing. Strain drop of 60 radial micro strains observed following sodium freezing.
4	High vacuum test, ~ 1E-5 torr vacuum to degas sodium, Freezing Pattern 1.	Similar results as in Test 3 observed.
5	Fast cooling test, same procedure as Test 4 but with increased cooling rate during sodium freezing.	Similar results as in Test 4 observed.
6	Same procedure as Test 4 but with Freezing Pattern 2.	Similar results as in Test 5, with slightly reduced strain drop during sodium freezing (7 axial micro strains).
7	Same procedure as Test 6 but with Freezing Pattern 3.	Physical phenomenon of solid sodium pulling the wall after freezing shifted from +4.8” location to the center of TS.
8	Same procedure as Test 4 but with Freezing Pattern 4.	In terms of solid sodium pulling the wall after freezing, slight improvement at the -4.8” location, negligible improvement at the center location, and reduced effect at the +4.8” location.

9	Same procedure as Test 4 but with Freezing Pattern 5.	No constant temperature corresponding to sodium freezing point observed. Sharp drop of ~ 50 micro strains right after freezing observed at the center location (hoop Strain 2)
10	Same procedure as Test 6 but with ~ 30 psig Ar.	No improvement in the measured strain drop during sodium freezing.
11	Same procedure as Test 8 but with ~ 10 psig Ar.	Prominent phenomenon of solid sodium pulling the wall observed at all three measurement locations.
12	Repeat of Test 3 with another 500°C heating of TS for ~ 24.5 hours and Freezing Pattern 2.	No appreciable effect of additional heating observed.
13	Repeat of Test 11 following 2nd 500°C wetting test.	No appreciable effect of additional heating observed.
Freezing Pattern 1: Free surfaces -> center of TS **Freezing Pattern 2**: Zones 6 and 7 -> free surfaces -> center of TS **Freezing Pattern 3**: Zones 6 and 3 -> free surfaces -> Zone 2, strengthened freezing plug on reservoir side **Freezing Pattern 4**: Center of TS -> free surfaces **Freezing Pattern 5**: Maintain Zone 1 at 115°C while turning all other heaters to form freezing plugs -> lower Zone 1 temperature to 102°C at 1°C/4 mins -> increase Zone 1 temperature to 137°C at 1°C/4 mins -> lower Zone 1 temperature to room temperature at 1°C/4 mins		

The maximum stresses arising from sodium freezing are measured to be quite mild. In the tests, a maximum strain change of 60 radial micro strains was measured, equivalent to a stress/negative pressure of 77 psi. This mild maximum stress is thought to reflect the low yield stress of solid sodium near the freezing temperature. Evidence for yielding of solid sodium is provided by the visual observation of a depression in the frozen sodium free surface inside of the sodium reservoir in one test. It is thought that contraction of sodium in the test section during freezing pulled downward on the frozen sodium at the free surface creating the depression. The authors are not aware of any data for the yield stress of solid sodium or the stress versus strain behavior of solid sodium (sodium is not a structural material). It is thus not possible to directly compare with the solid sodium yield strength. However, stress versus strain data at different temperatures up to the freezing temperature are available for solid lithium which is also a alkali metal and has a low yield strength similar to the maximum stresses determined from the Sodium Freezing and Remelting tests providing support for the interpretation of the results in terms of yielding of solid sodium. This is a good result for Sodium-Cooled Fast Reactors and sodium facilities. The maximum stress due to frozen sodium pulling inward upon a structural wall wetted by sodium and to which the sodium adheres will be limited by the low sodium yield stress.

Argon has a significant solubility in sodium. Cavitation due to nucleation of dissolved argon can offset the effects of sodium thermal contraction and alleviate the formation of stress/negative pressure. This is also a good result for Sodium-Cooled Fast Reactors and sodium facilities that operate with an argon cover gas. In the tests, it was found that due to the cavitation, the maximum measured strain change during sodium freezing was limited to 10 axial micro strains, or equivalently 55 psi of negative pressure.

Nonetheless, sodium components such as valves and tubesheets have sustained damage during sodium “freezing.” This leads to a question of whether the damage actually occurred during the sodium freezing phase or the liquid sodium cooldown phase prior to the onset of freezing. There is a need for experiment investigation of the stresses and strains from the cooldown-induced thermal contraction of trapped liquid sodium. It is planned to design and initiate such testing with a sodium capsule test section during FY 2019. In addition, the Sodium Freezing and Remelting facility will be upgraded with installation of a new cold finger providing a significantly greater surface area for precipitation of sodium oxide from oxygen dissolved in the sodium. New tests will examine the effects of sodium purity upon the freezing phenomena.

Acknowledgements

Argonne National Laboratory's work was supported by the U.S. Department of Energy Nuclear Technology Research and Development (NTRD) Program under Prime Contract No. DE-AC02-06CH11357 between the U.S. Department of Energy and UChicago Argonne, LLC. The work presented here was carried out under the Primary System Component Research and Development area of the NTRD Program. The authors are grateful to Chris Grandy (Argonne/Nuclear Science and Engineering), the Technical Area Lead, Bob Hill (Argonne/Nuclear Science and Engineering), the National Technical Director, as well as Tom Sowinski (U.S. DOE), Headquarters Program Manager for the Project.

Vince Novick, Rich McDaniel, Jim Grudzinski (Argonne/Nuclear Engineering Division) as well as Matthew Weathered (then at the University of Wisconsin Madison) also worked on the assembly and operation of the original Sodium Freezing and Remelting facility. The authors are indebted to them for their contributions through the preceding years.

References

[1] D. Southall and S. Dewson, "Innovative Compact Heat Exchangers," in *Proceedings of ICAPP'10*, San Diego, CA, June 13-17, 2010.

[2] [Online]. Available: www.heatric.com.

[3] J. Sienicki and C. Reed, "Small-scale Experiment Concepts for the Investigation of Fundamental Phenomena in Compact Sodium Heat Exchangers," ANL-GenIV-173, Argonne National Laboratory, 2010.

[4] J. Sienicki, C. Reed, S. Majumdar, Y. Momozaki and B. Size, Argonne National Laboratory, Unpublished Information, 2011.

[5] C. Reed, J. Sienicki, Y. Momozaki, J. Grudzinski and D. Chojnowski, Argonne National Laboratory, Unpublished Information, 2012.

[6] C. Reed, J. Grudzinski, V. Novick, Y. Momozaki, M. Weathered, J. Sienicki, R. McDaniel and K. Byme, Argonne National Laboratory, Unpublished information, 2013.

[7] C. Reed, J. Grudzinski, V. Novick, Y. Momozaki, M. Weathered, J. Sienicki and R. McDaniel, Argonne National Laboratory, Unpublished Information, 2014.

[8] Q. Lv, E. Boron, Y. Momozaki, D. Chojnowski, J. Sienicki and C. Reed, "FY 2017 Status of Sodium Freezing and Remelting Tests," ANL-ART-114, Argonne National Laboratory, 2017.

[9] E. Hodkin, D. Mortimer and M. Nicholas, "The Wetting of Some Ferrous Materials by Sodium," in *Liquid Alkali Metals, Proceedings of the International Conference*, Nottingham University, April 4-6, 1973.

[10] E. Shpil'rain, S. Skovorod'ko and A. Mozgovoi, "New Data on the Solubility of Inert Gases in Liquid Alkali Metals at High Temperature," *High Temperature*, Vol. 40, No. 6, pp. 825-831, 2002.

[11] "United Performance Metals," [Online]. Available: https://www.upmet.com/sites/default/files/datasheets/316-316l.pdf. [Accessed 14 May 2018].

[12] E. Griffiths and E. Griffiths, "The Coefficient of Expansion of Sodium," in *Proc. Phys. Soc*, London, 1915.

[13] D. McLachlan and E. Ehlers, "Effect of Pressure on the Melting Temperature of Metals," *Journal of Geophysical Research*, Vol. 76, No. 11, pp. 2780, 1971.

[14] R. Schultz, "Lithium: Measurement of Young's Modulus and Yield Strength," 2002.

Nuclear Science and Engineering Division
Argonne National Laboratory
9700 South Cass Avenue, Bldg. 208
Argonne, IL 60439

www.anl.gov

Argonne National Laboratory is a U.S. Department of Energy
laboratory managed by UChicago Argonne, LLC